Master's thesis

NTNU
Norwegian University of Science and Technology
Faculty of Engineering
Department of Energy and Process Engineering

August Brækken

Energy Use and Energy Efficiency Potential on Passenger Ships

Master's thesis in Energy and Environmental Engineering
Supervisor: Natasa Nord
Co-supervisor: Cecilia Gabrielii
June 2021

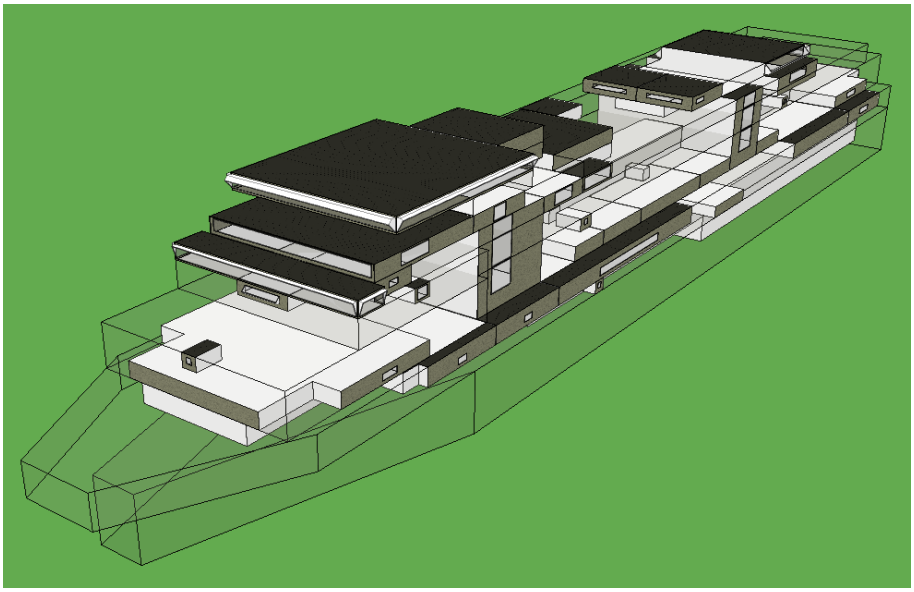

NTNU
Norwegian University of
Science and Technology

August Brækken

Energy Use and Energy Efficiency Potential on Passenger Ships

Master's thesis in Energy and Environmental Engineering
Supervisor: Natasa Nord
Co-supervisor: Cecilia Gabrielii
June 2021

Norwegian University of Science and Technology
Faculty of Engineering
Department of Energy and Process Engineering

NTNU
Norwegian University of
Science and Technology

Preface

This master's thesis is conducted as a part of the 2-year master's programme Energy and Environmental Engineering at Norwegian University of Science and Technology (NTNU) in Trondheim. The work was done at Department of Energy and Process Engineering under supervision of Professor Natasa Nord. The project's co-supervisor is research scientist Cecilia Gabrielii at SINTEF Energy Research. The master's project amounts to 30 ECTS.

The work was started in a summer job at SINTEF Energy Research in 2020, where the main task was developing an initial building simulation model for a cruise ship in IDA ICE. This was followed by a project thesis in autumn 2020, where the model was developed further and a parametric study was performed by varying the weather data and ship orientation. Preliminary energy efficiency scenarios were also developed and analysed using the simulation model. In this thesis, the model is developed further and more analyses are performed.

I would like to thank Natasa Nord for good advice regarding the project work, as well as help with IDA ICE. Thank you to Cecilia Gabrielii for assistance in the literature study, report writing and the analyses performed. I would also like to thank Torbjørn Krogh and Rosina Barbuscia at Fosen Design & Solutions for information about ship construction and ventilation systems. Thank you to technical contractor GK for cost estimates for air handling units.

Trondheim, 11 June 2021

August Brækken

August Brækken

Abstract

Energy systems on passenger ships have traditionally been based on fossil fuels, which contribute to large CO_2 emissions. The main focus has been on improving the propulsion system on ships, while a focus on reducing the energy use in the hotel system has been lacking. Hotel systems on passenger ships account for up to 40% of the energy consumption. To efficiently reduce greenhouse gas emissions from passenger ships, it is therefore important to also consider the hotel system.

This master's thesis is a part of the project CruiZE (Cruising towards Zero Emissions), which is a collaboration between SINTEF Energy Research, NTNU, Carnival Corporation & plc, as well as Norwegian suppliers of ship equipment and design solutions. The overarching goal of CruiZE is to reduce the energy use of hotel systems on passenger ships through innovative design solutions. The aim of this master's thesis is to analyse the energy use on passenger ships and possible energy saving solutions, using the building simulation tool IDA ICE.

The hotel system of a cruise ship was modelled in IDA ICE, mainly based on Color Line's ship Color Fantasy. At first, fan coils with unlimited heating and cooling were used in the model. The initial results were compared to energy use on the reference ships MS Birka Stockholm and a large cruise ship. The model was then calibrated by increasing the demand for domestic hot water (DHW) and reducing the ventilation rate in large galleys. This gave a total annual energy consumption of 19.2 MWh/passenger for the ship's hotel system. The energy demand for propulsion was found to be 0.156 kWh/ALB-km. ALB is available lower berth, set to two per cabin.

After calibration, an analysis of different ways to size fan coils was performed. The resulting thermal environment was similar when using design day data in heating and cooling simulations and when using the maximum heating and cooling power from a one year simulation. For most zones apart from the laundry room, the fan coils could be significantly undersized without affecting the thermal environment. The fan coil sizing did not significantly impact the ship's annual energy consumption.

The ship's energy supply system, consisting of engines and boilers, was considered through post processing of the simulation data in MATLAB. Two different fuels were considered: marine gas oil (MGO) and liquefied natural gas (LNG). A hot water storage tank of size 150 m^3 was included in order to utilise all unused recovered heat from engines in the MGO case. The tank was also used to reduce the peak demand for boilers from 12.3 to 9.2 MW.

Several energy efficiency scenarios were investigated to find their effect on the energy consumption and peak energy demand. Of the solutions investigated, ventilation heat recovery, variable air volume (VAV) ventilation and an air-to-water heat pump gave the largest reductions in fuel consumption. On the MGO ship, the annual boiler fuel consumption was decreased by 30, 23 and 66%, respectively.

The economic profitability was investigated to find the solutions most likely to be suitable for implementation in a cruise ship. All solutions were found to be more profitable on the MGO ship than on the LNG ship, due to more heat being recovered from LNG engines and MGO being more expensive. Ventilation heat recovery was clearly profitable on both ships with a net present value (NPV) more than twice as large as the investment costs. An air-to-water heat pump was very profitable only on the MGO ship. Solutions with heating setback had smaller reductions in fuel consumption, but they are likely to be profitable due to low investment costs. VAV ventilation was not profitable enough to recommend.

In further work, the model could be used to investigate the effectiveness of other energy saving solutions. This could include heat pumps utilising low temperature water on board as a heat source, steam producing heat pumps, and a combination of heat pumps and thermal energy storage.

Sammendrag

Energisystemer på passasjerskip har tradisjonelt vært basert på fossile brensler, som bidrar til store CO_2-utslipp. Hovedfokuset har vært på å forbedre fremdriftssystemet på skip, mens fokus på å redusere energiforbruk i hotellsystemet har vært mangelfullt. Hotellsystemet på passasjerskip står for opptil 40 % av energiforbruket. For å effektivt redusere klimagassutslipp fra passasjerskip, er det derfor også viktig å ta hensyn til hotellsystemet.

Denne masteroppgaven er en del av prosjektet CruiZE (Cruising towards Zero Emissions), som er et samarbeid mellom SINTEF Energi, NTNU, Carnival Corporation & plc, samt norske leverandører av skipsutstyr og designløsninger. Det overordnede målet til CruiZE er å redusere energiforbruket til hotellsystemer på passasjerskip gjennom innovative designløsninger. Målet med masteroppgaven er å analysere energiforbruket på passasjerskip og mulige energisparingsløsninger, ved hjelp av bygningssimuleringsverktøyet IDA ICE.

Hotellsystemet til et cruiseskip ble modellert i IDA ICE, hovedsakelig basert på Color Lines skip Color Fantasy. Først ble viftekonvektorer med ubegrenset oppvarming og kjøling brukt i modellen. De første resultatene ble sammenlignet med energiforbruk på referanseskipene MS Birka Stockholm og et stort cruiseskip. Modellen ble deretter kalibrert ved å øke energiforbruket til tappevann og redusere ventilasjonsmengden i store kjøkken. Dette ga et totalt årlig energiforbruk på 19,2 MWh/passasjer for skipets hotellsystem. Energibehovet for fremdrift ble funnet å være 0,156 kWh/ALB-km. ALB (available lower berth) er tilgjengelige underkøyer, satt til to per lugar.

Etter kalibrering ble det utført en analyse av forskjellige måter å dimensjonere viftekonvektorer. Det resulterende termiske miljøet var omtrent likt ved bruk av design værdata i varme- og kjølesimuleringer og ved bruk av maksimal varme- og kjøleeffekt fra en årssimulering. For de fleste soner bortsett fra vaskerommet, kan viftekonvektorene være betydelig underdimensjonert uten å påvirke det termiske miljøet. Dimensjonering av viftekonvektorene påvirket ikke skipets årlige energiforbruk i vesentlig grad.

Skipets energiforsyningssystem, bestående av motorer og kjeler, ble tatt hensyn til gjennom etterbehandling av simuleringsdataene i MATLAB. To forskjellige brensler ble vurdert: marin gassolje (MGO) og flytende naturgass (LNG). En varmtvannstank på 150 m^3 ble inkludert for å utnytte all ubrukt gjenvunnet varme fra motorer i MGO-skipet. Tanken ble også brukt til å redusere maksbehovet for kjeler fra 12,3 til 9,2 MW.

Flere energisparingsscenarier ble undersøkt for å finne deres effekt på energiforbruket og maks. energibehov. Av de undersøkte løsningene ga varmegjenvinning i ventilasjonen, VAV (variable air volume) ventilasjon og en luft-til-vann-varmepumpe de største reduksjonene i brenselforbruk. På MGO-skipet ble kjelenes årlige brenselforbruk redusert med henholdsvis 30, 23 og 66 %.

Den økonomiske lønnsomheten ble undersøkt for å finne løsningene som mest sannsynlig vil være egnet for implementering i et cruiseskip. Alle løsningene var mer lønnsomme på MGO-skipet enn på LNG-skipet, på grunn av at mer varme blir gjenvunnet fra LNG-motorer og at MGO er dyrere. Varmegjenvinning i ventilasjonen var tydelig lønnsomt på begge skip med en nåverdi over dobbelt så høy som investeringskostnadene. En luft-til-vann-varmepumpe var veldig lønnsom bare på MGO-skipet. Løsninger med periodevis redusert oppvarming hadde mindre reduksjoner i brenselforbruk, men de vil sannsynligvis være lønnsomme på grunn av lave investeringskostnader. VAV-ventilasjon var ikke lønnsomt nok til å anbefale.

I videre arbeid kan modellen brukes til å undersøke effektiviteten til andre energisparingsløsninger. Dette kan inkludere varmepumper som bruker lavtemperatur vann om bord som varmekilde, dampproduserende varmepumper, og en kombinasjon av varmepumper og termisk energilagring.

Project Description

Background and objective

Cruise or passenger ships are an energy-intensive ship sector where the energy use for the so-called "hotel system" on board (heating, air conditioning, cooling, appliances, etc.) accounts for an average of 40% of the ship's total energy use. Traditionally, ship energy needs are covered by burning fossil fuels, which leads to a high carbon footprint per passenger as well as emissions of substances that are harmful both to the environment and to human health. Developments towards "greener" passenger ships have largely shed light on alternative fuels and propulsion systems. However, in order to achieve "zero emissions", it is also important to reduce the energy use of the hotel systems. The project assignment is part of the innovation project CruiZE (Cruising towards Zero Emissions), which is a collaboration between SINTEF Energy Research, NTNU, the world's largest cruise line operator, Carnival Corporation & plc, as well as Norwegian suppliers of equipment and design solutions for cruise ships. The overall ambition of the CruiZE project is to help reduce the total energy use of hotels on board passenger ships and analyse the possibility of an energy efficient operation.

The aim of the master's thesis is to analyse energy use and energy efficiency possibilities for passenger ships by using a building simulation tool. Through a literature study, the student will familiarise with the problem of heating, ventilation, and cooling needs on passenger ships. Furthermore, the student will collect data on energy use for hotel systems on board passenger vessels. The IDA ICE model developed in the preceding project work will be further developed based on collected data on passenger ships. The student will analyse energy use in different usage patterns for passenger ships. Based on the energy use, the student will look further at the possibility for energy efficiency. As one of the assignment outputs, the student will develop background for energy efficient and suitable design and operation of the ship's hotel system.

The following tasks are to be considered:

1. Literature study on energy and fuel use in passenger ships considering total annual, monthly, and daily energy use. Performance indicators for passenger ship operation should be considered. The study should specifically include heating, cooling and ventilation systems on ships.
2. Based on the literature study and information available from the project partners, organise necessary data relevant for a hotel system on passenger ships. These should include information about heating, ventilation and cooling systems. Further, information about the operation of the ship's HVAC systems should also be organised, as well as information about internal heat gains.
3. Collect and develop relevant weather data. If necessary for the purpose of the project, develop own weather files that may be used as input.
4. Develop energy efficiency scenarios that are relevant for passenger ships. The scenarios should be discussed with the project partners.
5. Further develop the model for the ship's hotel system in IDA ICE based on points 1 and 2.
6. Calibrate the IDA ICE model based on the literature study or data available from the project partners.
7. Consider the integration of the hotel system with the ship's propulsion and energy supply systems. A hot water tank for energy storage could also be considered.
8. Perform energy efficiency analyses for the suggested scenarios. Evaluate the economic profitability of the energy saving solutions, as well as their effect on greenhouse gas emissions.

Contents

Nomenclature

Terms	
Bulkhead	Vertical wall in a ship, separating rooms or compartments
Deck	Horizontal structure separating levels of the ship, or the level itself
Galley	Kitchen in a ship
HVAC auxiliary	Fans and pumps in the HVAC systems
Roll on/off	Vehicles driving onto/off the ship
Superstructure	The part of the ship that extends above the main deck

Abbreviations	
AHU	Air handling unit
ALB	Available lower berth
BC	Base case
CAV	Constant air volume
CO_2e	CO_2 equivalent
COP	Coefficient of performance
DCV	Demand-controlled ventilation
DHW	Domestic hot water
ECA	Emission control area
ESBO	Early Stage Building Optimization
GHG	Greenhouse gas
HFO	Heavy fuel oil
HVAC	Heating, ventilation, and air conditioning
IWEC	International weather for energy calculation
LBG	Liquefied biogas
LNG	Liquefied natural gas
MDO	Marine diesel oil
MGO	Marine gas oil
MPI	Maximum permissible investment
NPV	Net present value
PCM	Phase change material
PV	Photovoltaic
TTP	Tank-to-propeller
VAV	Variable air volume
ws	Water surface
WTP	Well-to-propeller

Units	
kn	knots
met	metabolism, 1 met = 58 W/m^2 body surface [1]
MMBTU	1 million BTUs (British thermal units)

Symbols		**Unit**
η	efficiency	-
ρ	density	kg/m^3
a	annuity factor	-
B	net annual savings	NOK
C	costs	NOK
c_p	specific heat capacity	J/(kg K)
dt	time step length	h
E	energy	Wh or J
i	time step	-
I_0	additional investment cost	NOK
n	economic lifetime	years
P	power	W
Q	heat	J
r	real interest rate	-
S	residual value	NOK
T	temperature	°C
V	volume	m^3
v	speed	kn
x	load factor	-

Subscripts	
boil	boiler
cap	installed capacity
charge	charging of tank
discharge	discharging of tank
el	electrical
eng	engine
M	maintenance
max	maximum
O	operation
prop	propulsion
rec	recovered
tank	hot water storage tank
th	thermal

List of Figures

List of Tables

1 Introduction

1.1 Background

Traditional energy systems on passenger ships are based on fossil fuels, which contribute to large CO_2 emissions. There has been a large focus on improving the propulsion system on ships, for example by using hybrid solutions combining batteries with liquefied natural gas (LNG) or hydrogen. However, a focus on reducing the energy use in the hotel system on ships has been lacking. The hotel system on a passenger ship accounts for up to 40% of the energy consumption. To efficiently reduce greenhouse gas (GHG) emissions from passenger ships, it is therefore important to also consider the hotel system and find ways to integrate these systems in an optimal way, making use of any waste energy from the propulsion and auxiliary systems [2].

This report is a part of the project CruiZE (Cruising towards Zero Emissions), which is a collaboration between SINTEF Energy Research, NTNU, Carnival Corporation & plc, as well as Norwegian suppliers of ship equipment and design solutions. The long-term aim of the project is to achieve an average reduction of 10-20% in the ships' total energy use, facilitate zero emissions in ports and minimise emissions at sea. This is to be achieved through innovative design solutions [2].

1.2 Objective

The aim of this master's thesis is to analyse the energy use on passenger ships using a building simulation tool. This includes the hotel system on passenger ships and its integration with the propulsion and energy supply systems. By investigating several energy efficiency scenarios and their economic profitability, the goal is to find the solutions most likely to be suitable for implementation in a cruise ship.

1.3 Structure of the Thesis

Chapter 2 consists of a literature study, which describes relevant reference ships, ship construction and technical installations on passenger ships, as well as various energy saving solutions. This is followed by chapter 3, which presents the methods used in the study. In chapter 4, energy use data from reference ships and weather data are analysed. Chapter 5 describes how the ship was modelled in IDA ICE based on the literature study. It also describes post processing of the energy supply system done in MATLAB. This is followed by chapters 6 and 7, which present results for the different scenarios and discussion of these results. Lastly, there is a conclusion and presentation of possible further work.

1.4 Limitations

When modelling the ship, limited data were available for ship construction and technical installations on specific ships. The modelling was therefore based on several reference ships and the information available. Several assumptions, estimations and simplifications were made in the modelling.

The energy use data were also limited. In the reference ships used, there was limited knowledge about energy use for specific users and how much of the total energy was consumed by the ship's hotel system. There are uncertainties related to the interpretation of the energy use data, especially in regard to energy use for specific users.

Due to limitations of IDA ICE, the integration of the hotel system with the energy supply system was done through post processing in MATLAB. The interaction between the systems and the utilisation of recovered heat from the engines were therefore simplified.

The thesis focuses mainly on the energy consumption on the ship in different scenarios. In addition, there is some discussion of thermal environment and comfort. Daylight factors have not been considered. The effect of fan coil sizes and energy saving solutions on the ship's weight was not taken into account, as it was considered to be outside the scope of this thesis.

The economic profitability of the energy saving solutions was calculated based on implementation in an existing ship. Some discussion of what the profitability could be in a new ship was included. There were challenges related to finding specific installation and investment costs for some energy saving solutions. Prices were estimated and further considered in the analysis and discussion of the results.

2 Literature Study

2.1 Reference Ships

Color Fantasy and Color Magic

Color Line's sister ships Color Fantasy and Color Magic are the world's largest cruise ships with a car deck [3]. This is also known as a ro-ro passenger ship. The two ships sail between Oslo and Kiel throughout the whole year. One ship leaves the port in Oslo at 14:00 and arrives in Kiel at 10:00 the next day. The other ship will travel in the opposite direction [4]. Thus, the ships follow a regular cycle with 20 hours of travel and 4 hours in port. One full round trip lasts 48 hours, including the port stays.

Table 1 contains key information about the two ships. The engines have the same installed capacity and service speed. The ships also have the same size, but there are some differences in how much space there is for people and cars. Color Fantasy has fewer cabins and a lower guest capacity, but can fit more cars than Color Magic. They both have 1270 lanemetres for trailers [3, 5]. Color Fantasy has two trailer decks and three car decks, distributed across decks 2-5 [6].

Table 1: Key information about Color Fantasy and Color Magic [3, 5].

	Color Fantasy	**Color Magic**
Launched	2004	2007
Passenger capacity	2400	2600
Maximum capacity	2605	2812
Guest cabins	966	1016
Car capacity	750	550
Trailer lanemetres [m]	1270	1270
Length [m]	224	224
Width [m]	35	35
Number of decks	15	15
Service speed [kn]	22	22
Engine capacity [MW]	31.6	31.6

Both Color Fantasy and Color Magic offer different types of cabins, ranging from 3 to 5 stars. Some cabins have view to the ocean or the ships' promenades, while other cabins are internal with no windows. The maximum number of people that can stay in a cabin ranges from 2 to 5 people. All the cabins have a minibar [7].

The ships have 250 crew members, and there are 248 crew cabins located on deck 5. In addition, there are officers' quarters located behind the navigation bridge on deck 12 [6].

The public areas on the ships include several restaurants and shops, as well as a casino, a show lounge, a spa and fitness centre and an Aqualand. On deck 12, there is a conference centre with an auditorium and several meeting rooms. There is also a break and reception area [8].

Color Fantasy and Color Magic receive shore power in port both in Oslo and in Kiel. This means that the engines do not have to keep running to produce electricity to cover onboard electricity demand [9, 10].

Other Reference Ships

Table 2 shows key information for the ships MS Birka Stockholm and a large cruise ship, as well as TUI Cruises' ships Mein Schiff 3, 4 and 5.

Table 2: Key information about Birka Stockholm, the large cruise ship, and Mein Schiff 3, 4 and 5 [11, 12, 13, 14].

	Birka Stockholm	**Large cruise ship**	**Mein Schiff 3 and 4**	**Mein Schiff 5**
Launched	2004	-	2014 / 2015	2016
Passenger capacity	1800	5230	2506	2534
Guest cabins	900	2627	1253	1267
Length [m]	176.9	337	293.2	293.2
Width [m]	28.6	42	35.8	35.8

MS Birka Stockholm operates between Stockholm and Mariehamn, and it makes one round-trip every day of the year. The ship spends 33% of the time stopped in port or sea stays. This ship is smaller than Color Fantasy and Color Magic, both in terms of physical size and in number of passengers. Birka Stockholm has an energy supply system based on engines and auxiliary boilers using marine diesel oil (MDO) as fuel. There are four main engines covering the mechanical propulsion demand and four auxiliary engines covering the electricity demand on board [15]. Birka Stockholm does not receive shore power in port [16]. The ship does not have vehicle decks [12].

The large cruise ship operates in the Mediterranean Sea from May to October, and in the Caribbean Sea from November to April. In both cases, it travels between multiple ports on a regular schedule every week. The ship has long port stays, spending more than half of the time in port. This ship is significantly larger than Color Fantasy and Color Magic, in physical size and number of passengers. The total floor area of the ship is 180,854 m^2. This reference ship has LNG engines and gas boilers, and therefore runs entirely on LNG [13].

All the Mein Schiff ships have the same length and width [14], which can be seen in the table. They are longer than Color Fantasy and Color Magic, but very similar in width. The number of guest cabins is higher than in Color Fantasy and Color Magic.

2.2 Ship Construction

The main construction of a cruise ship is a structure with steel decks and bulkheads. When designing the ship construction, fire integrity is one of the most important factors to consider. A fire spreading on a ship can have disastrous consequences because passengers will have nowhere to escape. Each deck on the ship is therefore separated into fire zones with fire insulation between. These zones can be a maximum of 48 m long [17].

Another crucial factor is the weight of the ship. It is important to minimise the ship's weight to ensure stability and to reduce the energy required for propulsion. Lightweight materials should therefore be used, and this is especially important in the upper decks. Up to and including deck 9, the ship's superstructure will normally be made of steel. If weight reduction is required for stability, decks 10 and above will be made of aluminium. Seeing as aluminium does not provide fire integrity like steel does, additional fire insulation is needed when using this solution [17, 18].

To ensure a stable ship with a low enough weight, the distance between decks should be minimised. However, a certain ceiling height is needed to provide a comfortable environment for passengers and ship crew. Normally, cabins have a height of 2100 mm. In places with limited space this can be reduced to 2030 mm, which is the minimum requirement according to the Maritime Labour Convention. Public areas have a minimum height of 2300 mm [17, 19].

The cabin construction is based on a sandwich structure, using two steel or aluminium plates with insulation in between. The steel or aluminium plates have a thickness of 4 mm. Sound insulation is used between zones, in addition to fire insulation being used where needed. The external constructions

on the ship have comfort insulation to reduce heat losses. This is typically 150 mm insulation, similar to the standard mineral wool used in buildings [17].

In addition to the sandwich structure, the walls between cabins have wall panelling on each side. An example of such wall panelling is 25 mm thick tinplate steel cladding, which also provides fire resistance. Other walls in the cabin also have wall panelling, and the wall facing the corridor often has thicker panelling on the cabin side. On the corridor side, there is sometimes no panelling on top of the steel or aluminium. The external wall of the ship also has no such panelling [17].

The floor and ceiling of the cabin are based on the same sandwich structure as the walls. Spot levelling is used on the floor to give a surface that is as level as possible without increasing the weight of the ship an unnecessary amount. Cabin floors are usually covered with wool carpets, which means that it is acceptable for the floor not to be completely even. For decks separating two cabins, a limited amount of insulation is needed because the two zones have similar temperatures. If the zone below or above a cabin has a different temperature, more insulation is needed [17].

The construction materials used in public areas are similar to the cabins, with the same superstructure and insulation. The wall panels in public areas are usually not fire resistant, but they are non-combustible. This means that only the steel structure and fire insulation provide fire resistance in these areas. The type of wall and ceiling panels depends on the architect's choices. One example of wall panelling is honeycomb aluminium panels [17].

The windows in the cabins consist of a steel or aluminium frame welded into the ship's structure. Around the windowpanes, only steel or aluminium separates the inside from the outside. This creates significant thermal bridges in the construction. For windows in public areas, the glass panes are often glued directly to the steel or aluminium structure. The gap between the panes is typically 20 mm with a sealant used between. This construction has smaller thermal bridges than the windows used in cabins [17].

Doorways for external doors are welded to the construction or bolted and sealed with a sealant [17]. The way the windows and doors are attached to the ship's structure means that the construction is approximately airtight [18].

Shading is used in the ship to reduce unwanted solar radiation. Curtains are often used, both in cabins and in public areas [7, 8]. Internal roller sunshades can also be used, and this is most common in public areas. Another option is treated window glass [17].

2.3 Fire Safety

In case of a fire, decks and bulkheads should be insulated so that the average and maximum temperature on the unexposed side does not rise more than 140 °C and 180 °C, respectively, in a time frame given by the class. One example of a class is A-60, meaning that the temperature should not rise more than 140 °C or 180 °C in 60 minutes [20].

Bulkheads and decks in accommodation spaces must be at least class B-15, which is considered equivalent to A-0. Bulkheads and decks separating accommodation spaces from cargo rooms and machinery spaces should be at least class A-60 [21].

2.4 Ventilation

It is important to avoid the possible spread of fire and smoke throughout the ship. Each fire zone in the ship therefore has its own ventilation system [14]. In addition, solar radiation can cause large temperature differences between the sides of the ship, which leads to differences in heating and cooling

demand. Several air handling units (AHUs) are therefore used in each fire zone. This way, ventilation and temperature control are split between the sides of the ship, and sometimes the middle [17].

Different types of accommodation spaces are usually served by separate AHUs. These types of zones could for example be cabins or restaurants. As an example, Mein Schiff 3, 4 and 5 each have 50 different AHUs on board, with 15 of these serving cabins [14]. In the AHUs, the air is preheated or precooled to achieve the desired supply air temperature. In accommodation spaces, the supply temperature is often set to 18 °C [17].

The most common ventilation strategies in buildings are mixing ventilation and displacement ventilation. In mixing ventilation, air is supplied near the ceiling with high velocity. To ensure proper mixing, the supply air temperature should be lower than the temperature in the room. It can often be quite low without causing draught problems. It is also possible to have a supply air temperature higher than the room air temperature, but then it is important that the air is supplied with a large momentum to provide sufficient mixing. Mixing ventilation is the most common ventilation method in Norway, but it can be challenging in areas with high ceilings [1].

In displacement ventilation, air is supplied close to the floor and extracted near the ceiling. The supply air temperature must be lower than the average room air temperature, to ensure that the supplied air spreads throughout the room before rising. The supply air temperature is typically 2-6 °C lower than the average temperature in the room. Displacement ventilation is well suited in areas with high ceilings [1, 22].

In a standard cabin, there is no recirculation of air, which means that only fresh outdoor air is supplied to the room. To achieve the best possible indoor environment in the cabin, air is supplied to the sleeping room and extracted from the bathroom and corridor. Air flows between the zones through grilles placed right above the floor [17].

In public areas on ships, rainfall ventilation may be used to improve the distribution of air. This means that zones are split into supply and extract. The air is distributed above the ceiling panels and enters the zone through gaps or holes in the panels. Doors between different public areas can be closed for fire safety, but they are usually open. This means that the temperature difference is small between different areas [17].

DNV specifies requirements for the living and working conditions on a passenger ship. The requirements are separated into three comfort classes with comfort rating number (crn) from 1 to 3. Passenger ships should have crn = 1 [17]. For this comfort rating number, the minimum supply of fresh air is 36.0 m^3/h per person. This applies for all accommodation spaces in passenger ships, except hospitals and ward rooms [23].

According to NS-EN ISO 7547, the exhaust airflow rate in laundries on cruise ships should be at least 15 h^{-1}. In public bathrooms, it should be the highest of 15 h^{-1} and 0.3 m^3/s [24]. The ventilation rate in galleys varies depending on the size of the galley. For smaller galleys, it is around 30 h^{-1}, while large galleys can have ventilation rates above 90 h^{-1} [25].

For swimming pools, recirculation of air is typically used. The minimum requirement for fresh air supply is the highest of 1.4 l/s per m^2 total ground area and 2.8 l/s per m^2 water surface (ws) [26].

On passenger ships with more than 36 passengers, a closed vehicle deck should have an exhaust airflow rate of at least 10 h^{-1}. The ventilation rate must be increased to at least 20 h^{-1} when vehicles are driving on or off [27]. Vehicle decks usually have balanced ventilation provided by large fans. They could also have only supply of fresh air, with natural exhaust. There is typically no ventilation heating on the vehicle decks [28].

2.5 Ventilation Heat Recovery

On modern cruise ships, most AHUs have heat recovery. When there is a heating demand, the heat recovery unit transfers energy from the exhaust air to the supply air, heating the supply air. The reverse process takes place when there is a cooling demand. AHUs in galleys typically do not have heat recovery. Due to pollutants from cooking equipment, the exhaust air from galleys is released directly to the outdoor air [1, 29].

Rotary wheel heat exchangers and plate heat exchangers commonly have an efficiency around 80% [30]. For example, Systemair has compact AHUs with rotary wheel heat exchangers and a heat recovery efficiency of 80%. The largest AHUs have a capacity of 5250 m^3/h, for both supply and extract [31].

2.6 Variable Air Volume Ventilation

Traditionally, constant air volume (CAV) ventilation has been used in passenger ships. This is also the case in Mein Schiff 3, where alternatives have not yet been implemented due to their large investment costs [14]. However, alternatives to CAV have started being implemented in some cruise ships to reduce the energy use. During the low season, guests might be placed in cabins in one area of the ship, so that the ventilation rate and temperature can be reduced in other areas [18].

It is also possible to use motion detectors to control the temperature and ventilation rate in each cabin based on presence. This is an example of occupant-controlled ventilation, which is a type of variable air volume (VAV) ventilation. This can however cause discomfort for occupants, as the temperature can be too low or too high when they enter the room [1, 18].

Another type of VAV ventilation is demand-controlled ventilation (DCV), where the airflow rate, heating and cooling are adjusted based on real-time measurements done in the zone. Room states that are typically used include air temperature, CO_2 concentration and humidity. The measurements are compared to the setpoints, and the ventilation rate is adjusted between the predefined minimum and maximum rates. For unoccupied rooms, the minimum airflow rate should be 0.7 $m^3/(h\ m^2)$ due to emissions from materials and furniture, assuming low emitting materials [1].

Sensors in the system can be motion sensors, CO_2 sensors or temperature sensors, depending on the ventilation strategy. The sensors should be placed in a representative part of the room, away from open doors and other processes that may significantly affect the measured room states. When using CO_2 as a measured state, another CO_2 sensor should be placed in the supply air duct after the AHU. This makes it possible to control the airflow rate based on the difference in CO_2 concentration between indoor and outdoor air. The maximum CO_2 level in a room is typically set to 1000 ppm [1]. Without maintenance and calibration, CO_2 sensors should have a minimum lifetime of 15 years [32].

For rooms with airflow rates below 100 m^3/h, it is recommended to use CAV or occupant-controlled ventilation. This is because the possible energy savings from using DCV are smaller for rooms with a low airflow rate. In rooms with airflow rates above 500 m^3/h, it could be beneficial to use DCV with combined temperature and CO_2 control. For airflow rates between 100 and 500 m^3/h, it is recommended to use occupant-controlled ventilation, temperature controlled DCV, or a combination of these [1].

Compared to a CAV system, VAV systems require additional VAV controllers, silencers and sensors. The approximate prices for these components are shown in table 3. Annual maintenance costs are around 3 NOK/m^2 floor area for CAV and 5 NOK/m^2 for DCV [33].

Table 3: Approximate prices for VAV components [33].

	Price [NOK]
VAV controller	5400
Silencer	1300
CO_2 and temperature sensor	11,800
Motion sensor	1000

2.7 Swimming Pools

In Norway, the total annual energy consumption for swimming facilities is on average around 4000 kWh/m^2 ws. However, it can vary significantly between different pool facilities. It can be between 1000 and 11,000 kWh/m^2 ws [34].

2.8 Space Heating and Cooling

In Mein Schiff 3, 4 and 5, fan coil units are used to provide additional heating or cooling in both cabins and in public areas. When the temperature is outside the desired temperature range, the fan coil unit turns on and starts sucking air from the zone. The fan coil unit heats or cools the air to reach the temperature setpoint. In these particular ships, the fan coil units have electric heating and waterborne cooling [14]. The fan coil units used in cabins have electric power below 1 kW, while fan coils in public areas are up to 10 kW [35]. Alternative methods for space heating include electric heaters and water heaters placed in the room [17].

There is no space cooling on vehicle decks. There can be heating on the vehicle decks in the winter, using a waterborne heating system or electric heaters [28].

2.9 Energy Supply System

The energy supply system on a cruise ship is usually based on the use of diesel engines. The engines generate electricity for the propulsion system and for the hotel system. Heat from the engines is utilised through the production of steam and high temperature water. Steam is often used to cover high temperature heat demands in galleys and laundry, and to heat the engines and the fuel. The steam and high temperature water are also used to cover heat demands for ventilation and space heating, domestic hot water (DHW) and swimming pools. Oil boilers are used for additional heating or for heating when the ship is in port. All the energy used in such a system therefore comes from fossil fuels [36].

2.10 Fuels

The most common fuels for cruise ships are based on heavy fuel oil (HFO) and marine gas oil (MGO). HFO is almost pure residual oil, which is the heavier fractions of petroleum. MGO is made from pure distillates, the lighter fractions of petroleum. Medium fuel oil (MFO), intermediate fuel oil (IFO) and marine diesel oil (MDO) are combinations of these with increasing amounts of MGO [37].

From 2020, the maximum sulphur content in fuels was reduced to 0.5%. In emission control areas (ECAs), there is a stricter limit of 0.1%. The Baltic and North Seas are included in the ECAs. These strict requirements favour MGO and other lighter fuel oils [38].

As a more environmentally friendly alternative to fuel oils, LNG can also be used on cruise ships. As the desire to reduce GHG emissions increases, fuels with even lower CO_2 emissions become relevant and necessary. These alternative fuels include biofuels, methanol, hydrogen and ammonia. Batteries can

also be used as a part of the propulsion system on a ship and improve the overall efficiency. However, with today's technology, batteries cannot fully substitute combustion engines on longer ship journeys [39].

When considering alternative fuels for cruise ships, it is important to consider the fuel prices. Over the past 5 years, the average price for MGO was 12.9 USD/MMBTU or 0.378 NOK/kWh. For natural gas in the EU, the price was 5.50 USD/MMBTU or 0.161 NOK/kWh. These prices do not include supply costs for MGO and distribution costs for LNG [40]. Liquefied biogas (LBG) is liquefied methane produced from biomass, and it is therefore equivalent to LNG. The average price of biofuels in general is 86% higher than the price of LNG, though it depends on the type of fuel. Biofuels cannot compete with the price of fuels used today, but it could become a possibility in the future. Overall, fuel prices can vary significantly and are often not predictable [39].

GHG emissions are measured in CO_2 equivalents (CO_2e). GHG emissions from cruise ship are mainly in the form of CO_2, and they depend on the type of fuel used. For MGO, the total GHG emissions are very similar to the CO_2 emissions. However, for LNG engines, some unburned methane can be released. As methane has a high global warming potential (GWP), this can significantly increase the CO_2 equivalent for LNG. The amount of methane released varies with the type of engine [39].

MGO has total well-to-propeller (WTP) GHG emissions of 314 gCO_2e/kWh, while LNG has emissions of 289 gCO_2e/kWh. WTP includes both direct and indirect emissions in production and use of the fuel. For fossil fuels, the tank-to-propeller (TTP) emissions make up the majority of the emissions, as CO_2 is released during combustion [39].

Seeing as biomass is considered carbon neutral, LBG has no TTP emissions. LBG therefore has relatively low CO_2 emissions around 72 gCO_2/kWh. Today, most hydrogen is produced from methane and therefore has higher CO_2 emissions than MGO. However, if produced from water using renewable energy, the emissions can be around 7 gCO_2/kWh [39].

2.11 Propulsion

A ship's required propulsion power depends on the ship speed in the moment. With a linearly increasing ship speed, the propulsion power increases exponentially. The relation between required propulsion power, installed engine capacity and their corresponding ship speeds is shown in equation 1 [41].

$$P_{prop} = P_{prop,cap}\left(\frac{v}{v_{max}}\right)^k \tag{1}$$

where P_{prop} [W] is the required propulsion power at speed v [kn], $P_{prop,cap}$ [W] is the installed capacity of the engines, and v_{max} [kn] is the maximum speed at installed capacity. For a theoretical ship, the exponent k would be 3. However, a real ship will move slightly up and down in addition to the horizontal movement. With increasing horizontal speed, the vertical movement will increase due to larger waves. The exponent should therefore be above 3, and will be somewhere between 3 and 4 [41].

2.12 Performance Indicators

When comparing the performance of different cruise ships, the energy consumption is often given per m^2, per cabin or per passenger. Another option is energy use per available lower berth (ALB). It is common to assume two passengers, and thus two ALBs, per cabin. To account for cruise ships with different routes and operational profiles, the energy use can also be given per km travelled. A combination of these would be to use the unit ALB-km, giving the energy consumption per ALB and km travelled [42].

2.13 Thermal Energy Storage

Hot water storage tanks

Thermal energy can be stored in many different ways and in different media, one of which is water. The sensible heat stored in water can be expressed using equation 2 [43].

$$Q_{sensible} = \rho \; V \; c_p \; \Delta T \tag{2}$$

where $Q_{sensible}$ is the heat [J], ρ [kg/m^3] is the density of water, V [m^3] is the water volume, c_p [J/(kg K)] is the specific heat capacity of water, and ΔT [K] is the change in water temperature.

On cruise ships, water tanks are usually used to store freshwater produced on board that will be used for DHW. These tanks therefore have temperature requirements similar to DHW tanks in buildings, in order to avoid legionella [44]. The amount of legionella will generally increase when the temperature is below 46 °C and decrease at higher temperatures [45].

Some examples of installed thermal energy storage in ships include the cruiseferry Color Hybrid, which has a hot water tank of size 340 m^3. The temperature variation in this tank is 15 °C. The cruiseferry Viking Grace has two storage tanks with a total volume of 88 m^3 [42].

In a previous report, a hot water storage tank was sized to deliver all necessary DHW to a large cruise ship with a total capacity of 5000 people. With storage temperatures of 60 and 85 °C, the required tank size was found to be 143 and 61 m^3, respectively. The necessary power for the heat exchanger heating the tank was 4.30 and 5.58 MW, respectively [46].

Phase change materials

In addition to heat storage using sensible heat, latent heat can also be used in thermal energy storage. Phase change materials (PCMs) are materials that store latent heat through phase changes. During a phase change, the temperature of the material is close to constant. Many different materials can be used as PCMs depending on the application and necessary phase change temperature. For heat storage in buildings, paraffins are commonly used [47].

It is common for PCMs to have thermal hysteresis, which means that the melting temperature and the solidification temperature are different. The specific heat capacity of the material is high during the phase changes around the melting and solidification temperatures, and lower and constant otherwise. The specific heat capacity is the derivative of the enthalpy with respect to the temperature [48].

PCMs can be used in storage tanks, typically requiring a lower volume than a hot water tank to store the same amount of heat. Heat losses from the tank will also be smaller due to relatively low temperatures in the tank. Commonly for both sensible and latent thermal energy storage, they can be used in peak shaving by storing heat during low demand and releasing heat during higher demand. They can also be used to store waste heat until there is a heating demand [47].

Another application is PCM layers in walls, ceilings and roofs. In cold climates with dominating heating demands, the main benefit is a potential reduction of the heating demand. It can also improve thermal comfort by evening out the indoor temperature. From a profitability perspective, it is best to place the PCM only in the inner part of external walls. For application in flat roofs in Istanbul, it has been found most suitable to use a PCM thickness of 2 cm [49]. To reduce the heating demand, it is beneficial to use a PCM with a melting point close to the heating setpoint. Similarly, to reduce the cooling demand, the melting point should be close to the cooling setpoint [50].

2.14 Heat Pumps

Heat pumps work by extracting heat from a heat source and delivering it to the heating system. The heat pump requires a relatively small amount of electrical energy to run, which means that it delivers more heat to the zone than the electricity it uses. The ratio between the heat delivered and the electrical power needed is called the coefficient of performance (COP). Common heat sources for heat pumps include outdoor air, bedrock, soil and sea water. To use sea water as the heat source, the sea water inlet should be at least 20 m below the water surface [51]. Large air-to-air heat pumps usually have a COP between 2 and 4 [52]. Heat pumps are not commonly used on cruise ships today [16].

It is important not to oversize heat pumps because this leads to very high investment costs, and the COP can be lower at part load operation. In order to avoid oversizing heat pumps, they should always be dimensioned based on the net thermal power demand and the net annual energy demand. The net thermal power demand is the heating demand at design outdoor temperature (DOT) when internal heat gains and solar radiation are included. Similarly, the net annual energy demand is the annual energy demand with all heat gains included [53].

The ratio between the heat pump's heating capacity and the net thermal power demand is called the power coverage factor. For buildings, it is typically between 40 and 70%. The ratio between the annual delivered heat from the heat pump and the net annual energy demand is the energy coverage factor, which is usually 70 to 95%. The remaining heating demand will be covered by a peak load system, for example a fuel boiler or electric boiler [53].

The specific investment cost for heat pumps, i.e. cost per kW, tends to decrease with the size of the heat pump. This means that large heat pump systems are more likely to be profitable. Small heat pumps usually have an economic lifetime of 10-15 years, while larger heat pumps have a lifetime of 20-25 years. Air-source heat pumps typically have an economic lifetime of 10-15 years [54].

2.15 PV Panels

Photovoltaic (PV) panels have traditionally not been used on cruise ships, but some applications have been seen in the latest years. PV panels produce electricity that can cover electricity demands for both the hotel system and propulsion system on board. They can thus reduce the demand for electricity produced by the engines. To be applicable for use at sea, the PV panels must be resistant against corrosion from seawater. There must also be space available for installing the PV panels on deck or other external surfaces of the ship [55].

Including all necessary equipment, a PV panel system for ships is estimated to have installation costs of 2.8 to 3.4 USD/W. Due to technological advancements, this price is expected to drop in the future [55]. PV panels generally have negligible maintenance costs throughout their lifetime [56].

SunPower delivers 360 W PV panels with a copper foundation that are resistant to corrosion. The panels' dimensions are 1558 mm by 1046 mm, which gives a total area of 1.63 m^2. The efficiency of these panels is 22.2%, and they have a 25-year warranty [57].

2.16 Profitability Analysis

When evaluating the economic profitability of an energy saving solution, it is common to perform a profitability analysis. One example of such an analysis is calculating the net present value (NPV) for the measure. First the net annual savings must be calculated using equation 3. Then the NPV is calculated using equation 4. NPV expresses the absolute profitability of the investment. If the NPV is above zero, the solution is considered profitable. If the NPV is several times larger than the additional investment costs, it is very profitable [54].

$$B = \Delta C_O - \Delta C_M \tag{3}$$

where B [NOK] is the net annual savings, ΔC_O [NOK] is the reduction in operating costs and ΔC_M [NOK] is the increase in maintenance costs, for solutions where this is relevant.

$$NPV = \frac{B}{a} + S \cdot (1+r)^{-n} - I_0 \tag{4}$$

where a is the annuity factor, which is calculated using equation 5. S [NOK] is the residual value of the solution after its lifetime, r is the real interest rate, n [years] is the economic lifetime and I_0 [NOK] is the additional investment cost relative to alternative solutions. The economic lifetime is the time the measure is estimated to give annual savings. The economic lifetime is always shorter than the technical lifetime of the measure. The real interest rate is the bank interest adjusted for inflation, risk and profit [54].

$$a = \left(\frac{r}{1-(1+r)^{-n}} \right) \tag{5}$$

As a part of the profitability analysis, the pay-back time (PB) is often calculated, using equation 6. The pay-back time is a rough estimate of how long it takes to earn back the investment [54].

$$PB = \frac{I_0}{B} \tag{6}$$

A more accurate method is calculating the pay-off time (PO). This takes the real interest rate into account, as shown in equation 7 [54].

$$PO = \frac{ln\left[\left(1 - \left(\frac{I_0}{B}\right) \cdot r\right)^{-1}\right]}{ln(1+r)} \tag{7}$$

A sensitivity analysis can also be performed for the profitability. Such an analysis could include calculating the maximum permissible investment (MPI) for the solution, using equation 8. The MPI is the additional investment cost when the NPV is zero, assuming no residual value. Investment costs below the MPI would give a profitable solution [54].

$$MPI = \frac{B}{a} \tag{8}$$

3 Method

3.1 IDA ICE

IDA Indoor Climate and Energy (IDA ICE) is a simulation tool used to study the energy consumption for a building. The building model can consist of one or more zones, and the indoor climate of individual zones can also be evaluated. Predefined building components, heating and cooling units, and heat loads can be selected from a database and included in each zone. Weather data is usually supplied using weather files. Wind and temperature driven airflows can also be considered in the model [58].

The standard energy supply system consists of a boiler for heating and DHW, as well as a chiller for cooling. If an Early Stage Building Optimization (ESBO) plant is used, more complex energy supply solutions can be implemented, including heat storage, heat pumps and PV panels. The default AHU includes a heating coil, a cooling coil, and a heat recovery unit. The building can have one or more AHUs divided between the zones. The operation of the energy supply system and AHUs can be controlled through the user interface [58].

The IDA ICE extension "Ice rinks and pools" allows the implementation of swimming pools in the model. The heat and mass transfer between the pool surface and the zone is taken into account, as well as the heating of the pool water [59].

3.2 MATLAB

MATLAB is a computer program and programming language used for calculations, data analysis and graphical presentation of data. The script function makes it possible to construct a program where data can be imported and used in analysis and computations [60].

3.3 Modelling

IDA ICE was used to model the hotel system on a cruise ship, and an ESBO plant was used for the energy supply system. The "Ice rinks and pools" extension was used to model swimming pools. The model was mainly based on Color Line's cruise ship Color Fantasy. Information about the ship's cabins, restaurants and other public areas was found on colorline.no. A 3D model of Color Fantasy available from Color Line was also used [8]. The deck plan for the ship was used to provide additional information [61]. TUI Cruises' ships Mein Schiff 3, 4 and 5 were used as a reference when modelling the HVAC system. The modelling is described further in chapter 5.

3.4 Speeding up Simulation

In order to speed up computation when simulating an entire year, the solver's tolerance and maximal timestep were considered. According to EQUA's user manual for IDA ICE, the tolerance can often be increased from the default value 0.02 to 0.1-0.3. The maximal timestep can also be increased from the default 1.5 h [58].

Tests were done varying the tolerance and maximal timestep when simulating one month. It was found that the simulation time was shortest with a tolerance of 0.4, without significantly impacting the energy consumption. Increasing the maximal timestep gave no difference in simulation time or energy use. The tolerance was therefore set to 0.4 and the maximal timestep remained at 1.5 h, when doing simulations of one year. This change in tolerance can lead to a loss of accuracy in the computation. However, for quantities accumulated over one month, the loss of accuracy was found to be insignificant. When simulating a whole year, the relative deviation is likely to be even smaller.

For heating and cooling load simulations used when dimensioning HVAC components, it may not be appropriate to use a large tolerance and maximal timestep [58]. In this case, the tolerance was therefore set to 0.1.

3.5 Initial Model

At first, unlimited heating and cooling were used in the model. This means that the room units deliver as much heating and cooling needed to reach the temperature setpoint at any time. To enable connection between the heating and cooling units and the waterborne heating and cooling systems in the ESBO plant, fan coils with waterborne heating and cooling were used instead of ideal loads. The fan power was set to zero. The maximum power was increased so that the fan coils could always deliver the necessary heating or cooling. The vehicle decks only have heating, as there is no cooling in these zones. All efficiencies in IDA ICE were set to 1 to find the actual heating and cooling demands.

A custom weather file was made to represent the different weather conditions the ship passes through. This is further described in section 3.6. To mimic the wind conditions at sea, the wind profile in IDA ICE was set to Ocean and the pressure coefficients were set to "Exposed" according to the Air Infiltration and Ventilation Centre (AIVC).

It is not possible to rotate the ship in IDA ICE while a simulation is performed. The ship's varying orientation was therefore taken into consideration when the results were analysed. The ship is not always facing directly north or south, which can be seen in figure 1. However, as a simplification, the ship was assumed to be facing south on the way from Oslo to Kiel, and north from Kiel to Oslo. One simulation was performed for each of these situations, and the results were then combined so that the ship turns around every 24 hours when it docks in Oslo or Kiel.

3.6 Combined Weather File

To approximate the weather conditions the ship experiences between Oslo and Kiel, IWEC files for several locations on the route were combined into one file. IWEC files contain weather data for a location generalised over several years. The files include hourly values for air temperature, wind speed, relative humidity, solar irradiation and sky cover over a leap year, i.e. 8784 hours.

The chosen IWEC files are from onshore weather stations located close to the ship's route. Weather data for Kiel is not available in IDA ICE, and the coastal town of Eckernförde was used instead. The weather station is located in Holzdorf, which is close to the ocean and close to Kiel. For Oslo, both Gardermoen and Fornebu are available in IDA ICE. Fornebu was used because it is close to the ocean and likely to give more realistic weather conditions than Gardermoen, which is further inland.

When combining weather files, it is essential that the files contain the same information. Fornebu had two IWEC files available, one located near the ocean and another further inland in Hakadal. The one close to the ocean did not contain sky cover like the other IWEC files. The mean annual temperature for Hakadal is 6.8 °C, while it is 6.6 °C in the other Fornebu file. In addition, the temperature duration curves were similar for the two locations. It was therefore considered acceptable to use the Hakadal file for Fornebu.

To represent the area between Oslo and Kiel, another four weather files were used. These locations were chosen due to their proximity to the ship route, and to get an even distribution of locations on the journey. All locations used can be seen below, listed from north to south. Figure 1 shows the locations marked on a map. The approximate ship route was found from CruiseMapper [62] and is also marked on the map.

1. Oslo, Fornebu

2. Sandefjord, Tjøme
3. Fredrikshavn, Skagen
4. Fornæs (cape)
5. Odense, Beldringe
6. Eckernförde, Holzdorf

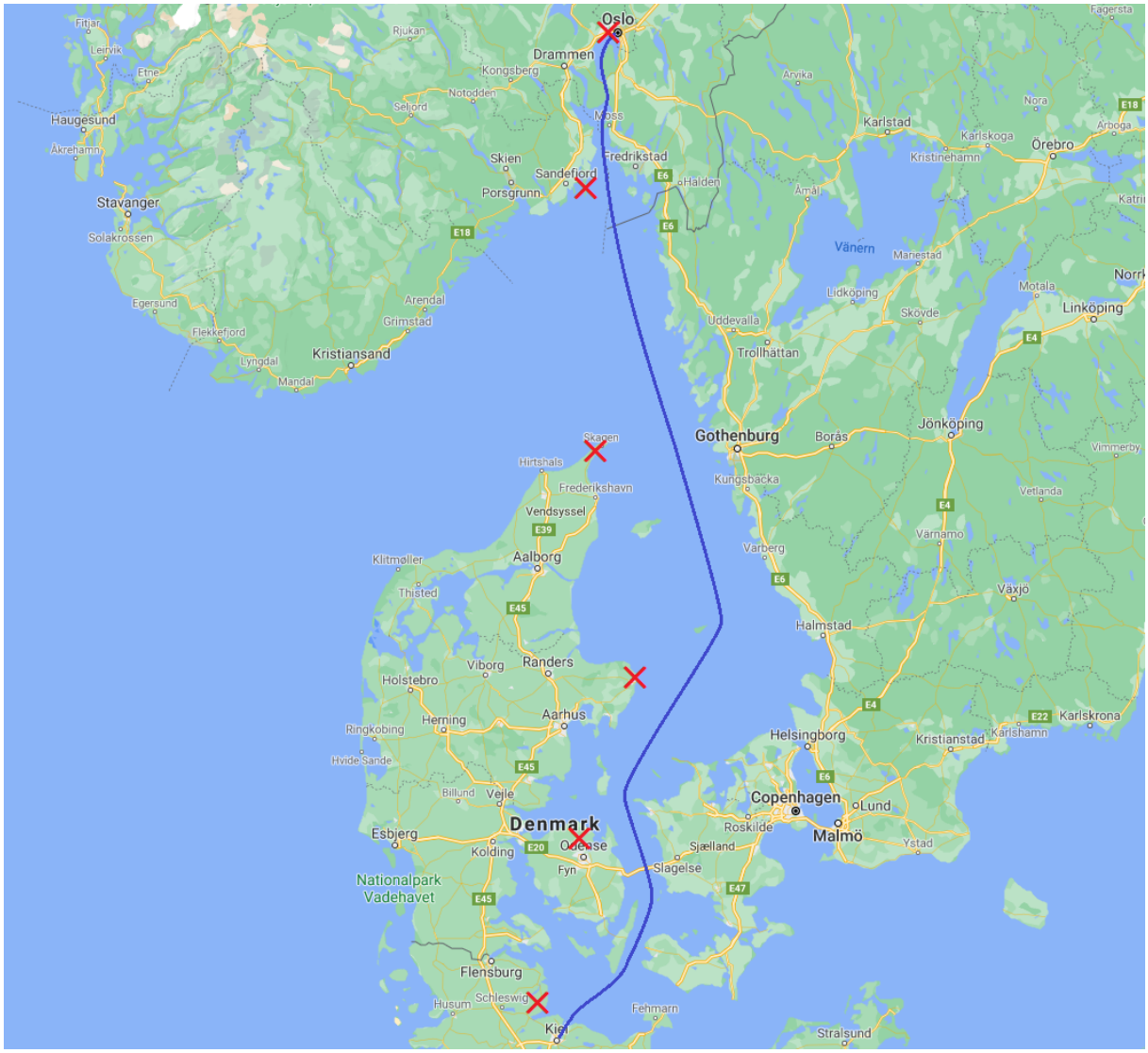

Figure 1: The six locations used in the combined weather file, marked with red crosses. The ship's approximate route is marked in blue [63].

Säve, Gothenburg was considered as an alternative to Skagen, Fredrikshavn, as it is slightly closer to the ship route. However, Säve's weather station is located further from the open sea, and it was therefore assumed that Skagen would have weather conditions closer to what the ship experiences.

The movement of Color Fantasy and Color Magic was studied using a map from Color Line showing where each ship is currently located [4]. The amount of time spent in each region on the journey was then estimated. Table 4 shows the estimated number of hours spent in each section on the 20-hour journey between Oslo and Kiel. The time spent in port is thus not included here. The ship was set to

leave Oslo at 14:00 on the 1st of January. The weather file starts at midnight and therefore starts with Skagen when the ship is on its way north towards Oslo.

Table 4: Estimated time spent in each geographical region on the 20-hour journey between Oslo and Kiel. The time in port is not included.

	Time spent in region [h]
Fornebu	1
Tjøme	4
Skagen	5
Fornæs	4
Beldringe	4
Holzdorf	2

The location selected in IDA ICE decides the position of the sun throughout the day. This cannot be varied during a simulation, and one single location therefore had to be used with the combined weather file. Fornæs (cape) was chosen because it is closest to the middle of the route, when the travel time is taken into account.

In the preceding project work, a wind data analysis was performed by using offshore wind data from Anholt Offshore Wind Farm outside Fornæs [64]. The ship speed was also taken into account in the wind speed. As shown in figure 2, using offshore wind data and taking into account the ship speed did not significantly affect the energy consumption for the ship's hotel system. It was therefore considered sufficient to use the onshore wind data from the IWEC files.

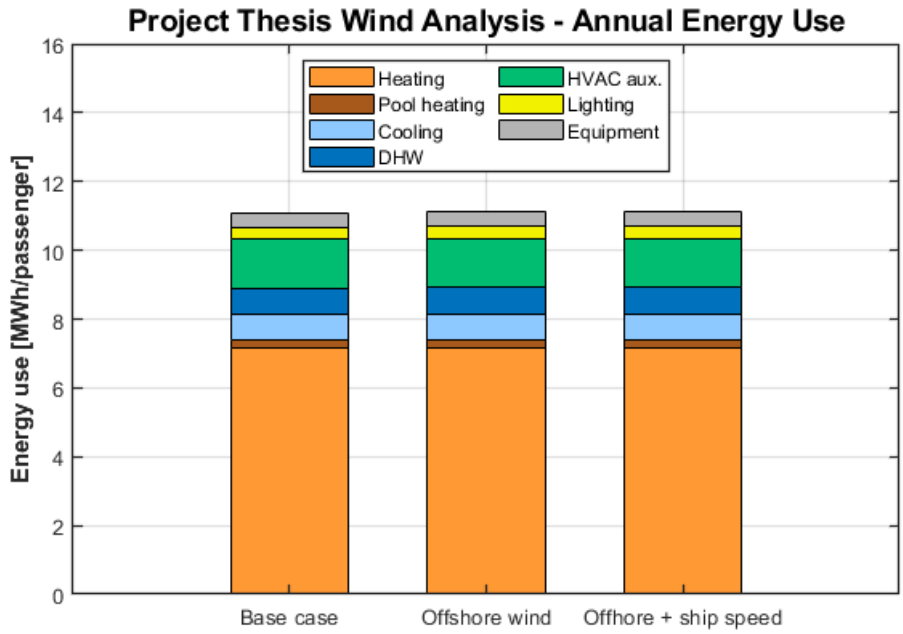

Figure 2: Annual energy consumption when offshore wind data were used, and when the ship speed was taken into account.

3.7 Calibration

The energy consumption was calculated for hotel and propulsion systems on the reference ships Birka Stockholm and the large cruise ship. This is described further in section 4.1. The simulated energy consumption was compared to this and the model was calibrated accordingly. First, the DHW demand

was increased to match with the reference ship Birka Stockholm. The accommodation heating was then decreased by reducing the ventilation rate in large galleys.

3.8 Performance Indicators

ALB-km was calculated for Color Fantasy, i.e. the simulated ship, and for the reference ships Birka Stockholm and the large cruise ship. The ALB, shown in table 5, was calculated by assuming two passengers per guest cabin. The distance travelled by Color Fantasy between Oslo and Kiel was estimated to be 700 km [63]. For Birka Stockholm, the distance travelled between Stockholm and Mariehamn was estimated to be 150 km [65]. For the large cruise ship, the total distance travelled was estimated for the Mediterranean and the Caribbean cruises [13, 66, 67]. Taking the operational profiles into account gave the total distance travelled per year, shown in the table. Multiplying ALB by the distance travelled gives ALB-km/year for the ships.

Table 5: ALB and distance travelled for the reference ships.

	Color Fantasy	**Birka Stockholm**	**Large cruise ship**
ALB	1932	1800	5254
Distance travelled [km/year]	256,200	109,800	118,000

3.9 Fan Coil Sizing Analysis

Due to weight limitations on the ship, it might not be beneficial to size the fan coils based on extreme hot and cold conditions. To investigate the effect of the fan coils' size on the ship's energy consumption and thermal environment, an analysis was done by sizing the fan coils in different ways. The calibrated model was used in this analysis. When sizing the fan coils, the fan power was set to the default in IDA ICE. This default is 3% of the cooling power, or 3% of the heating power if the cooling power is zero.

In Case A, the fan coils were sized by using design day weather conditions in heating and cooling simulations. Simulations were run with the ship facing north and south, and the highest required heating and cooling power were chosen for each zone.

For the heating simulation, none of the internal gains or solar radiation were included, to simulate the highest possible heating demand from fan coils. Design day data for Fornebu was used, as it gave the highest required heating power in all zones due to a low winter design day temperature.

Design day weather data is decided by the location file in IDA ICE. Fornebu is not available as a location, and the design day data therefore had to be entered manually. Values from ASHRAE were used for most of the parameters [68], while others were assumed. The design day data used for Fornebu can be seen in appendix A. The minimum dry-bulb temperature is -17.2 °C.

For the cooling simulation, all internal gains were included. Design day data for Holzdorf was used, as it gave the highest required cooling power in most zones. This is due to a high maximum dry-bulb temperature of 32.4 °C.

In Case B, the components were sized based on the maximum power reached by the fan coils during one year simulations when the ship is facing north and south. The custom combined weather file was used here. In Case C, the fan coils were undersized by reducing the design heating and cooling power in Case B by 50%.

The method used for fan coil sizing in Case B was used further in the base case model. In contrast to the initial model, the fan coils in the base case represent real systems for space heating and cooling on a ship. For simplification, the vehicle decks were also assumed to have fan coils for heating.

3.10 Energy Supply System

The electricity and heat produced by the ship's engines cannot easily be included in the IDA ICE model. This was therefore considered in post processing of the simulation data using a MATLAB script. This is described further in section 5.12, and the script is shown in appendix F.1. A hot water storage tank was also included here to utilise unused heat recovered from the engines and reduce peak demand for boilers. A resolution of 0.125 h was used for all results from IDA ICE and for post processing.

For the main analysis, the ship was set to have engines and boilers using MGO. MGO was used instead of other fuel oils due to the strict requirement for sulphur content in fuels, mentioned in section 2.10. Efficiencies of MDO engines and boilers on Birka Stockholm were used in the calculations.

An alternative propulsion system using LNG as fuel was also investigated, to see how this affects use of engines and boilers. For LNG engines, the exhaust gas can be cooled down more than for MGO engines, and more heat can therefore be recovered [16]. The amount of heat recovered from LNG engines was therefore set higher than for the MGO engines. This is discussed further in section 5.12.

3.11 Energy Efficiency Analysis

Relevant energy efficiency scenarios were developed for the ship. The cases are presented below and described further in section 5.14.

1. Reducing the heating in port and at night by reducing supply air temperatures and the supply water temperature for heating.
2. Turning off heating on the vehicle decks in port.
3. Increasing the amount of insulation in external constructions.
4. Switching out all windows with ones that have a lower U-value and reducing the size of many large windows.
5. Implementing PCM layers in all external and internal walls.
6. Implementing heat recovery units in every AHU, except in vehicle decks and galleys.
7. Implementing VAV ventilation strategies suitable for each zone.
8. Installing a heat pump as base heating on the ship.
9. Placing PV panels on the roof of the ship.
10. Increasing the size of the hot water storage tank to reduce the use of boilers in port.

Energy efficiency analyses were performed, considering the suggested energy saving solutions. The solutions were implemented in the IDA ICE model, to investigate how they affect the energy consumption, peaks in energy demand, and thermal comfort. Post processing in MATLAB was then performed for each scenario, mainly focusing on the case with MGO engines and boilers.

3.12 Profitability Analysis

The profitability of the energy saving solutions was investigated for the two ships using MGO and LNG as fuel. The fuel costs for MGO and LNG were considered based on the information in section 2.10. In order to consider the distribution costs for LNG, an online tool was used. The current total costs for LNG in the Baltic and the North Seas were found to be 4381 NOK/ton [69]. Without distribution costs, the current price in the EU was found to be 2722 NOK/ton [40]. This indicates that the distribution costs account for 38% of the total price for LNG. Considering the price for LNG without distribution

costs in section 2.10, the average total price for LNG over the past 5 years, including distribution costs, was calculated to be 0.259 NOK/kWh.

Similarly, the total costs for MGO in Rotterdam in February 2021 were found to be 4651 NOK/ton [70]. In the same period, the price without supply costs was 4535 NOK/ton [40], which was assumed to be representative for Rotterdam. This indicates that the supply costs account for 2.5% of the total price for MGO. This gives an average total cost over the past 5 years of 0.388 NOK/kWh.

The price of electricity from shore power was set to 0.999 NOK/kWh. This was based on the average electricity price for households in Norway for the past 5 years, including grid rent and taxes [71].

The MATLAB script was used to find the fuel consumption and use of shore power for each energy efficiency scenario listed in section 3.11. The annual reductions in fuel and shore power were used to find the reduction in operating costs. Equation 3 was then used to find the net annual economic savings for each case.

Estimates of investment costs were found for some of the solutions. For Cases 1 and 2, the investment costs depend on the control equipment already present on the ship, and this was not known. Cases 3, 4 and 5 would require large renovations to be implemented on an existing ship, and investment costs were therefore not found. For solutions where an estimate of investment costs was available, the NPV was calculated using equation 4, and the pay-off time was calculated with equation 7. Lastly, the MPI was calculated for all solutions using equation 8.

In all cases, the real interest rate was assumed to be 5%, and the residual value of the measures was set to zero. For windows and constructions with insulation and PCM layers, the economic lifetime was assumed to be 60 years. The lifetime of solutions needing only control equipment was set to 15 years.

3.13 Greenhouse Gas Emissions

The total GHG emissions in the base case and for each energy efficiency scenario were calculated for the MGO and LNG ships. This was done using the total WTP CO_2 equivalents for the fuel types, mentioned in section 2.10. The emission factor for shore power was set to 130 gCO_2e/kWh [72].

4 Data Analysis

4.1 Energy Use on Reference Ships

MS Birka Stockholm

Data for energy use on Birka Stockholm was found using two previous reports [11, 15]. This information is presented in table 6. As mentioned in section 2.1, the ship's main engines cover the mechanical propulsion demand and the auxiliary engines cover the electricity demand. For simplification, the mechanical efficiency of the main engines was used for all engines. Calculation of the amount of heat recovered from engines can be seen in appendix B.

Table 6: Energy use data for the reference ship Birka Stockholm.

	Value	**Source**
Fuel consumption engines [MWh/year]	100,000	[15]
Mechanical efficiency main engines [%]	44	[15]
Heat recovered from engines [%]	9.38	[11]
Fuel consumption boilers [MWh/year]	4000	[15]
Efficiency boilers [%]	79	[15]

Taking into account accommodation heating, hot water heating, high temperature heat demand in galleys and electric cooling, the hotel system accounts for 24.6% of the energy demand on Birka Stockholm. The ship has pools, but it is unknown where the heating demand for this is included. Hot water heating was assumed to only include DHW, but it is possible that pool heating is included here. The propulsion demand, including electricity demand for bow thrusters, amounts to 46.0% of the total energy demand [11].

26% of the ship's energy demand is electricity where the exact use is unknown. Some of this is used by the hotel system, for example in lighting, fans and pumps [11]. The remaining electricity could be used for pumps in the engine room, as well as auxiliary and safety systems. Two values were therefore calculated for the ship's energy consumption, with low and high estimates for the hotel system's share of this electricity consumption. For the low value, the hotel system was assumed to have 30% of the unidentified electricity consumption. For the high value, this was set to 90%.

As mentioned in section 2.1, Birka Stockholm has a capacity of 1800 passengers. The calculated energy use per passenger is shown in table 7. "Other" includes electricity use for lighting, fans, pumps, etc. Detailed calculations are presented in appendix B.

Table 7: Calculated energy use for Birka Stockholm, divided into different energy users. All values are in kWh/passenger/year.

	Low estimate	**High estimate**
Propulsion	14,449	14,449
Accommodation heating	4994	4994
Fuel/tank heating	1068	1068
Galley	974	974
Hot water heating	1508	1508
Accommodation cooling	251	251
Other	2450	7350
Total	25,694	30,594

Birka Stockholm has a peak thermal demand around 7200 kW for a typical winter day [15]. This

demand includes accommodation heating, hot water heating and fuel heating. The variation in thermal demand is based on a hotel, with peaks from 6:00 to 8:00 and from 19:00 to 21:00 [73]. This means that the demand for fuel heating is evenly distributed throughout the day, even though it should be zero when the ship is in port. Fuel heating is estimated to account for 10% of the total thermal demand [11].

In the summer, the thermal demand only covers hot water heating, and it has a peak of 2400 kW, or 1.33 kW/passenger. The peak demand for accommodation heating in the winter was therefore estimated to be 4080 kW, or 2.27 kW/passenger. The peak cooling demand for a typical summer day is around 1200 kW, or 0.67 kW/passenger [15].

Large Cruise Ship

On the large cruise ship, 13.1% of the total energy consumption goes to the HVAC systems, including cooling, fans and pumps. Propulsion amounts to 35.6% of the energy use. 51.0% goes to other users, which includes electricity for lighting and equipment, as well as heat demands for DHW, laundry, galleys and pools [13]. It is unknown how much of this is used by the hotel system on board. Again, high and low estimates were therefore calculated for the hotel system's energy use. For the low estimate, 30% of the "other" category was included. For the high estimate, this was set to 70%.

As mentioned in section 2.1, the large cruise ship has a capacity of 5230 passengers. Table 8 shows the calculated energy use per passenger. The ship has no known accommodation heating, which is likely due to the warm climate in the Mediterranean and Caribbean Seas. HVAC auxiliary includes energy use for fans and pumps in the HVAC system.

Table 8: Calculated energy use for the large cruise ship, divided into different energy users. All values are in kWh/passenger/year.

	Low estimate	**High estimate**
Propulsion	21,989	21,989
Accommodation cooling	3499	3499
HVAC auxiliary	4576	4576
Other	9465	22,084
Total	39,528	52,147

As seen in the table, the total energy use varies significantly depending on how much of the "other" energy use is included. Around 24% of the "other" energy use goes to production of freshwater [13], which is not included in energy use for the hotel system. This means that the hotel system at most has 76% of the "other" energy use. However, it was considered likely that this category includes more processes that are not related to the hotel system. It is also possible that less than 30% of this category should be included in the low estimate.

In between the cruise in the Mediterranean and the Caribbean, the ship sails from one area to the other without passengers on board. This adds up to around 30 days that are not included in the energy consumption [13]. This means that the energy use would be higher if a whole year was included.

For a week in July on the Mediterranean cruise, the total cooling power reaches peaks of around 18 MW, or 3.44 kW/passenger. In the same week, the peak thermal power for DHW is around 2.7 MW, or 0.52 kW/passenger [13].

Comparison

In general, the energy consumption varies a lot between different cruise ships. The hotel system's share of the total energy use can also vary significantly [74]. The analysed data show that there is a significant difference in the energy use depending on how much of the ship's energy consumption is assumed to go to the hotel system. The actual energy use for the hotel and propulsion systems combined could be outside the range of the low and high estimates. These are important sources of error in the calculations and in the following calibration.

The energy consumption per passenger is generally higher on the large cruise ship compared to Birka Stockholm, and the exact reasons for this difference are unknown. It is difficult to directly compare these ships, as the climate zones they sail in differ significantly. Birka Stockholm has a dominating heating demand, while the large cruise ship mainly has cooling. The energy use on Birka Stockholm does not include heating demand for laundry. This could indicate that laundry is not done on the ship, but instead left in port. This could be part of the reason why the energy use per passenger is lower on Birka Stockholm.

4.2 Temperature Data

Figure 3 shows duration curves for the air temperature in the six IWEC files used in the custom combined weather file, mentioned in section 3.6. Holzdorf stands out by having significantly higher temperatures than the other locations for around 3000 hours. The maximum temperature here is 34.5 °C. Fornebu stands out by having lower temperatures than the other locations for almost 6000 hours. However, Holzdorf has a lower minimum temperature than Fornebu, with Holzdorf at -18.3 °C and Fornebu at -16.7 °C. The remaining four locations have similar duration curves, categorised as mild coastal climate with moderate temperatures in both winter and summer. The annual temperature variation for the six locations can be seen in appendix D.

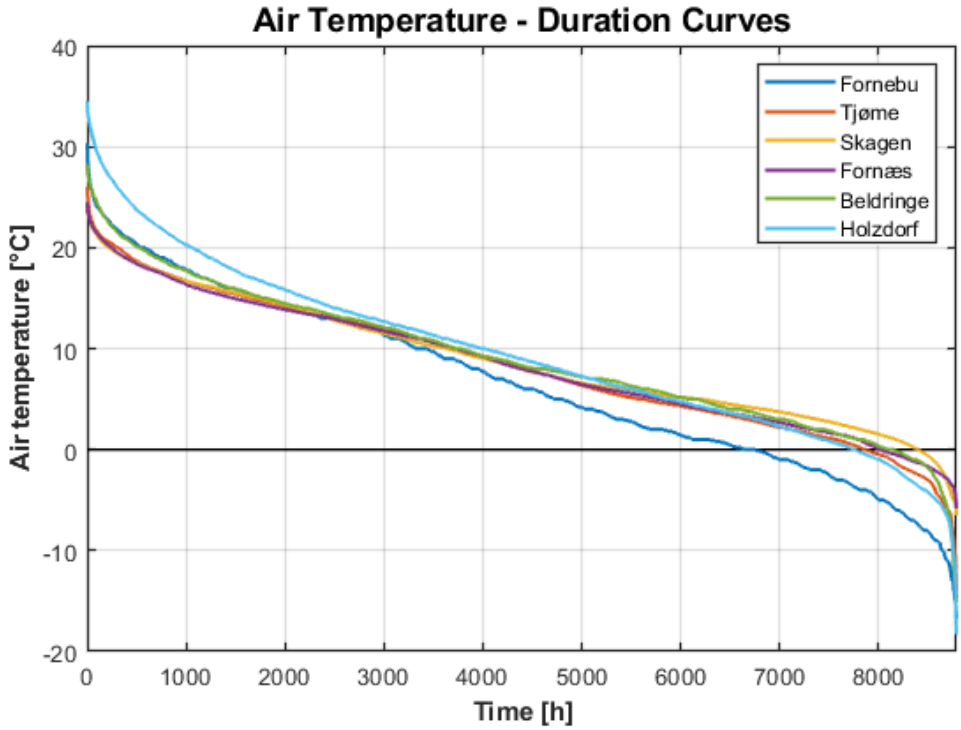

Figure 3: Duration curves for air temperature in the six IWEC files.

Combined Weather File

Figure 4 shows the air temperature in the combined weather file for the first 48 hours of the year. The ship starts in the Skagen region on its way north. At hour 9, it reaches the Fornebu area, where it stays for 6 hours. Then the ship travels south again and reaches the Holzdorf region at hour 32, where it stays for 8 hours. There are large and fast variations in temperature due to how the weather file has been made. In reality, the temperature variations would be gradual, but they could still be as large as shown in the figure. The same applies for the other weather data in the combined file. The annual temperature variation in the combined weather file is shown in appendix D. The minimum temperature is -16.1 °C, while the maximum temperature is 34.5 °C.

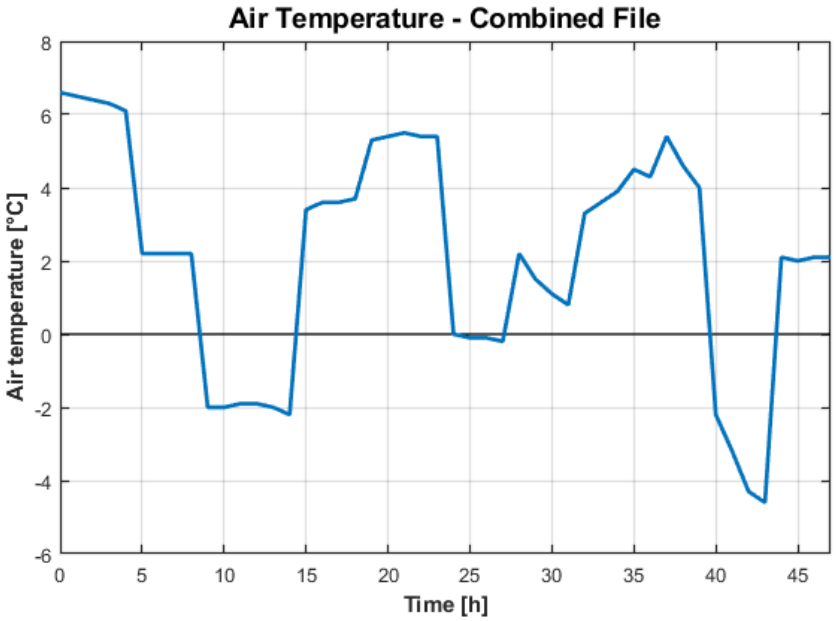

Figure 4: Air temperature for the first 48-hour travel cycle in the combined weather file.

5 Case Study

5.1 Zone Modelling

The zone modelling was based on Color Line's Color Fantasy. The building structure in IDA ICE was based on the ship's deck plan [61]. Seeing as the ship's shape changes in the vertical direction, several building bodies were used. Each building body contains 1-3 decks.

To reduce the modelling and simulation time, the model should not be made more complex than necessary. Representative zones were therefore identified. Zones with similar size, orientation and internal loads were represented by one zone, and zone multipliers were used to get the correct number of zones. The types of zones were analysed using information from colorline.no, the 3D model of Color Fantasy [8], and the deck plan for the ship [61].

The zone multipliers were especially useful for cabins, as there are 966 similar cabins on the ship. The different types and sizes of cabins were identified using Color Line's cabin overview [7]. A few cabins of each size were included in the model. For ocean view cabins, one cabin of each size was placed on each side of the ship. Internal cabins and cabins facing the promenade were included where relevant. Cabins located on several decks were placed near the middle of the given decks. The cabins were modelled as one zone each, with sleeping room and bathroom combined. A total of 16 cabins were used to represent all cabins on Color Fantasy.

Figure 5 shows the 3D model of the ship in IDA ICE, where the ship is facing towards the left. The front half of the ship is shown on top and the back half is shown on the bottom. The smallest zones in the figure are the ship's cabins.

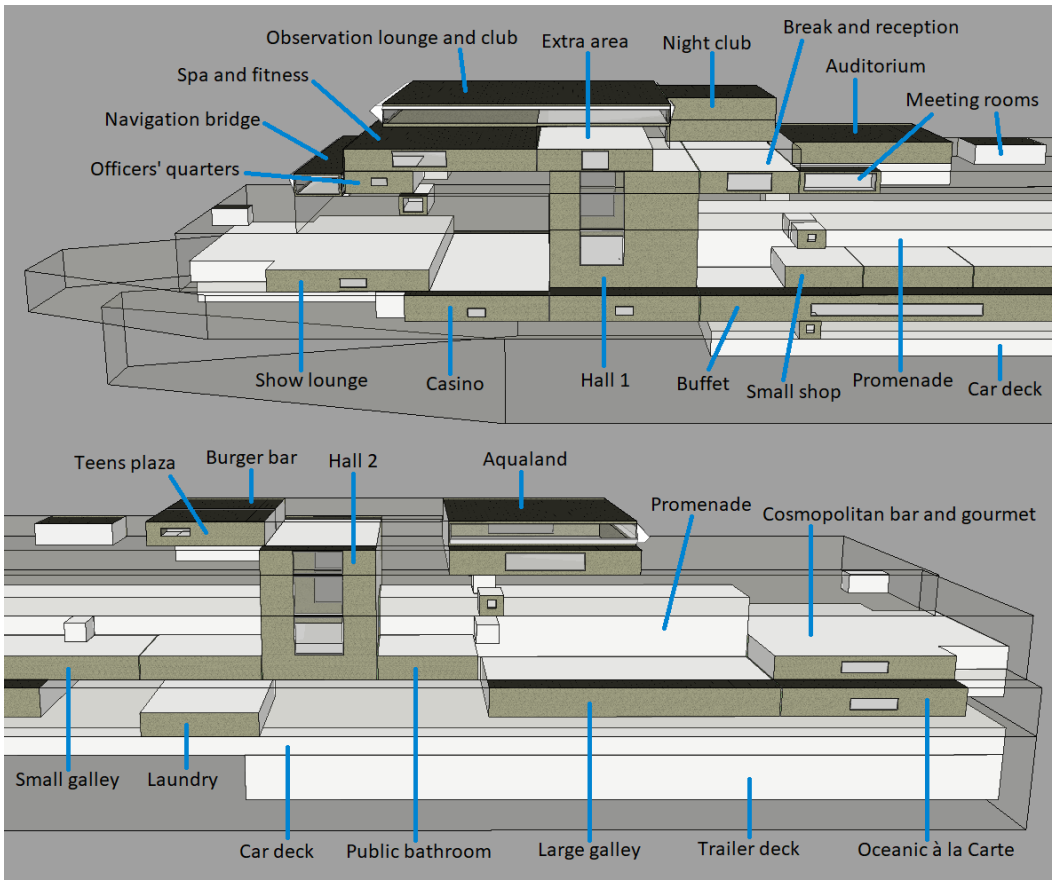

Figure 5: Ship model in IDA ICE with several zones marked. The ship is facing towards the left.

The contents of deck 5 are largely unknown, including the size and location of guest and crew cabins. A few guest cabins are located here, and these cabins have view to the ocean [7]. The number of guest cabins on deck 5 was decided so that the total number of guest cabins on the ship would be correct. Seeing as the guest cabins have view to the ocean, it is likely that most of the crew cabins on the deck are internal. It was estimated that there are five crew cabins on each side of the ship, and that the rest of them are internal cabins. It was assumed that the crew cabins with ocean view are similar to the guest cabins on deck 5, and they were therefore modelled together using zone multipliers.

Corridors between cabins were not included. Compared to other accommodation areas, the corridors are small and sheltered from the ship's external walls. They were therefore assumed to have a small energy demand. Some other corridors were also ignored, or simply included in the larger space they are part of.

The officers' quarters on deck 12 were assumed to be three identical zones on each side of the ship with two windows each. Meeting rooms in the conference centre on deck 12 were modelled using one representative meeting room on each side of the ship. Galleys for the ship's restaurants were combined into one large galley on deck 6 and one smaller galley on deck 7. The configuration of laundry rooms was unknown. The laundry rooms were therefore assumed to be one large room on deck 5.

For the larger areas of the ship with specific shapes and usage, each zone was modelled individually. This includes the restaurants, show lounge, promenade and the spa and fitness centre, among others. Open seating areas for restaurants and bars in the promenade were merged into the promenade zone. Shops were also modelled separately due to differing sizes and locations. Zones with complex shapes were simplified, and the size was chosen so that the total area would be correct. The area of each zone is not known precisely, and this was therefore estimated based on the deck plan [61].

The height of cabin decks was set to 2.1 m, based on the literature study in section 2.2. For decks with public areas, the height was set to 2.5 m, except deck 6 which was estimated to be 3 m. There are two large halls in the ship which are connected to the promenade and extend over several decks. It is unknown exactly how tall these halls are, but they were estimated to go up to deck 12 [8].

For walls with several windows, the windows were combined to simplify the model. The total area of the windows was estimated based on the 3D model [8]. Internal windows in the promenade were not included, as they were found to have an insignificant impact on the heat transfer between zones and the total energy consumption.

Some zones on the ship have angled walls with windows. This includes the navigation bridge, Aqualand, observation lounge and the largest cabins. The effect of the angled walls was approximated using tilted windows in IDA ICE. The angle of the windows was estimated using the 3D model and a video of Color Fantasy [75].

Similarly to internal windows, closed internal doors were found to not significantly impact the heat transfer between zones and the total energy use, and they were therefore not included. Internal doors that were assumed to be open a significant amount of the time were given an opening schedule based on the opening hours of the zone [76, 77]. Internal doors were sized according to the 3D model, and doors on the same wall were combined. External doors were not included, as they were assumed to not significantly affect the thermal insulation of the ship envelope.

According to the IDA ICE user manual, openings should not be used in the model unless the flow through the opening is to be studied. Large leaks should be used instead [58]. Leaks were therefore used for large openings in the ship that were assumed to always be open under normal operation. The area of the leak was set equal to the area of the opening. This was used mainly in the promenade and the large halls, and the zones connected to these.

The floor area and heights of the vehicle decks are not known precisely. The floor area was therefore estimated based on the car capacity and the trailer lanemetres. Using zone multipliers, the car decks were modelled as three decks of equal size, and the trailer decks were modelled as two decks. The height of the car decks was estimated to be 3 m [78], and the height of the trailer decks was assumed to be 5 m.

The length of a car parking space should be 5.0 m, while the width should be at least 2.5 m [79]. Together with the maximum number of cars, this was used to calculate the necessary total area for the car decks. For trailers, the lanes were estimated to be 2.8 m wide, based on the fact that trucks, trailers and buses usually are 2.5 m wide [80]. Considering the total number of trailer lanemetres on the ship, this was used to calculate the total area of the trailer decks.

The external door on the vehicle decks was estimated to be 50 m^2 [78]. In the model, this door area was divided evenly between the five vehicle decks. The doors were set to be open for 30 minutes during both roll on and roll off. However, during simulation the airflow through the external doors was found to be insignificant compared to the large ventilation rate on the vehicle decks. To simplify the model, the doors were therefore not included.

Using the deck plan for Color Fantasy [61], the gross internal area of the ship was estimated to be 62,271 m^2. Assuming 1% of this is internal walls, the required net internal area is 61,648 m^2. At this point in the modelling, the net internal area was lower than this, and a general zone was therefore made to represent the extra area. As most corridors in the ship had not been modelled, the zone was modelled after a large corridor outside the spa and fitness, with windows facing both sides of the ship. To achieve the desired total area, a zone multiplier of 57.7 was used for this zone. In total, 54 different zones were modelled on the ship. When zone multipliers are taken into account, this gives a total of 1323.7 zones.

5.2 Ship Construction

The ship construction in IDA ICE was based on the literature study in section 2.2. Steel was used in the construction for decks 9 and below, while the decks above this have aluminium. As mentioned, this reduces the weight of the upper parts of the ship, thereby increasing the stability. The basic construction used for walls, ceilings and floors consists of two 4 mm steel or aluminium plates with insulation between. Vertical air gaps, wall panelling, and carpets were included where relevant.

A 25 mm thick steel plate was used as an estimation for tinplate steel cladding used as wall panelling. This was used in all zones, as the wall panelling was assumed to have similar thermal properties. As a simplification, the cabin wall facing the corridor was set equal to the other internal walls.

Default air gaps in IDA ICE specify that the surfaces are non-metallic. Therefore, new gaps were made, and the thermal conductivity of the gaps was calculated according to NS-EN ISO 7547 [24], using surfaces with high emissivity. For 10 mm gaps, the thermal resistance was interpolated.

Most zones in the ship have carpet floors, including public areas [8]. For simplification, carpet was therefore included in all internal floors. An 8 mm wool carpet was included, using a specific heat capacity of 1380 J/(kg K) [81], a thermal conductivity of 0.193 W/(m K) and a density of 226.3 kg/m^3 [82].

The insulation used in the whole ship construction is "light insulation" in IDA ICE, which has a thermal conductivity of 0.036 W/(m K). The external walls, roofs and floors were set to have comfort insulation with thickness 150 mm. The internal constructions were given insulation of thickness 40 or 55 mm to achieve U-values close to Isover's bulkhead and deck insulation constructions [83].

Isover has insulation constructions for steel bulkheads of class A-15 and A-60. The U-values of these constructions are similar. When simulating energy use, the U-value of the wall is of high importance, while the fire resistance is less important. For simplification, the same construction was therefore used for all internal steel walls. 40 mm insulation was used in the internal steel walls, which gives a U-value of 0.7805 W/(m^{2}K) before air gaps and panelling were added. This is in the range of both the A-15 and A-60 insulation constructions [84, 85].

U-values for different classes are also similar for the deck insulation and the aluminium constructions. One construction was therefore used for each of these as well. Table 9 shows the thickness of insulation used in the various constructions and the U-value achieved.

Table 9: Insulation thickness and U-value for ship constructions used in the model.

Construction	**Insulation thickness [mm]**	**U-value [W/(m^{2}K)]**
External steel wall	150	0.2228
External aluminium wall	150	0.2228
Steel roof	150	0.2306
Aluminium roof	150	0.2306
Steel bulkhead	40	0.6542
Steel deck	40	0.7560
Aluminium bulkhead	55	0.5141
Aluminium deck	55	0.5750

Figure 6 shows the different constructions used in IDA ICE, with the ship viewed from two different angles. As a simplification, the walls of the halls were made entirely out of steel even though these halls span across decks 7-12.

The typical thermal properties of ship windows are unknown. The window glazing was estimated as 2-pane glazing in IDA ICE, which has a U-value of 2.9 W/(m^{2}K). In the Aqualand, a high temperature setpoint and large windows cause significant heat losses when it is cold outside. It was therefore assumed that these windows have a better insulating capacity. 3-pane glazing with a U-value of 1.9 W/(m^{2}K) was therefore used.

For cabins, the window frame is made entirely out of steel or aluminium. The frame was assumed to be 50 mm thick, which gives a U-value of about 5.9 W/(m^{2}K) for both steel and aluminium. This U-value was used for the window frame in all cabins. For other windows, less is known about the thermal properties of the window frame. The default U-value of 2.0 W/(m^{2}K) was therefore used. The thermal bridge for external window perimeters was estimated to be "poor" in IDA ICE, meaning a thermal bridge of 0.4 W/K/(m perimeter).

Glass doors were estimated to be 20 mm thick. For simplification, the material of other internal doors was set to default in IDA ICE, which is 40 mm wood.

As mentioned in section 2.2, the ship's construction is approximately airtight. The infiltration was therefore set to 0 h^{-1}.

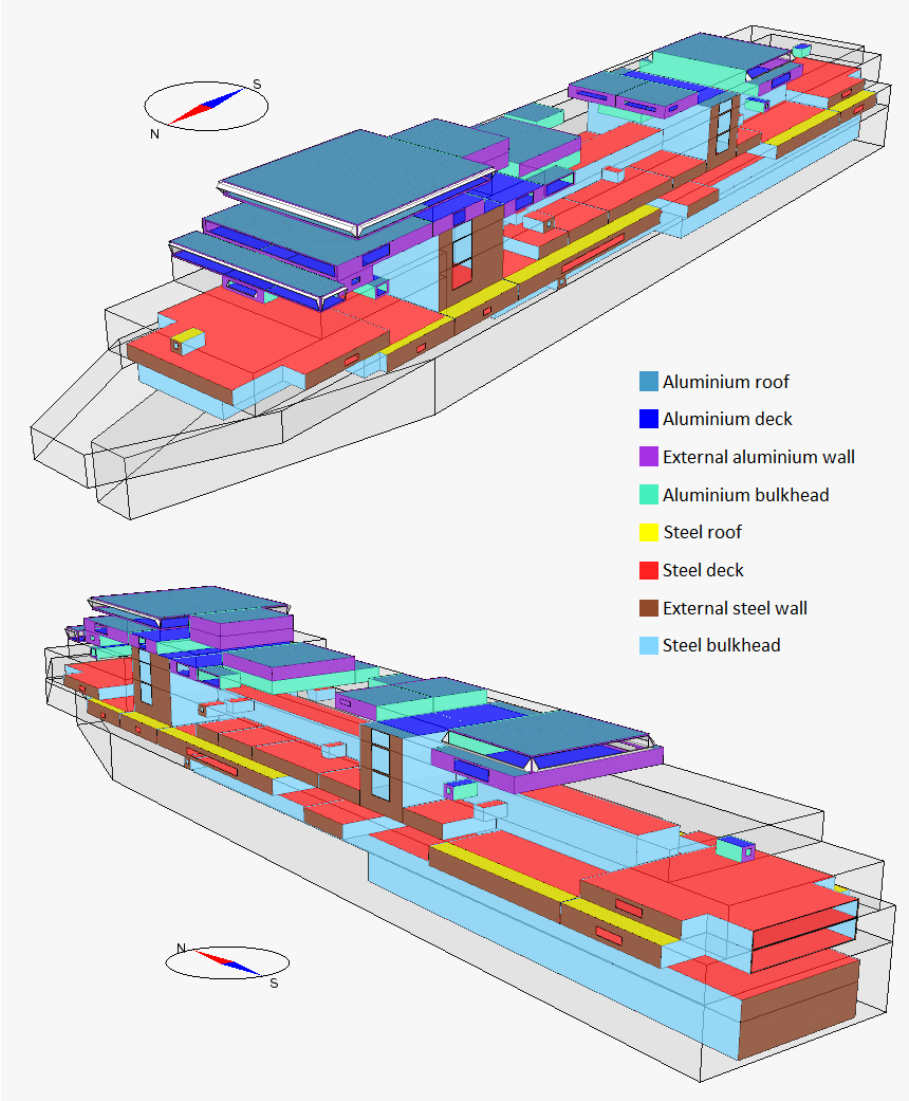

Figure 6: The different constructions used in the ship model.

5.3 Internal Gains

Internal gains include heat loads from occupants, lighting, and electrical equipment. All schedules for internal gains were set equal for every day of the week, as Color Fantasy normally is in operation every day of the week most of the year [4].

5.3.1 Occupancy

The number of occupants in the cabins was set to the maximum number of adults that can sleep there [7]. The guest cabins on deck 5 can be used by two occupants, while it was assumed that each crew cabin houses one employee. The number of occupants in the ocean view cabins on deck 5 was therefore set as an average based on the total number of people staying in the guest cabins and the crew cabins.

The average activity level for occupants in cabins was assumed to be seated and relaxed. The internal heat production for an average sedentary, relaxed person is 58 W/m^2 body surface, which is defined as 1 met [1].

The cabins were assumed to have an occupancy schedule similar to a hotel room. The schedule used in IDA ICE was based on a hotel schedule from NS-EN 15232-1:2017 [86], which is shown in figure 7. Occupancy is at 100% during the night and at 0% during the day, which fits with the assumed use of the cabins.

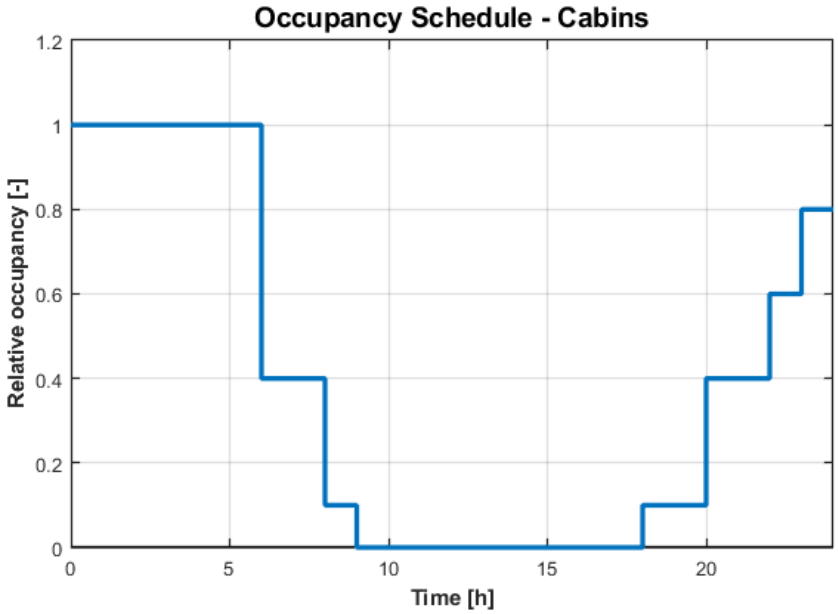

Figure 7: Occupancy schedule used for cabins in IDA ICE, from NS-EN 15232-1 [86].

It was assumed that the ship has six officers in total, and that two of them are always in the navigation bridge. The activity level in the navigation bridge was set to 1.2 met, which corresponds to sedentary activity [87]. Further, it was assumed that the four remaining officers are in the officers' quarters the whole day, as they will sleep at different times. The activity level here was set to 1.0 met. It was assumed that the number of people in the navigation bridge and officers' quarters is significantly reduced when the ship is in port between 10:00 and 14:00. The occupancy was set to 10% to account for cleaning.

Use of the auditorium and the meeting rooms in the conference centre was assumed to be similar to the use of an office building. Schedules for an office were taken from SN-NSPEK 3031:2020 [88], and the

occupancy was set to 10% during port stays. For the break and reception area, a similar schedule was used but without the peaks in occupancy. The activity level was set to 1.2 met for the entire conference centre.

The maximum number of people in the auditorium and meeting rooms was estimated based on the number of seats available [8]. The maximum number of people in the break and reception area was set equal to the maximum in the auditorium. Table 10 shows the maximum number of people used for each zone.

Table 10: Maximum number of people estimated for each zone.

Zone	Max number of people
Restaurants	
Oceanic à la Carte	180
Cosmopolitan bar and gourmet	130
Private dining	8
Observation lounge and club	180
Grand buffet	500
Burger bar	25
Promenade and shops	
Promenade	448
Halls	80
Large corridors	48
Public bathrooms	5
Shops	10-30
Taxfree market	40
Other public areas	
Adventure planet	20
Aqualand	50
Casino	80
Night club	140
Show lounge	200
Teens plaza	20
Spa and fitness	60
Extra area	10
Conference centre	
Auditorium	272
Meeting rooms	18
Break and reception area	272
Employee areas	
Small galley	20
Large galley	40
Laundry	20
Navigation bridge	2
Officers' quarters (total)	4
Vehicle decks	0

For the public areas on the ship, the occupancy schedules were based on the opening hours of the zone [76, 77]. During opening hours, occupancy was set to 50-100% depending on the assumed occupancy in a given time period. For zones assumed to have a significant number of employees, occupancy was

set to 10-20% one hour before and after opening hours. As an example, the occupancy schedule for the restaurant Oceanic à la Carte can be seen in figure 8. Occupancy schedules used for other large zones are shown in appendix E.1. The spa and fitness occupancy schedule was also used in the extra area. Occupancy schedules in the galleys were based on the occupancy in the restaurants they are serving.

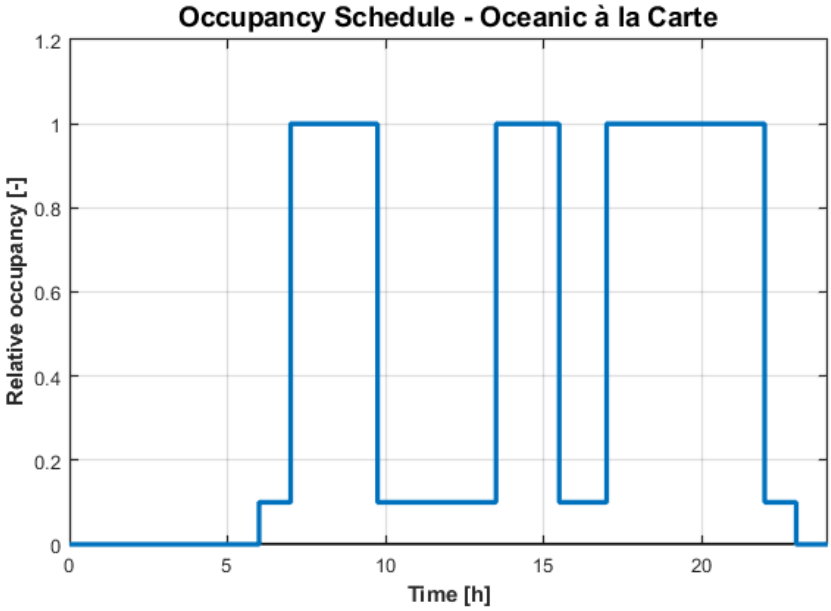

Figure 8: Occupancy schedule for the restaurant Oceanic à la Carte.

To reduce peak demand, laundry is often done on the ship at night or while it is in port [89]. Seeing as the ship model already had large heat demands in port, it was decided to set the laundry steam demand high at night. As a simplification, occupancy in the laundry room was set constant during the night, and zero otherwise.

The maximum number of occupants was estimated based on the number of seats available or the area of the zone [8]. For zones not available in the 3D model, estimations are especially crude and based on pictures from colorline.no. For the promenade, public bathrooms, observation lounge, and spa and fitness, it was assumed that there are no guests present when the ship is in port. The occupancy was set to 10% to account for the ship crew. Some restaurants and other public areas open before 14:00. As guests could remain on the ship during port stays, the occupancy was set according to these earlier opening hours. For public bathrooms, occupancy was set constant outside the port stays from morning until evening.

For restaurants, bars, and other zones where people were assumed to be sitting, the activity level was set to 1.2 met. For the promenade, shops, public bathrooms and extra area, the activity level was set to 1.6 met. This corresponds to standing, light activity [87]. For the spa and fitness centre, an average activity level of 3.0 met was assumed, which corresponds to fast walking. The Aqualand and the night club were set to have an activity level of 2.5 met. The activity level in the galleys and laundry was set to 2.0 met, meaning standing with medium activity.

As mentioned in section 2.1, the maximum capacity of Color Fantasy is 2605 people. The occupancy schedules and maximum number of occupants were therefore adjusted to achieve approximately 2600 people as the total occupancy for the ship. For cabins of size 10.5 m^2, two different variations exist where 2 or 5 people can stay. The number of occupants was set to 2.5 for all these cabins to achieve the correct total occupancy. Figure 9 shows the total number of occupants on the ship throughout the day. The schedule is automatically smoothed out in IDA ICE to avoid sharp transitions in the number of

occupants. Cabins include the crew cabins on deck 5, as some of these were modelled together with the guest cabins. The zones included in the other zone categories can be seen in table 10.

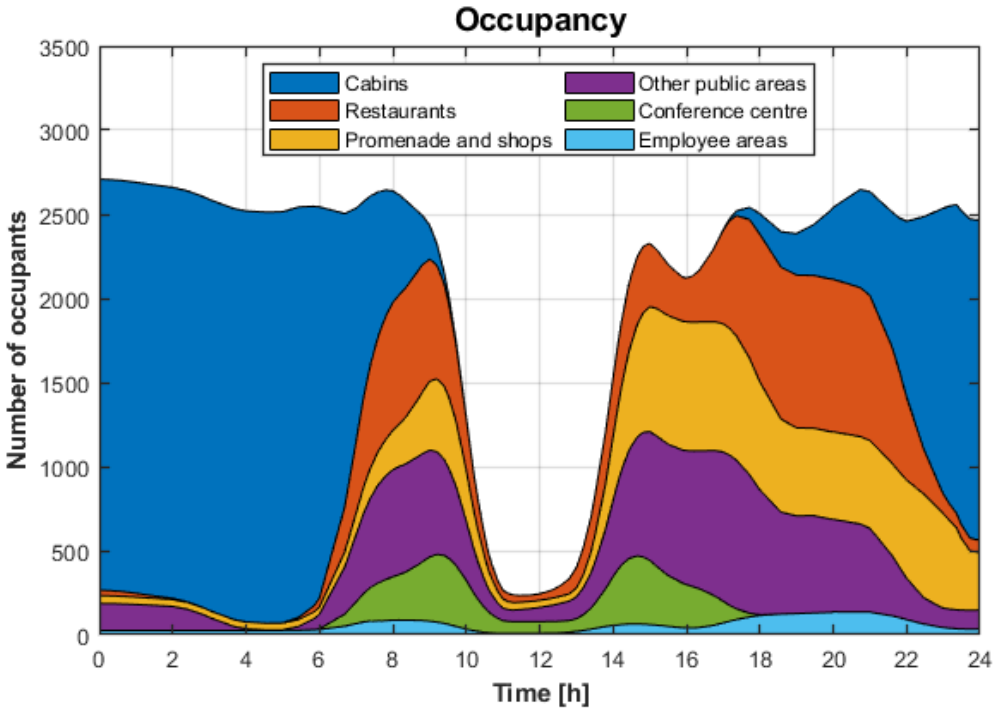

Figure 9: Total number of occupants on the ship, divided into zone types.

During the night it was assumed that everyone is inside the ship, while some people will go outside on deck during the daytime. Small reductions in total occupancy during the daytime are therefore considered realistic. There is for example a dip in the total occupancy around 16:00. There is also a reduction in number of occupants in restaurants, caused by the opening hours of all the restaurants. This reduction in total occupancy on the ship can therefore represent people going outside on deck before or after their meals.

5.3.2 Lighting

LED lights are usually used on passenger ships, which gives small internal gains. Especially in cabins, the heat load is very low and is considered negligible [17]. Therefore, no lighting was included in the cabins.

The lighting schedules in the rest of the ship were based on SN-NSPEK 3031 [88]. The values given in the standard are based on an efficient system using LED lighting. The schedules have maximum lighting level during occupancy hours and a lower level for the rest of the day. In the conference centre, the lighting schedule for an office building was used in all zones. This schedule has a peak of 3.7 W/m^2. For all other zones, the schedule for a hotel was used, with a peak of 2.4 W/m^2. The basic schedules for office buildings and hotels are shown in appendix E.2. For areas with opening hours that differ significantly from the hotel schedule, the schedule was shifted to the correct hours. This can be seen in the lighting schedule for the night club in figure 10.

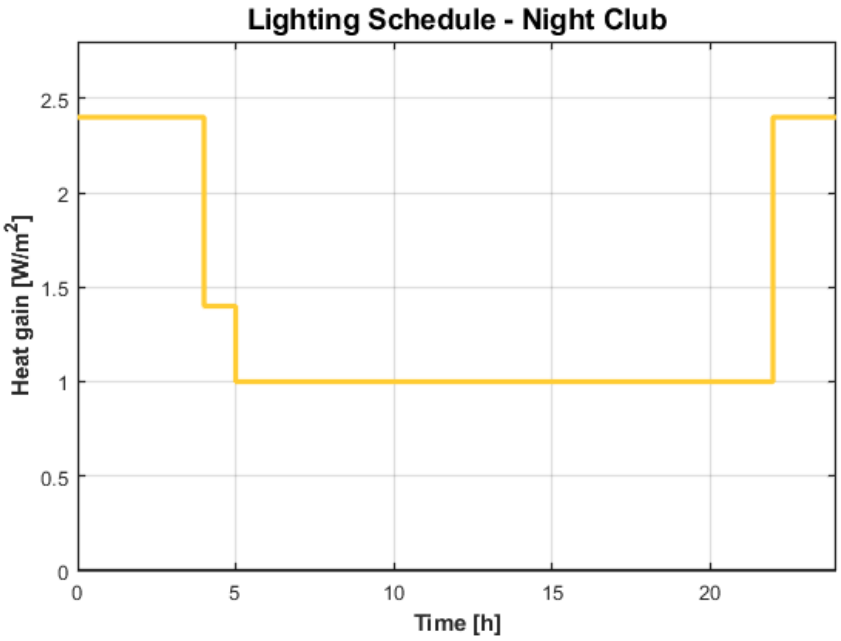

Figure 10: Lighting schedule for the night club, based on SN-NSPEK 3031.

As the two large halls in the ship are several decks tall and contain half floors open to the halls, the lighting load was assumed to be twice as large as the floor area would indicate.

In the large reference cruise ship, LED lights are set to have a heat gain of 5 W/m^2 [13], which is larger than the peak values used in the IDA ICE model. This difference could be caused by inaccuracies in the Norwegian standard about the power requirements of LED lights, different types of LED lights being used, or different practices for how many LED lights are placed in a space.

5.3.3 Equipment

According to NS-EN ISO 7547, the heat gain from refrigerators should be set to 0.3 W/l storage capacity [24]. The minibar in the cabins was estimated to have a volume of 60 l, which gives a total output of 18 W. The standard also specifies that heat gains from temporary electrical appliances, such as TVs and hair dryers, should be ignored. The internal gain was therefore set to a constant 18 W in all cabins.

The equipment schedules for the rest of the ship were based on SN-NSPEK 3031 [88]. The equipment schedule for an office building was used in all zones in the conference centre. This schedule has a peak heat gain of 8.6 W/m^2. The other zones have schedules for a hotel, with a peak of 1.3 W/m^2. These two schedules can be seen in appendix E.3. If occupancy differed significantly from the hotel schedule, the schedule was simplified and shifted to the correct hours. This can be seen in the equipment schedule for the night club in figure 11.

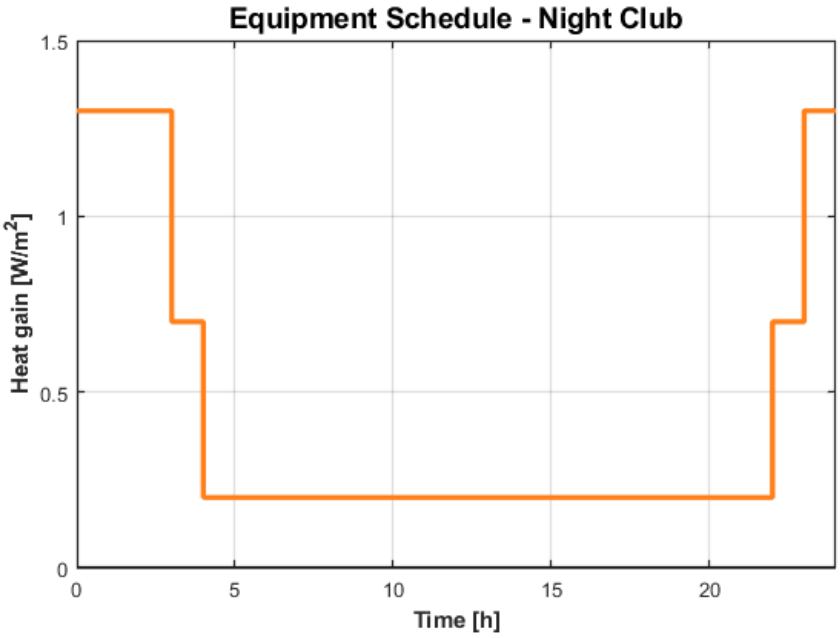

Figure 11: Equipment schedule for the night club, based on SN-NSPEK 3031.

As for lighting, the two large halls in the ship were assumed to have an equipment load twice as large as the floor area indicates.

5.4 Steam Demand

The schedules for the steam demand in galleys and laundry were based on the energy demand per passenger in a smaller expedition cruise ship. This reference ship is fuel cell-driven, and the energy demands in galleys and laundry are covered by electricity [89]. The steam demand for galleys and laundry was assumed to be similar to this. The steam demand was added as equipment in the zones with energy carrier fuel.

In galleys, the schedule for the steam energy use was based on the opening hours of the connected restaurants. The schedule was adjusted based on the expedition reference ship to achieve the same total energy use per passenger. The peak demand was set higher for dinner due to hot meals being prepared [89]. For the large galleys, the peak demand was set to 1400 kW, and the schedule used in IDA ICE can be seen in figure 12. The small galleys have a peak demand of 700 kW and the schedule is shown in figure 13. It was assumed that there is no other equipment used in the galleys.

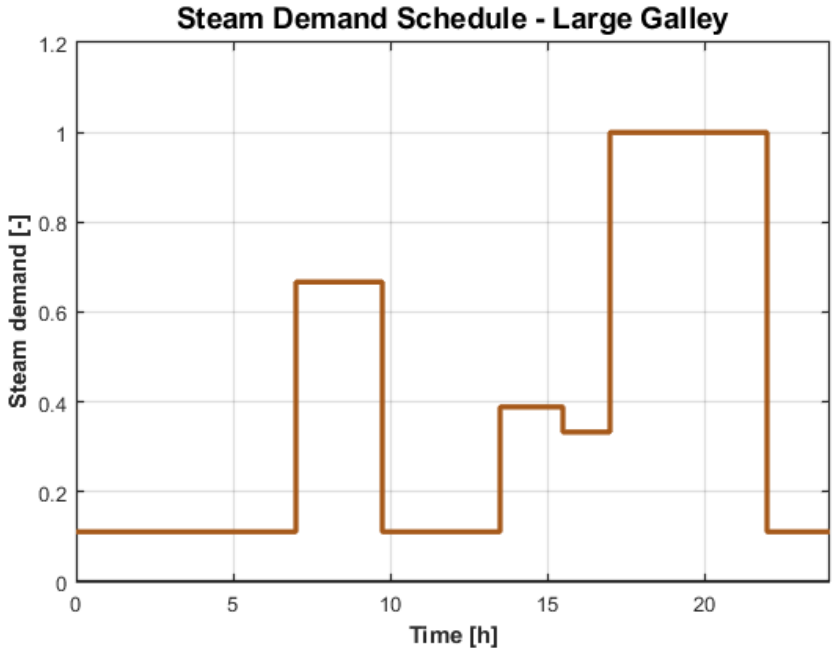

Figure 12: Steam demand schedule for the large galleys, based on the expedition reference ship.

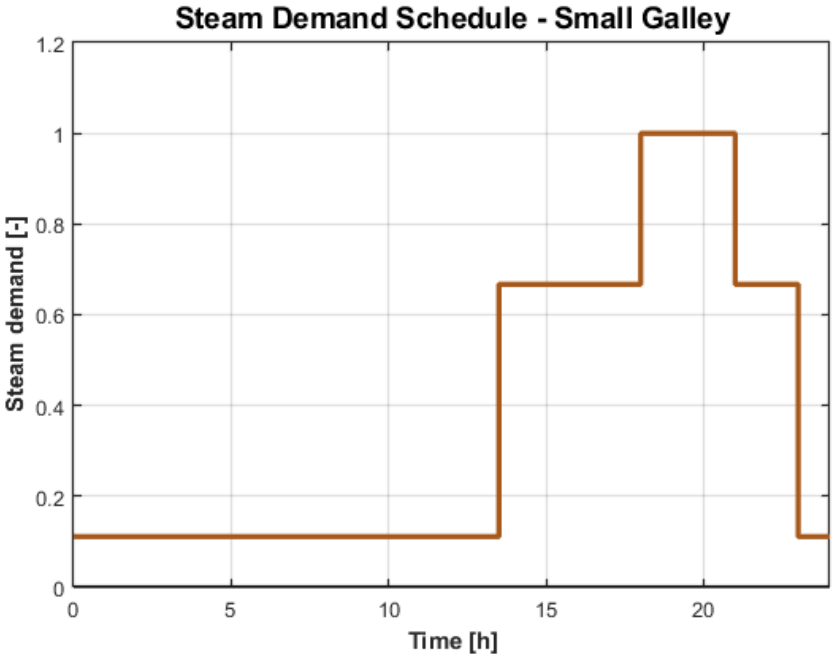

Figure 13: Steam demand schedule for the small galleys, based on the expedition reference ship.

The heat released to zones was set using a utilisation factor. For simplification, only ovens were included in the heat gain from equipment in galleys. The ovens were assumed to be similar to electric full-size ovens with rated power 12 kW. With an exhaust hood, these ovens have a heat gain of 850 W [90]. It was assumed that the galleys have the same number of ovens as employees. The maximum heat load in the zones was set as the total heat gain from all ovens. This gave a utilisation factor of 2.43% for the galleys.

The schedule used for the laundry steam demand was based on the expedition reference ship and

is shown in figure 14 [89]. The peak demand was set to 2160 kW to achieve a total energy use per passenger equal to the reference ship. The utilisation factor in the laundry was assumed to be similar to the one in the galleys. Again, it was assumed that no other equipment is used in the laundry room.

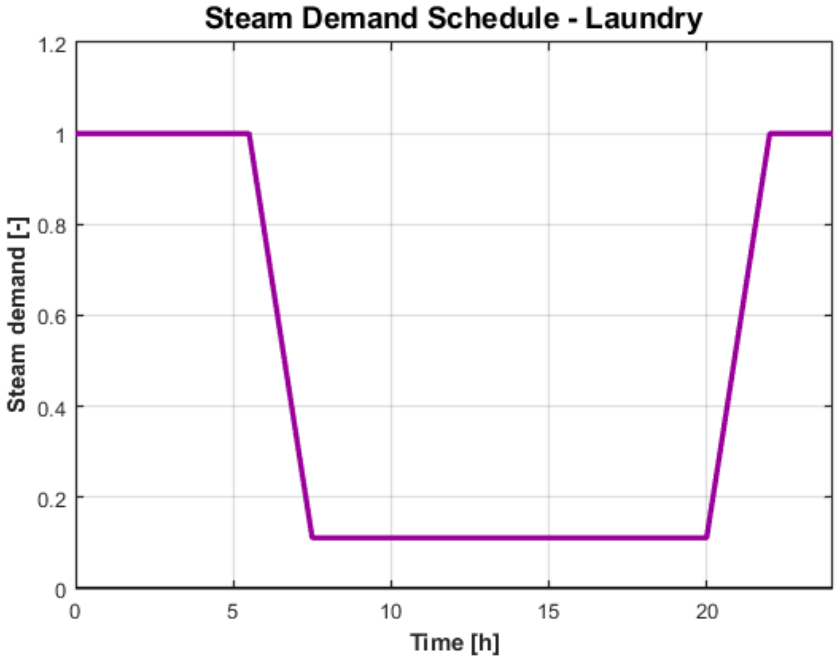

Figure 14: Steam demand schedule for the laundry, based on the expedition reference ship.

5.5 Domestic Hot Water

The use of DHW in the hotel system on the ship is relatively large due to frequent showering and dish-washing. The DHW use was assumed to be similar to the use in hotels, and the schedule implemented in IDA ICE was taken from SN-NSPEK 3031. This gives an annual energy use for DHW of 30.1 kWh/m^2 [88].

5.6 Swimming Pools

The swimming pools in the Aqualand were estimated to cover 25% of the floor area, which gives a pool area of 136.8 m^2. The average water depth was estimated to be 1.2 m [8]. The pools were modelled as one rectangular pool with uniform depth. For an indoor water park, the water temperature should be at least 28 °C [26]. The temperature setpoint for the pool was therefore set to 28 °C.

In the model, no zones were connected to the floor of the Aqualand. To simulate heat losses from the pool to the zones below, an extra zone was added. This zone was made 1 m tall covering the entire floor area of the Aqualand. No ventilation, heating, cooling or internal gains were included in this zone. In IDA ICE, heat losses through the sides of the pool construction are not included. However, this is realistic for the Aqualand as the pools are not lowered into the floor, but are instead raised up [8]. Any heat losses through the sides of the pools would therefore go into the zone.

The evaporation from the pool is affected by the activity in the pool. The activity level is assigned using its own activity factor in IDA ICE. Outside occupancy hours, the activity factor was set to 0.5 for unoccupied pools. Public and school pools have an activity factor of 1.0, while water slides have an activity factor of 1.5 [91]. There are two water slides in the Aqualand [8], and the activity factor was therefore estimated to be 1.2 during occupancy hours.

5.7 Temperature Requirements

According to the Norwegian Maritime Authority, the heating system in accommodation areas should be dimensioned for maintaining a temperature of at least 20 °C [92]. This means that 20 °C should be reached even on the coldest days that are likely to occur. According to SN-NSPEK 3031, the heating setpoint for hotels should be 21 °C during the operating hours, and the cooling setpoint should be 24 °C [88]. These setpoints were used in the model.

For pool facilities, the air temperature should be 2 °C higher than the water temperature to reduce evaporation from the pool [26]. The heating setpoint in the Aqualand was therefore set to 30 °C. The cooling setpoint was set to 32 °C.

For the vehicle decks, the heating setpoint was assumed to be 5 °C, to avoid freezing and unfavourable conditions for the vehicles.

5.8 Ventilation

Several AHUs were included in the model. As mentioned in the literature study in section 2.4, Mein Schiff 3, 4 and 5 have 50 AHUs. Considering that these ships are larger, it was assumed that Color Fantasy has slightly fewer AHUs. However, it is not necessary to include all these AHUs in the model. Including more AHUs will not change the energy use for fans because the total airflow rate stays the same. It will only affect the energy use if different supply air temperatures are chosen for the different AHUs. Zones were therefore grouped together in the same AHU based on the supply air temperature chosen for the zone. Galleys, cabins and the navigation bridge were given their own AHUs to enable easier implementation of the energy saving solutions. A total of 8 AHUs were included in the model.

As a simplification, the supply air temperature was set constant the whole year regardless of the outdoor temperature. The supply air temperature was adjusted to ensure that the temperature in each zone was within the temperature setpoint range as much as possible. In zones with large internal or solar heat gains, it is important to avoid a high supply air temperature because this could lead to large cooling demands in the zone. In zones with large cooling or heating demands, the supply air temperature was therefore decreased or increased accordingly.

It was assumed that mixing ventilation is used in cabins and other zones with low ceilings. Here, a low supply air temperature can be used without negatively affecting the indoor climate, as mentioned in section 2.4.

In public areas with high ceilings, rainfall ventilation or displacement ventilation may be used. To ensure proper ventilation in these areas, the supply air temperature was set 2-6 °C lower than the average temperature in the room, based on the literature study. To account for the zone temperature range being 21-24 °C, the supply air temperature was set to 18 or 19 °C in these zones. In the Aqualand, the supply air temperature was set as low as possible to avoid large cooling demands due to solar heat gains in the summer. As the maximum temperature setpoint is 32 °C, the supply air temperature was set to 26 °C.

In many of the zones, including the cabins, the supply air temperature was set to 18 °C. Table 11 shows the AHUs, which zones they serve and the chosen supply air temperature.

It is unknown if Color Fantasy has CAV or VAV ventilation. Seeing as CAV ventilation is used in the reference ship Mein Schiff 3 and is commonly used in cruise ships in general, it was decided to use CAV ventilation in all zones in the base case. It is also unknown if Color Fantasy has heat recovery in the AHUs. In the base case, the ship was modelled with no heat recovery units. As a simplification, all AHUs were set to only use fresh air supply, including the Aqualand.

Table 11: AHUs included in the model, which zones they serve, and the supply air temperature.

AHU	Zones served	Supply air temp. [°C]
1	Officers' quarters, laundry	10
2	Spa and fitness, extra area	12
3	Promenade and halls, restaurants, casino, shops, taxfree market, conference centre, adventure planet, Burger bar, Teens plaza, observation lounge, night club	18
4	Guest and crew cabins, navigation bridge	18
5	Private dining, show lounge, public bathrooms	19
6	Galleys	19
7	Aqualand	26
8	Car and trailer decks	-

Ventilation rates in the model were based on the literature study in section 2.4. In the Aqualand, the ventilation rate was set to 1.4 l/s per m^2 total ground area, which is the requirement for fresh air supply [26]. The ventilation rate in the laundry and public bathrooms was set to 15 h^{-1}, in accordance with NS-EN ISO 7547 [24]. In the small galleys, the ventilation rate was set to 30 h^{-1}, and in the large galleys it was estimated to 50 h^{-1}. In the other zones, the ventilation rate was set to 36 m^3/h per person based on the requirement from DNV [23]. The ventilation rate was calculated from the maximum number of occupants in each zone. In reality, most of the air would be extracted through bathrooms, galleys, and hallways. As a simplification, the supply and extract rates were set equal to each other in all zones.

For the vehicle decks, the standard air change rate was set to 10 h^{-1} for both supply and extract. This was increased to 20 h^{-1} for 30 minutes during roll on and roll off. No ventilation heating or cooling was included on the vehicle decks.

5.9 Shading

Curtains were included in all cabins. They were estimated as "light, tightly woven internal drapes" in IDA ICE. The schedule for when the curtains are drawn was based on the cabins' occupancy schedule in figure 7, with the curtains being drawn during the night. These curtains and curtain schedule were also used in the officers' quarters.

The choice of shading type for public areas was based on the 3D model [8]. Internal blinds were used in the spa and fitness and the casino, while meeting rooms, restaurants, Aqualand and Teens plaza have curtains. In all these public areas, the shading was assumed to be drawn when there is sun. The remaining public areas have little or no shading, and shading was therefore not included.

5.10 Internal and Thermal Masses

In IDA ICE, internal masses can be used to represent furniture, while thermal masses can represent internal walls and floor slabs inside the zone. According to the IDA ICE user manual, internal masses can significantly impact fast temperature variations, but they can usually be omitted in energy calculations [58]. Therefore, the default setting was used, where 20% of the floor area is covered with furniture. Thermal masses were also assumed to have a small impact on the energy use and were therefore not included in the model.

5.11 Propulsion

The energy use for propulsion was added in the model by using electrical equipment with no heat released to zones. The equipment was added in the trailer decks, but it will not affect the energy use in the zone, and it is therefore arbitrary which zone is used. The ship's average speed on the open sea was estimated to be 18 knots [4]. Closer to Oslo and Kiel it was assumed to be 12 knots. One hour from port, the speed was set to 5 knots. This resulted in the assumed ship speed operational profile shown in figure 15.

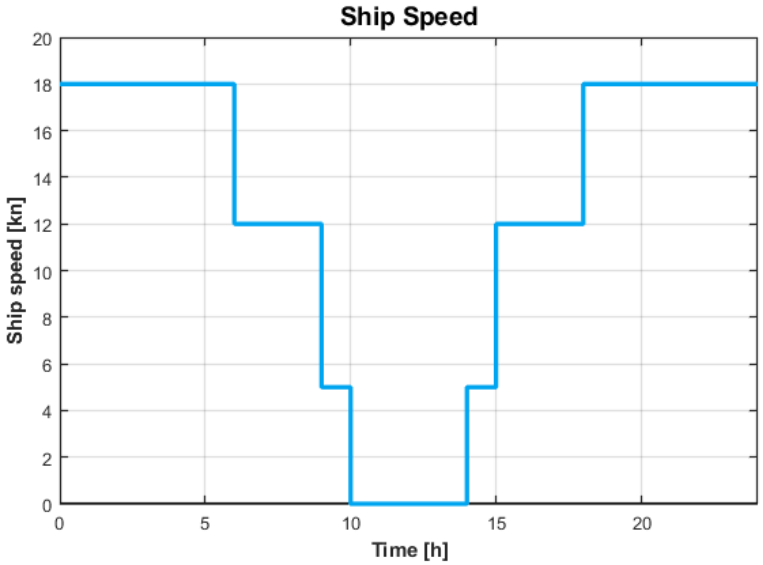

Figure 15: Operational profile for the ship speed.

Based on the ship speed, equation 1 was used to calculate the propulsion power throughout the day. The installed capacity and maximum speed were based on Color Fantasy and were set to 31.6 MW and 22 knots, respectively. Seeing as the real value for the exponent k was unknown, it was assumed to be 3.5. The calculated propulsion power can be seen in figure 16. The propulsion demand was assumed to be covered by electricity produced by the engines.

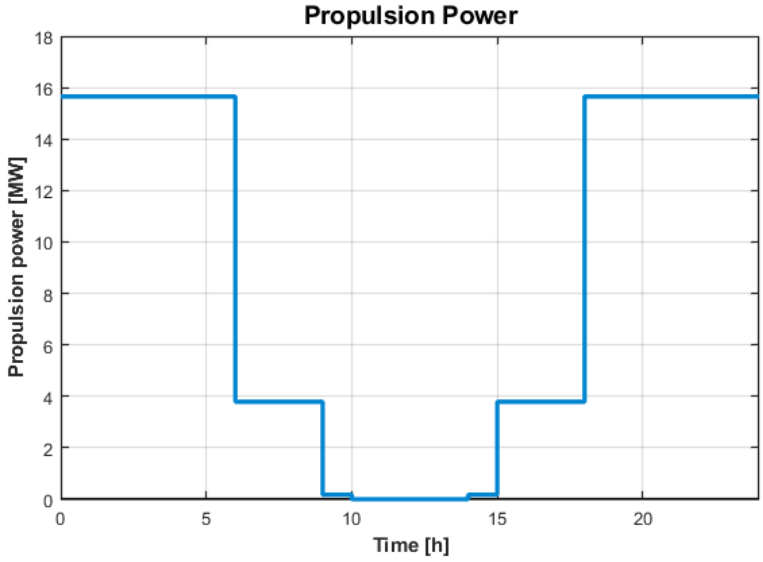

Figure 16: Operational profile for the propulsion power.

5.12 Energy Supply System

An ESBO plant was used in the IDA ICE model, allowing more complex energy supply solutions. All the heating on board is covered by a fuel boiler to find the total heating demands. The cooling system on the ship was modelled as an electric chiller. Both the boiler and chiller were modelled with unlimited capacity.

The heating and cooling rates in fan coils are defined based on a heating supply water temperature of 50 °C and a cooling supply water temperature of 7 °C. The temperature of cold water from the chiller used for zone cooling was therefore set to 7 °C. The supply water temperature for the waterborne heating system was set constant to 60 °C.

Post processing of the energy supply system was then done using a MATLAB script, which is shown in appendix F.1. The total electricity and heating demands were imported from IDA ICE into MATLAB. The cooling systems on board were assumed to have a COP of 3, which was included when calculating the total electricity demand. When the ship is not in port, the electricity produced by the engines was set equal to the electricity demand on board. In port, the engines were assumed to be completely off, and the electricity demand would then be covered by shore power. The efficiency of the electricity from shore power was assumed to be 1.

Daylight Saving Time (DST) is taken into account in the schedules in IDA ICE. Therefore DST also had to be considered in the post processing when deciding whether the ship is in port or at sea.

The engines' electricity production and electrical efficiency were used to calculate the engines' total fuel consumption, which was then used to find the waste heat recovered from the engines. The remaining heating demand was set to be covered by auxiliary boilers, and the boilers' fuel consumption was calculated. Efficiencies and the share of heat recovered from the MGO engines were assumed to be similar to the reference ship Birka Stockholm.

The change in efficiencies at varying load was taken into account. Using a best fit line, a relation for the boiler efficiency in Birka Stockholm was found based on a reference report [15]. This is shown in equation 9 and plotted in figure 17a. Here, the maximum boiler efficiency occurs at a load of 30%. According to the reference report, this is due to boilers in marine applications typically having high efficiency at low loads.

$$\eta_{th,boil} = -0.118\, x_{boil}^2 + 0.0708\, x_{boil} + 0.7891 \tag{9}$$

where $\eta_{th,boil}$ is the thermal efficiency of the boilers and x_{boil} is the load factor, i.e. the ratio of the boiler power to the installed capacity. The installed capacity of the boilers was set to the peak demand over the year. In reality, the installed capacity could be higher to account for unexpected high heating demands due to extreme weather or other problems.

The electrical efficiency for auxiliary engines on Birka Stockholm [15] was used for all electricity demand on the simulated ship, including propulsion. Using a best fit line, equation 10 was found. The plot can be seen in figure 17b.

$$\eta_{el,eng} = -0.0814\, x_{eng}^2 + 0.1612\, x_{eng} + 0.3486 \tag{10}$$

where $\eta_{el,eng}$ is the electrical efficiency of the engines and x_{eng} is the load factor.

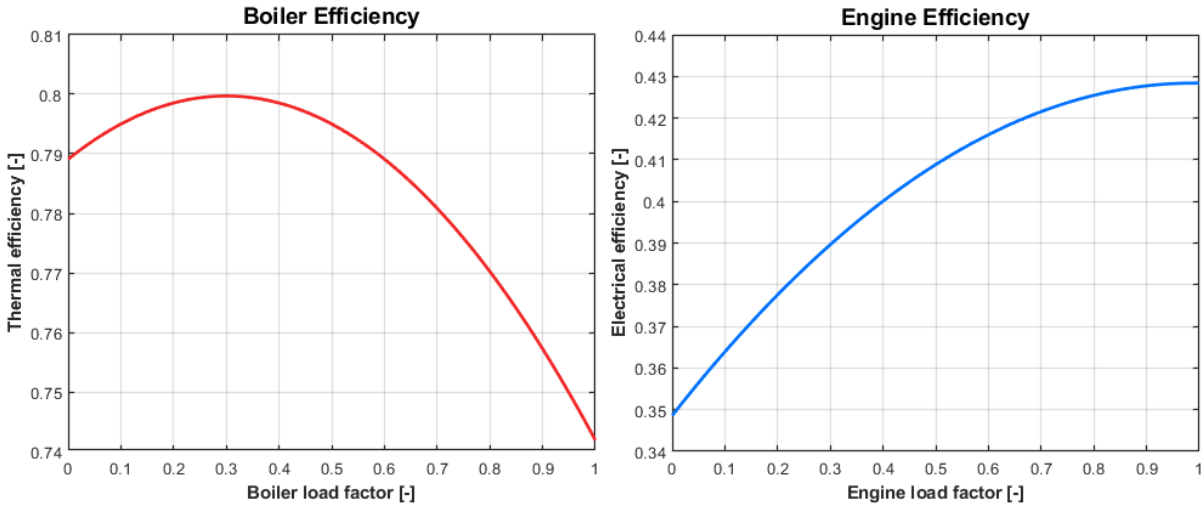

(a) Thermal efficiency for boilers.

(b) Electrical efficiency for engines.

Figure 17: Efficiencies at part load used in the MATLAB script.

The amount of heat recovered from the MGO engines was based on the thermal efficiency for the auxiliary engines on Birka Stockholm [15]. The equation for the thermal efficiency was multiplied by a correction factor of 0.189 so that the share of the engines' total fuel consumption recovered as heat in the base case was 9.38%, as calculated for Birka Stockholm in appendix B. The resulting relation can be seen in equation 11 and is shown graphically in figure 18.

$$\eta_{heat,rec} = 0.189\ (0.0812\ x_{eng}^2 - 0.1611\ x_{eng} + 0.5519) \tag{11}$$

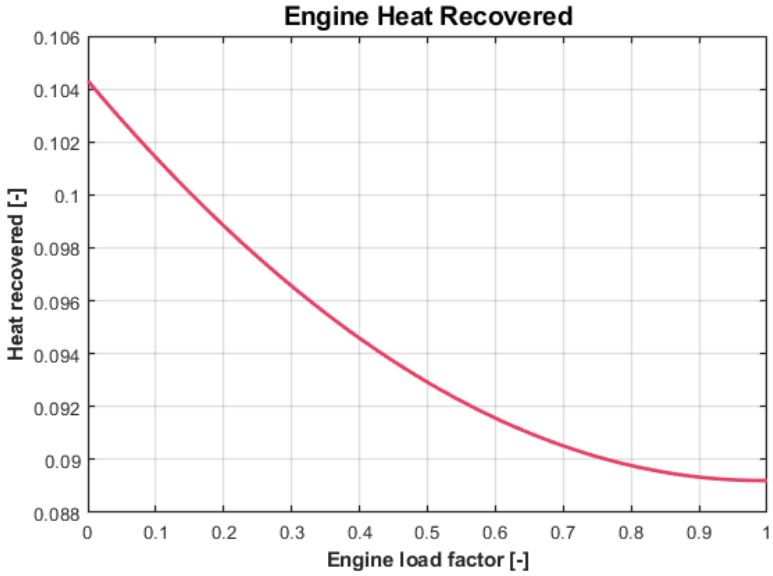

Figure 18: Share of the engines' fuel consumption recovered as heat, for the MGO ship.

On the LNG ship, gas boilers were assumed to have the same efficiency as the MGO boilers. LNG engines were assumed to have the same electrical efficiency as the MGO engines. However, more heat can typically be recovered from LNG engines, as mentioned in section 3.10. It varies significantly

between different ships how much of the thermal energy from the engines can be recovered, but it is typically around 10 percentage points higher for LNG engines than for diesel engines [16]. Based on this, the share of the engines' fuel consumption recovered as heat was calculated to 14.1% for the LNG ship. Detailed calculations are seen in appendix C. For the LNG ship, the correction factor in equation 11 was therefore set to 0.283 to achieve an average amount of heat recovered of 14.1%.

5.13 Hot Storage Tank

The use of a hot water storage tank was included in the MATLAB script, shown in appendix F.1. The tank could be charged using a heat exchanger between the tank and the waterborne heating system. When using the tank for DHW, water from the tank would be mixed with cold freshwater to reach the desired temperature. For uses other than DHW, the tank could be discharged using a heat exchanger.

First, the maximum heat storage capacity of the tank was calculated using equation 2. The water level in the tank, and thus the water volume, was assumed to be constant. The density of water was set to 1000 kg/m^3 and the specific heat capacity of water was set to 4180 J/(kg K). To avoid legionella in the tank, the temperature was set to be between 50 and 80 °C, based on the literature study in section 2.13.

In the summer, there is sometimes recovered heat available from the engines that is not being utilised. Storing this unutilised heat in the tank could reduce overall fuel consumption. The hot storage tank was sized based on the base case with MGO engines and boilers. To store all unused recovered heat throughout the year, the necessary tank volume in this case was found to be 150 m^3. Based on the examples of thermal energy storage on ships mentioned in section 2.13, this was considered a reasonable size, and this tank size was therefore used further. The tank has an energy storage capacity of 5.23 MWh.

In the base case, there is no extra recovered heat available in the winter. Instead, it is useful to use the tank for peak shaving to reduce the maximum power delivered by auxiliary boilers and reduce the needed boiler size. The operation of the tank was therefore separated into summer and winter operation modes. Winter mode is used in the months November through February, and the remaining months use summer mode.

In the summer, the tank should be fully discharged to 50 °C as often as possible, to enable storage of any unused recovered heat. The base level for the tank was then set to zero. For winter mode, the base level for the tank was set to 33%, corresponding to a temperature of 60 °C. This means the tank temperature is at 60 °C as often as possible to enable shaving of any large peak that occurs. The base level was set relatively low to allow for storage of unused recovered heat in the winter for the LNG ship and in the energy efficiency scenarios. This tank level was high enough to not impact the peak shaving in this case. If larger peaks in heating demand are expected, the winter base level should be increased.

In both modes, the tank is charged when there is extra recovered heat available. When there is a demand requiring heat from the auxiliary boilers, the tank is discharged down to the base level. A peak shaving level is set for the boiler in the winter, and the tank is charged when the boiler power is below this level. When the boiler power is above the shave level, the tank is discharged.

The chosen tank volume is large enough to reduce the boiler peak power by 3.1 MW. This was therefore set as the maximum for charging and discharging. This was considered a realistic heating power for the heat exchanger, based on the heat exchanger power used in [46] as mentioned in section 2.13. The peak shaving level was then set 3.1 MW below the annual peak boiler demand.

In each time step, the charging and discharging rates are used to calculate the new energy level of the storage tank. This was done using equations 12 and 13. Heat losses from the tank were assumed to be small and were therefore neglected.

$$\Delta E_{tank}(i) = (P_{charge}(i) - P_{discharge}(i))\ dt \tag{12}$$

where $\Delta E_{tank}(i)$ [MWh] is the change in energy level of the storage tank in the current time step, $P_{charge}(i)$ [MW] is the charging rate, $P_{discharge}(i)$ [MW] is the discharging rate, and dt [h] is the length of each time step i.

$$E_{tank}(i) = E_{tank}(i-1) + \Delta E_{tank}(i) \tag{13}$$

where $E_{tank}(i)$ [MWh] is the total energy in the tank in the current time step, and $E_{tank}(i-1)$ [MWh] is the energy in the tank in the previous time step.

Finally, the temperature change in the tank was calculated using equation 14, based on equation 2. Equation 15 was used to find the new temperature in this time step. For simplification, it was assumed that the water in the tank has a uniform temperature.

$$\Delta T_{tank}(i) = \frac{\Delta E_{tank}(i)}{\rho\ V\ c_p} \tag{14}$$

where $\Delta T_{tank}(i)$ [K] is the change in tank temperature in the current time step. $\Delta E_{tank}(i)$ [J] is the change in tank energy, ρ [kg/m^3] is the density of water, V [m^3] is the tank volume and c_p [J/(kg K)] is the specific heat capacity of water.

$$T_{tank}(i) = T_{tank}(i-1) + \Delta T_{tank}(i) \tag{15}$$

where $T_{tank}(i)$ [°C] is temperature in the tank in the current time step, and $T_{tank}(i-1)$ [°C] is the tank temperature in the previous time step.

In reality, maintaining an exact peak shaving level is not important as long as the demand for heat from boilers is below the boilers' maximum capacity. The shave level achieved could however be used to find the necessary boiler size and determine whether the size of boilers on the ship could be reduced.

When investigating energy saving solutions, the hot storage tank size was kept the same. The peak shaving level was adjusted to the lowest it could be in each case.

5.14 Energy Efficiency Scenarios

Case 1 - Heating setback in port and at night

When the ship is in port, most of the guests were assumed to leave the ship. In addition, most zones were assumed to be unoccupied at night. Reducing the heating during these times was therefore investigated as an energy saving solution. The Aqualand was not included because reduced air temperature would increase evaporation from the pools. Heating setback in port was therefore used in all zones except the Aqualand. Night setback from midnight to 6:00 was included in all zones except the Aqualand, the cabins and the navigation bridge, as occupants will stay in the cabins and navigation bridge at night.

Heating setback was achieved by reducing the supply air temperatures to 10 °C. The supply air temperature was not reduced in the officers' quarters and the laundry, as these already have low supply temperatures. Additionally, the supply water temperature for zone heating was reduced from 60 to 10 °C, to limit the heating from fan coils. This strategy was only implemented during the winter months, from November through February, when the outdoor temperature is almost always below 10 °C.

Case 2 - Turning off vehicle deck heating in port

Seeing as the ventilation rate on the vehicle decks is doubled during roll on and roll off, the heating demand is significantly increased at these times. Turning off heating on the vehicle decks during roll on and roll off could decrease the total heating demand and be used as an energy saving solution. It was assumed that there are no vehicles on the vehicle decks when in port, and the heating was therefore turned off for the entire port stay period. The heating was turned off in the model by decreasing the heating setpoint to -30 °C.

Case 3 - Increased insulation

The insulation in the external constructions was increased from 150 to 300 mm. The insulation thickness in internal constructions was not changed, as these were considered to be sufficiently insulated.

Case 4 - Improved windows

In the Aqualand, 4-pane glazing was implemented, which means the U-value decreased from 1.9 to 1.4 W/(m^2K). In all other windows, 3-pane glazing was used, so the U-value decreased from 2.9 to 1.9 W/(m^2K). Additionally, the size of large windows was reduced by 50% in the halls, restaurants, conference centre, Aqualand, observation lounge, and the spa and fitness.

Case 5 - PCM layers in walls

IDA ICE allows the integration of PCM layers in constructions. This can even out variations in heating and cooling demands, and thus reduce the energy use. For this energy saving solution, a 2 cm thick PCM layer was implemented in all external and internal walls, based on the literature study in section 2.13. For external walls, the PCM layer was placed on the inside of the sandwich structure, as this gave the largest energy savings. This was also done for internal walls not connected to other zones. For internal walls connected to other zones, the PCM layer was divided in two and placed on either side of the sandwich structure.

The default PCM in IDA ICE has thermal hysteresis with a melting temperature around 2 °C higher than the solidification temperature. The behaviour of the material is described using a series of temperature coordinates, and the average specific heat capacity between these temperatures. The melting temperature for the default PCM was adjusted by shifting the temperature coordinates, while keeping the average specific heat capacities the same.

Seeing as the phase change occurs over a small temperature interval, the melting point was defined as the temperature with the highest average specific heat capacity. Based on the literature study in section 2.13, several melting temperatures around 21 and 24 °C were tested. These are the heating and cooling setpoints for all zones in the ship, except the Aqualand. A melting temperature around 24 °C gave the lowest total energy consumption for the ship and was therefore used in this case. The properties for this PCM with the shifted melting point can be seen in appendix G. To account for the higher temperature in the Aqualand, the melting point for the PCM in these walls was set to 32 °C, i.e. the cooling setpoint.

Because the PCM layer was added to the walls in addition to the existing insulation, the U-value of the walls was slightly decreased. However, the PCM layer is thin and has a high thermal conductivity compared to the insulation. Therefore, the reduction in U-value was small.

Case 6 - Ventilation heat recovery

Heat recovery units were included in all AHUs, except for the vehicle decks and galleys. Vehicle decks were not included as they in reality have large fans for ventilation instead of AHUs. Galleys usually do not have ventilation heat recovery, as mentioned in the literature study in section 2.5. The efficiency of the heat recovery units was set to 80%, based on the literature study.

When considering the economic profitability of this energy saving solution, it was assumed that every AHU would be fully replaced. This would give easier installation and likely reduce installation costs. Systemair's largest AHUs with capacity 5250 m^3/h were used, as mentioned in section 2.5. An estimate for investment and installation costs was provided by Scandinavian technical contractor GK and is shown in appendix H [93]. The total cost per AHU is 132,500 NOK, not including VAT. These costs were based on typical commercial buildings and were assumed to be similar in cruise ships. The total supply airflow rate for the relevant AHUs was simulated to be around 257,000 m^3/h. To achieve this total airflow rate, 49 AHUs were required, which gives a total investment cost of 6.49 MNOK.

According to Fosen Ventilasjon, maintenance costs are very similar for AHUs with and without a heat recovery unit [94]. The maintenance costs were therefore assumed to not change after implementing this solution. Based on a previous master's thesis, the economic lifetime of the AHUs was estimated to be 15 years [33].

Case 7 - VAV Ventilation

As mentioned in section 2.6, the recommended ventilation strategy varies with the airflow rate in the room. Rooms with airflow rates below 100 m^3/h were therefore left with CAV ventilation. This includes the navigation bridge, officers' quarters and many of the cabins. For rooms with airflow rates between 100 and 500 m^3/h, occupant-controlled ventilation with motion sensors was used. This includes the smallest shop, private dining, extra area, 14 m^2 and 24.5 m^2 cabins, and most 10.5 m^2 cabins. Rooms with airflow rates above 500 m^3/h were given DCV with combined temperature and CO_2 control. This was done for the remaining zones, which includes most public areas and the conference centre.

The minimum ventilation rate for all the VAV strategies was set to 0.7 $m^3/(h\ m^2)$, based on the literature study in section 2.6. For DCV, the maximum airflow rate was set 50% higher than the one used for CAV ventilation, so that less local cooling is needed to avoid overheating. The maximum CO_2 setpoint was set to 1000 ppm, based on the literature study.

For galleys, bathrooms and the laundry with specific ventilation requirements, VAV ventilation with a schedule was implemented. During the whole occupancy period, the ventilation rate was left the same as in the base case, according to the requirement. Otherwise, the airflow rate was set to 10% of this. The ventilation was not changed in the Aqualand and on vehicle decks, due to the requirements.

For the profitability analysis, it was assumed that the existing AHUs and ductwork could be left as it is, and that only additional controllers, silencers and sensors would be needed. Based on meeting rooms and recreation areas with DCV in a previous master's thesis, it was estimated that there are 0.1 VAV controllers and 0.1 silencers per m^2 [33]. For each zone, the number of components was rounded up to the nearest whole number. It was assumed that all rooms would need only one sensor each, to reduce total costs. For the rooms with DCV, the cost of an additional CO_2 and temperature sensor for the supply duct was added, based on the literature study in section 2.6.

Investment and maintenance costs were based on the reference master's thesis and are mentioned in section 2.6. Appendix I shows the chosen ventilation strategies and the total costs for each zone. The total investment costs for this energy saving solution were 31.6 MNOK. Installation costs are not included here, and they can be difficult to determine because they vary significantly for different

ventilation systems [33]. The additional annual maintenance costs for the VAV solution were set to 2 NOK/m^2. This gave total additional maintenance costs of 87,585 NOK for the whole area covered by the solution. All additional components needed for VAV ventilation were set to have an economic lifetime of 15 years, based on the reference thesis [33].

Case 8 - Heat Pump

IDA ICE enables implementation of ambient air-to-water and brine-to-water heat pumps. Seeing as the ship moves, the ground or sea water could not be used as the heat source for heat pumps. Cruise ships have large cooling demands related to the propulsion system, and water from these systems was considered the most appropriate heat source for heat pumps. This would increase the heat recovered from the engines. This cooling water would also have a more stable temperature throughout the year compared to outdoor air, giving a higher average COP. However, these cooling demands were not included in IDA ICE, and it would therefore be challenging to consider this heat source.

It was therefore decided to use outdoor air as the heat source in air-to-water heat pumps. Having multiple large air-source heat pumps on the ship would take up a lot of space and could therefore be challenging to implement. Air-source heat pumps are unlikely to be the best heat pump solution for cruise ships, but could give an indication of the potential for heat pump solutions in general.

Heat pumps in the IDA ICE model cannot be used to cover the steam demand for galleys and laundry, as these were modelled as equipment. The thermal power demand for accommodation heating, including pool heating, and DHW was therefore used. The net thermal power demand for the base case was found by running a heating simulation with 100% of the internal gains and solar radiation in the model. The design day data for Fornebu in appendix A was used, as this had the lowest minimum winter temperature. For accommodation heating and DHW combined, the power demand was 11.6 MW.

Due to high peak heating demands, the power coverage factor was set quite low at 27%. This gave a heating capacity of 3.12 MW for the heat pump. Based on the duration curve for accommodation heating and DHW, this gave an energy coverage factor of 93%, which was considered appropriate based on the literature study in section 2.14. An air-to-water heat pump with this capacity was inserted as the base heating in the model, while a fuel boiler with unlimited capacity was kept as the peak heating.

Seeing as air-source heat pumps are unrealistic for implementation in a cruise ship, it was challenging to find specific investment costs for this solution. An estimate for the heat pump's investment costs was based on typical specific investment costs for heat pumps of various sizes. Based on prototype and demonstration heat pump systems, SINTEF Energy Research has found that heat pump units with heating capacity 3 MW have specific investment costs around 2000 NOK/kW [95]. Installation costs are likely not included in this price.

For the chosen heat pump, this gives investment costs of 6.24 MNOK. The source is from year 2000, and inflation was therefore taken into account. This gave total investment costs around 9.5 MNOK. Some additional equipment is likely needed for the heat pump solution, and the price could therefore be higher. There are large uncertainties related to these investment costs. The annual maintenance costs were assumed to be 2% of the investment costs [96]. The economic lifetime of the heat pump was estimated to be 15 years, based on the literature study in section 2.14.

Case 9 - PV Panels

In order to utilise as much solar radiation as possible throughout the day, it was considered beneficial to place the PV panels horizontally on the ship roof. PV panels could also be placed on the sides of the ship, between cabin windows. These panels would have higher production than the roof panels when

the sun is low in the sky, but low production when that side of the ship is facing away from the sun. To investigate the difference in production, identical PV panels were placed on the roof and on one side of the ship. Seeing as the ship orientation changes, the annual production will be the same for panels placed on the starboard and port sides of the ship. The panels placed on the roof gave a total annual production around 50% higher than the panels on the side of the ship.

Based on this, it was decided to place PV panels on the ship roof. It was estimated that half the roof of the observation lounge could be covered with PV panels. This amounts to an area of 450 m^2. The PV panels used in the model were based on SunPower's 360 W PV panels, mentioned in the literature study in section 2.15. Even though PV panels for use at sea might have to be even more robust than these panels, they were expected to have a similar efficiency and warranty. The panel efficiency was therefore set to 22.2%.

To achieve the chosen PV panel area, 276 of SunPower's PV panels are needed, which gives an installed capacity of 99.36 kW. Seeing as the price of PV panels is expected to drop in the future, the price was assumed to be in the lower end of the range found in section 2.15. The price was therefore set to 2.8 USD/W, giving total investment costs of 2.4 MNOK. Based on the literature study, the maintenance costs were expected to be small and were therefore neglected. The economic lifetime was set to 25 years, based on the warranty for SunPower's panels.

In post processing, the electricity delivered by engines and shore power was reduced due to the production from PV panels. Otherwise, the script was kept the same as in the base case.

Case 10 - Hot storage tank for heat demands in port

In order to facilitate zero emissions in port and reduce local pollution, it is important to reduce the use of boilers in port. The energy storage section of the MATLAB script was therefore rewritten to use the storage tank instead of the boiler in port. This is shown in appendix F.2. To cover the entire heating demand with the hot storage tank in port, the maximum discharge rate had to be increased to the peak heating demand in port, which was 12.3 MW. The maximum charging rate was left at 3.1 MW.

In port, the tank will be discharged as much as necessary to cover the heating demands. The charging was separated into summer and winter modes. At sea in the winter, the boiler will be used to charge the tank until it is full. In the summer, the maximum capacity for the tank was set to 75%. At sea, any unused recovered heat from the engines is first used to charge the tank. Then, the boilers will continue charging the tank until it is 75% full. This means that there is always capacity available in the tank to utilise unused heat from the engines in the summer.

The tank volume was increased until the boilers were no longer needed to cover the heating demands in port. This gave a tank size of 1105 m^3 with a storage capacity of 38.5 MWh. In addition, it was investigated how much the use of the boiler in port was reduced when using a tank with size between 0 and 1105 m^3.

6 Results

6.1 Initial Model

Figure 19 shows the heating demand for accommodation throughout the year. This includes heating in the AHUs, zone heating from fan coil units and heating of water in pools. The peak heating demand is 11.9 MW, which is significantly higher than most other peaks. The peak heating demand for a typical winter day was estimated to be 7.5 MW, or 3.13 kW/passenger. This is significantly higher than the peak heating demand for Birka Stockholm, which is 2.27 kW/passenger, as mentioned in section 4.1.

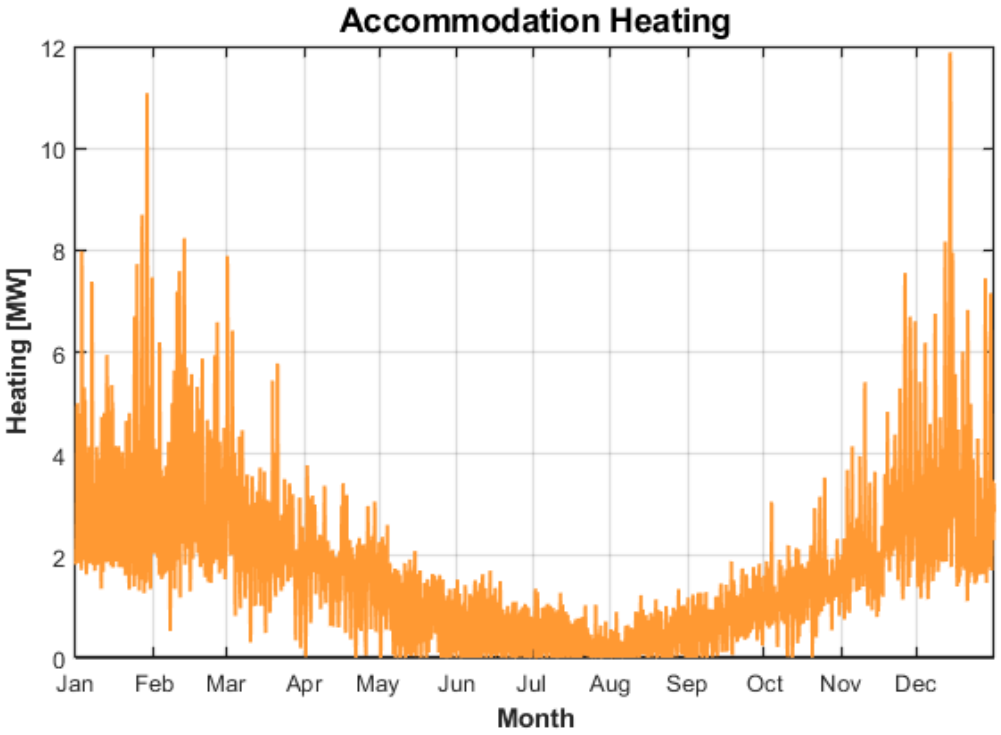

Figure 19: Accommodation heating demand throughout the year, with unlimited heating.

The duration curve in figure 20 shows that there is a heating demand throughout the whole year, which is typical for cold climates. In the combined weather file, the temperature frequently goes below 18 °C in the summer, which will require heating in most of the AHUs. In zones with small internal heat gains, space heating is also needed to bring the supply air temperature up to the zones' setpoint temperature.

Figure 21 shows the accommodation heating demand per passenger as a function of the outdoor temperature. The resolution of this graph is 1 hour due to the resolution of the temperature data. The graph shows that the heating demand clearly depends on the outdoor temperature. There are two significant breaks in the graph. Below 18 °C, heating is needed in many of the AHUs to bring the temperature of the supply air up to the desired level.

Below 4 °C, the slope of the curve increases even more. This is caused by heating on the vehicle decks where the heating setpoint is 5 °C. The reason the slope does not increase until the outdoor temperature is below 4 °C could be the heat supplied to the vehicle decks from equipment and lighting. The spread in the data points below 4 °C is due to increased heating demands during roll on and roll off when the ventilation rate on vehicle decks is doubled.

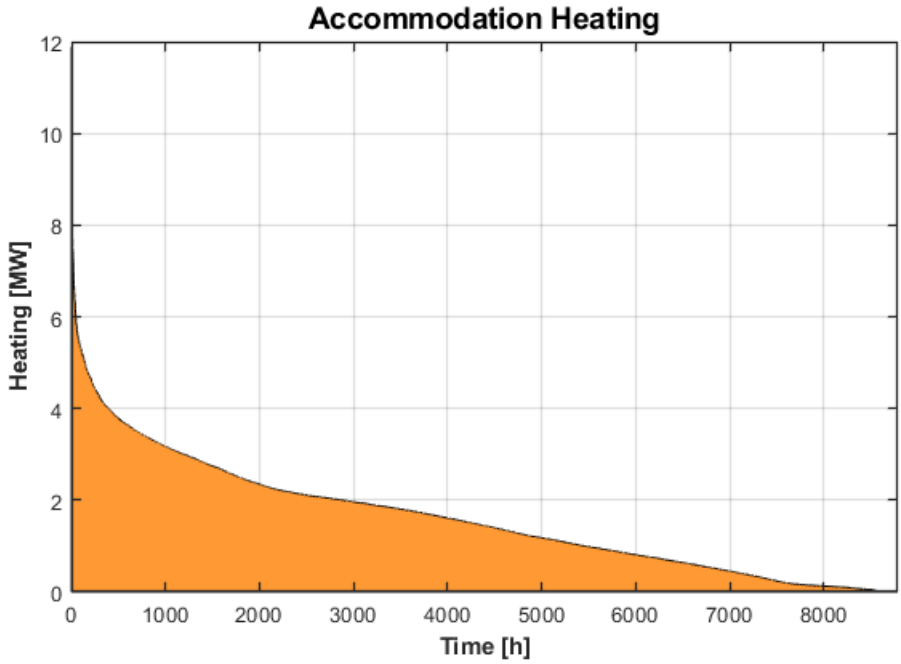

Figure 20: Duration curve for the accommodation heating demand, with unlimited heating.

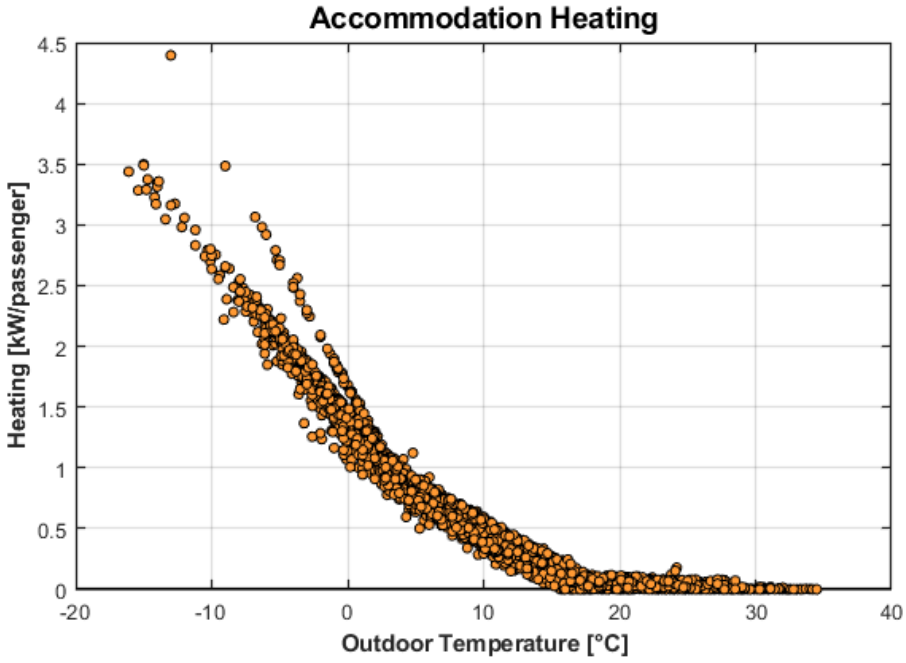

Figure 21: Accommodation heating demand as a function of outdoor temperature, with unlimited heating.

Figure 22 shows the total cooling demand throughout the year. This includes cooling in the AHUs and zone cooling from fan coils. The cooling demand is mainly in the summer months, with very low demand during the winter. The large equipment loads in galleys and laundry do not cause large cooling demands due to high ventilation rates in these zones.

The peak cooling demand is 2.53 MW, or 1.05 kW/passenger. As mentioned in section 4.1, the large cruise ship has a peak cooling power of 3.44 kW/passenger for a week in July. This is over three times larger than the peak cooling demand for the simulated ship. If a COP of 3.0 is included for the simulated

ship, the difference would be even larger. The large cruise ship is however expected to have a much higher cooling demand, as it sails in the Mediterranean Sea during July.

As mentioned in section 4.1, Birka Stockholm has a peak cooling demand of 0.67 kW/passenger for a typical summer day. Based on figure 22, the peak cooling demand for a typical summer day was estimated to be 2 MW, or 0.83 kW/passenger. This is thus higher than the reference ship.

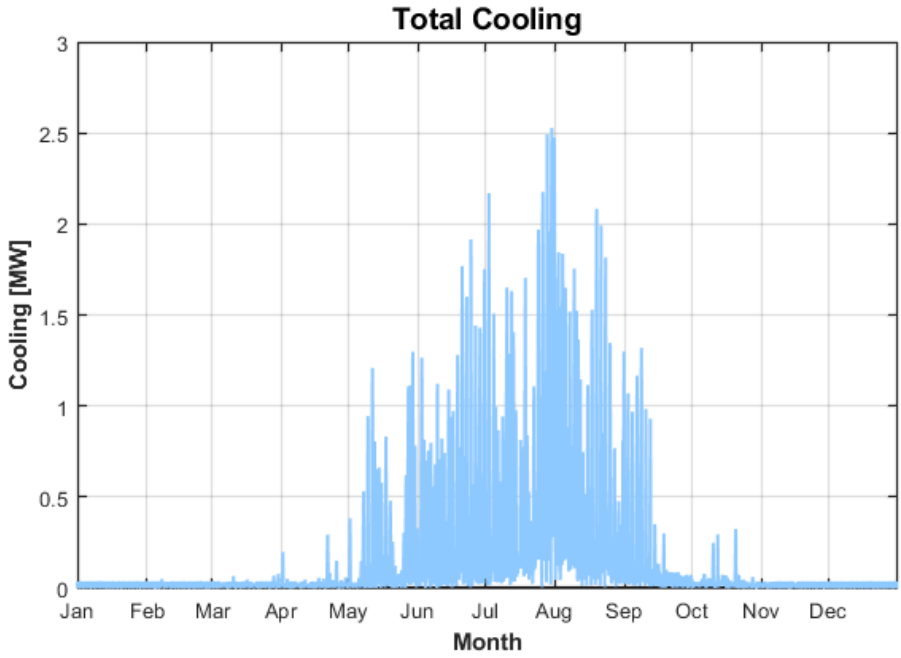

Figure 22: Total cooling demand throughout the year, with unlimited cooling.

The duration curve in figure 23 shows that high cooling demand occurs a relatively small part of the year. This is because the ship sails in a cold climate, and cooling is mainly needed during the summer months.

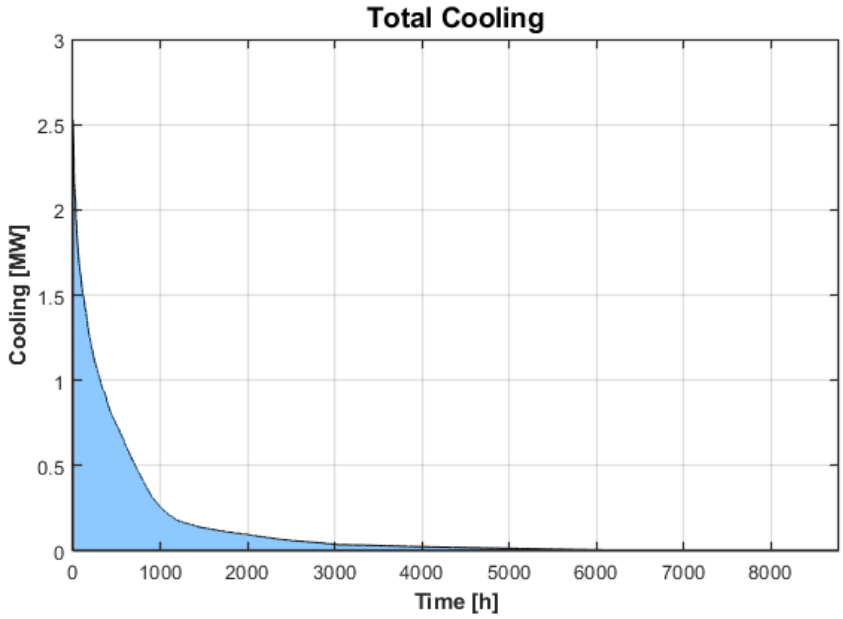

Figure 23: Duration curve for the cooling demand, with unlimited cooling.

Figure 24 shows the total cooling demand per passenger as a function of the outdoor temperature. Again, the resolution is 1 hour. The figure shows that the cooling demand increases significantly at outdoor temperatures above 18 °C. Above this temperature, the cooling demand is also largely dependent on the outdoor temperature. This is because 18 °C is the supply air temperature in many of the zones, and temperatures above this will require cooling in most of the AHUs.

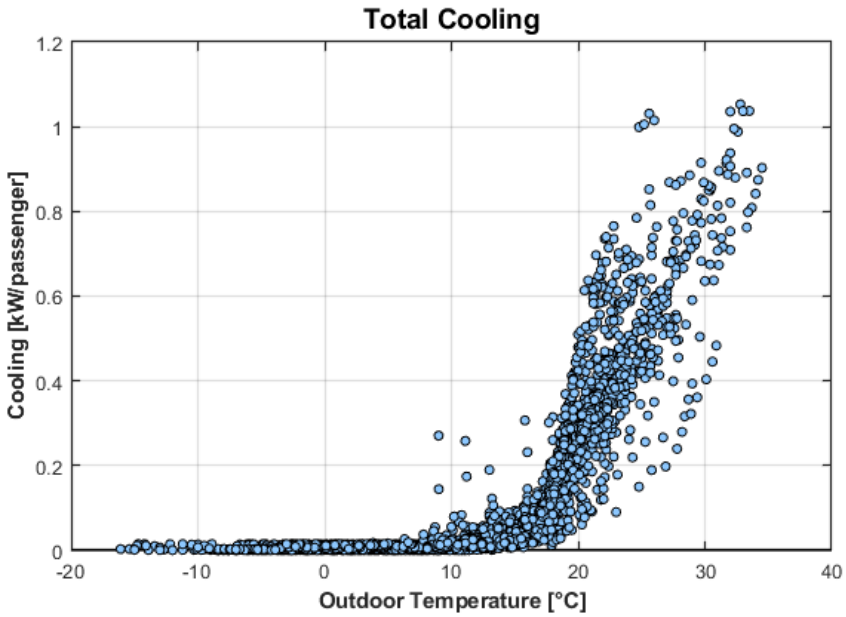

Figure 24: Cooling demand as a function of outdoor temperature, with unlimited cooling.

Figure 25 shows a duration curve for the steam demand throughout the year. This includes the steam demands in galleys and laundry. These demands are the same every day due to the schedules used in IDA ICE. The peak demand is 5.2 MW, which occurs in the evening when steam demands are high in all galleys and relatively high in the laundry.

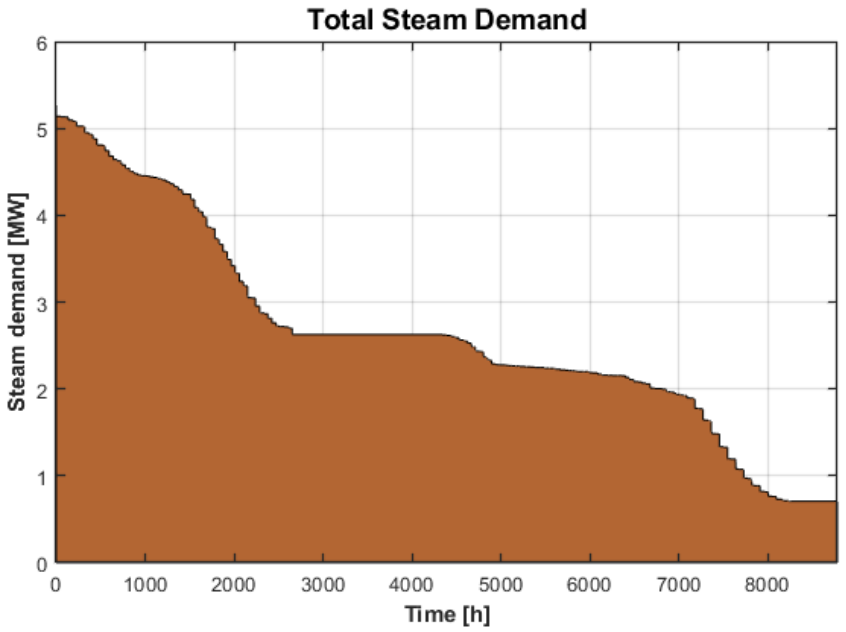

Figure 25: Duration curve for the steam demand in galleys and laundry.

Figure 26 shows a duration curve for the propulsion demand. Again, the demand is the same every day of the year. As expected, the peak consumption matches the peak in the propulsion power schedule in figure 16. The transition between different propulsion powers is not as sharp here due to automatic smoothing in IDA ICE.

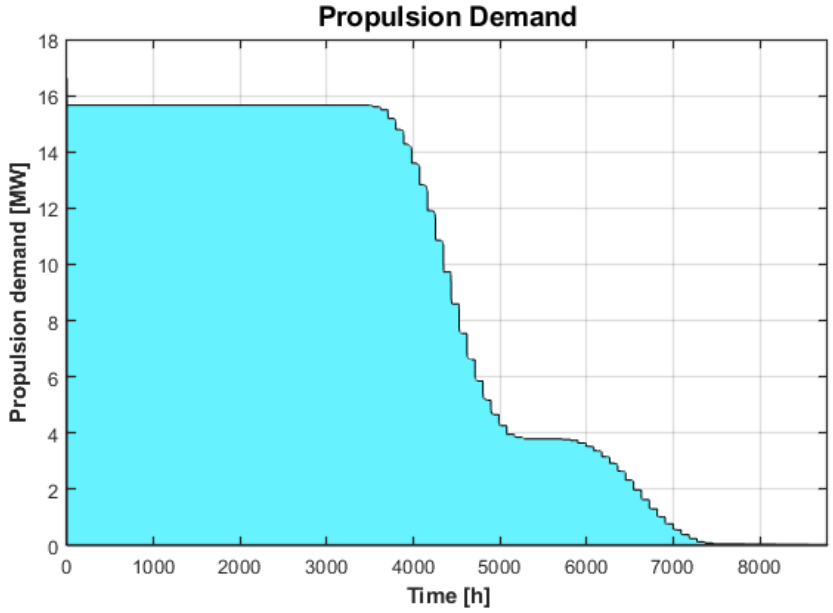

Figure 26: Duration curve for the propulsion demand.

In addition to cooling and propulsion, the electricity use on board includes equipment and lighting, as well as fans and pumps in the HVAC systems. Equipment, lighting and fans have the same electricity consumption every day due to the schedules in IDA ICE. The consumption for pumps varies depending on the heating and cooling demands. Figure 27 shows a duration curve for the HVAC auxiliary electricity demand, i.e. fans and pumps. The highest peaks in this graph are caused by the ventilation rate on vehicle decks being increased for a total of one hour every day during roll on and roll off.

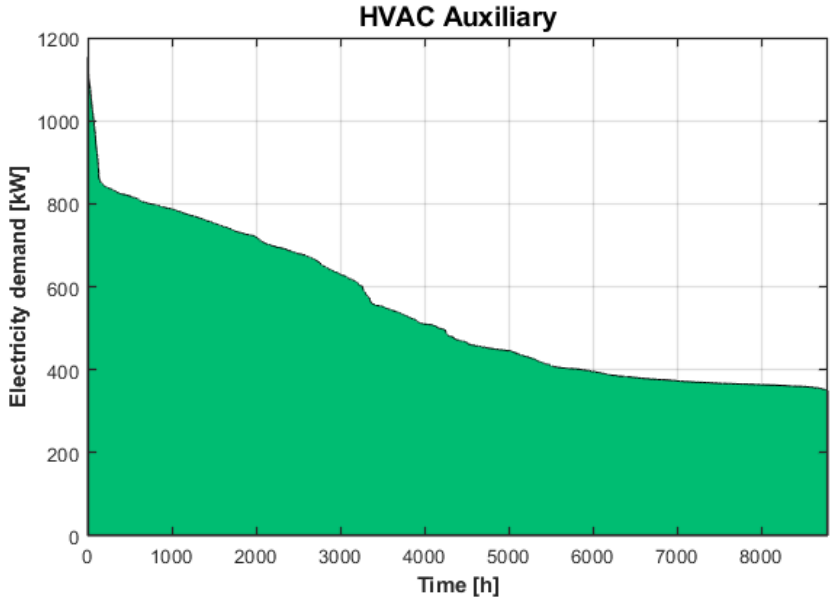

Figure 27: Duration curve for the HVAC auxiliary electricity demand.

The duration curve in figure 28 shows the electricity demand for lighting and equipment. Compared to the other energy demands on the ship, the demand for lighting and equipment is relatively small.

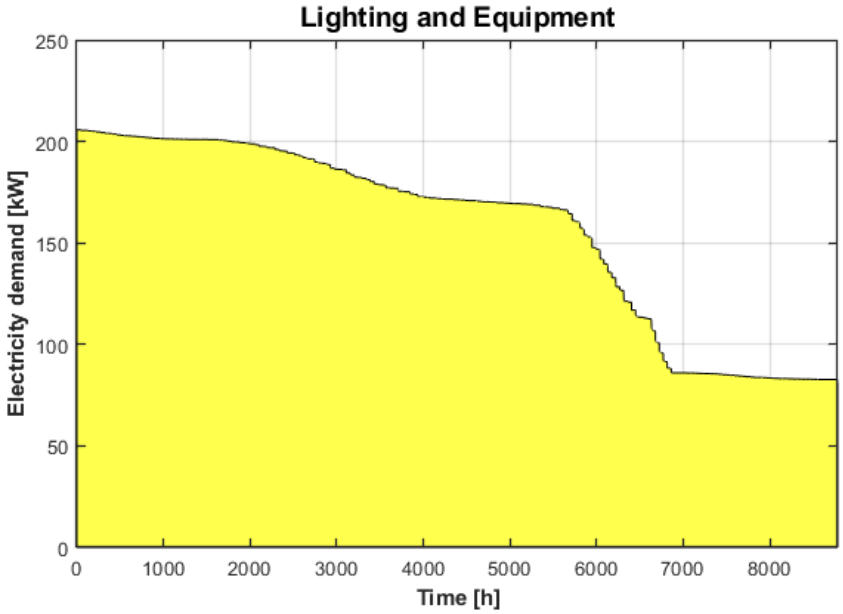

Figure 28: Duration curve for the lighting and equipment electricity demand.

Figure 29 shows the duration curve for the DHW heating demand. The demand is the same every day due to the schedule used in IDA ICE. The peak DHW demand is 684 kW, or 0.29 kW/passenger. This is much lower than the peak demand for hot water heating in Birka Stockholm at 1.33 kW/passenger, as mentioned in section 4.1.

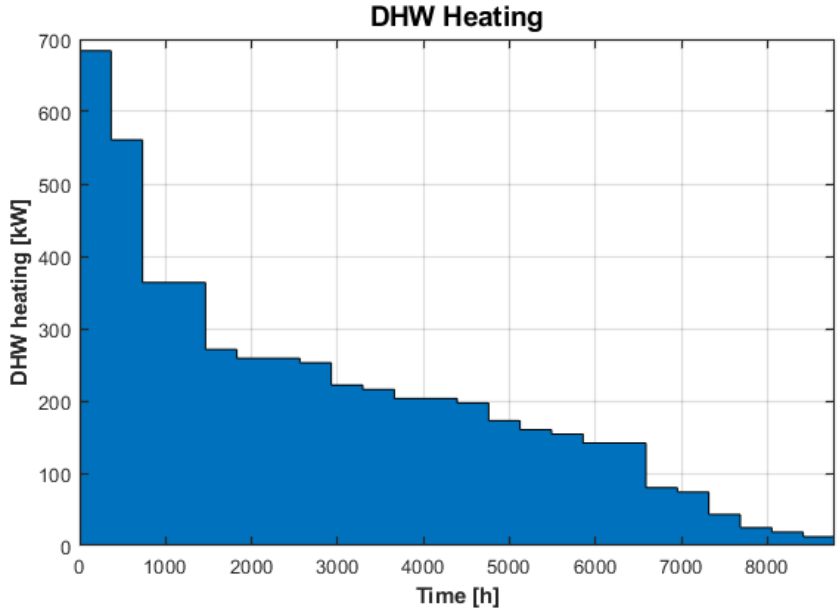

Figure 29: Duration curve for the heating demand for DHW.

It is possible that the hot water heating on Birka Stockholm includes pool heating. However, the peak demand for pool water heating in the simulated model was 0.02 kW/passenger. Therefore, this would likely not significantly impact Birka Stockholm's hot water heating demand, unless Birka Stockholm

has a large number of pools. The simulated peak DHW demand is also lower than the peak demand in the large cruise ship at 0.52 kW/passenger. It is possible that the schedule used in IDA ICE does not accurately represent the DHW use on cruise ships, and that the demand should be higher.

Figure 30 shows the annual propulsion demand per passenger for the simulated ship and reference ships. The simulated ship has a much higher propulsion demand per passenger compared to the reference ships. This can be explained by the simulated ship travelling a much larger distance per year, as seen in table 5. To take this into account, the energy use per ALB-km was calculated based on section 3.8, and is presented in figure 31. The simulated propulsion demand is 0.156 kWh/ALB-km, which is between the two reference ships. This is therefore considered a reasonable result. This shows how important it is to use appropriate units when comparing the energy use on cruise ships.

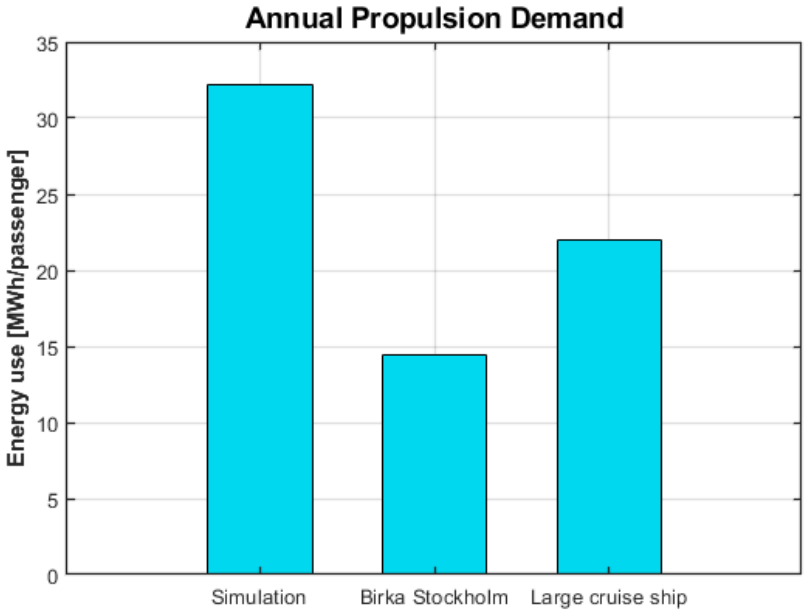

Figure 30: Annual propulsion demand per passenger for the simulated ship and the reference ships.

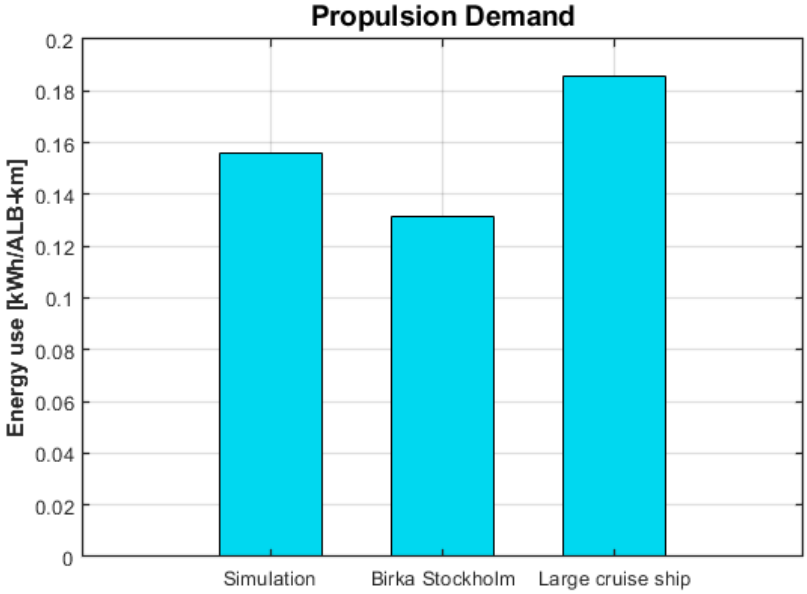

Figure 31: Propulsion demand per ALB-km for the simulated ship and the reference ships.

Figure 32 shows the annual energy consumption per passenger for the hotel system on the simulated ship and reference ships. For Birka Stockholm, the energy use for fuel and tank heating is also included. Seeing as the hotel system's energy consumption is usually similar in port and at sea, it was considered most appropriate to compare the energy use per passenger and not per ALB-km. Appendix K.1 shows the exact results, and includes more detailed energy use categories for the simulated ship.

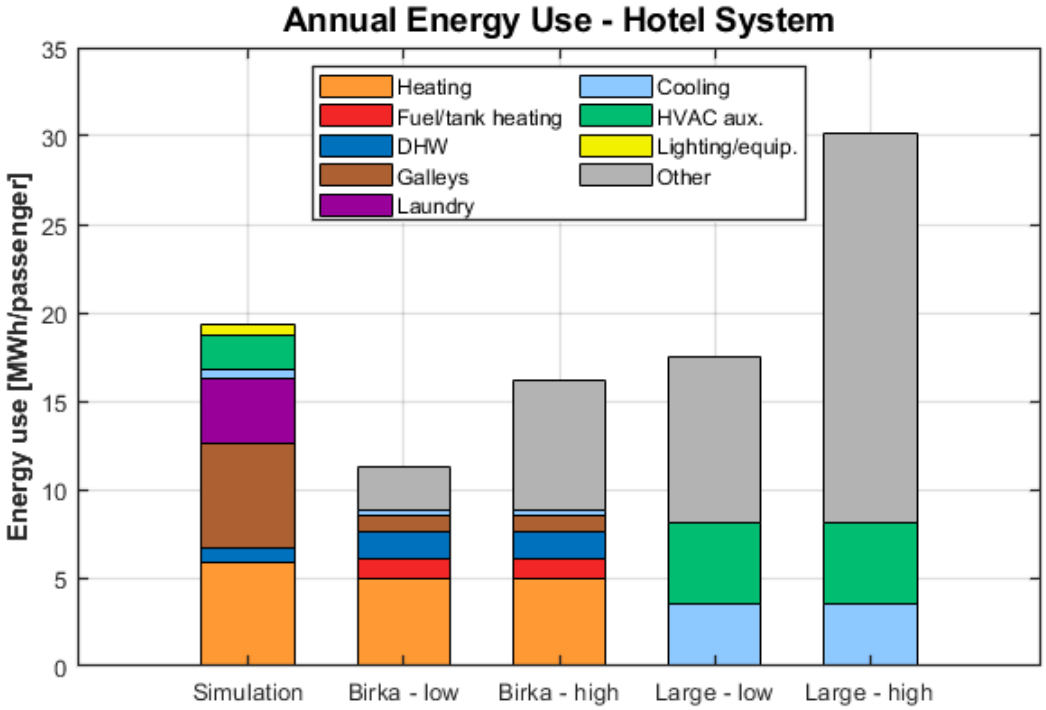

Figure 32: Annual energy consumption for the hotel system on the simulated ship, and high and low estimates for the reference ships.

When comparing the simulated ship to Birka Stockholm, the energy use for accommodation heating is 17% higher in the simulation. As these ships sail in similar climates, they were expected to have similar heating demands. For the simulated ship, heating of the pool water makes up 0.8% of this heating demand. This small heating demand for the pool can be explained by the ship having more than 1300 zones with accommodation heating, while there is only one pool.

The demand for DHW is significantly larger in Birka Stockholm than in the simulated ship. Even if the hot water heating demand in Birka Stockholm includes pool heating, this is unlikely to make a large difference, unless Birka Stockholm has many pools. The difference could also be due to the DHW schedule used in IDA ICE not accurately representing the DHW use on cruise ships.

The steam demand for galleys in the simulated ship is much larger than the demand on Birka Stockholm. Seeing as the simulated ship has steam demand based on a small expedition cruise vessel, it is possible that such a small vessel has a higher steam demand per passenger compared with larger cruise ships. It is also possible that the high temperature heat demand on Birka Stockholm does not represent the whole energy demand in galleys. The steam demand for laundry could not be investigated, as this data was not given for the reference ships.

Figure 32 also shows that with a COP of 1, the simulated ship has a larger use of electricity for cooling than Birka Stockholm. If a COP of 3.0 is taken into account, the electricity use for cooling in the simulated ship is 0.16 MWh/passenger. This is significantly lower than Birka Stockholm, where the cooling electricity use is 0.25 MWh/passenger.

The large cruise ship has no accommodation heating, and it has a much larger energy use for cooling than the simulated ship. These ships are however not directly comparable because the large cruise ship sails in much warmer climates in the Mediterranean and Caribbean Seas. In addition, the large cruise ship has much higher energy use for fans and pumps than the simulated ship. This could be caused by a large demand for air conditioning due to the warm climate. It could also be caused by inefficient fans and pumps.

The energy use for lighting and equipment is included in "other" for both the reference ships and could therefore not be investigated. However, energy use for lighting is likely higher in the large cruise ship than in the simulated ship due to the higher energy use per m^2 for LED lights, as seen in section 5.3.2.

Aqualand

The annual energy consumption for the Aqualand was found to be 2570 kWh/m^2 ws. This includes heating and cooling from the AHU and fan coil, heating of the pool water, as well as electricity demand for lighting, equipment and fans. Assuming the same heating demand for DHW as the rest of the ship, the total annual energy use is 2690 kWh/m^2 ws. Compared to the energy use for Norwegian swimming facilities mentioned in section 2.7, this is below the average but between the minimum and maximum. This is therefore considered a realistic result. AHU heating, zone heating and pool water heating make up the majority of the energy use. Detailed energy use for the Aqualand is presented in appendix K.3.

The fact that heat losses through the walls of the pool construction are not included could be one reason the energy use is lower than the average for Norwegian swimming facilities. In addition, the weather conditions experienced by the ship are likely warmer than for most Norwegian swimming facilities. The energy use for pumps in the waterborne heating system was not taken into account, as these are common for all zones in the model.

To investigate the effect of a swimming pool, the indoor climate in the Aqualand was compared to the indoor climate in an identical model without a pool. Figure 33 shows duration curves for the air temperature in the Aqualand with and without a pool.

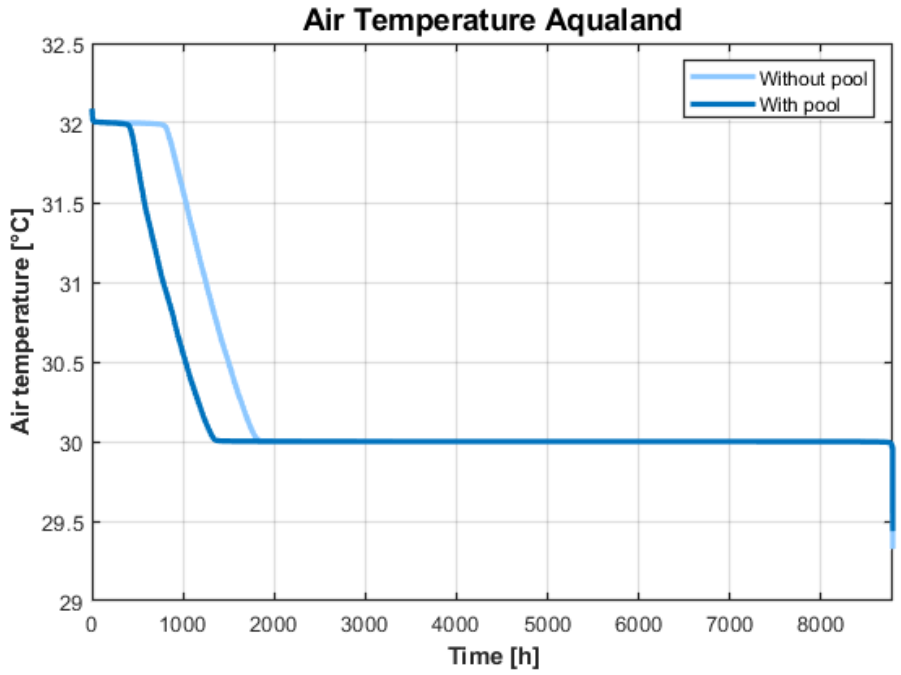

Figure 33: Duration curves for the air temperature in the Aqualand with and without a pool.

The air temperature is at the lower setpoint for a large part of the year due to relatively high ventilation rates and low supply air temperature. Otherwise, the air temperature is generally lower with a pool. This is due to the pool temperature always being lower than the air temperature, which causes heat transfer from the air to the pool.

Figure 34 shows duration curves for the relative humidity in the Aqualand with and without a pool. In the model with a pool, the humidity is significantly higher overall. This is expected due to evaporation from the pool. Control of the humidity and the effect of humidity on indoor climate have not been considered here.

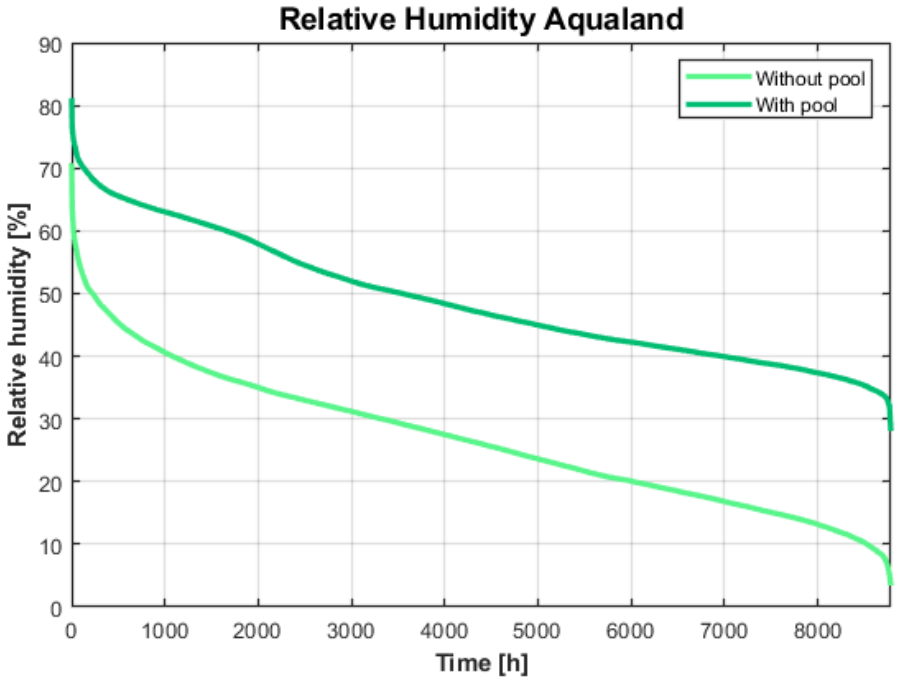

Figure 34: Duration curves for the relative humidity in the Aqualand with and without a pool.

6.2 Calibration

As seen in figure 32, the DHW demand is significantly higher in Birka Stockholm than in the simulated ship. As mentioned, this could be caused by inaccuracies in the Norwegian standard about the DHW demand, or cruise ships could have a higher demand than hotels. During calibration, the specific DHW demand in IDA ICE was increased to 58.7 kWh/m^2, which gave an annual demand very close to Birka Stockholm. This also slightly increases the annual energy consumption in the Aqualand discussed in section 6.1, making it closer to the average for Norwegian swimming facilities.

In addition, the accommodation heating demand on the simulated ship was larger than the demand on Birka Stockholm. The ventilation rates used in the model are uncertain and could be different in reality. Especially the ventilation rates in the galleys could be different from what was assumed. The accommodation heating was therefore decreased by reducing the ventilation rate in the large galleys from 50 to 30 h^{-1}. This resulted in accommodation heating only 2.8% higher than Birka Stockholm.

The total annual energy demand for the simulated ship's hotel system was then 19.2 MWh/passenger. Figure 35 shows the annual energy consumption before and after calibration, alongside Birka Stockholm, as this was the reference ship used for calibration. Exact values for the results after calibration are shown in appendix K.1, along with the values for the reference ships.

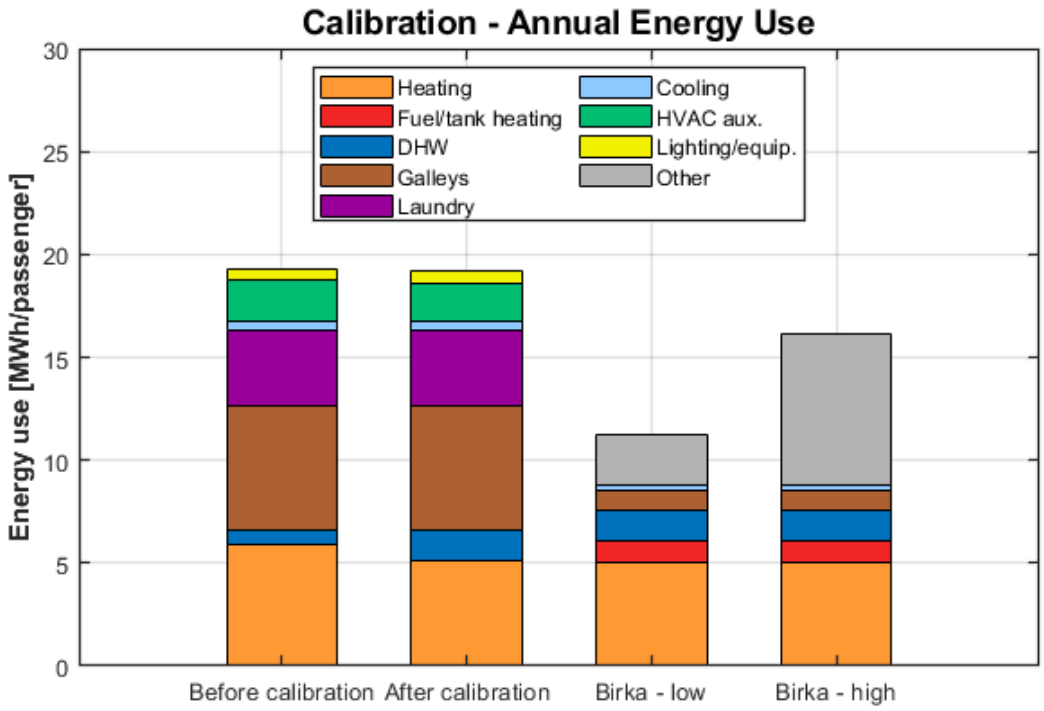

Figure 35: Annual energy consumption for the hotel system on the simulated ship, before and after calibration.

After calibration, the total energy demand for the hotel system was above the energy use for Birka Stockholm, but below the high estimate for the large cruise ship. The model was therefore considered adequately calibrated in relation to the reference ships. Including propulsion, the total annual energy demand for the simulated ship is 51.4 MWh/passenger. Due to the large propulsion demand on the simulated ship, this is close to the high estimate for the large reference ship.

After calibration, the ventilation rate in the large galleys was still large enough to cover the cooling demands most of the year. The cooling demand was therefore not increased, but instead decreased by 5.5%. This was caused by reduced cooling in the AHU for the galleys on hot summer days due to a lower ventilation rate. With a COP of 3.0, the new electricity use for cooling is 0.15 MWh/passenger. This is now even further from Birka Stockholm's cooling electricity use of 0.25 MWh/passenger. The difference in energy use for cooling could be due to higher solar or internal heat gains in Birka Stockholm, or different ventilation rates.

The energy demand for fans and pumps also decreased by 6.2% due to reduced ventilation rates and reduced heating and cooling demands. It is still much lower than the energy demand for fans and pumps on the large cruise ship, as seen in figure 32. It is possible that the energy use for fans and pumps should have been increased in the calibration. The energy use for lighting, equipment, galleys, laundry and propulsion is the same before and after calibration, as the schedules used in IDA ICE were not changed.

Figure 36 shows duration curves for the DHW heating demand before and after calibration. The consumption profile is the same due to the same schedule being used in IDA ICE. The peak demand is now 1335 kW, or 0.56 kW/passenger. This is still much lower than the peak demand for Birka Stockholm at 1.33 kW/passenger, but around the same as the large cruise ship at 0.52 kW/passenger. The new peak demand after calibration is therefore considered realistic.

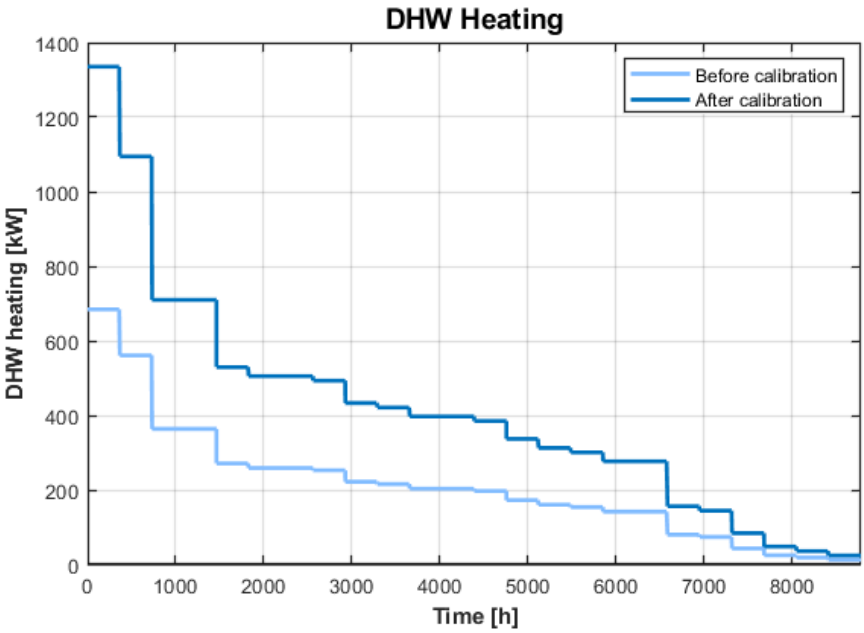

Figure 36: Duration curves for DHW heating demand before and after calibration.

Figure 37 shows the accommodation heating demand throughout the year after calibration. The shape of the curve is very similar to the curve before calibration, shown in figure 19. The peak heating demand is now 11.1 MW. The peak demand for a typical winter day is estimated to be 7 MW, or 2.92 kW/passenger. This is now closer to the peak heating demand for Birka Stockholm, at 2.27 kW/passenger. This is due to the reduced heating demand caused by reduced ventilation in the large galleys.

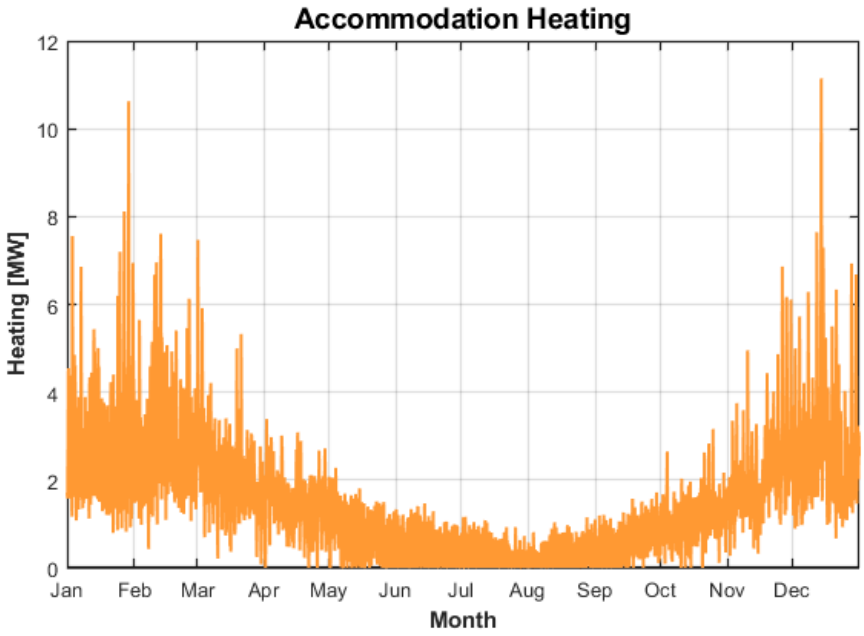

Figure 37: Accommodation heating demand throughout the year after calibration.

In the simulated ship, heating of the vehicle decks causes significant increases in the heating demand, especially during roll on and roll off. As mentioned in section 2.1, Birka Stockholm does not have a vehicle deck. The difference in peak heating demand could therefore represent the demand for vehicle

deck heating during roll on and roll off. It is also possible that real boilers cannot react as quickly to a heating demand as the boiler in IDA ICE. The peak heating might therefore be lower in reality.

Figure 38 shows duration curves for the accommodation heating demand before and after calibration. The heating demand is now slightly lower through the whole year, and the largest difference is when the demand is high. This can be explained by the reduced ventilation rate causing a larger decrease in heating demand when the outdoor temperature is low.

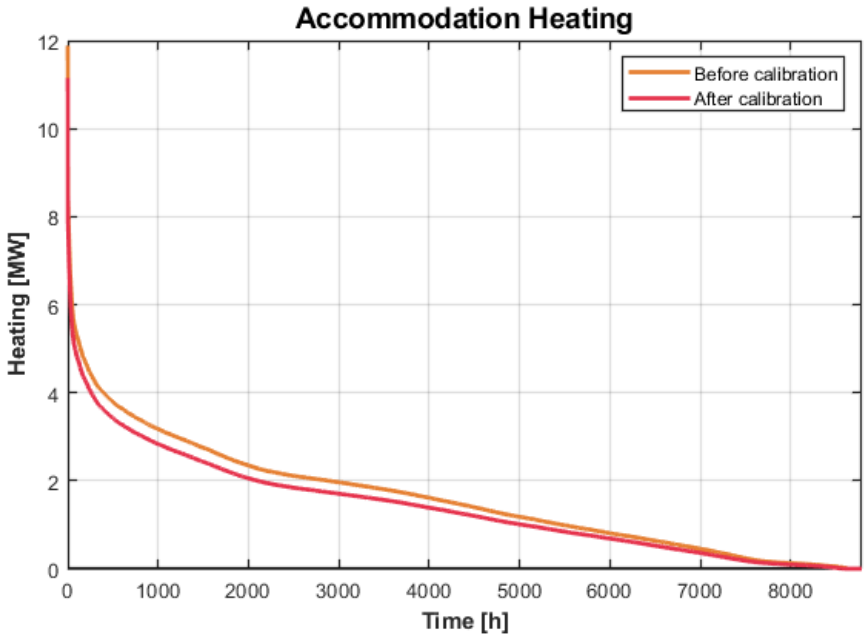

Figure 38: Duration curves for accommodation heating demand before and after calibration.

Figure 39 shows the cooling demand throughout the year after calibration. Again, the shape of the curve is similar to what it was before calibration, shown in figure 22.

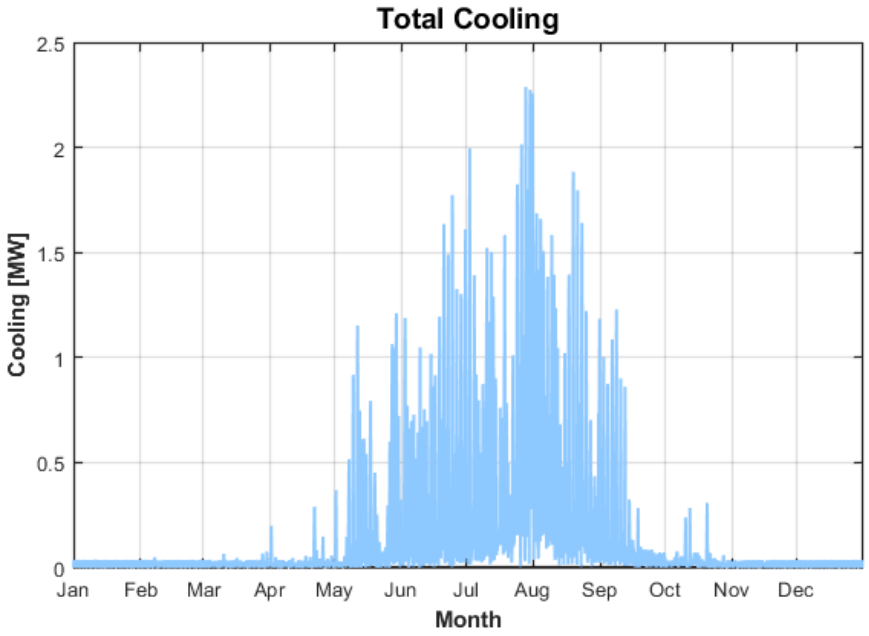

Figure 39: Total cooling demand throughout the year after calibration.

The peak cooling demand for a typical summer day was estimated to be 1.8 MW, or 0.75 kW/passenger. This is now only slightly higher than the peak cooling demand for Birka Stockholm, at 0.67 kW/passenger. This reduction in peak cooling demand was expected due to the lower annual cooling demand in the simulated ship after calibration.

The results show that the simulated ship has a lower annual energy use for cooling compared to Birka Stockholm, but a higher peak cooling demand. This could be caused by the cooling demand on the simulated ship being more intermittent, for example with occasional large solar heat gains, but with lower demand for cooling in galleys and laundry.

Figure 40 shows duration curves for the total cooling demand before and after calibration. The cooling demand was mainly decreased in hours with high demand. This is due to the reduced ventilation rate in the large galleys decreasing the cooling demand when the outdoor temperature is high.

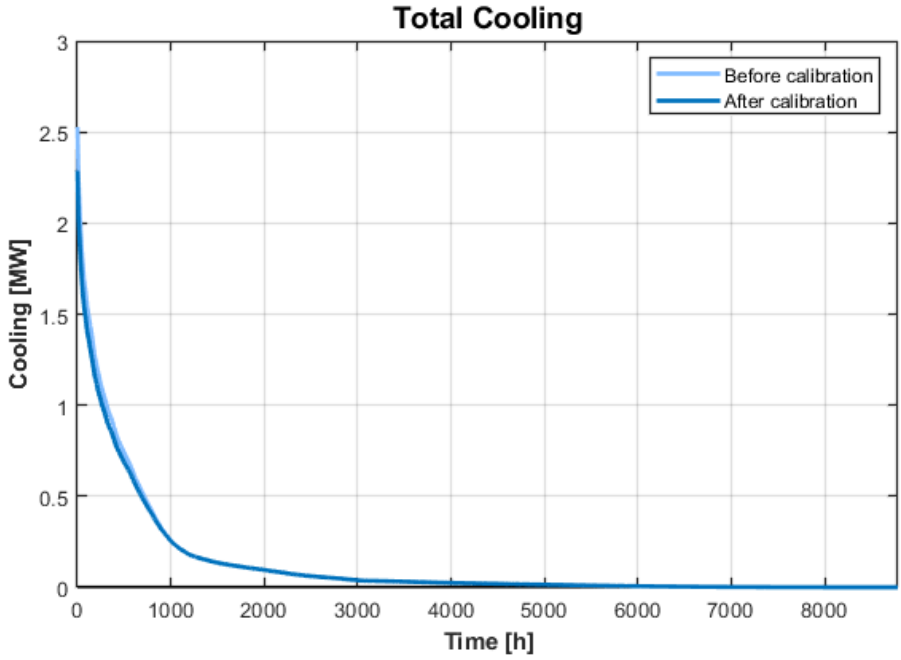

Figure 40: Duration curves for total cooling demand before and after calibration.

Figure 41 shows duration curves for the HVAC auxiliary electricity consumption before and after calibration. The electricity consumption decreased due to reduced ventilation rates and reduced heating and cooling demands in the large galleys.

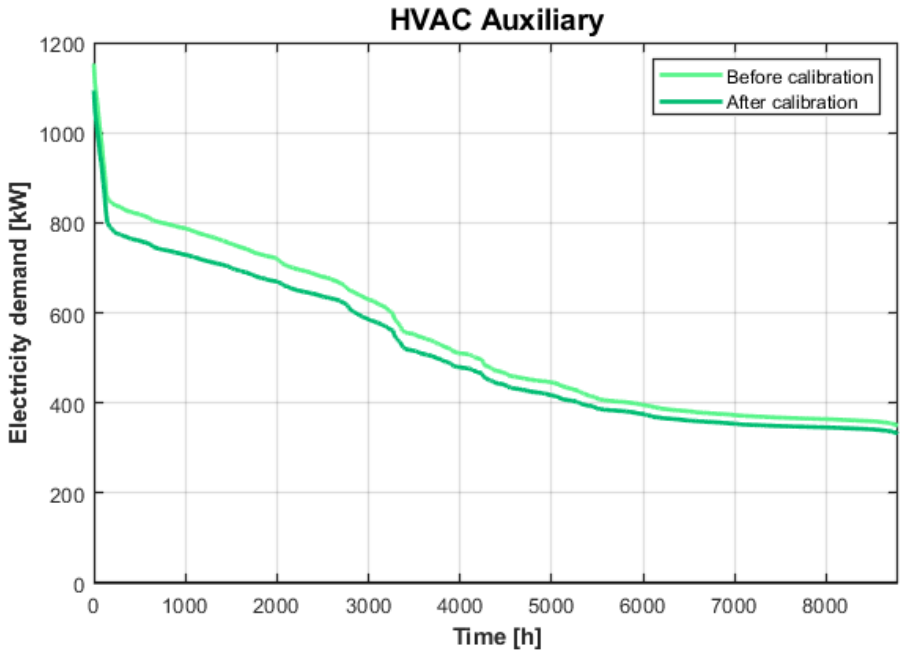

Figure 41: Duration curves for HVAC auxiliary electricity demand before and after calibration.

6.3 Fan Coils Sizing Analysis

As mentioned in section 3.9, the fan coils in Case A were sized based on design day data in heating and cooling simulations. In Case B, the fan coils were sized based on the maximum power delivered during a one year simulation. The heating and cooling rates used for the fan coils in Cases A and B can be seen in appendix J. Many of the fan coils in large public areas have heating and cooling power above 10 kW. In reality, it is likely that these areas would have several fan coils, which would enable a better temperature distribution in the zone and reduce the maximum power of each fan coil.

Case A was expected to have higher required heating power than Case B due to the minimum temperature in the design day data being lower than the minimum temperature in the combined weather file, as seen in sections 3.9 and 4.2, respectively. However, Case B had higher heating power in almost half of the zones. This could be due to the minimum outdoor temperature in Case A occurring at a time with lower heat demand than the minimum temperature in Case B. Another reason could be the function of the PI controller in the fan coils. The given PI parameters can lead to the heating in Case B sometimes being higher than in Case A even if the outdoor temperature is higher.

For cooling, Case B had higher required power in most zones. This is likely caused by Fornæs being used as the location for the combined weather file. This means the position of the sun is lower and gives more solar heat gains than Holzdorf in the cooling simulation. In addition, the maximum temperature in the combined file is slightly higher than the maximum design day temperature for Holzdorf. Such a high temperature combined with the low solar angle would not happen as frequently in reality, and is therefore unrealistic. The function of the PI controller in the fan coils could also have an impact here.

As mentioned in section 5.12, the supply water temperature for cooling was set based on the fan coil power requirement. The fan coils should therefore be able to deliver power equal to the chosen cooling rates. The heating rate in fan coils is defined for a supply water temperature of 50 °C, and the fan coils can therefore deliver slightly more when the supply water temperature is 60 °C.

Figure 42 shows histograms with the air temperature in the Aqualand throughout the year for the three fan coil sizing cases. The heating and cooling setpoints are shown with blue and red dashed lines, respectively. For Cases A and B, the temperature is sometimes outside the desired range, but the deviation is usually small. The minimum temperature is below 27 °C, while the maximum temperature is almost 33 °C. However, such deviations occur for very short periods of time and are therefore negligible. Overall, the thermal environment is therefore considered good. The air temperature is usually far from the pool temperature at 28 °C, and the risk of evaporation from the pool is therefore small.

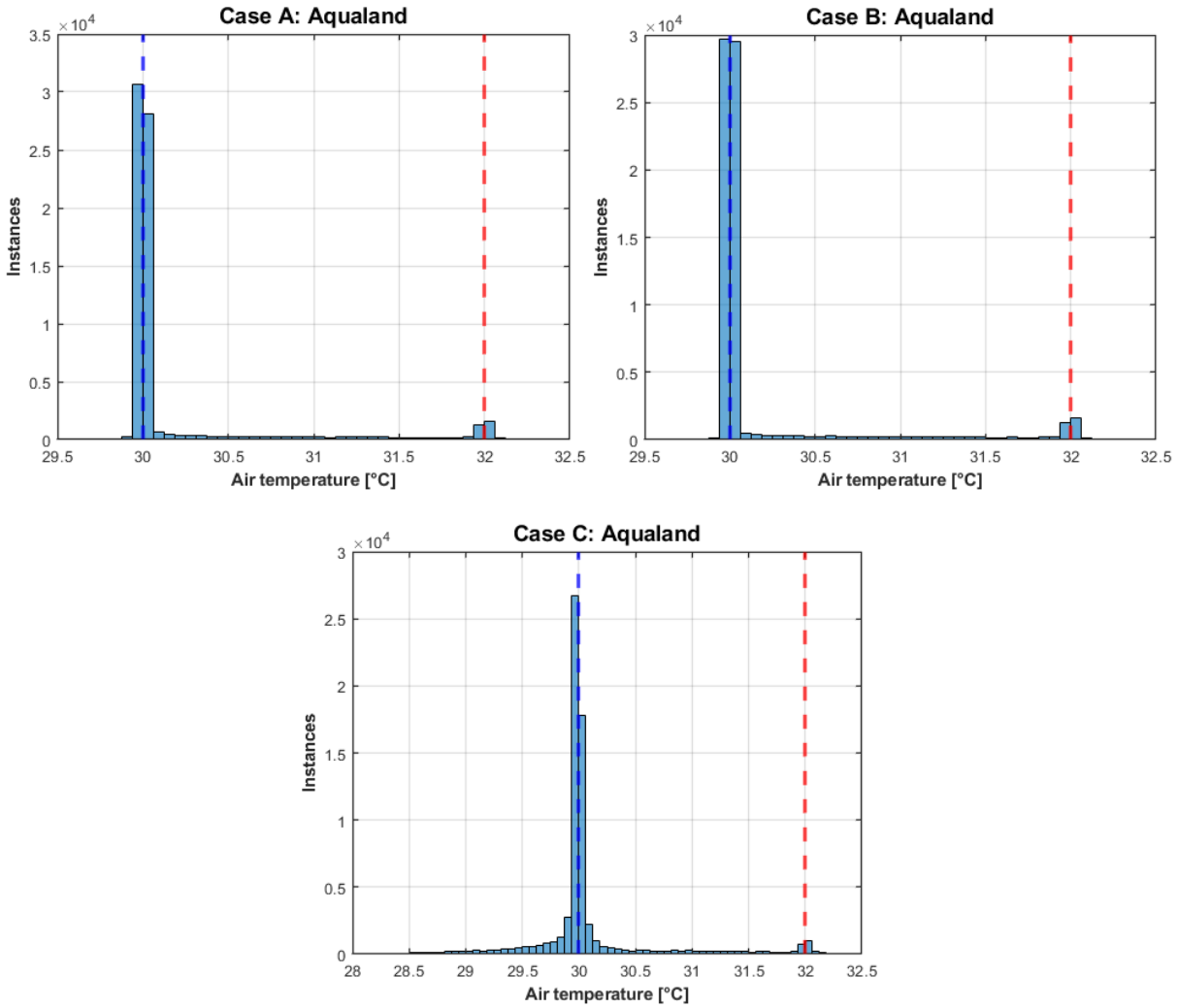

Figure 42: Air temperature in the Aqualand for the three fan coil sizing cases. Heating setpoint in blue, cooling setpoint in red.

In Case C, the heating and cooling powers in Case B were reduced by 50%. Here, the air temperature in the Aqualand is below the heating setpoint a significant amount of the time. However, the temperature is usually above 28.5 °C, and the occupants are therefore likely to still be comfortable in the zone. The risk of evaporation from the pool is increased, but not drastically. Reducing the cooling power in the Aqualand did not cause overheating in the zone.

Figure 43 shows histograms for the air temperature in the large galleys. In all cases, the air temperature is usually below 22 °C due to the large ventilation rate in the zone. The air temperature is sometimes below the heating setpoint, but with a relatively small deviation. The thermal environment in the large galleys is therefore considered satisfactory in all cases. Case C has similar temperatures to Case A due to the heating power in Case B being around twice as large as in Case A. Reducing the heating power further would likely cause lower temperatures in the zone. Similar trends were found for the air temperature in the small galleys.

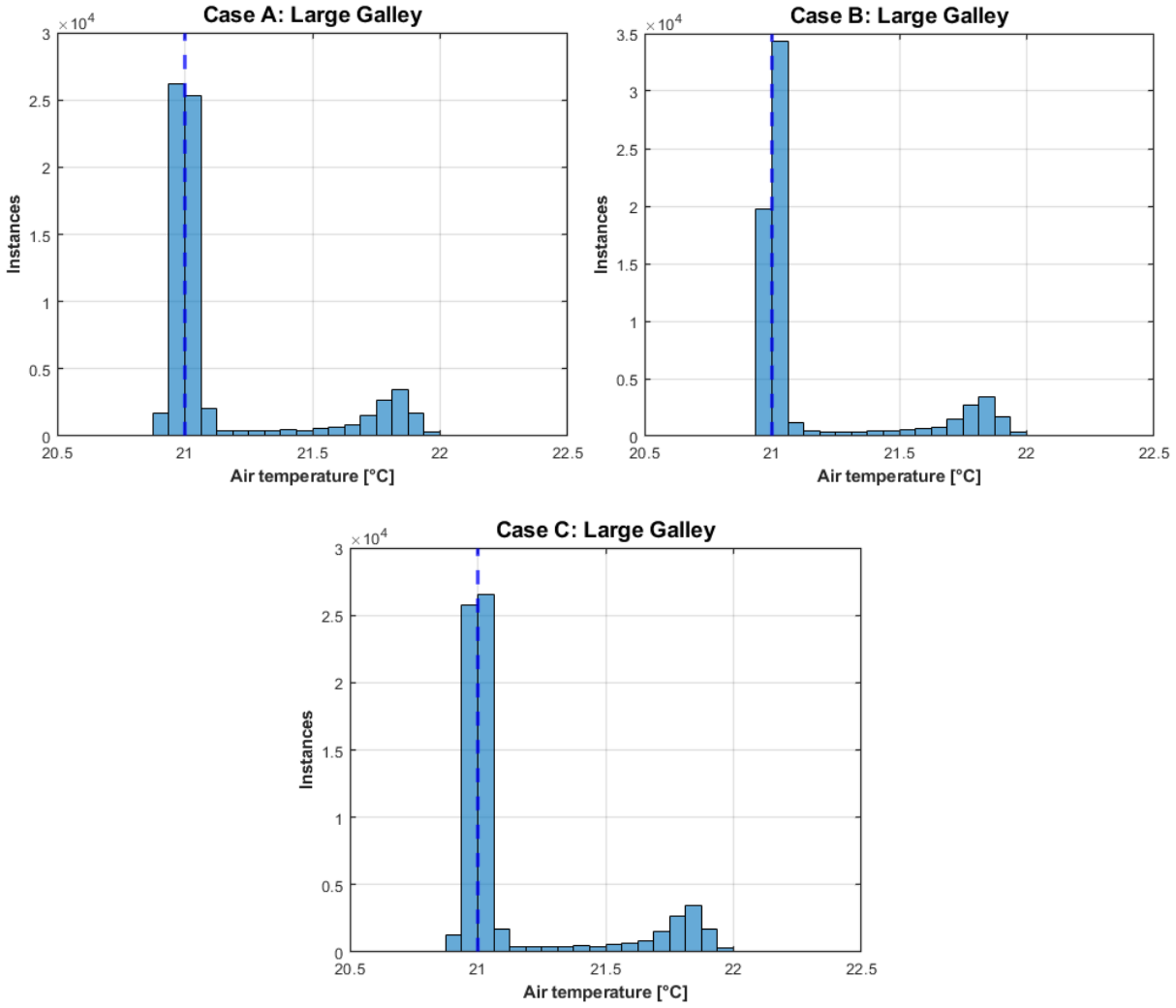

Figure 43: Air temperature in the large galleys for the three fan coil sizing cases. Heating setpoint in blue.

Figure 44 shows histograms for the air temperature in the laundry. In all cases, the temperature goes below the heating setpoint only by a small amount. For Case B, the temperature goes above the cooling setpoint a significant amount of the time, but stays below 24.5 °C. The thermal environment here is therefore considered acceptable.

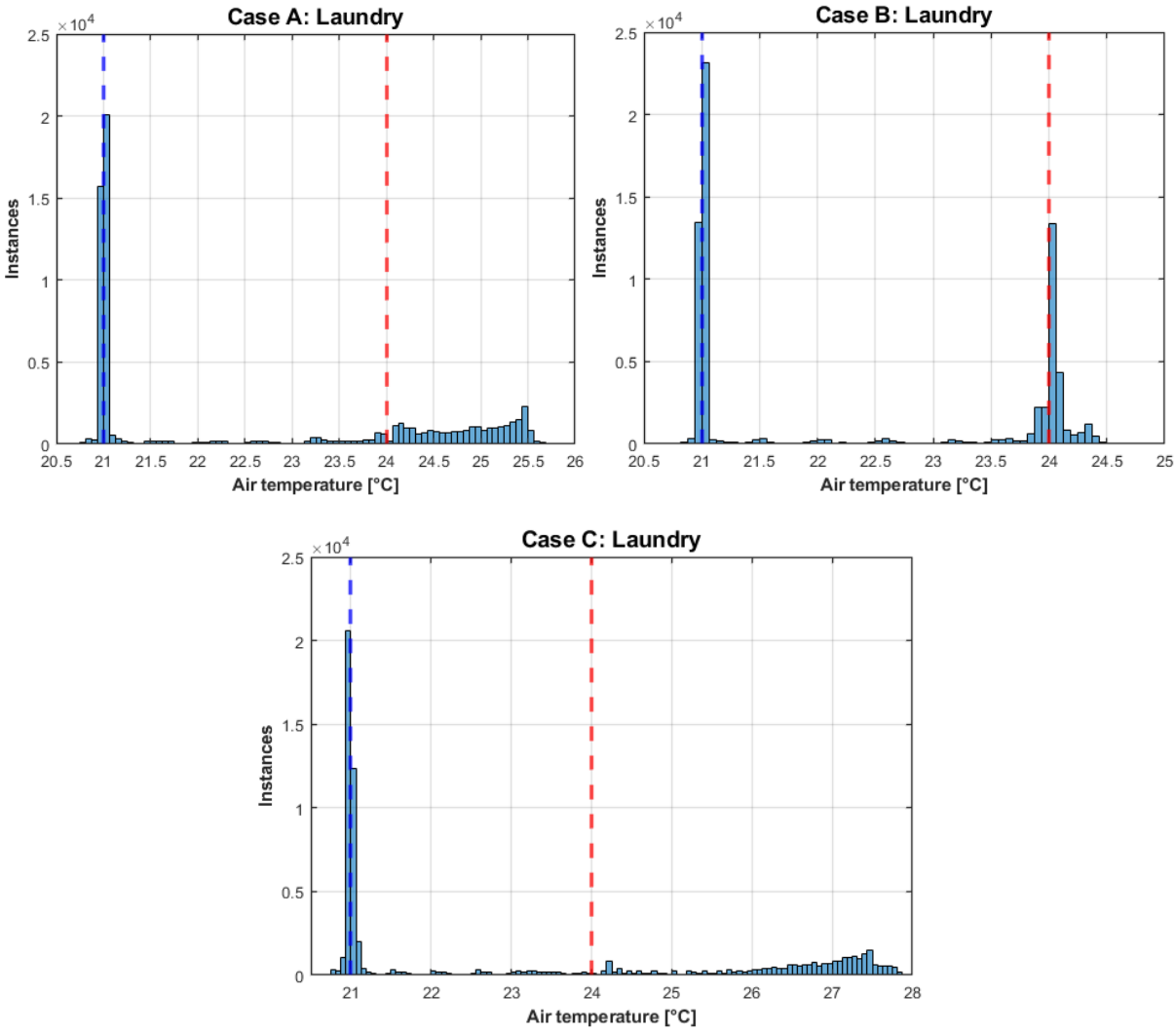

Figure 44: Air temperature in the laundry for the three fan coil sizing cases. Heating setpoint in blue, cooling setpoint in red.

For most zones, the reduced cooling capacity in Case A did not significantly impact the thermal environment in the zone. As seen in figure 44, the temperature in the laundry was increased in Case A, causing significant overheating. This could be due to the laundry having large cooling demands every night due to the laundry steam demand. In other zones, there are high cooling demands for shorter periods of time due to solar and internal heat gains. In such cases, the reduced cooling capacity means it might take longer to reach the cooling setpoint, but is it still reached relatively quickly. In Case C, this overheating was increased even more. This shows that the choice of design cooling power in zones with large internal heat gains is important to provide an adequate thermal environment in the zone.

Figure 45 shows histograms for the air temperature in the navigation bridge. In all cases, the air temperature stays within or close to the setpoints most of the time. Case C has temperatures up to 25 °C, but this occurs very rarely and is therefore considered acceptable. Overall, the thermal environment in the navigation bridge is good in all cases and was not significantly impacted by undersizing the fan coil.

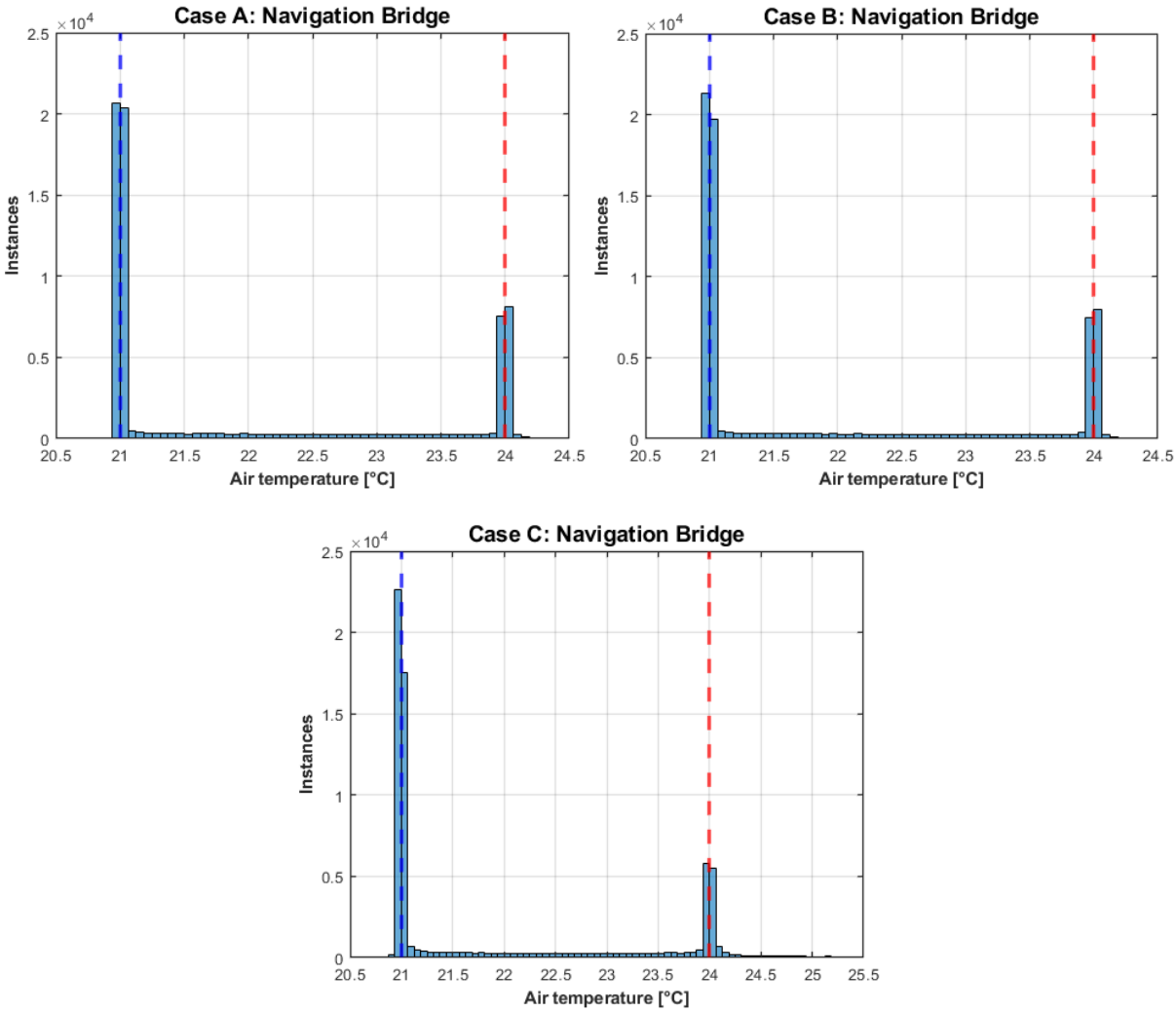

Figure 45: Air temperature in the navigation bridge for the three fan coil sizing cases. Heating setpoint in blue, cooling setpoint in red.

Figure 46 shows histograms for the air temperature in a 10.5 m^2 ocean view cabin. In all cases, the temperature rarely goes above 22.5 °C. Cases A and B also have small deviations below the heating setpoint. In Case C, the temperature is reduced further below the heating setpoint for a significant amount of time. However, the temperature is rarely below 20.5 °C, and the thermal environment is therefore considered acceptable. Similar trends were found for the air temperature in many other ocean view cabins. Internal cabins typically had less variation in the air temperature, with the temperature largely staying between 21 and 22 °C. This is due to no solar heat gains in internal cabins, as well as less heat transmission through the constructions.

These results show that there generally is a small difference between using design day data or a one year simulation for fan coil sizing. However, if more extreme weather conditions were to occur, it could

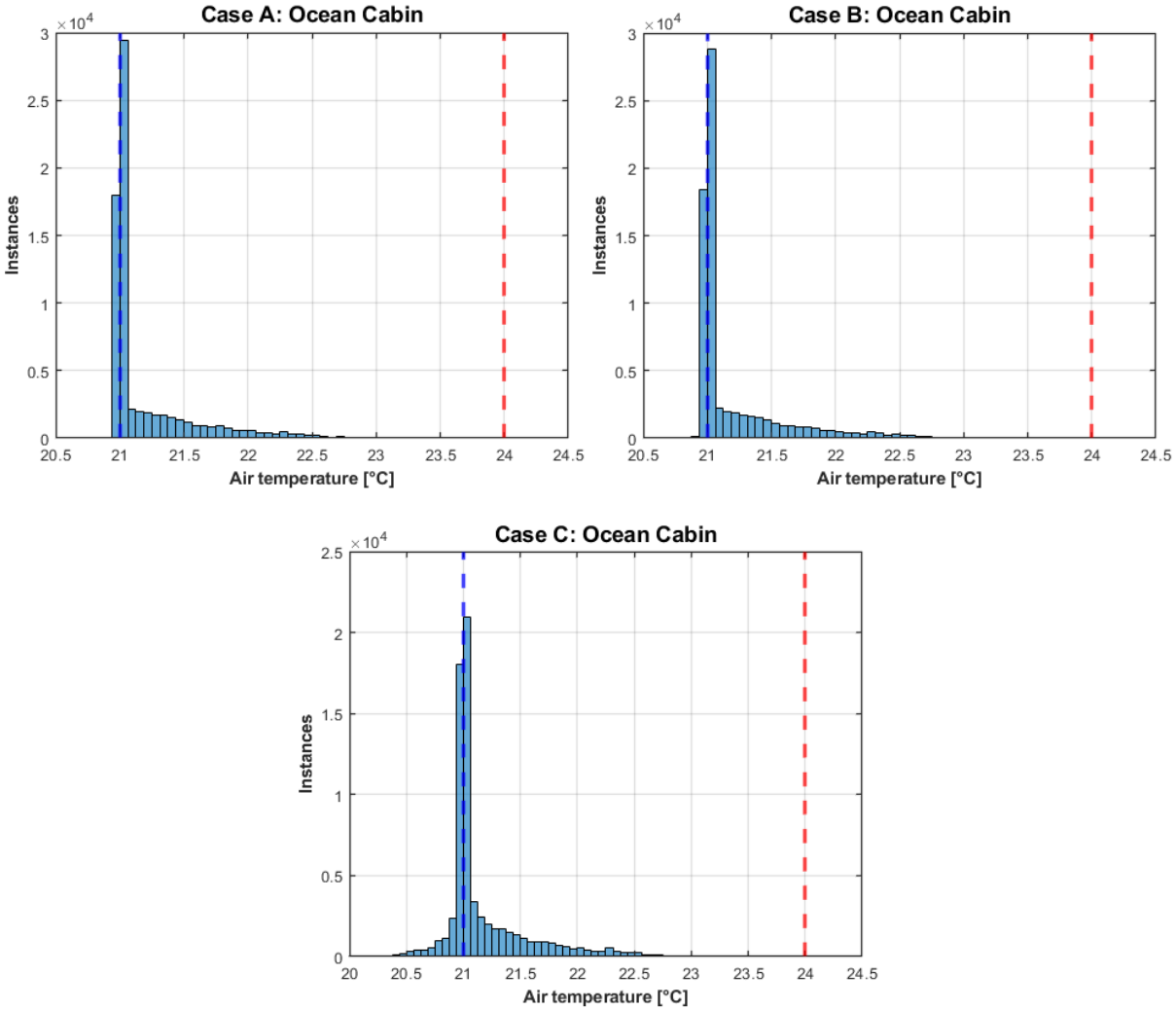

Figure 46: Air temperature in an ocean view cabin for the three fan coil sizing cases. Heating setpoint in blue, cooling setpoint in red.

be beneficial to use the highest power given from these two methods. In laundries and other zones with high internal heat gains, the design cooling power is especially important to avoid overheating and provide a satisfactory thermal environment in the zone. For most other zones, the fan coils can be significantly undersized without affecting the thermal environment. This could however become a problem if extreme weather were to occur.

Figure 47 shows the annual energy consumption for the hotel system with unlimited heating and cooling after calibration, and for each of the three fan coil sizing cases. It is clear that the total energy use is almost identical in all cases. The biggest difference is the energy use for fans and pumps increasing by around 2% in all fan coil sizing cases compared to the unlimited model. This is due to the fan power in the fan coils being set to 3% to represent real fan coils.

In Case C, the cooling decreased by 1.5% compared to the unlimited case. This is due to the undersized fan coils not being able to cover the whole cooling demand, as seen in the temperature for the laundry in figure 44. Most zones still had their cooling setpoint reached in Case C, and the difference in total cooling is therefore small. The heating in Case C decreased by 0.5% compared to the unlimited case. This small difference is due to the reduced heating capacity having a small impact on the heating in

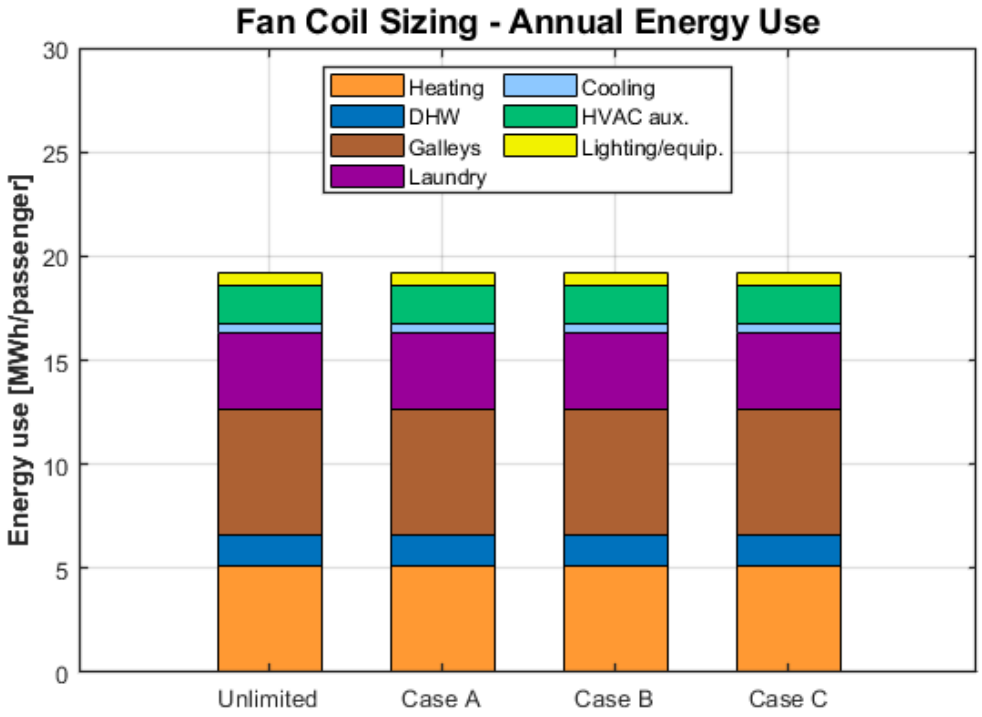

Figure 47: Annual energy consumption for the hotel system, with unlimited heating and cooling, and for the three fan coil sizing cases.

the zones. For Cases A and B, the change in heating and cooling was insignificant due to the fan coils largely being able to cover the heating and cooling demands.

The energy use for DHW, galleys, laundry, lighting and equipment was once again not affected seeing as the schedules in IDA ICE remained the same.

Duration curves for heating and cooling for the fan coil sizing cases can be seen in appendix K.4. The curves are almost identical apart from the peak demand. For cooling, Case C has a slightly lower peak demand than the other cases. For heating, Cases A and B have a slight reduction in the peak demand, while Case C has a larger reduction. This was expected due to the reduced heating and cooling capacities in Case C. In such a case, the necessary size of the boiler would be decreased.

During the simulation, there was condensation on surfaces in the Aqualand, and on the vehicle decks. This was expected as the Aqualand has high air temperatures, and the external constructions were not additionally insulated in this area. On the vehicle decks, condensation was expected because the air temperature goes down to 5 °C most of the winter, and the internal surfaces will therefore be cold.

As the fan coil sizing method used in Case B was the most effective for reaching the heating and cooling setpoints in the model, this case was used further as the base case of this project. The exact annual energy use for this case can be seen in appendix K.1.

6.4 Energy Supply System

Figure 48 shows the electricity delivered by the engines and by shore power on 5 August, as calculated by the post processing script. This graph is identical for the MGO and LNG ships. Most of the electricity delivered by the engines clearly goes towards the propulsion demand, as seen in figure 16. In port, only the hotel system has electricity demands and this is covered by shore power.

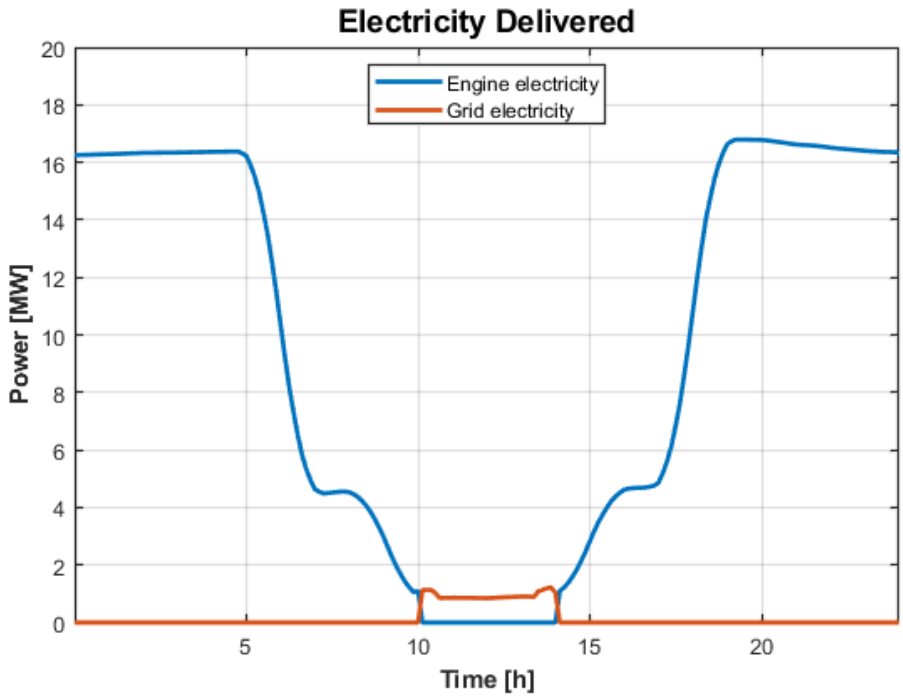

Figure 48: Electricity delivered by the engines and by shore power on 5 August.

For the same day, figure 49 shows the delivered heat and heating demands for the MGO ship. The graph shows the heat recovered from engines and the heat from auxiliary boilers, as well as the total heating demand and the wasted recovered heat.

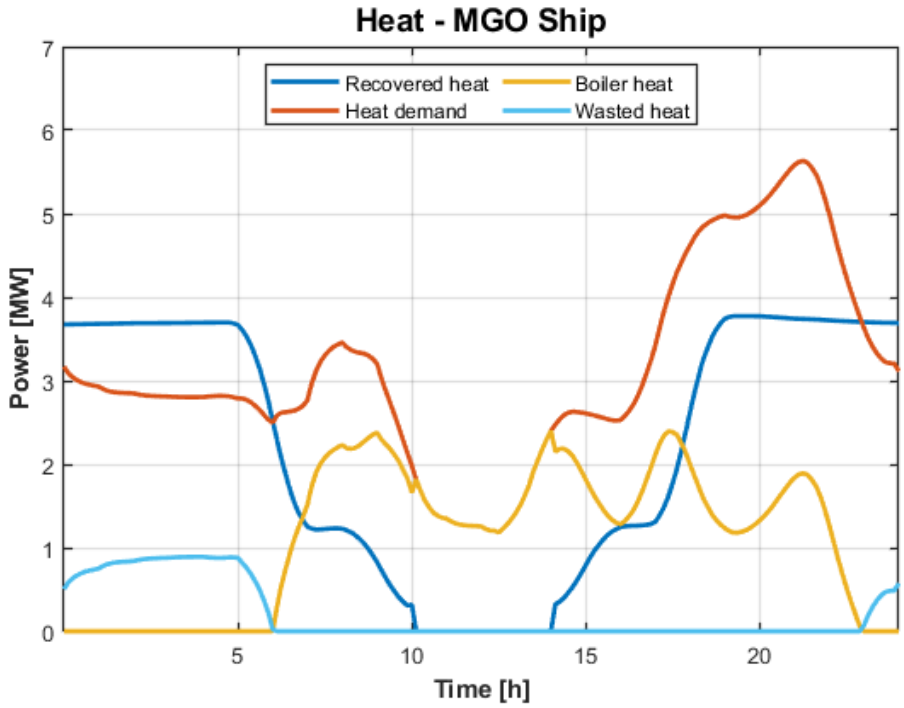

Figure 49: Heat recovered from engines, heat delivered by boilers, total heat demand and wasted heat, 5 August on the MGO ship.

This shows the direct correlation between the heat recovered from engines and the electricity from engines, shown in figure 48. No hot water storage tank was included here, and the boilers therefore cover all heat demands that are not covered by the recovered heat. During the night, the recovered heat is larger than the heating demand, due to a large propulsion demand and a relatively small heating demand. This means that in a case with no hot water tank, some recovered heat will be wasted, as shown in the figure. Throughout the whole year, 244 MWh of recovered heat was wasted.

The same case is shown for the LNG ship in figure 50. Here, the amount of heat recovered from the engines is higher due to the exhaust gas being cooled down more, as discussed in section 5.12. This leads to an increased amount of wasted heat and reduced use of the boiler. In this case, 3320 MWh of recovered heat was wasted in one year. This large increase in wasted heat could be due to the heating demands already being covered by recovered heat a significant part of the summer. At these times, the additional recovered heat can therefore not be utilised.

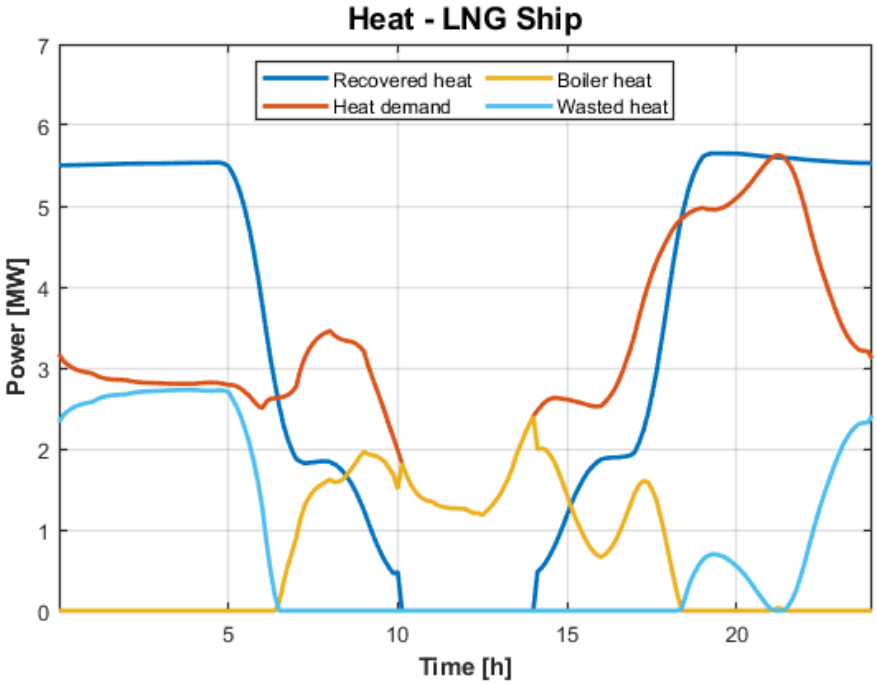

Figure 50: Heat recovered from engines, heat delivered by boilers, total heat demand and wasted heat, 5 August on the LNG ship.

6.5 Hot Storage Tank

MGO Ship

The use of the 150 m^3 hot storage tank on the MGO ship was investigated. Figure 51 shows the cumulative heat rate for charging and discharging of the hot water storage tank throughout one year. Seeing as heat losses have been neglected, the cumulative charging and discharging rates are equal. At the end of the year, the charging energy is slightly higher than the discharging energy due to the tank being discharged at the start of the year and 33% charged at the end, i.e. the base level for the winter mode.

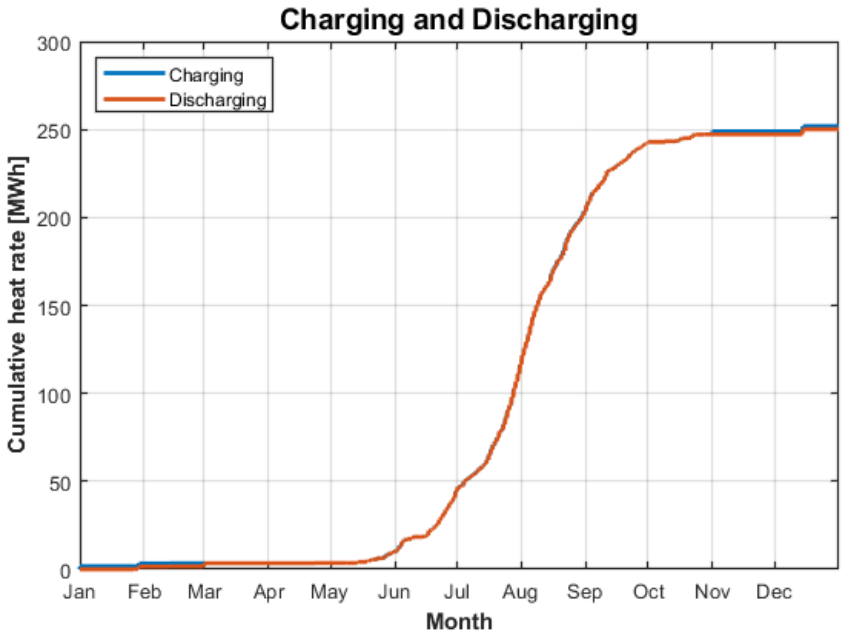

Figure 51: Cumulative heat rate for charging and discharging of the hot water storage tank, for the MGO ship.

Figure 52 shows the heat rate for the hot storage tank throughout the year. When the heat rate is positive, the tank is charging, and when the heat rate is negative, the tank is discharging. The maximum charging and discharging rates are 3.1 MW, as decided in section 5.13. The maximum charging rate is reached at the start of the year and in the beginning of the winter mode in November, when the tank is being charged up to the winter base level. The maximum discharge rate occurs in December, when the peak boiler demand is reduced to the peak shaving level.

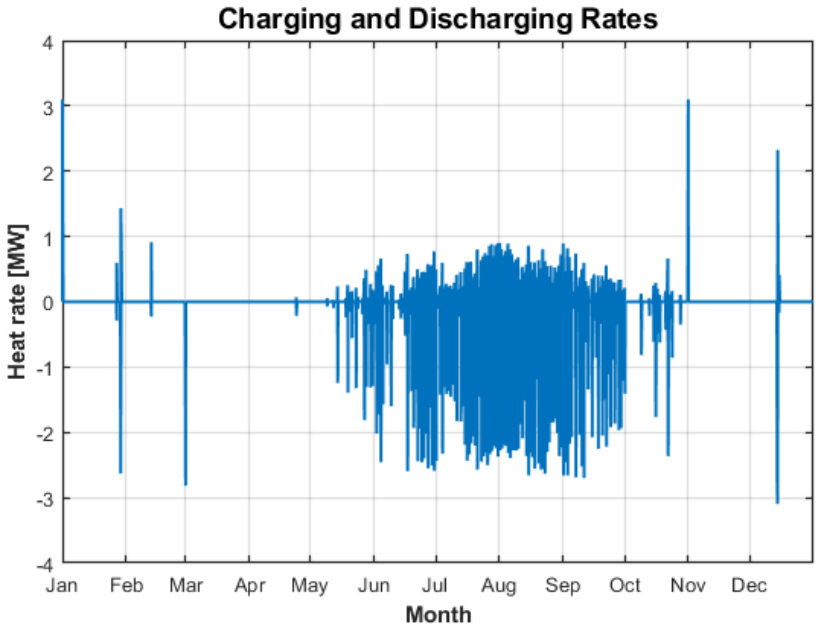

Figure 52: Heat rate for the storage tank throughout the year, i.e. the charging and discharging rates, MGO ship.

Figure 53 shows the temperature in the hot water storage tank throughout the year. The temperature varies between 50 and 80 °C, with the maximum temperature in this case being 79.7 °C. The energy

level of the tank has the same variation between 0 MWh and the tank's maximum capacity. In a real tank with heat losses, it would be beneficial to reduce the use of the winter mode to only the coldest months to reduce the average temperature in the tank. Using a relatively low base temperature in the winter also helps with this.

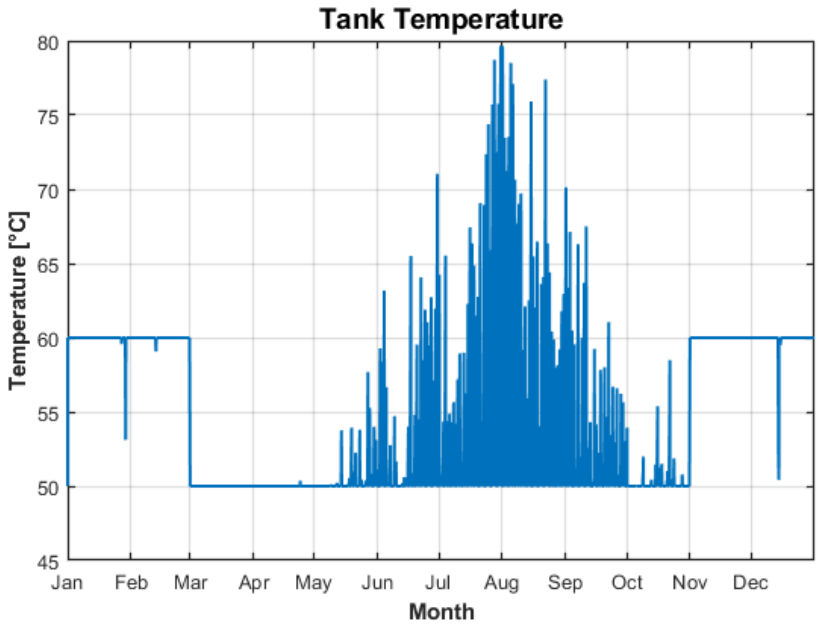

Figure 53: Temperature in the hot water storage tank throughout the year, for the MGO ship.

Figure 54 shows the same case as figure 49, but including a 150 m^3 hot storage tank. Charging and discharging rates for the tank are also included. Compared with figure 49, the wasted heat is now recovered by charging the storage tank. Later, the boiler demand is reduced by discharging the tank.

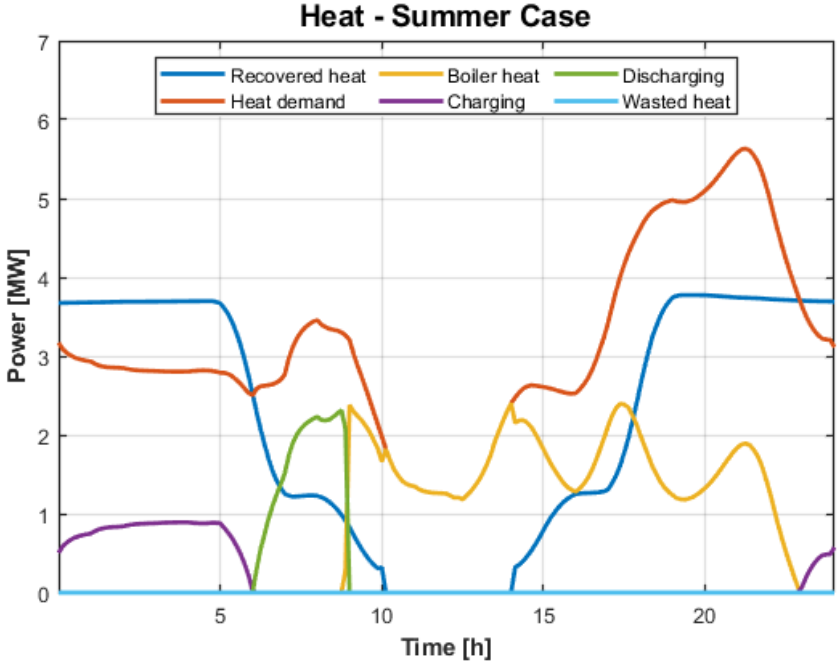

Figure 54: Heat from engines, boilers and the storage tank, as well as total heat demand, charging power and wasted heat, 5 August on the MGO ship.

Figure 55 shows the energy level of the hot storage tank throughout the day on 5 August. It is clear that the change in energy level corresponds with the charging and discharging rates in figure 54. On this day, the storage tank reaches 95% of its full capacity, which is 5.23 MWh.

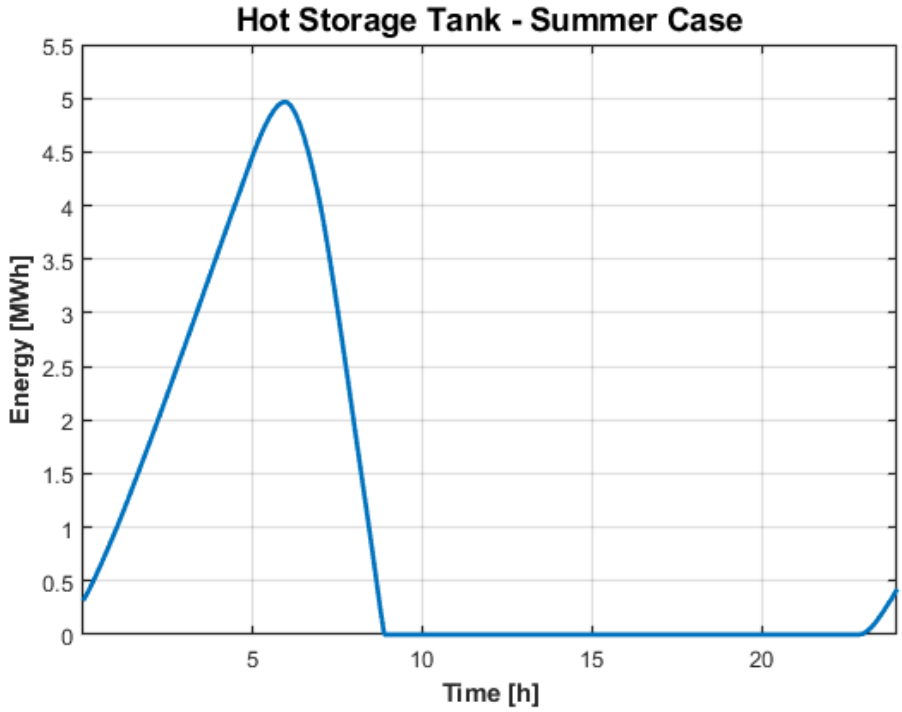

Figure 55: Energy level of the hot storage tank on 5 August, for the MGO ship.

The amount of energy saved over the year was 244 MWh, which corresponds to the amount of wasted heat before the storage tank was included. The energy savings are only 0.62% of the total heating demand. If heat losses from the tank had been included, the total energy savings would be even smaller.

However, the energy savings depend on the electricity demand, heating demand, engine efficiencies and the amount of waste heat recovered. The tank can therefore have larger savings in other ships that have more unused recovered heat. For example, if the steam demand used in the model is too large, there would be more available heat recovered from the engines that is not utilised, and a larger amount of energy would be saved by the tank. Then, a larger tank volume would likely be required to store all unutilised recovered heat. The amount of unused recovered heat also depends on the weather conditions. In weather conditions that differ from the combined weather file, the energy saving potential could be larger.

The winter case with peak shaving is shown in figure 56, which shows the heat from engines, boilers and storage tank, as well as the total heating demand and charging rate for 29 January. For this day, the boiler peak was reduced by 2.63 MW. Figure 57 shows the energy level of the hot storage tank throughout the day. The tank starts off at the winter base level, at 33% of the maximum capacity. Again, the change in energy level corresponds with the charging and discharging rates in figure 56.

The maximum reduction in boiler peak power in the winter was 3.1 MW, as decided in section 5.13. The peak shaving level was then 9.2 MW. The demand from boilers would be different on other ships and in different weather conditions. For the chosen tank size, the maximum possible reduction of boiler peak power therefore might be different.

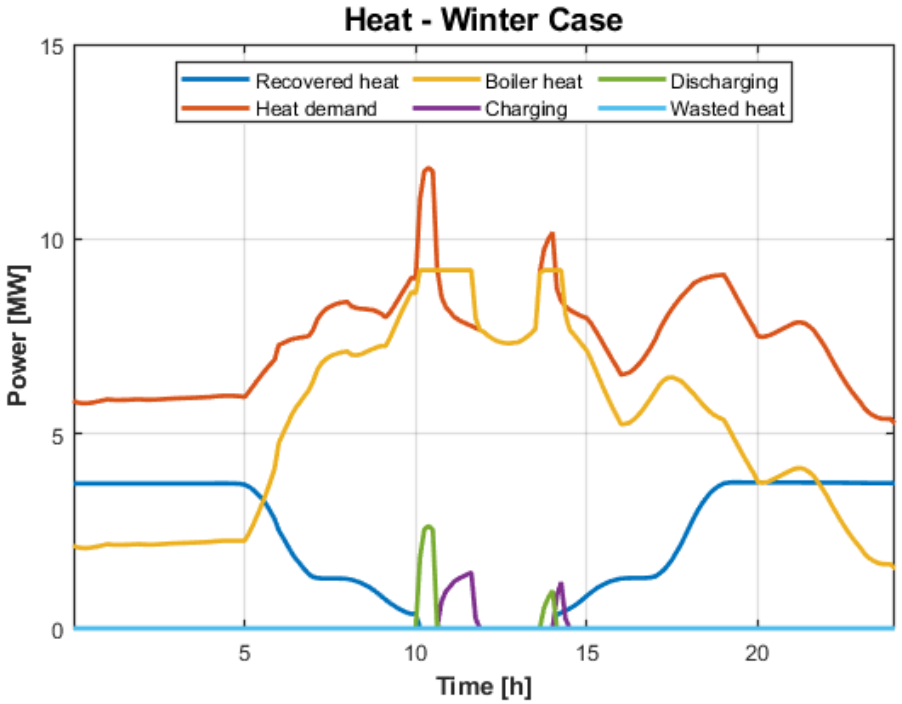

Figure 56: Heat from engines, boilers and the storage tank, as well as total heat demand and charging rate, 29 January on the MGO ship.

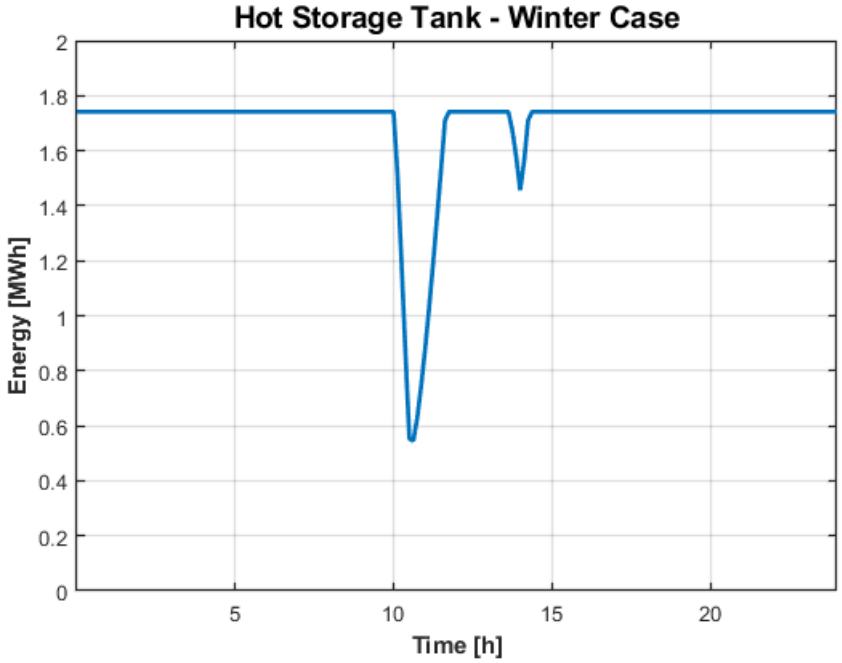

Figure 57: Energy level of the hot storage tank on 29 January, for the MGO ship.

In addition to boiler peak shaving, the hot storage tank could be used to run the boiler as close to 30% load as possible to give the highest possible efficiency, as seen in figure 17a. At load factors below 30%, the boiler power could be increased to charge the tank. At load factors above this, the boiler power could be decreased and the tank discharged.

Figure 58 shows the total annual electricity and heat delivered by engines, boilers and shore power, as well as the fuel consumption for engines and boilers. The heat delivered by engines is all the recovered heat regardless of how much was actually utilised. The amount of electricity delivered by shore power is very small due to low electricity demands in port when the propulsion system is not used. About half of the delivered heat is from boilers and the other half is recovered heat from engines. This ratio is caused by the relation between the electricity demands and heating demands on board, and could differ significantly in other ships. Exact values for these results can be seen in appendix K.2.

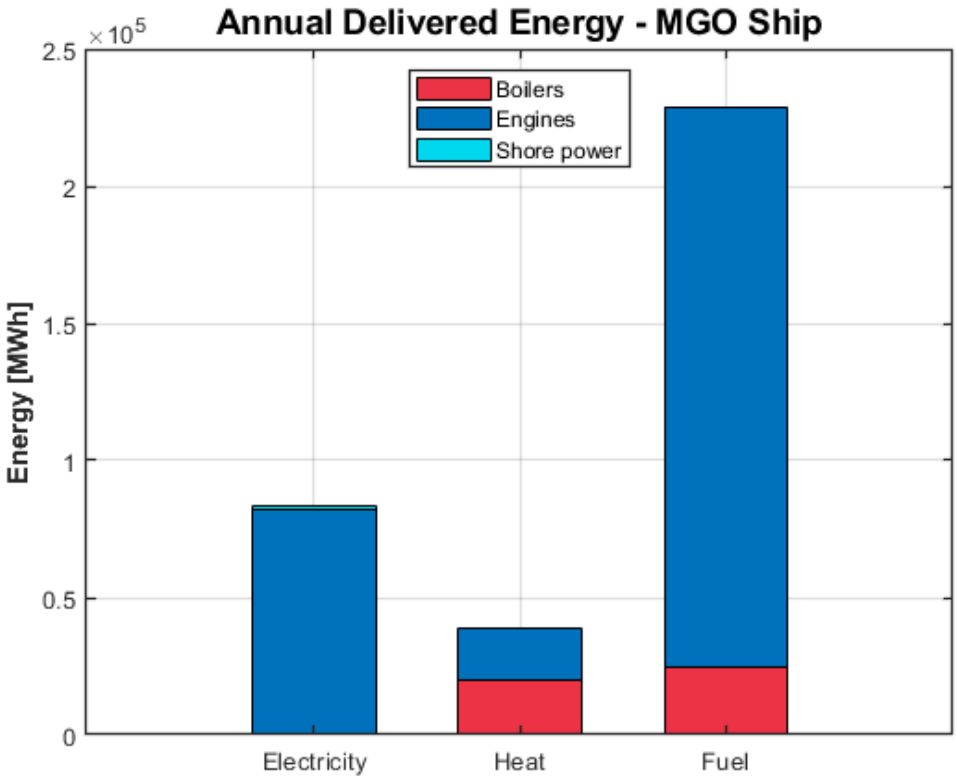

Figure 58: Delivered electricity and heat, as well as fuel consumption, for the MGO ship.

The boilers consume 10.9% of the fuel on board. On Birka Stockholm, the boilers only use 3.8% of the fuel, as seen in table 6. Seeing as Birka Stockholm does not use shore power, this difference could be caused by this ship using engines to cover electricity demands in port, which increases the use of engines and decreases use of boilers. The results are also affected by the relation between the heating demands and electricity demands on board.

LNG Ship

Seeing as the LNG ship has more unused recovered heat from the engines than the MGO ship, the 150 m^3 storage tank was not large enough to utilise all of it. Figure 59 shows the tank temperature throughout the year in the LNG ship. In the winter, the tank temperature increases above the base level in order to utilise unused recovered heat. The peak shaving in the winter was the same as for the MGO ship, with the boiler peak being reduced from 12.3 to 9.2 MW. In both the summer and the winter, the tank reaches its full capacity a significant amount of the time, and some heat was therefore wasted. Throughout the year, 1785 MWh of heat was wasted and 1535 MWh was saved.

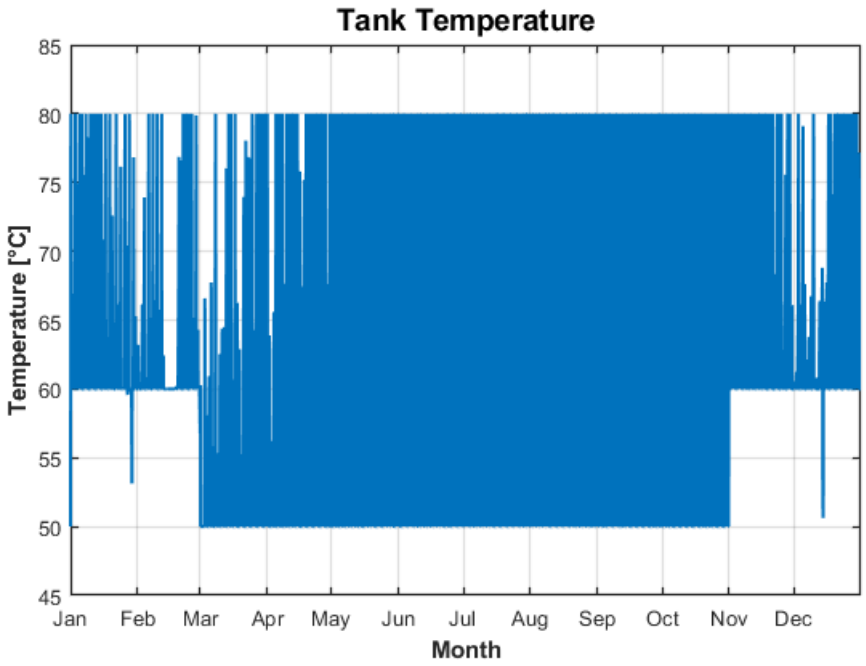

Figure 59: Temperature in the hot water storage tank throughout the year, for the LNG ship.

Figure 60 shows the recovered heat from engines, heat from boilers, heating demand and wasted heat, as well as charging and discharging rates on 5 August for the LNG ship. This is thus the same case as figure 54 for the MGO ship. The energy level of the hot storage tank throughout the day is shown in figure 61. Due to the large amount of heat recovered from engines, the tank reaches its full capacity and a lot of the unused recovered heat was wasted.

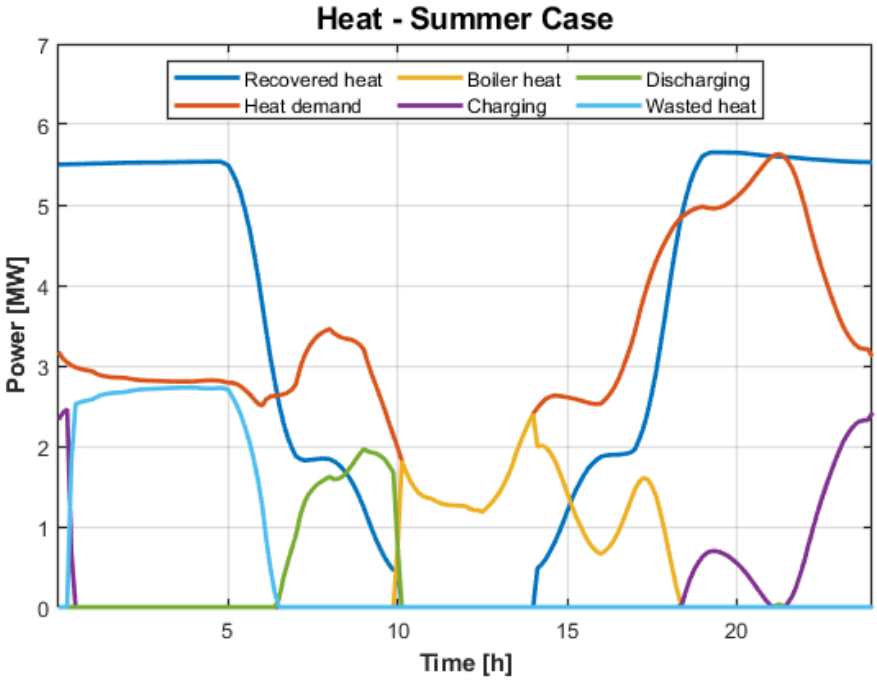

Figure 60: Heat from engines, boilers and the storage tank, as well as total heat demand, charging rate and wasted heat, 5 August on the LNG ship.

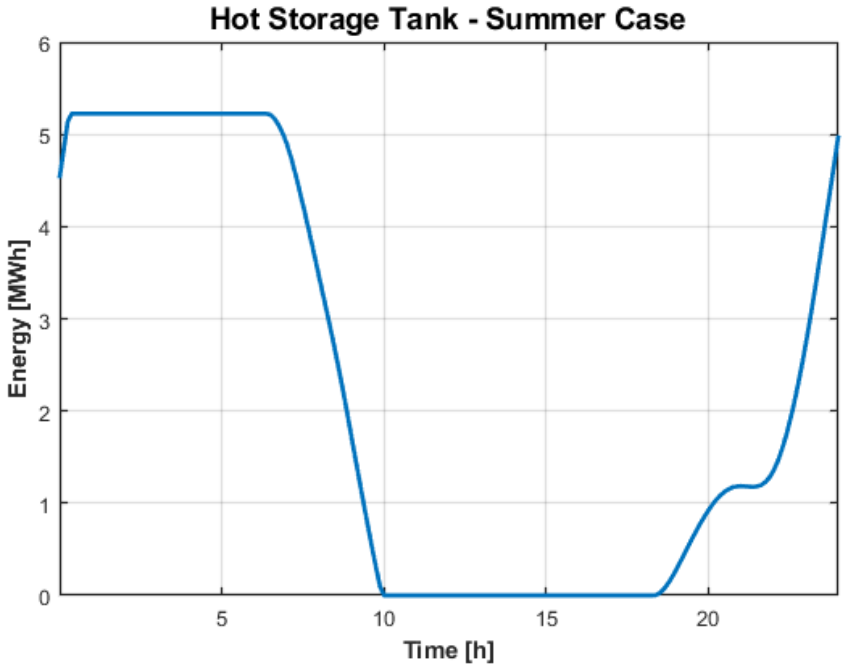

Figure 61: Energy level of the hot storage tank on 5 August, for the LNG ship.

In order to store all unused recovered heat throughout the year on the LNG ship, the tank size would need to be increased to 1853 m^3. This is considered unreasonably large and is likely too large to implement on most cruise ship. It would be very challenging to fit on an existing ship.

Figure 62 shows the total annual electricity and heat delivered by engines, boilers and shore power, as well as the fuel consumption for engines and boilers on the LNG ship.

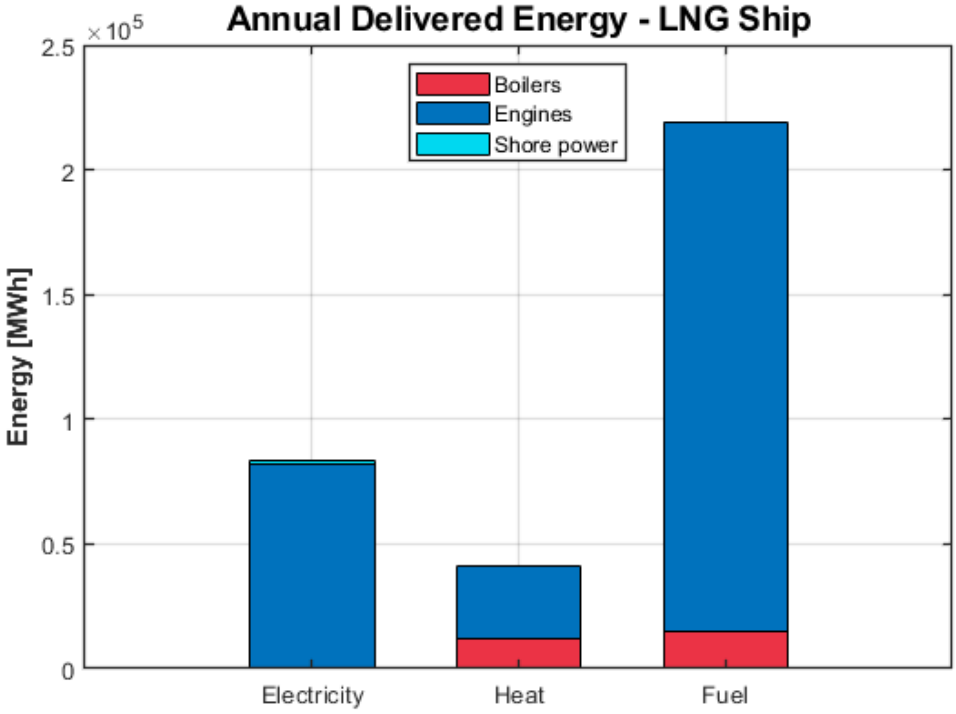

Figure 62: Delivered electricity and heat, as well as fuel consumption, for the LNG ship.

For the LNG ship, the electricity delivered by engines and shore power, as well as the engine fuel consumption, are the same as for the MGO ship in figure 58. This is due to identical electricity demands, and the same electrical efficiency being used for the engines. The amount of heat recovered from the engines is 50% higher for the LNG ship. This in turn reduces both the heat delivered from boilers and the boiler fuel consumption by 39%. This shows that the amount of heat recovered from engines can significantly impact the heat needed from boilers and the boilers' fuel consumption. Again, exact values for the results can be seen in appendix K.2.

6.6 Energy Efficiency Analysis

Figure 63 shows the annual energy consumption for the hotel system for the different energy efficiency scenarios, as well as the base case. Boiler heating is accommodation heating covered by the boiler in IDA ICE, while electric heating is electricity used by the heat pump to cover accommodation heating. Cases 9 and 10 are not included, as they were identical to the base case at this stage.

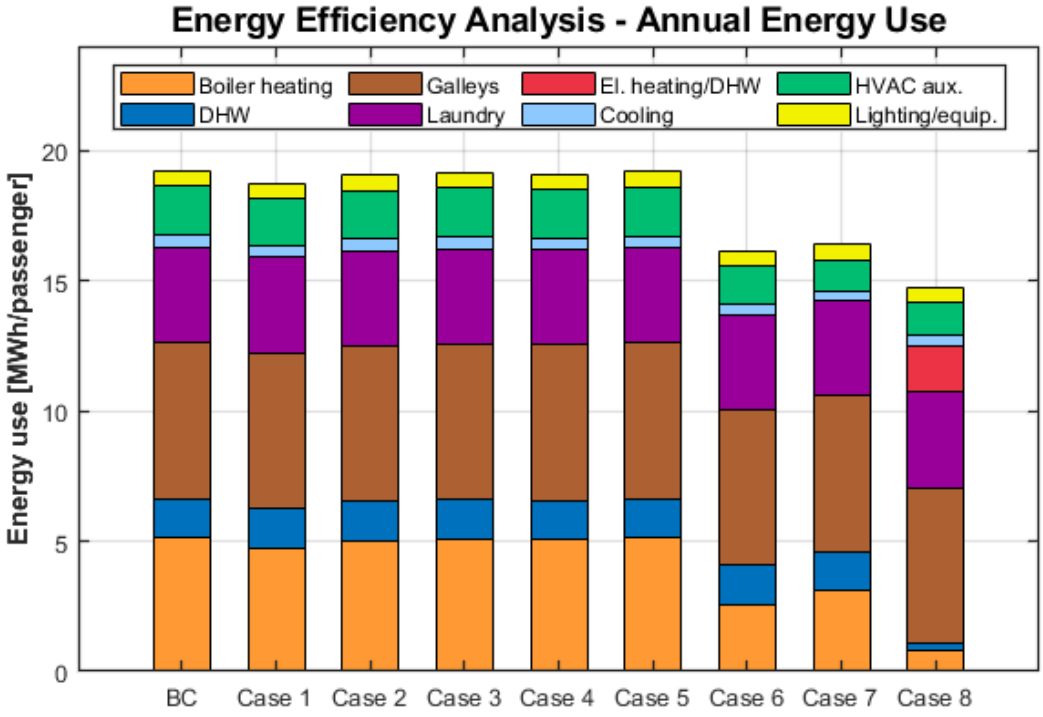

Figure 63: Annual energy consumption for the hotel system for the energy saving solutions.

Case 1 with heating setback shows a relatively small reduction in energy consumption. This reduction is mainly due to the accommodation heating being reduced by 7.5%. The energy use for fans and pumps was also decreased by 4.2% due to the reduced heating demand. The energy savings could be increased by expanding this solution to include the summer months. In the summer, the supply air temperature could be adjusted based on the outdoor temperature to avoid unnecessary cooling.

Case 2, where vehicle deck heating was turned off in port, has a slight reduction in energy consumption. This is caused by the accommodation heating being reduced by 2.4%. This small reduction could be due to the short setback period and the increased demand when heating is turned back on. Here, night setback is not an alternative as cars are still on the vehicle decks. Another option could be to lower the setpoint temperature on the vehicle decks by 1-2 °C at all times.

Case 3 with increased insulation thickness has a small reduction in annual energy consumption, with the heating being reduced by 1.1%. This small change is due to most of the heating demands in

the model being caused by heat losses through the ventilation system, and not through the external facades. In addition, the cooling increased by 0.6%, due to less heat being lost through the facades.

In Case 4 with improved windows, the heating was reduced by 1.4%. Again, it is relevant that much more heat is lost through the ventilation system than the external facades. Improving the windows reduced the heating more than increasing the insulation in Case 3. This is likely because the external walls were already relatively well insulated, while the windows were not. The cooling was reduced by 2.2%, likely due to reduced window sizes and reduced solar heat gains. The reduced window sizes would also affect the amount of daylight and the view from the ship, and could therefore negatively impact the indoor environment.

Case 5 with PCM layers in walls had very small total energy savings. The cooling was reduced by 1.4%, while the accommodation heating decreased by 0.07%. The cooling was reduced due to the varying cooling demands in the summer. The PCM layers absorb excess heat in the summer and thereby help keep the temperature below the cooling setpoint longer. During periods of the summer with lower temperatures, heat is released from the PCM.

As mentioned in section 5.14, the PCM melting temperature was set equal to the cooling setpoint in each zone. This means that the PCM layer is likely solid most of the time in the winter due to lower temperatures, and thus the PCM will not release heat to the zone and reduce the heating demand. This could be the reason the reduction in heating was so small. Even if the PCM had a lower melting point, there was no significant reduction in the heating demand. This could be because the ship sails in a relatively cold climate with cold winters where there are small variations in the heating demand.

Case 6 with heat recovery in the AHUs is one of the most efficient solutions. The energy use for heating was reduced by 50%. This is due to a large amount of the heat losses on the ship occurring in the ventilation system. Efficient recovery of this heat therefore provides significant energy savings. The energy use for cooling was also reduced by 6.2%, due to opposite operation of the heat recovery units when there is a cooling demand. The energy use for fans and pumps was reduced by 24%.

It is possible that a high heat recovery efficiency of 80% is not realistic for an existing ship, as the heat recovery system could be old and worn after years of use. However, a new heat recovery system should be able to have an efficiency around this level.

For Case 7 with VAV ventilation, the reduced ventilation led to a 40% reduction in heating, a 19% reduction in cooling and a 37% reduction in energy use for fans and pumps. In zones with temperature controlled DCV, this solution also enabled increased ventilation when there is a cooling demand, which contributes to the reduced cooling need.

Case 8 with a heat pump has the largest energy savings of all the solutions. In IDA ICE, the boiler's energy use for DHW is presented together with the accommodation heating. When separating these results, it was assumed that the ratio of peak heating and base heating was the same for both. The total energy use for DHW and accommodation heating, including electricity for the heat pump, was reduced by 58% compared to the base case. The boiler heating was reduced by 84%, and the energy use for all fans and pumps was reduced by 34% due to the reduced heating. The total electricity demand was increased by 38% due to electricity demand for the compressor in the heat pump.

Figure 64 shows duration curves for accommodation heating covered by the boiler for the energy efficiency scenarios. Again, Cases 9 and 10 were not included as they were identical to the base case.

Case 1 with heating setback had a small reduction in heating demand throughout the whole year. The annual peak for accommodation heating was reduced from 10.8 to 10.4 MW. In the base case, the peak occurred in port due to large heating demands when the vehicle deck ventilation rate is doubled

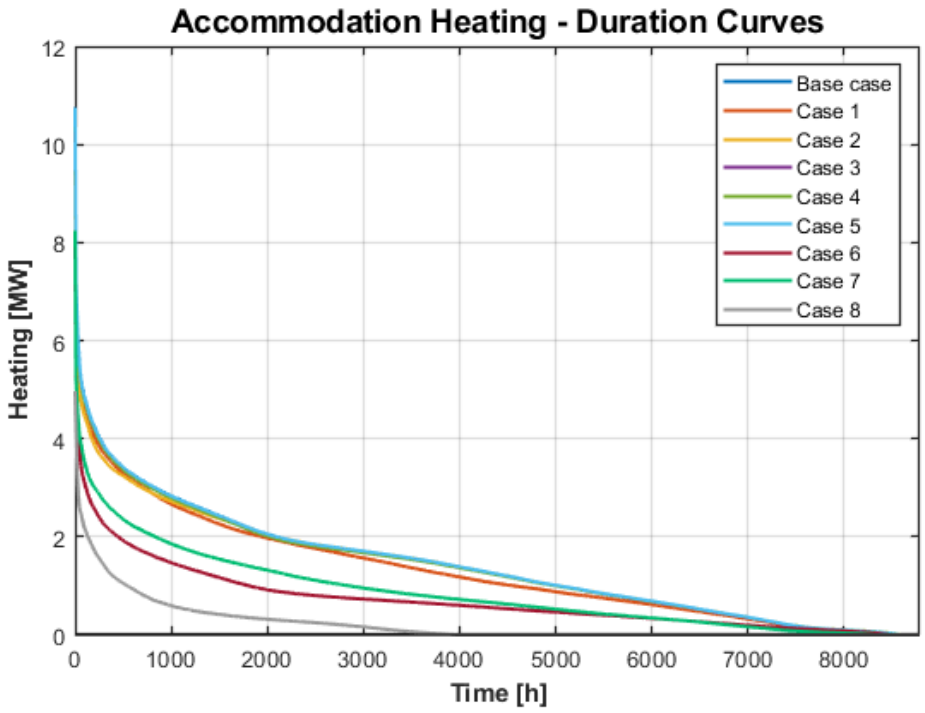

Figure 64: Duration curves for accommodation heating covered by the boiler for the different energy saving solutions.

during roll off. In Case 1, this heating demand was drastically reduced due to setback in port. Instead, the peak occurred right after the port stay.

Seeing as the highest heating demand in the base case occurred due to doubled ventilation rate during roll off, this was also significantly reduced in Case 2, where vehicle deck heating was turned off in port. The peak heating was reduced down to 9.5 MW.

Cases 3 and 4 with increased insulation and improved windows have duration curves almost identical to the base case. This is due to very similar total accommodation heating and no significant change in peak heating demand. This was also true for Case 5, with PCM layers in walls.

Case 6 with ventilation heat recovery and Case 7 with VAV ventilation have lower energy use for heating throughout the whole year. The peak reduction was 26 and 23%, respectively. This is in line with the results in figure 63 and was therefore expected.

In Case 8, most of the heating demand was covered by the heat pump. Seeing as figure 64 only includes heating covered by the boiler in IDA ICE, the curve for Case 8 is significantly lower than the other cases. The peak was reduced by 54% compared to the base case.

Figure 65 shows duration curves for cooling for the energy efficiency scenarios and the base case. Case 6 with heat recovery shows a small reduction in cooling demand when the cooling demand is highest, and the peak was reduced by 11%. The reason the cooling was not reduced throughout the whole year could be the cooling demand in the fan coils which is not affected by the ventilation heat recovery.

Case 7 with VAV ventilation has reduced cooling for a larger part of the year due to the overall reduced ventilation rate when the weather is warm. Temperature controlled DCV also means that the ventilation rate is increased when there is a cooling demand instead of local cooling starting immediately. For this case, the peak cooling demand was reduced by 8.9%. The remaining scenarios have cooling duration curves very similar to the base case.

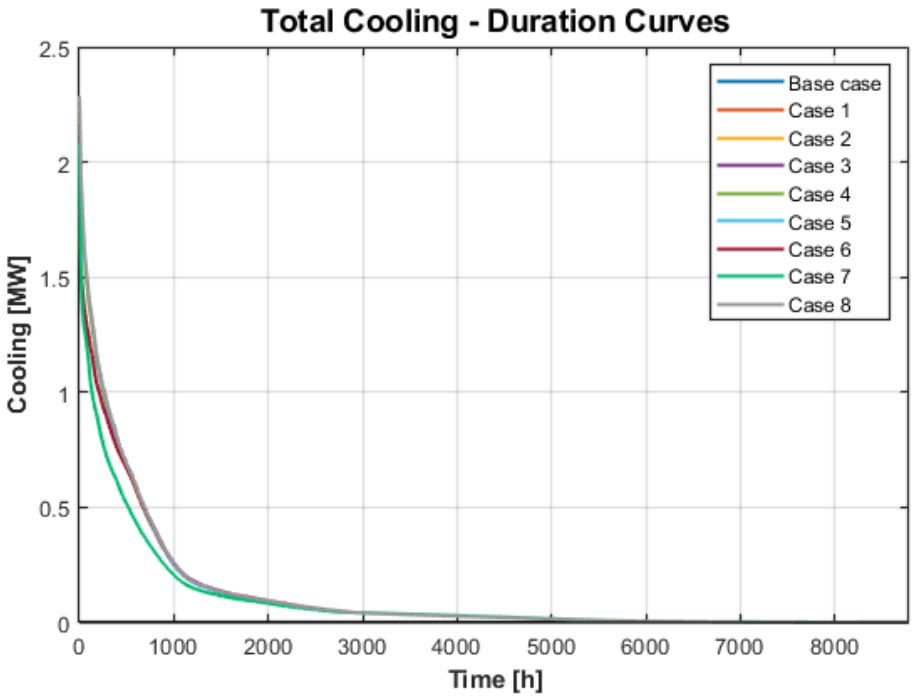

Figure 65: Duration curves for cooling demand for the different energy saving solutions.

Figure 66 shows duration curves for the hotel system's total electricity use. Case 6 with ventilation heat recovery and Case 7 with VAV ventilation had reductions in electricity consumption caused by the reduced use of fans and pumps and reduced cooling. Case 8 had a large increase in electricity consumption due to use of the heat pump. The remaining cases were similar to the base case.

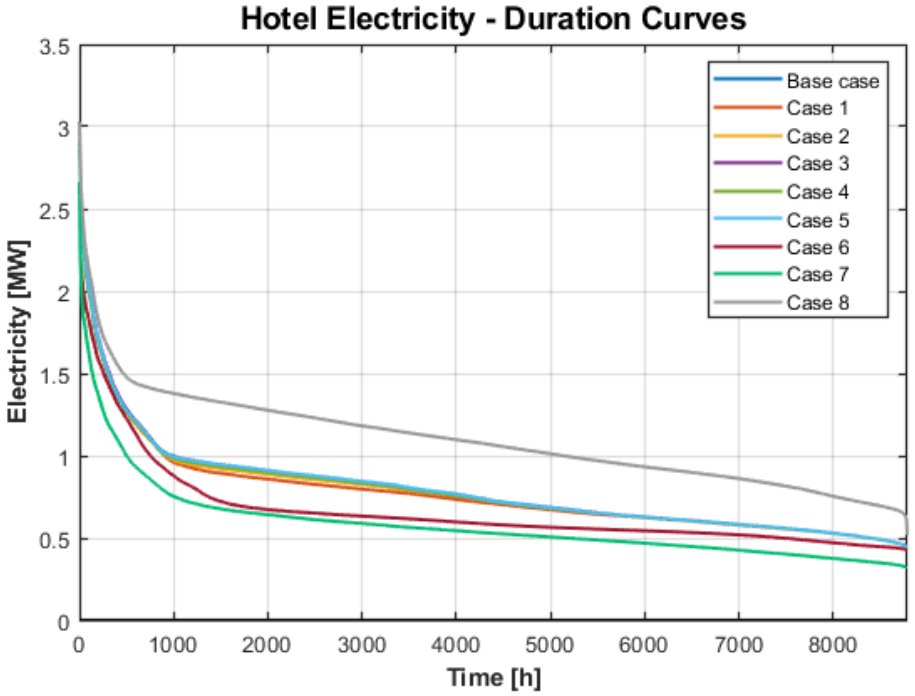

Figure 66: Duration curves for hotel electricity use for the different energy saving solutions.

Implementing energy saving solutions that significantly lower the peak heating and cooling demands

on an existing ship would lead to the fan coils, chillers and boilers being oversized. The weight of the ship and the energy demand for propulsion could then be unnecessarily high. In the case of large reductions in peak demand, one should investigate if it is beneficial to downsize these components to reduce the weight of the ship.

The energy demand for galleys and laundry was not decreased in any of the energy efficiency scenarios. This therefore represents a large potential for reduced energy use. It could be beneficial to improve the heat recovery from the engines to reduce the use of boilers to cover these large heating demands. However, in the future it will likely become more common to use batteries and fuel cells in the propulsion system, which will reduce the amount of waste heat available. In this case, energy saving solutions will not lead to any heat going to waste, and reducing the hotel system's energy consumption becomes even more relevant.

6.6.1 Case 1 - Heating Setback in Port and at Night

Air temperatures and zone heating were investigated for 29 January because this day had the lowest air temperatures in most of the zones in January. This was considered a representative winter day.

Figure 67 shows the air temperature in the large galleys on 29 January when heating setback was implemented. During both setback periods, the air temperature decreases gradually to around 11 °C. When normal heating resumes, the zone temperature reaches the heating setpoint after about 45 minutes, and it increases above the setpoint by a small amount. The temperature is above 20 °C most of the occupancy period, and the heating setpoint is reached relatively quickly. The thermal environment is therefore considered acceptable. The fact that the heating setpoint is reached quickly can be explained by the fan coils in the large galleys having a high heating capacity to accommodate the large ventilation rate.

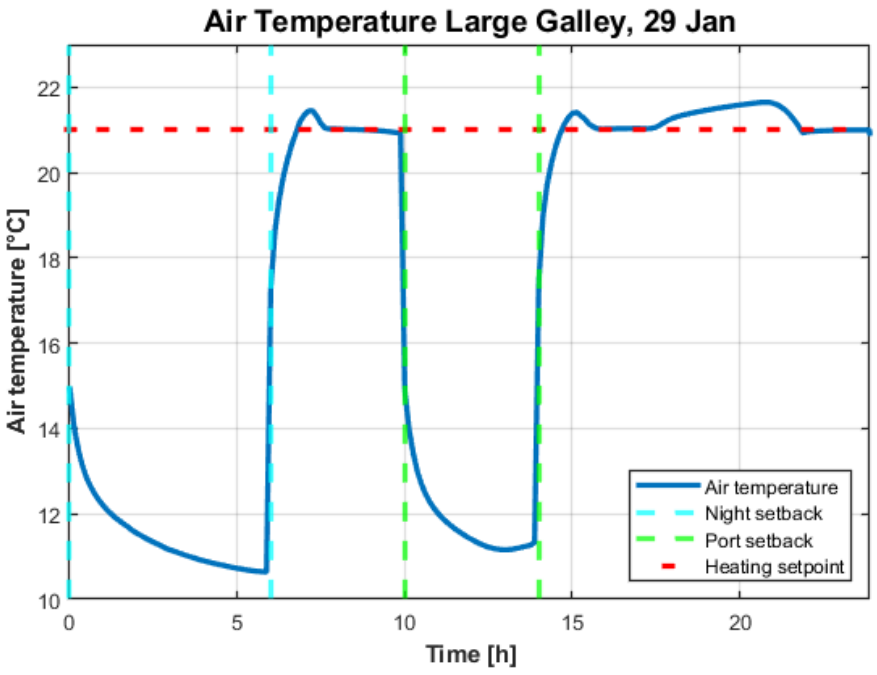

Figure 67: Air temperature in the large galleys on 29 January with heating setback.

Figure 68 shows the zone heating provided by fan coils in the large galleys throughout the day. There was no heating during the setback periods due to the reduced supply water temperature for zone heating. When normal heating resumes, there are significant peaks in the zone heating.

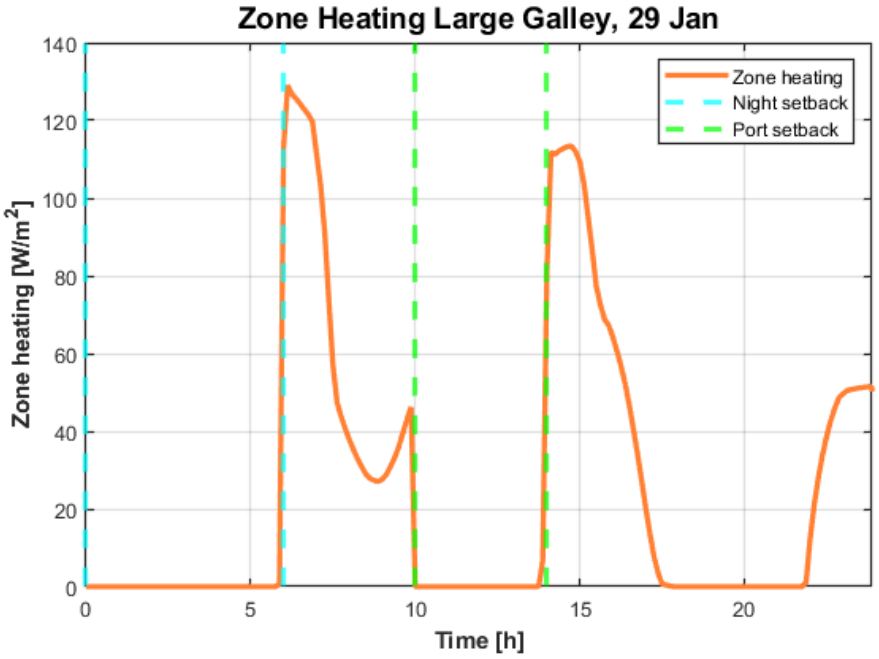

Figure 68: Zone heating in the large galleys on 29 January with heating setback.

Figure 69 shows the air temperature in the smallest shop. After the first setback period, the temperature does not reach the heating setpoint. After the second period, it takes over 8 hours before the setpoint is reached. This is caused by the fan coils in the small shop having no heating, due to the heating demand in the calibrated model being zero. The temperature goes down to around 18 °C in the occupancy period, which is not considered acceptable. Similar trends were found in other zones with low or no heating capacity in the fan coils. If this measure were to be implemented, the heating capacity in these zones should be increased.

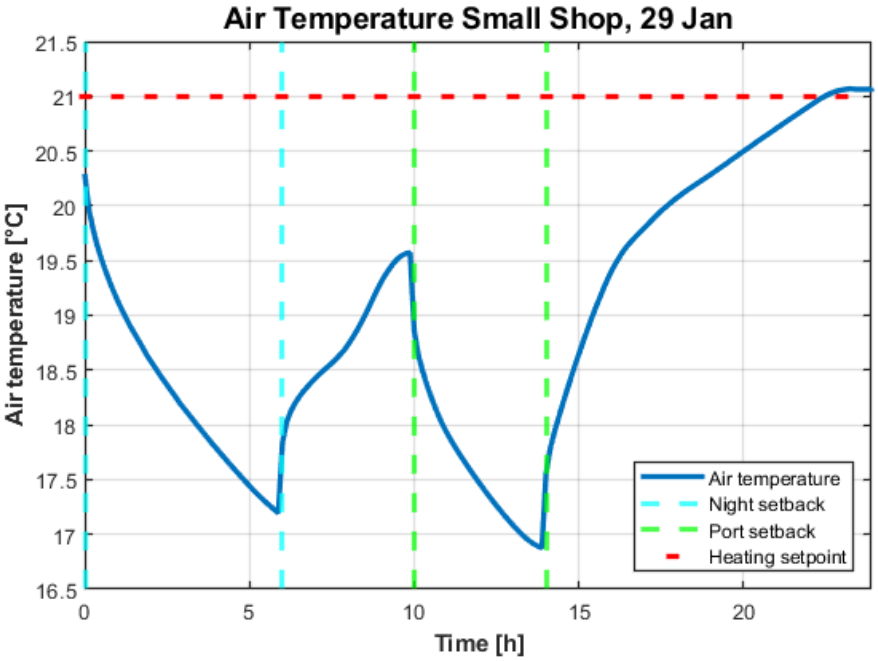

Figure 69: Air temperature in the small shop on 29 January with heating setback.

Figure 70 shows the air temperature in a 10.5 m^2 ocean view cabin on 29 January. The supply air temperature was not reduced at night, as guests are staying in the cabin. However, the air temperature in the zone was somewhat reduced at night due to the reduced supply water temperature for zone heating. In this cabin, the temperature goes down to 19.6 °C. Many people prefer to sleep in a colder environment, and this might therefore be acceptable. For some larger cabins, the temperature goes down to around 15 °C at night, which is likely to be too cold. To avoid this problem, the heating system for cabins would have to be separate from the rest of the heating system and have no reduction in supply water temperature at night.

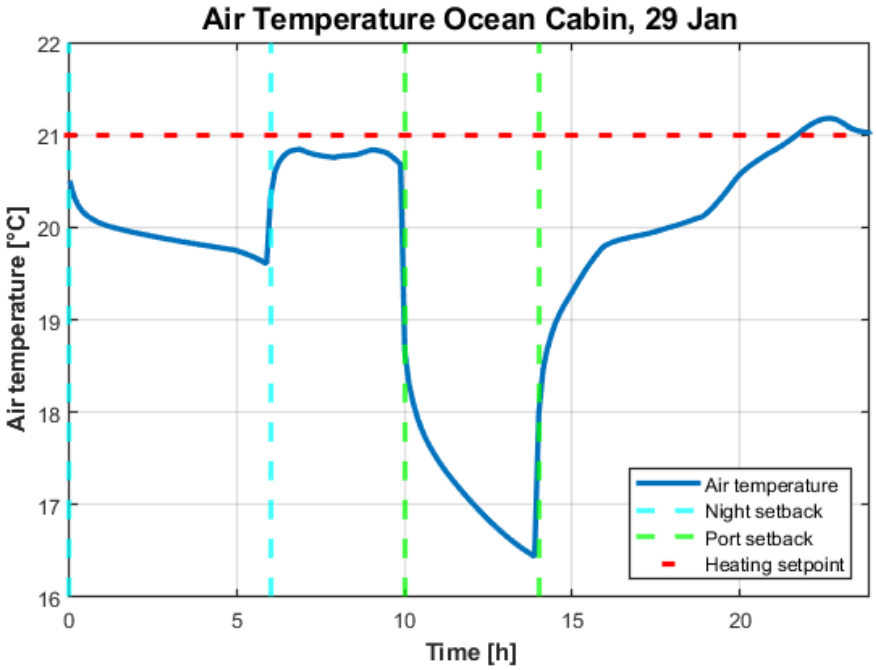

Figure 70: Air temperature in an ocean view cabin on 29 January with heating setback.

After the first setback period, the air temperature in the ocean cabin stays below the heating setpoint by a small amount. After the second setback period, it takes almost 8 hours until the setpoint is reached. Figure 71 shows the zone heating in the cabin throughout the day. For a large part of the day, the heating is below the maximum due to the supply water temperature for heating being below 60 °C. This is the reason it takes so long for the heating setpoint to be reached. To improve this, the heating capacity for fan coils in these cabins should be increased, or measures should be done to ensure a high enough supply water temperature.

The results show that the heating setpoint is reached fast in some zones and slowly in others. If this energy saving measure is to be used, the heating rate in the fan coils in some zones should be increased to reach the heating setpoint faster and provide a better thermal environment after the setback period. However, this would require bigger fan coils, which would increase the weight of the ship. It is unknown how large this difference would be, but considering the large number of fan coils on the ship, it could be significant. Increasing the heating in these zones would also reduce the energy savings provided by the solution.

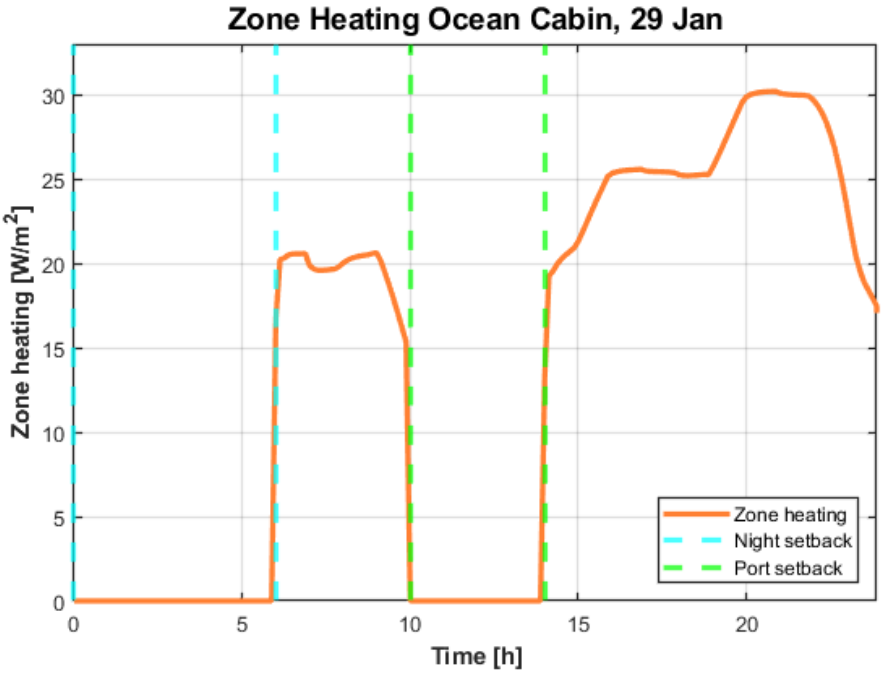

Figure 71: Zone heating in an ocean view cabin on 29 January with heating setback.

Figure 72 shows the air temperature in the Aqualand on 29 January. Even though the Aqualand was not included in this energy saving solution, the temperature in the zone was significantly reduced due to the reduced supply water temperature for zone heating. The air temperature goes as low as 19.1 °C, which would drastically increase evaporation from the pool. In reality, the supply water used for heating the Aqualand would likely be separate from the supply water heating other zones, to ensure adequate temperatures in the Aqualand at all times. This solution is therefore not entirely realistic.

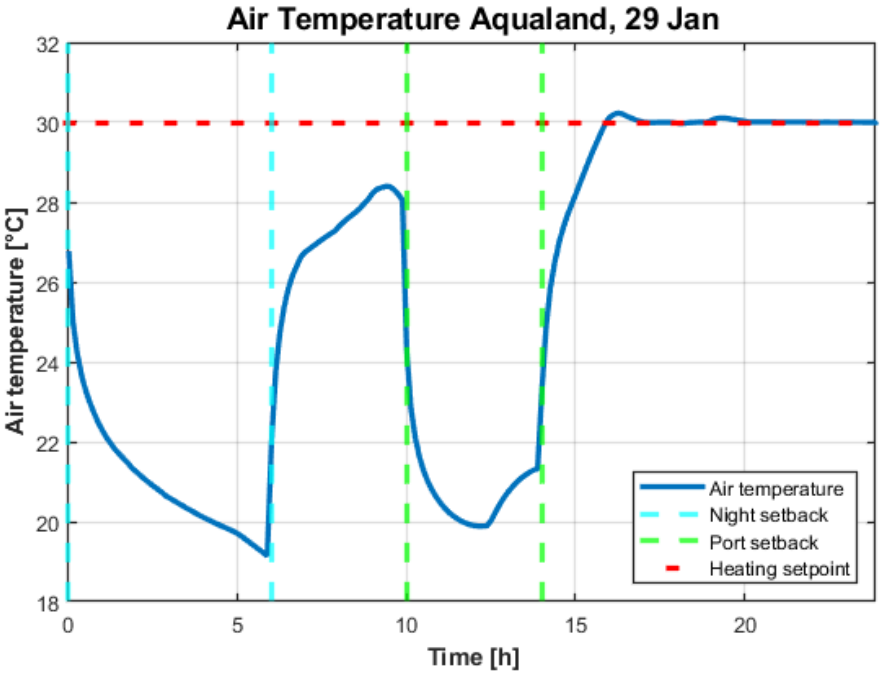

Figure 72: Air temperature in the Aqualand on 29 January with heating setback.

Some zones, including the casino and the night club, are open longer than midnight. In this case, the temperature in these zones would therefore decrease while people are there. In reality, it would be beneficial to shift the night setback in these zones, so that it fits better with the opening hours. This can be done only if these areas are served by their own AHU. To maintain the temperature setpoints during occupancy, the zone heating in these zones should also be separate from other zones.

Adjustments might also have to be made if some guests stay on the ship when in port. Then, the heating could be reduced only in areas the guests will not visit. This would maintain a satisfactory indoor environment for the guests, but also reduce energy savings from this measure.

Implementing heating setback led to occasional large reductions in the heating demand in the winter. During these periods, more of the recovered heat from engines will not be utilised and must be stored in the tank. Figure 73 shows the tank temperature throughout the year for Case 1 on the MGO ship. The amount of unused recovered heat is lower in the winter than in the summer. The summer months were identical to the base case, as they did not have heating setback. The 150 m^3 tank was therefore large enough to store all unused recovered heat, and no heat was wasted.

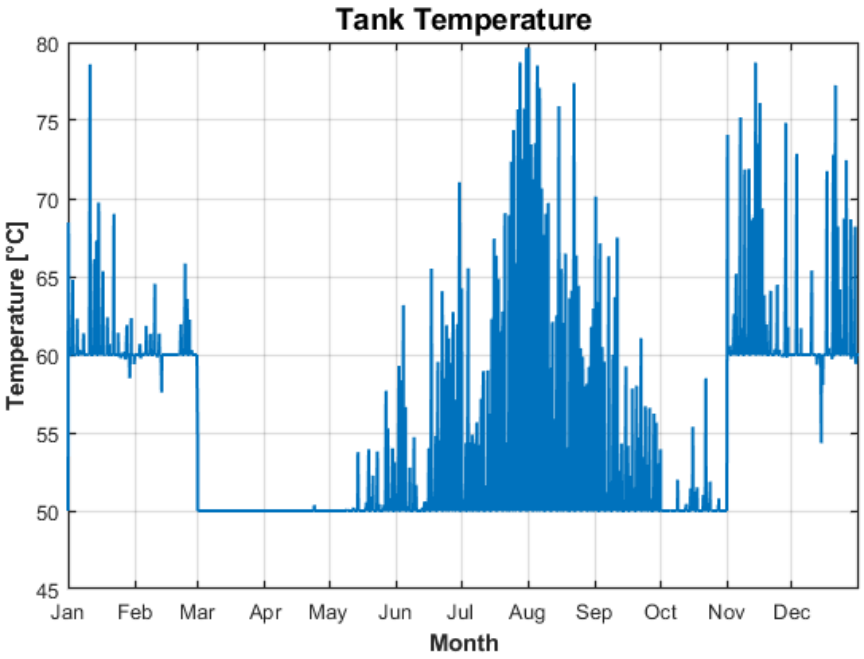

Figure 73: Temperature in the hot water storage tank throughout the year, for Case 1 on the MGO ship.

6.6.2 Case 2 - Turning off Vehicle Deck Heating in Port

Again, air temperatures and zone heating were investigated for 29 January because this day had the lowest air temperatures on the vehicle decks in January. Similar trends were found for both the car decks and the trailer decks.

Figure 74 shows the air temperature in the car decks on 29 January when the heating was turned off in port. When the heating is shut off, the air temperature quickly goes down to around -7 °C. This is due to the large ventilation rate during roll off at 10:00. When normal heating resumes, the zone temperature goes back above the heating setpoint in the first timestep. This fast increase is caused by the fan coils being dimensioned for the heat rate required during roll on and roll off when the ventilation rate is doubled. The temperature increases to 7.5 °C and oscillates slightly before settling at the heating setpoint.

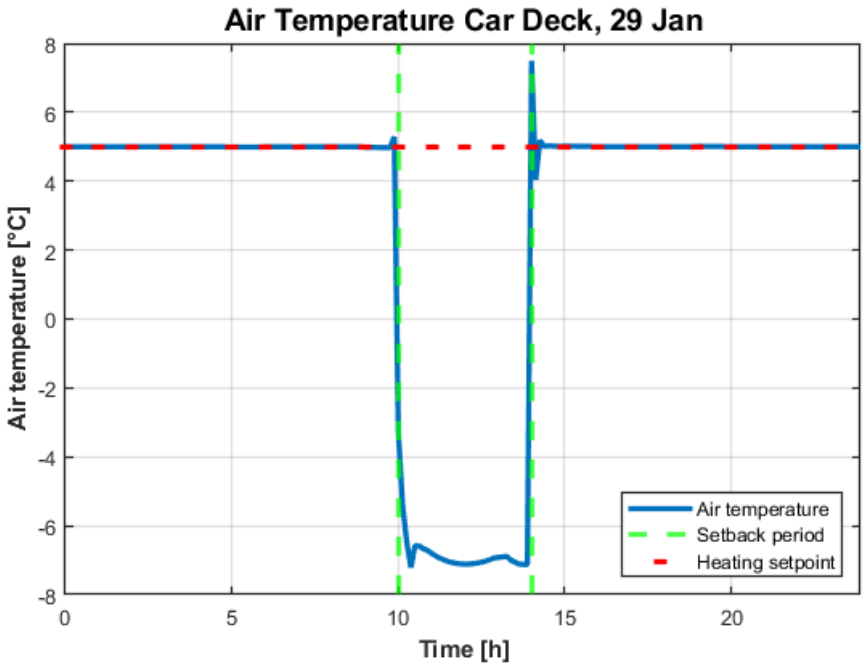

Figure 74: Air temperature in the car decks on 29 January when vehicle deck heating was turned off in port.

Figure 75 shows the zone heating on the car decks on 29 January. There is a large peak when the heating is turned on after the setback period, in order to bring the air temperature back to the heating setpoint. The variation in heating throughout the day strongly correlates with the outdoor temperature.

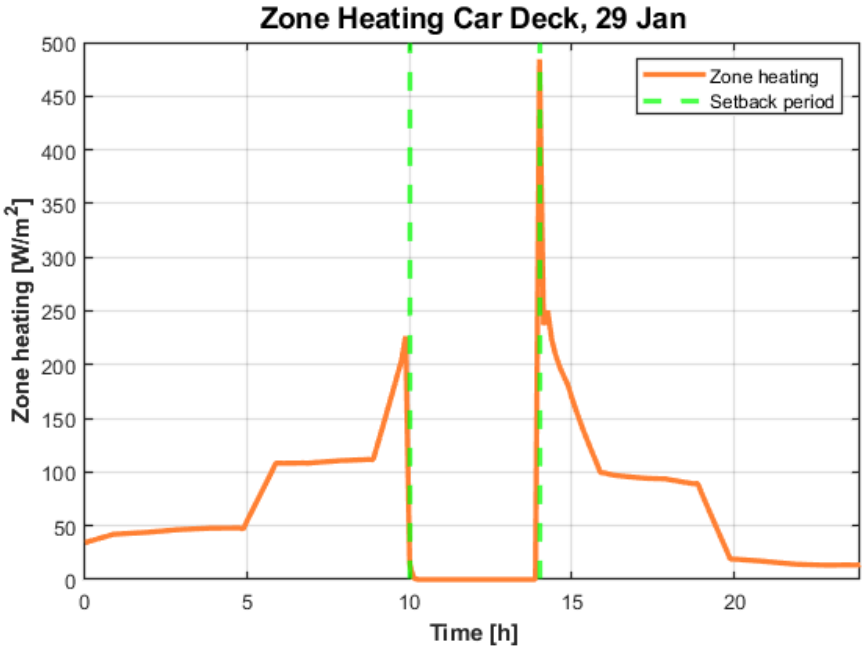

Figure 75: Zone heating in the car decks on 29 January when vehicle deck heating was turned off in port.

Figure 76 shows the total accommodation heating on the ship on 29 January when the vehicle deck heating was turned off in port. The total heating is significantly reduced in port, which shows that heating of the vehicle decks is a large part of the total energy use for heating. When the heating is turned back on, there is a subsequent peak in the heating rate.

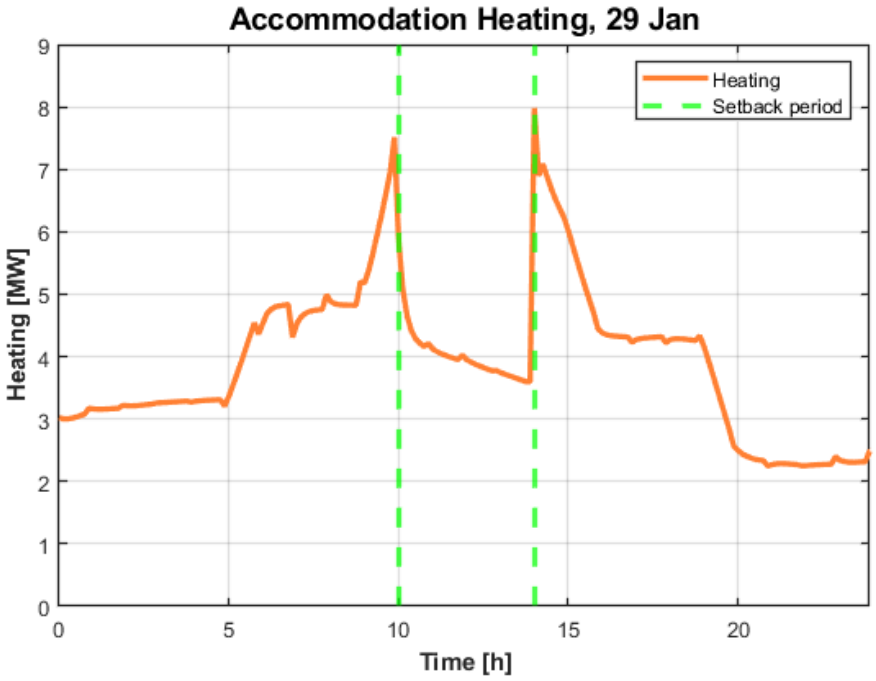

Figure 76: Total accommodation heating on 29 January when vehicle deck heating was turned off in port.

In comparison, the total accommodation heating on the ship for the base case is shown in figure 77. The heating is increased during roll on and roll off due to the ventilation rate on vehicle decks being doubled. For the base case, the peak heating on 29 January was 10.4 MW. When the heating on vehicle decks is turned off in port, the peak is at 8.0 MW, shown in figure 76. This lower peak is due to there being no heating on the vehicle decks when the ventilation rate is doubled.

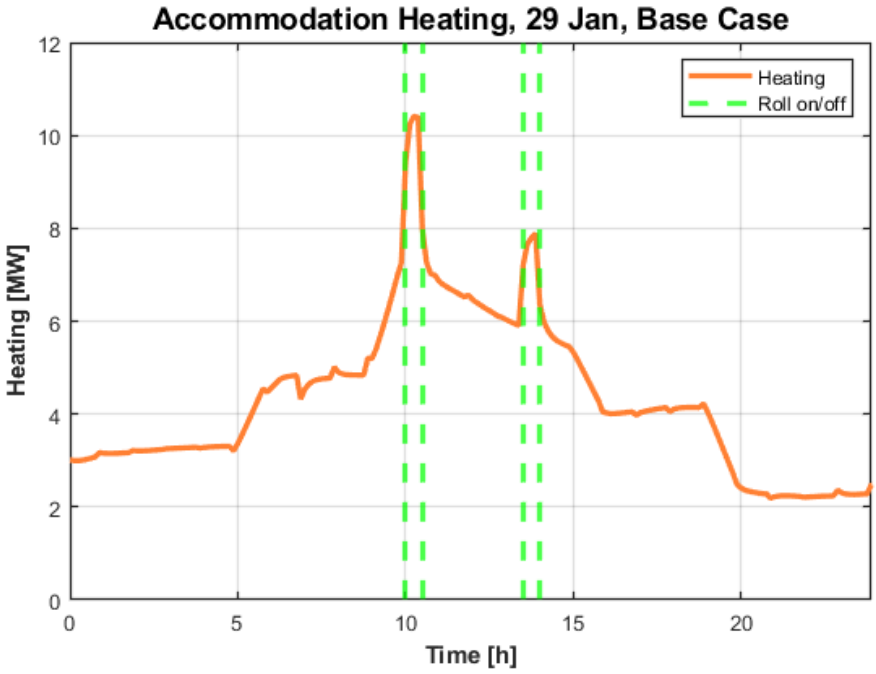

Figure 77: Total accommodation heating on the ship on 29 January for the base case.

For the MGO ship, the post processing for this case was very similar to the base case. When the vehicle deck heating was turned off in port, heating demands in port were reduced, while heating demands at sea increased. However, this only happened in the winter, when vehicle deck heating was needed. Seeing as there was no unused recovered heat in the winter in this case, and there is no recovered heat in port, there was no change in the amount of unused recovered heat.

6.6.3 Case 6 - Ventilation Heat Recovery

As seen in figure 63, implementing ventilation heat recovery led to a large reduction in the heating demand. This means that more of the recovered heat from engines is not utilised and must be stored in the tank. Figure 78 shows the tank temperature throughout the year for Case 6 on the MGO ship. In the winter, unused recovered heat was used to charge the tank, but the amount of unused heat is significantly lower than in the summer.

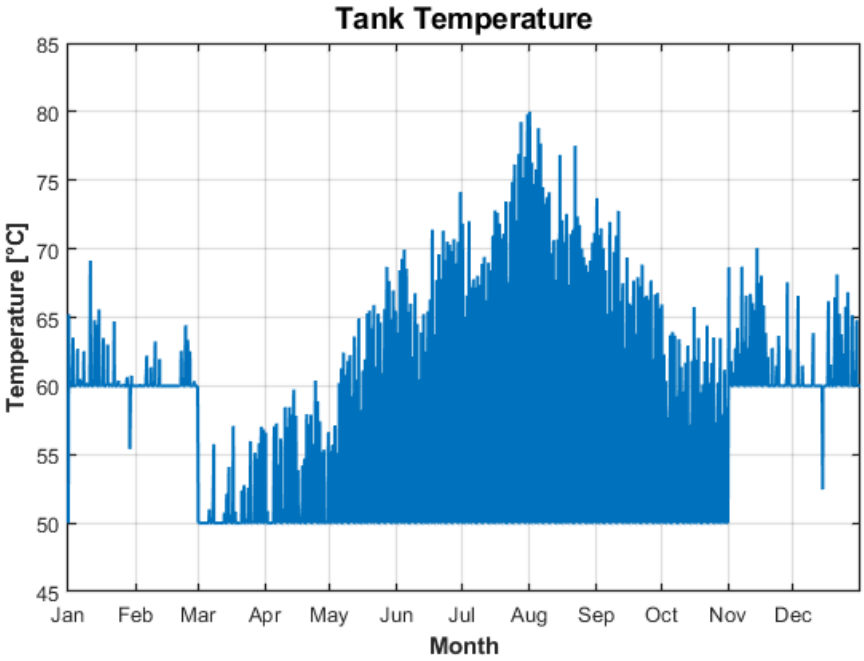

Figure 78: Temperature in the hot water storage tank throughout the year, for Case 6 on the MGO ship.

In the summer, the days with the highest amount of unused recovered heat looked almost identical to the base case. This is due to insignificant demands for ventilation heating on these days, meaning that the total heating demands were not affected by the ventilation heat recovery. Due to this, the 150 m^3 tank was still large enough to store all unused recovered heat, and no heat was wasted.

6.6.4 Case 7 - VAV Ventilation

Figure 79 shows the tank temperature throughout the year for Case 7 on the MGO ship. Reduced heating demands led to some unused recovered heat being used to charge the tank in the winter. In the summer, the amount of unused recovered heat is also higher than in the base case. Due to this, a small amount of heat was wasted.

This energy saving solution has more unused recovered heat than Case 6 in both the summer and winter, despite having a higher annual heating demand. This is due to Case 7 having reduced heating especially at night when the demands are already relatively low. This leads to larger amounts of unused recovered heat during these periods.

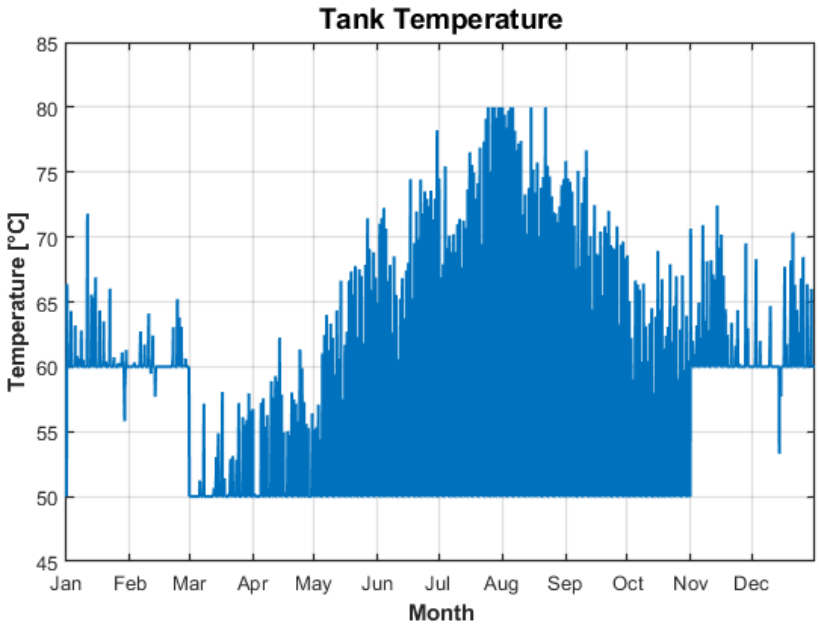

Figure 79: Temperature in the hot water storage tank throughout the year, for Case 7 on the MGO ship.

6.6.5 Case 8 - Heat Pump

The air-to-water heat pump in the model was expected to have similar COP to large air-to-air heat pumps. Figure 80 shows a duration curve for the heat pump's COP throughout the year. The COP is usually between 2 and 4, and it therefore fits with the literature study in section 2.14. In reality, several smaller heat pumps would likely be used for this solution. This would improve the overall COP by avoiding low COP at part load by instead turning off some of the heat pumps.

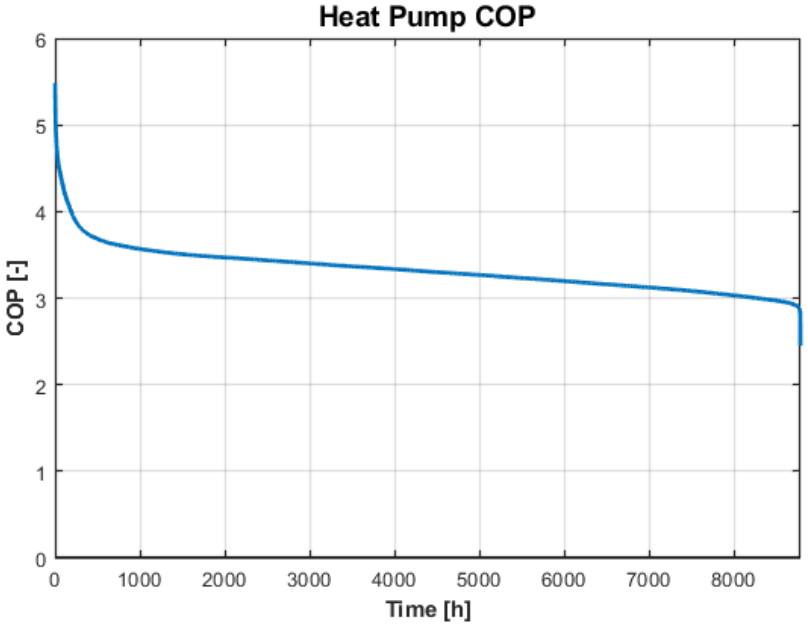

Figure 80: Duration curve for the heat pump's COP.

Figure 81 shows a duration curve for the total heating delivered by the heat pump and by the peak heating. This includes accommodation heating and DHW heating. There is significant variation in the

condenser heating throughout the year, shown as a black area in the graph. This could be caused by variations in outdoor temperature that do not match up with the total heating demand. These fast variations are also related to the control of the heat pump in IDA ICE, where the heat pump delivers as much as it can to cover the heating demands at any time. When the heating demand is largest, the condenser heating is reduced due to low outdoor temperatures reducing the heat pump's performance.

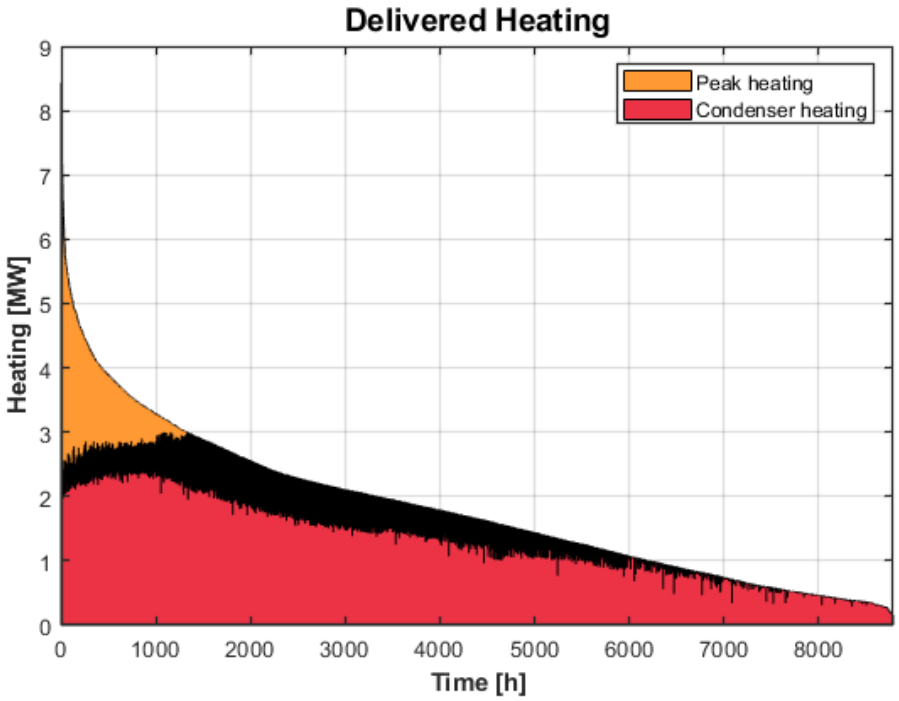

Figure 81: Duration curve for heating delivered by the heat pump and by peak heating.

Figure 82 shows the temperature in the hot water tank throughout the year for Case 8 on the MGO ship.

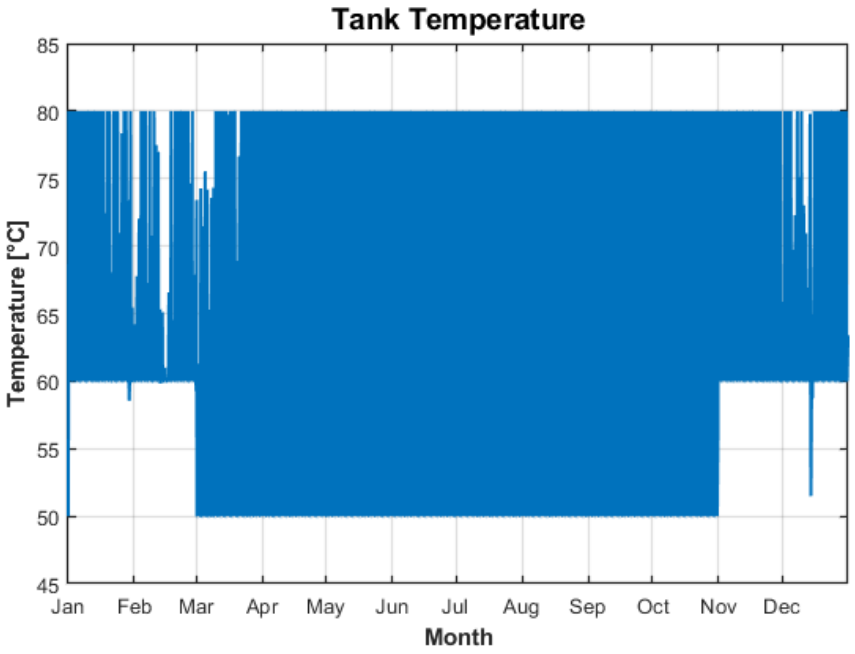

Figure 82: Temperature in the hot water storage tank throughout the year, for Case 8 on the MGO ship.

This shows that the tank reaches full capacity frequently throughout the whole year. This is due to the large reduction in heating demand giving a large increase in unused recovered heat. The increase in electricity demand caused by the heat pump also contributes to more recovered heat, though this electricity demand was small compared to the propulsion demand. When there is unused recovered heat available, it would be beneficial to use this instead of running the heat pump. As the recovered heat was calculated in post processing, this could not be prioritised in this case. 1634 MWh of unused recovered heat was saved using the tank, while 633 MWh was wasted.

6.6.6 Case 9 - PV Panels

Figure 83 shows the electricity production from PV panels throughout the year. As expected, the production is highest in the summer and low in the winter. The peak production is 83.3 kW.

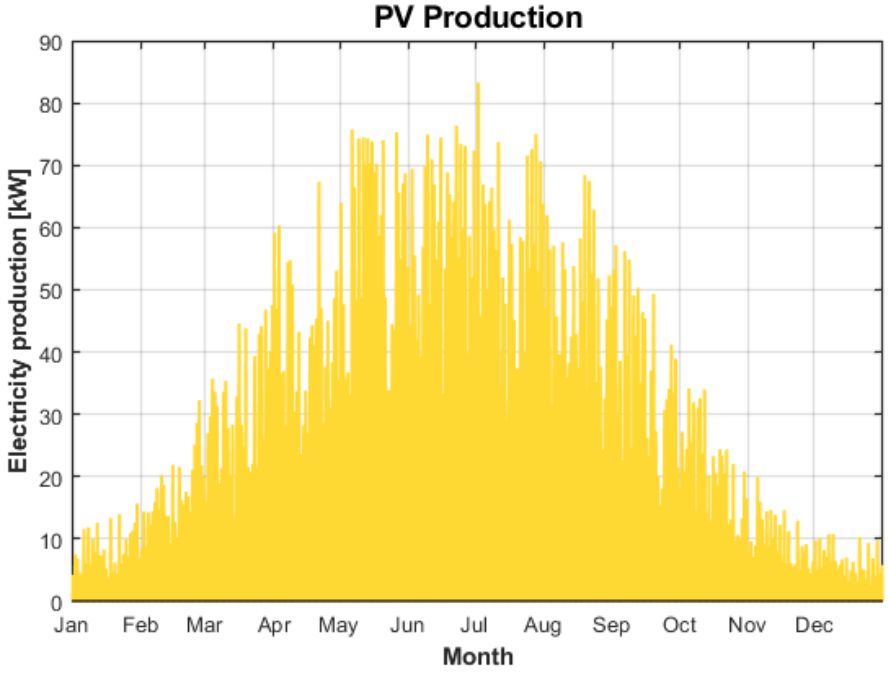

Figure 83: Electricity production from PV panels throughout the year.

Figure 84 shows a duration curve for the electricity production from PV panels. This shows the production being zero around half of the time due to there being no sun at night. The total annual production from PV panels is 84.2 MWh, or 0.04 MWh/passenger. For reference, this is 6.1% of the electricity demand for lighting and equipment.

Figure 85 shows the electricity delivered by the engines and by shore power on 2 July, as well as the production from PV panels. This was the day with the highest peak in PV electricity production. It is clear that the electricity from PV panels is very small compared to the electricity demand. More PV panels could be added to the ship, ideally on the roof, to increase the production. On existing ships, it could be challenging to find appropriate locations for the PV panels where they will not cause problems for guests or operation of the ship, and where other constructions do not block the sun.

Due to the relatively low production from PV panels, the post processing was almost identical to the base case. In a case with much more onboard electricity production, the electricity delivered from engines would be reduced, and thus also the amount of recovered heat available. This would give a larger demand for heat from the boilers.

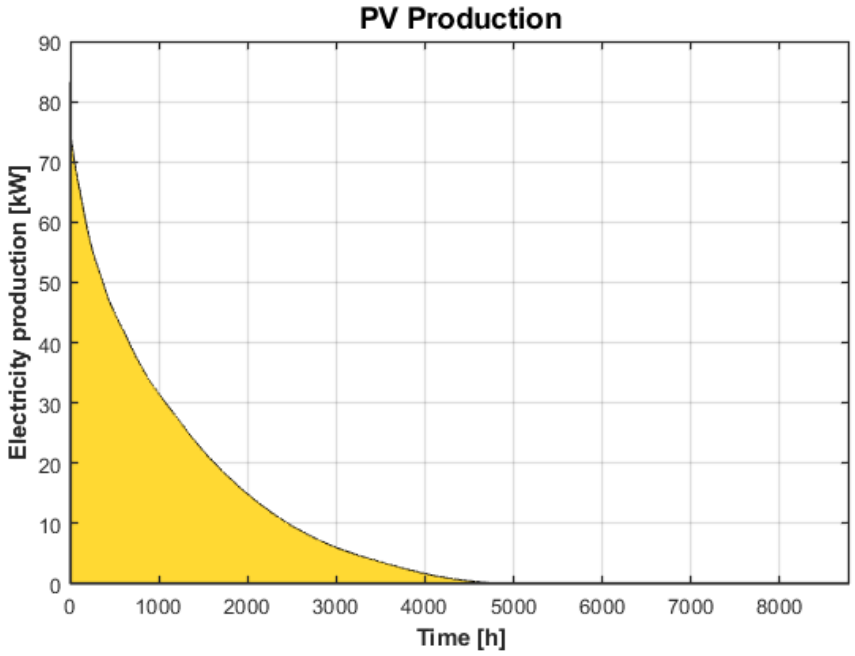

Figure 84: Duration curve for the electricity production from PV panels.

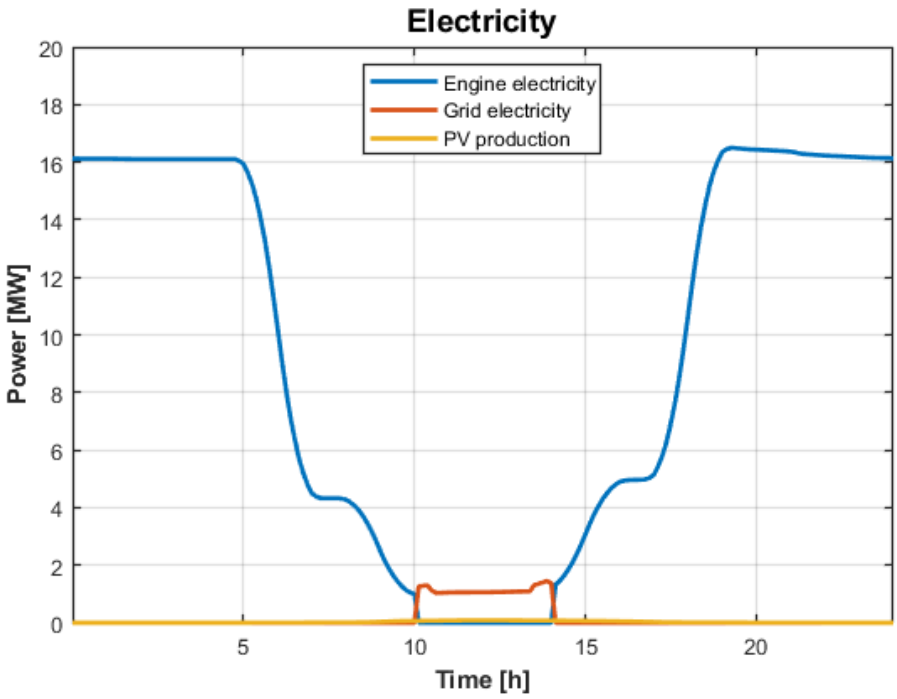

Figure 85: Electricity delivered by the engines, shore power and PV panels on 2 July.

6.6.7 Case 10 - Hot Storage Tank for Heat Demands in Port

The results presented here are for the case with MGO engines and boilers. Figure 86 shows the cumulative heat rate for charging and discharging of the hot water storage tank throughout the year, with a tank size of 1105 m^3, which was needed to cover all heat demands in port. Compared to the base case shown in figure 51, the charging and discharging are more similar in the summer and the winter due to having almost the same operation, with charging and discharging every day.

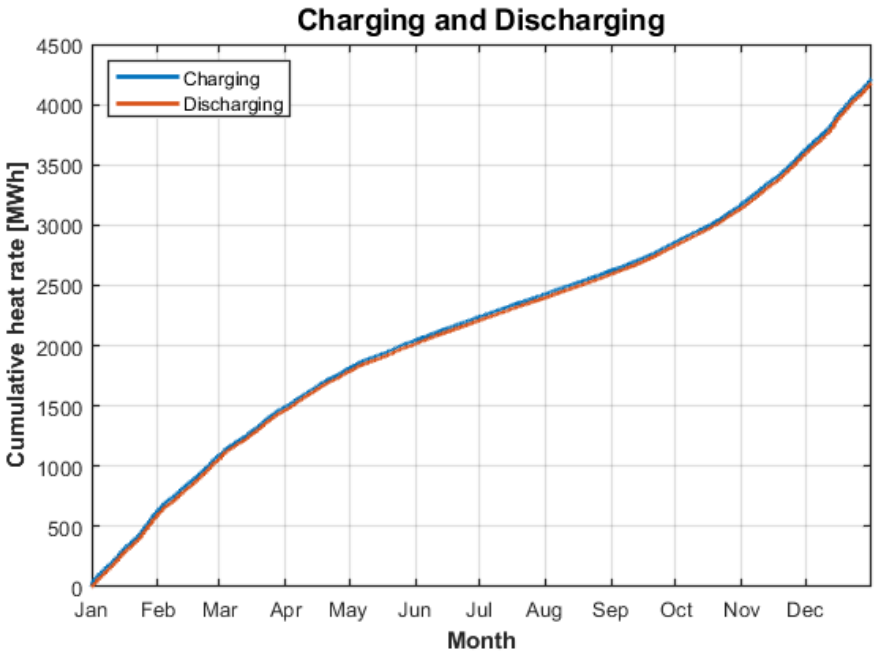

Figure 86: Cumulative heat rate for charging and discharging of the hot water storage tank, for the MGO ship.

Figure 87 shows the temperature in the hot water storage tank throughout the year. This shows that the tank was charged up to 75% in the summer, so that all unused recovered heat could be utilised.

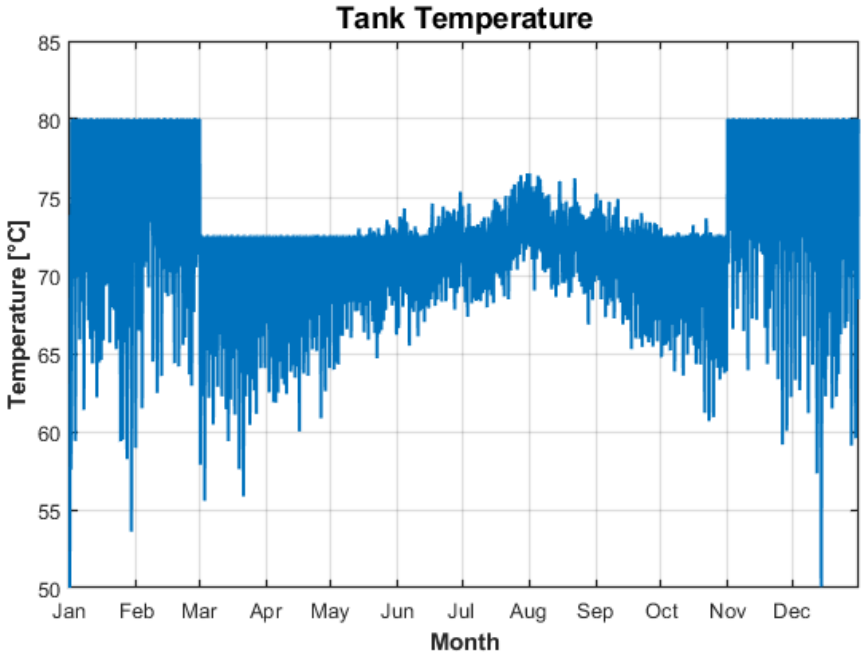

Figure 87: Temperature in the hot water storage tank throughout the year, for the MGO ship.

Figure 88 shows the recovered heat from engines, heat from boilers, heating demand, as well as charging and discharging rates for 5 August. Similarly to the base case shown in figure 54, all the unused recovered heat is used to charge the tank and no heat is wasted. In port, the entire heating demand is covered by the hot tank. After the port stay, the tank is charged briefly to reach 75% of the tank capacity, which creates a peak in boiler heat.

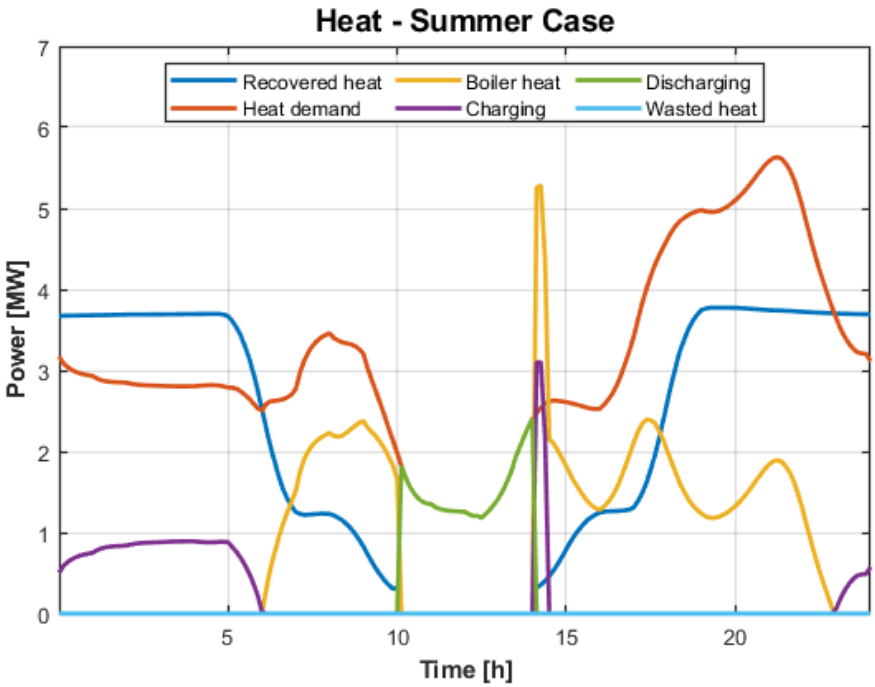

Figure 88: Heat from engines, boilers and the storage tank, as well as total heat demand and charging rate, 5 August on the MGO ship.

Figure 89 shows the energy level of the hot storage tank throughout the day on 5 August. The energy in the tank increases in the beginning as the unused recovered heat is used to charge the tank. The energy level decreases as the tank is discharging in port. At the end of the port stay, the energy level in the tank is just below 28.9 MWh, which is 75% of the total tank capacity. The boiler therefore charges the tank for a very short period of time until it reaches 75%. This explains the peak in boiler heat at 14:00 in figure 88.

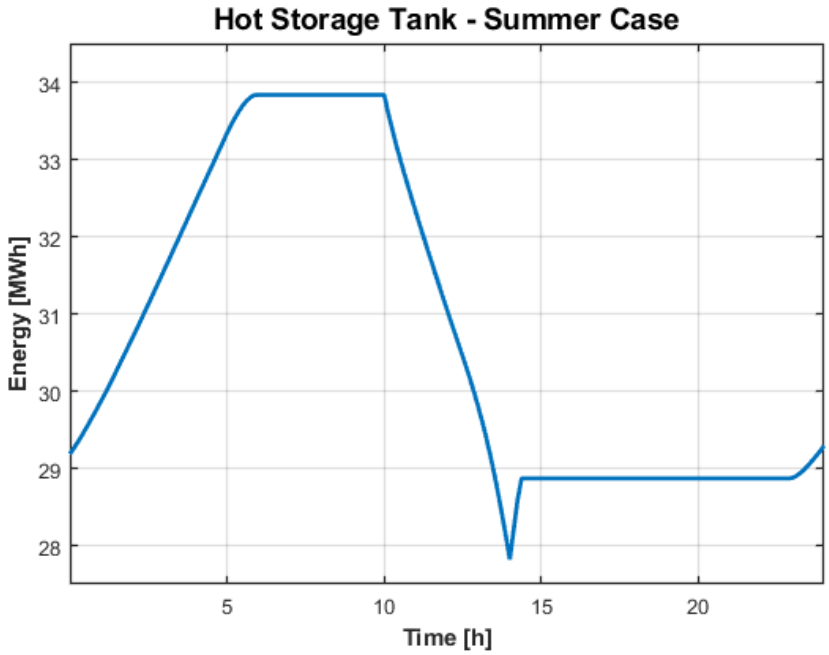

Figure 89: Energy level of the hot storage tank on 5 August, for the MGO ship.

The winter case is shown in figure 90. The figure shows the recovered heat from engines, heat from boilers, heating demand, as well as charging and discharging rates for 29 January. Again, the tank covers the entire heating demand in port. After the port stay, the tank is charged at maximum power until it is full. The boiler power increases to cover this demand.

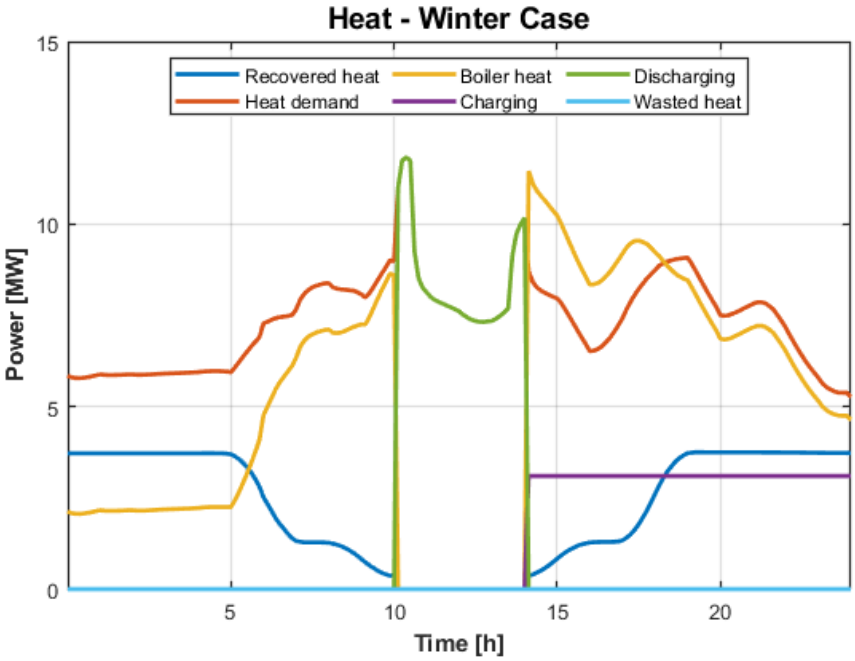

Figure 90: Heat from engines, boilers and the storage tank, as well as total heat demand and charging rate, 29 January on the MGO ship.

Figure 91 shows the energy level of the hot storage tank throughout the day on 29 January. Here, the tank is fully charged in the beginning. The change in energy level corresponds to the charging and discharging shown in figure 90.

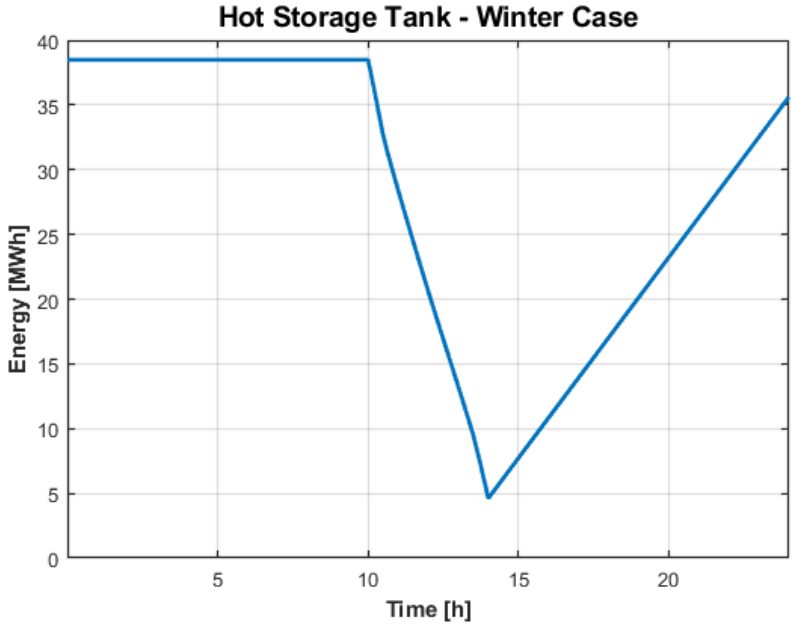

Figure 91: Energy level of the hot storage tank on 29 January, for the MGO ship.

For this model, the tank had to be charged by the boilers a significant amount of the time. This is due to the relatively small amount of unused recovered heat from engines. This solution therefore did not provide any reduction in fuel consumption. The solution could still be relevant in cases where it is required or desired for the ship to have no emissions in port, to reduce local pollution. In other ships with more unutilised recovered heat at sea, it could give large reductions in boiler fuel consumption.

The tank had to be 1105 m^3 to eliminate all use of the boilers in port. For most ships, this is considered unreasonably large. For existing ships, it would likely be very challenging to find space on board for such a large storage tank. The weight of the ship would also increase, which increases the propulsion demand. In addition, it could cause problems with stability depending on the placement of the tank.

To investigate the effect of the tank size, the annual heat delivered by the boilers in port was found for tanks with sizes between 0 and 1105 m^3. The maximum capacity for the tank in the summer was left at 75%, and some recovered heat was therefore wasted for tanks below 600 m^3. The energy delivered by the boilers in port is plotted in figure 92. A tank of size 200 m^3 reduces the use of boilers in port by 54%, while a 600 m^3 tank has a reduction of 97%. This shows that a tank significantly smaller than 1105 m^3 can cover almost all of the heating demands in port. Unless it is crucial to ensure absolute zero emissions in port, it would therefore be more reasonable to use a smaller tank.

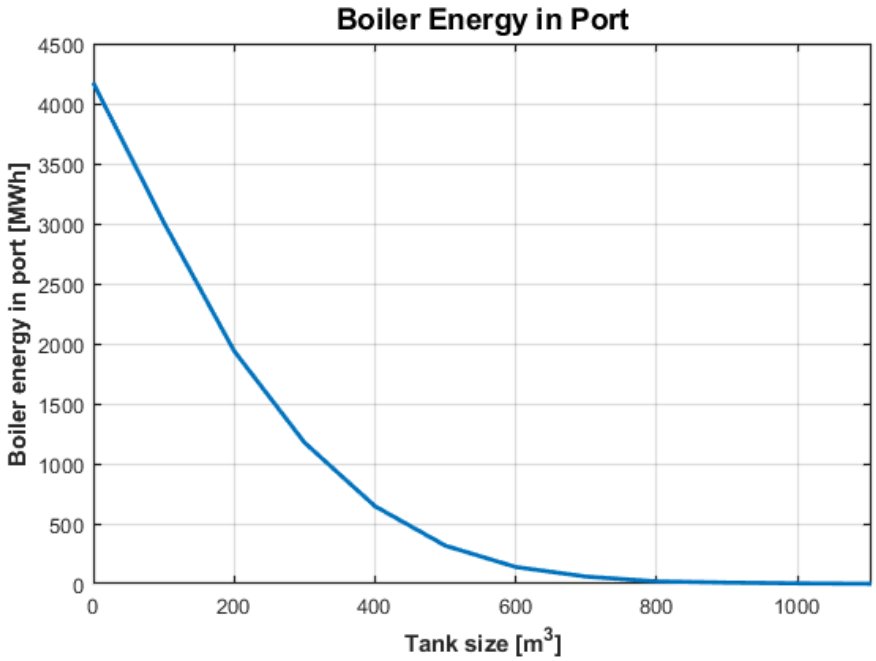

Figure 92: Annual boiler energy in port as a function of the tank size, for the MGO ship.

For the LNG ship, the necessary tank size for this case would be the same, due to the heat demands in port being the same. Some unused recovered heat was wasted both in the summer and winter due to a higher heat recovery efficiency for the LNG engines.

6.6.8 Energy Supply System

For Cases 2, 3, 4, 5 and 9, the post processing was very similar to the base case, due to small changes in energy consumption. Therefore, no recovered heat was wasted in any of these cases in the MGO ship. As mentioned, no heat was wasted in Cases 1, 6 and 10 either. Case 7 with VAV ventilation had a small amount of wasted heat, while Case 8 with a heat pump had a relatively large amount of wasted heat due to reduced heating demands.

Figure 93 shows duration curves for the heating power delivered by the boilers in each energy efficiency scenario, as calculated by the post processing script for the MGO ship. The annual peaks in boiler heating depend on the possible peak shaving in each case. As mentioned, the base case originally had a boiler peak of 12.3 MW without a hot storage tank. With the storage tank, the peak shaving level could be set to 9.2 MW.

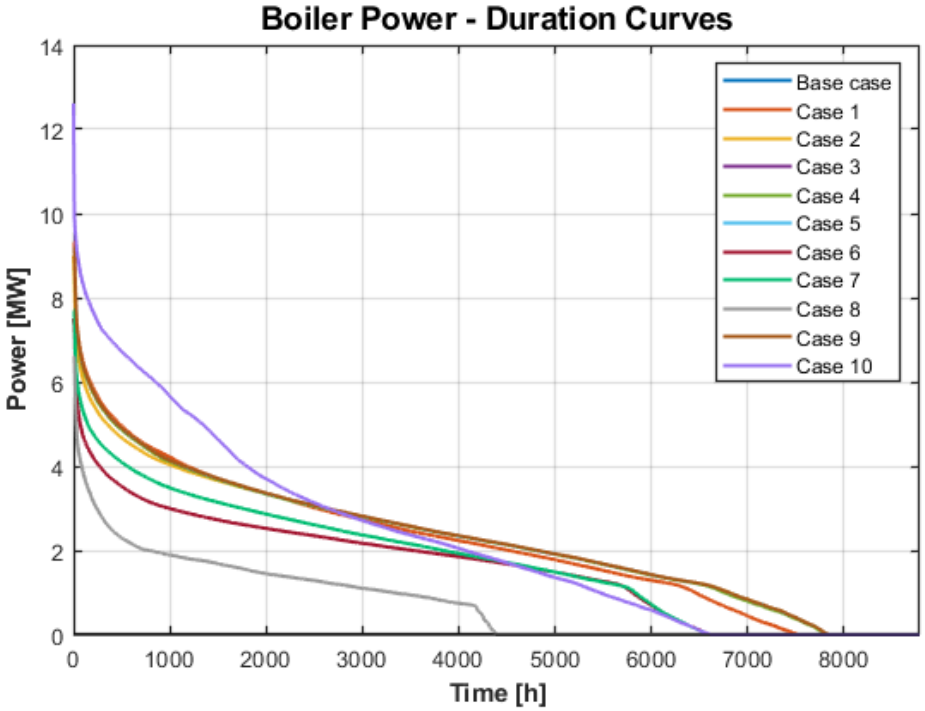

Figure 93: Duration curves for boiler heating power for the different energy saving solutions, for the MGO ship.

In Case 10, the hot storage tank was used to cover the heating demands in port. No peak shaving was therefore included in the script. In addition, the boiler had to be used to charge the tank at sea. This led to the peak boiler demand increasing to 12.6 MW.

For Case 1 with heating setback, the increased heating demands after the port stay period meant that the peak shaving level could not be set lower than 9.3 MW with the chosen tank size. For Case 6 with ventilation heat recovery, the reduced heating demands meant that the boiler peak demand could be reduced to 7.5 MW. Similarly for Case 7 with VAV ventilation, the boiler peak demand was reduced to 7.7 MW. For Case 8 with a heat pump, the peak was reduced to 6.6 MW. Case 2, where vehicle deck heating was turned off in port, had a reduction down to 9.0 MW. In the remaining cases, the peak shaving level was set equal to the base case at 9.2 MW.

Many of the duration curves have a clear break where they decrease quickly. This is due to the relation between the heating demands and the heat recovered from engines.

Figure 94 shows the results from post processing for each energy saving solution in the case where engines and boilers use MGO as fuel. The graph shows annual fuel consumption by engines and boilers. The difference in engine fuel consumption is relatively small between the different cases due to the propulsion demand being the same.

Case 6 with ventilation heat recovery and Case 7 with VAV ventilation had small reductions in engine fuel consumption due to reduced electricity demands for fans and pumps and for cooling. The reduction was 1.1 and 1.6% for Cases 6 and 7, respectively. Case 8 with a heat pump had a 2.6% increase

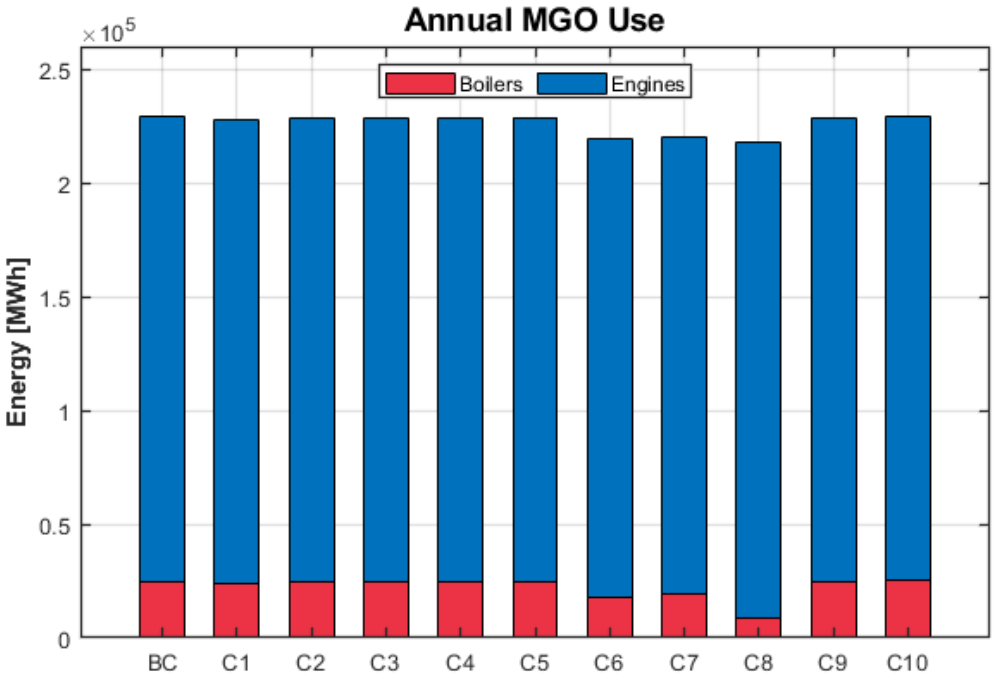

Figure 94: Fuel consumption for engines and boilers in each energy efficiency scenario for the MGO ship.

in engine fuel consumption due to electricity needed to run the heat pump.

The largest changes in boiler fuel consumption also occurred in Cases 6, 7 and 8. Cases 6 and 7 had a reduction of 30 and 23%, respectively. Case 8 had a reduction of 66% due to the heat pump covering a large portion of the heating demand. Cases 1 and 2 with heating setback had reductions of 4.5 and 1.5%, respectively. The remaining cases had less than 1% change in boiler fuel consumption.

Case 10 with a larger hot storage tank had negligible energy savings compared to the base case. This was due to all the unused recovered heat already being utilised by the smaller hot storage tank in the base case. The only difference was a small change in boiler fuel consumption due to the varying efficiencies at part load and the use of the boilers being different in the two cases. In reality, there would also be heat losses from the tank that would increase with increased tank size. For this specific ship, increasing the tank size would therefore increase the energy use.

The LNG ship had engine fuel consumption identical to the MGO ship for all the cases due to the same electrical efficiency being used for the engines. The boiler fuel consumption was lower in the LNG ship due to the engines' higher heat recovery efficiency. However, the change in boiler fuel consumption in each energy efficiency scenario was similar to the MGO ship. This can be seen in appendix K.5.

In addition to the changes in fuel consumption, there were some changes in the use of shore power. These were identical for the MGO and LNG ships due to the electricity demand being the same. The largest reduction in shore power was in Case 7 due to reduced use of fans and pumps and reduced cooling. Case 8 had an increase in shore power due to use of the heat pump. The shore power consumption for each case is shown in appendix K.5.

6.7 Profitability Analysis

Case 10, with a hot storage tank for heat demands in port, had negligible energy savings compared to the base case for both the MGO and LNG ships. This case was therefore assumed to not be profitable and was not included in the profitability analysis.

Input values and results calculated in the profitability analysis are shown in appendix K.6.

6.7.1 Net Present Value

The NPV was calculated for all energy saving solutions where an estimate of investment costs was available. This was done for both the MGO and LNG ships, and the results are presented in table 12.

Table 12: NPV for energy saving solutions, for the MGO and LNG ships.

	MGO ship - NPV [NOK]	LNG ship - NPV [NOK]
Case 6	34,475,792	15,586,766
Case 7	7,442,000	-10,575,436
Case 8	29,668,709	645,711
Case 9	-1,297,755	-1,494,196

As mentioned in section 2.16, an investment is profitable if the NPV is above zero. Overall, one can therefore see that Case 6 with ventilation heat recovery and Case 8 with a heat pump are profitable. Case 7 with VAV ventilation is only profitable for the MGO ship, while Case 9 with PV panels is not profitable. However, how large the profitability is also depends on the size of the additional investment costs, given in section 5.14 for each of the solutions. To compare how profitable each solution is, the ratio between the NPV and the investment cost I_0 is shown in figure 95.

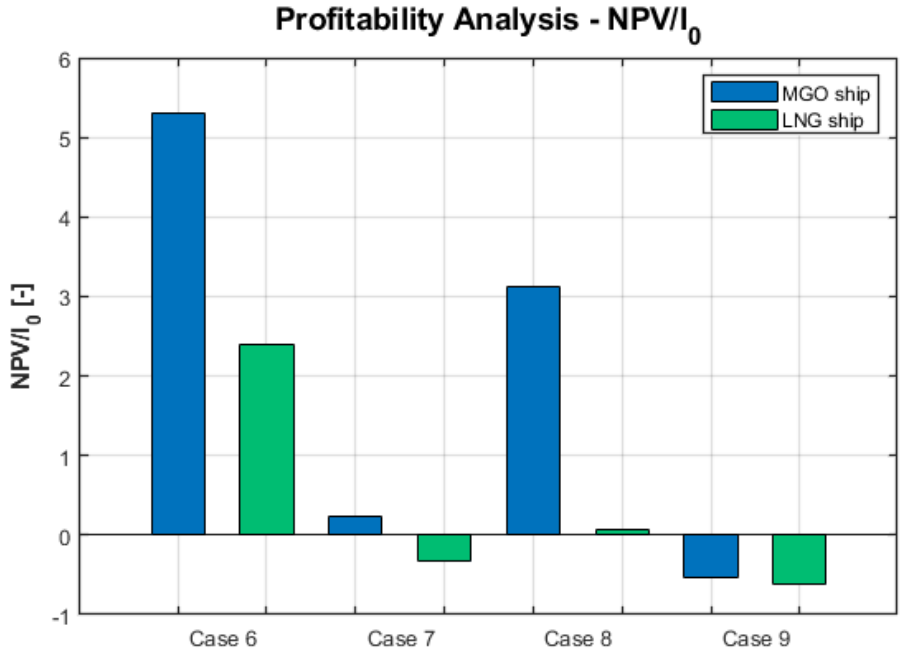

Figure 95: Ratio between NPV and I_0 for energy saving solutions for the MGO and LNG ships.

All these energy saving solutions are more profitable on the MGO ship than on the LNG ship. This is due to the price of MGO being higher than the price of LNG. Reductions in fuel use therefore lead to larger cost reductions in the MGO ship. The LNG ship also has more heat recovered from the engines

and thus a lower demand for heat from boilers. The potential for reduced boiler fuel consumption is therefore smaller on the LNG ship.

Seeing as Case 6 with ventilation heat recovery has an NPV more than two times larger than the investment costs for both ships, it is considered to be very profitable. The maintenance costs for AHUs with heat recovery are likely somewhat higher than for AHUs without heat recovery. The profitability of this solution would then be slightly lower, but it is unlikely to become unprofitable. These results suggest that ventilation heat recovery should be implemented in ships that do not already have this. For implementation in a new ship, the additional investment costs compared to alternative solutions will be lower. Then, this solution would be even more profitable. The same applies for existing ships with old AHUs that have to be switched out anyway.

Case 7 with VAV ventilation is barely profitable on the MGO ship, and just not profitable on the LNG ship. As the ratio NPV/I_0 is close to zero for both ships, the profitability of the solution could change if there are changes in investment costs, fuel costs, interest rate or economic lifetime. A small sensitivity analysis was performed to see how changes in these parameters would affect the profitability of the VAV solution. For the MGO ship, the solution would stop being profitable in each of these cases:

- Investment costs increase by 24%
- MGO costs decrease by 21%
- Real interest rate increases to 8.3%
- Economic lifetime decreases to 11 years

Installation costs were not included for the VAV solution, which means that the investment costs would be higher in reality. This should be investigated further, but it is possible that this could lead to a 24% increase in investment costs. In addition, when calculating the investment costs, it was assumed that all zones only need one sensor each. In reality, large zones might need several temperature and CO_2 sensors to enable efficient and accurate control of the indoor environment. However, a 24% increase in investment costs would only happen if the zones with DCV have more than 24 sensors on average, which is considered unlikely.

Considering the large variations in fuel prices, a 21% decrease could potentially happen in the future. For the real interest rate and economic lifetime, such large changes are considered unlikely to happen. However, a combination of smaller changes in these factors could lead to the solution not being profitable. Based on this analysis, the solution would be risky to implement for the MGO ship even though the NPV is positive. It is therefore not considered beneficial in this case. If this solution were to be implemented in a new ship, the additional investment costs compared to CAV ventilation would be lower. The solution would then be more profitable and likely beneficial to implement.

Similarly, for the LNG ship, the solution could become profitable in any of these cases:

- Investment costs decrease by 34%
- LNG costs increase by 58%
- Economic lifetime increases to 32 years

Seeing as the installation costs were not included, a decrease in investment costs is considered unlikely to occur. The large changes in LNG costs and economic lifetime are also considered unlikely. Changes in the real interest rate could not make the solution profitable. Again, implementation in a new ship would significantly reduce the additional investment costs and the solution could then be profitable.

Even though the VAV solution is not considered profitable enough to implement, it is possible that it

would be beneficial to implement in only some zones, especially on the MGO ship. For the base case, the ventilation rates are highest in the galleys, bathrooms and laundry. VAV ventilation in these zones therefore provides larger energy savings than in other zones, and this could be more profitable than the whole energy saving solution.

Figure 95 shows that Case 8 with a heat pump is very profitable on the MGO ship, as the NPV is more than three times as large as the investment costs. However, the solution is barely profitable on the LNG ship. This could be due to Case 8 on the LNG ship having 10.8 times more wasted recovered heat than on the MGO ship. In reality, the unused recovered heat should be used before running the heat pump, and the amount of wasted heat would therefore be lower.

Seeing as installation costs were not included for the heat pump, the investment costs are higher in reality and the solution would be less profitable. For the MGO ship, the high NPV means that it is still likely to be profitable. On the LNG ship, the solution becomes unprofitable after only a 6% increase in the investment costs, and it is therefore likely not profitable. Similarly, small changes in fuel costs, interest rate or economic lifetime could also make this solution unprofitable on the LNG ship.

Thus, the results indicate that a heat pump solution is profitable on the MGO ship. For the LNG case, it is likely not profitable enough to implement. As mentioned in section 5.14, it is important to note that air-source heat pumps are unlikely to be the best solution for cruise ships. It would be more appropriate to use cooling water from the engines as the heat source. This should be investigated further, to see how profitable such a solution would be.

Figure 95 shows that Case 9 with PV panels is clearly not profitable for either ship, and this solution should therefore not be implemented. This result is caused by a relatively high investment cost for PV panels on ships, combined with relatively low fuel prices. These results would be the same for implementation in a new ship. No maintenance costs were included, as mentioned in section 5.14. Some maintenance is likely needed, and this would make PV panels even less profitable.

Due to harsh weather conditions at sea, it is possible that the economic lifetime of the PV panels is shorter than 25 years. In addition, harsh weather conditions could lead to lower efficiency and increased maintenance costs. These factors would further reduce the profitability of this solution.

As mentioned in section 2.15, the price of PV panels is expected to drop in the future. For the MGO ship, the PV panels would become profitable if the investment costs are reduced by 55%. This is a large reduction, but could potentially happen with enough technological advancements. PV panels could also become profitable in the future if the fuel prices increase, more expensive fuels are used, or the efficiency of commercially available PV panels increases.

It could be beneficial to use angled PV panels that can be rotated, in order to utilise as much of the solar radiation as possible when the ship rotates. This could increase the annual production and possibly make the panels profitable. However, such panels would likely be more expensive. This would also increase the need for maintenance due to more moving parts, combined with wear and tear from salt water and harsh weather conditions.

6.7.2 Pay-Off Time

Table 13 shows the pay-off time for Cases 6-8 on the MGO and LNG ships. For Case 9 with PV panels, the savings are so small compared to the investment costs that the pay-off time could not be calculated.

These results show similar trends to the ratio NPV/I_0 in figure 95. Cases 6-8 all have an economic lifetime of 15 years, as mentioned in section 5.14. Case 6 with ventilation heat recovery has pay-off times well below the economic lifetime, which shows the profitability of this solution. This is also true for Case 8 with a heat pump on the MGO ship. Case 7 with VAV ventilation on the MGO ship and

Case 8 on the LNG ship have pay-off times just below the economic lifetime and are therefore slightly profitable. Case 7 on the LNG ship has a pay-off time longer than the economic lifetime, and is thus not profitable.

Table 13: Pay-off time for energy saving solutions, for the MGO and LNG ships.

	MGO ship - Pay-off time [years]	LNG ship - Pay-off time [years]
Case 6	1.8	3.4
Case 7	11.2	31.0
Case 8	2.8	13.6

6.7.3 Maximum Permissible Investment

The MPI was calculated for all solutions on both the MGO and LNG ships. The results are presented in table 14.

Table 14: MPI for energy saving solutions, for the MGO and LNG ships.

	MGO ship - MPI [NOK]	LNG ship - MPI [NOK]
Case 1	6,318,710	2,484,786
Case 2	2,294,735	1,603,782
Case 3	1,629,566	908,398
Case 4	2,598,121	1,483,413
Case 5	231,903	156,186
Case 6	40,968,292	22,079,266
Case 7	39,042,430	21,024,994
Case 8	34,068,467	10,034,711
Case 9	1,102,245	905,804

Case 1 involves heating setback in port and at night, while Case 2 has vehicle deck heating turned off in port. These cases mainly require control equipment to implement, and this equipment could already be present on the ship. If additional control equipment is needed, the investment costs should be considered. However, the MPI for these solutions is likely high enough that it would still be profitable.

In Case 1, the peak demand for boilers was slightly increased, as mentioned in section 6.6.8. This would probably not require a larger boiler, as the boilers are likely oversized in the first place. As seen in section 6.6.1, the heating capacity in some fan coils should be increased to provide a satisfactory indoor climate after the setback periods. This would increase the heating and reduce the energy savings from this solution. However, the MPI is so high that it is considered likely to still be profitable, especially on the MGO ship. If it is not profitable, the solution could be implemented only in some areas of the ship where the heating capacity is already sufficient.

In Case 2, the peak demand for boilers was not increased, and the relevant fan coils already have the required heating capacity. This solution therefore has no investment costs, unless additional control equipment is needed. For ships that have vehicle deck heating and already have the necessary control equipment, this solution should be implemented.

For Cases 3, 4 and 5, it is important to note that increasing the insulation thickness, improving the windows or implementing PCM in walls on an existing ship would require a drastic renovation of the ship envelope, which would be expensive. Especially for Case 5 with PCM, the MPI is so low that this is considered unlikely to be profitable. Even on a new ship, the costs for the PCM itself are probably higher than this. Cases 3 and 4 with increased insulation and improved windows are also considered

unlikely to be profitable for implementation in an existing ship. However, when building a new ship, it would likely be beneficial to use well insulated constructions and windows.

For Cases 6-9, comparing the MPI to the investment costs leads to results similar to the NPV in table 12 and figure 95. For Case 7 with VAV ventilation on the MGO ship, the MPI is 39.0 MNOK and the investment costs are 31.6 MNOK. Thus, the installation costs could be up to 7.4 MNOK for the solution to still be profitable. This is also seen in the NPV for this solution.

6.7.4 Discussion

As mentioned in section 2.10, fuel prices can vary significantly and are often unpredictable. The distribution and supply costs are considered most uncertain here. The profitability of each energy saving solution could therefore change depending on the fuel prices. In addition, the investment costs for the solutions are uncertain, especially for the heat pump.

There are also uncertainties related to the chosen economic lifetimes and real interest rate. In the sensitivity analysis conducted for Case 7, relatively large changes in these parameters were needed for the solution to change from being profitable to unprofitable and vice versa. Thus, these uncertainties are not likely to significantly change the profitability found for the different solutions.

With future technological advancements, the efficiency of fuel engines might increase. This would reduce the fuel consumption and costs for each case. It would however reduce the economic savings provided by the energy saving solutions. An increase in efficiency would also occur in the case of batteries and fuel cells becoming more frequently used on ships.

The profitability of a solution depends on the energy demands, which could vary significantly between ships. The profitability analysis should therefore only be taken as an indication of which energy saving solutions would be profitable to implement. Further analyses should be conducted for individual ships, especially for cases that are not clearly profitable or unprofitable.

Some energy saving solutions will increase the weight of the ship and therefore increase the energy use for propulsion. This will in turn increase the fuel consumption and related costs. It could also affect the stability of the ship. The solutions with PCM in walls, heat pumps and a large hot water storage tank are assumed to give the largest weight increase. Due to the ship's weight already being very high, it is considered unlikely that there will be a significant change in fuel costs. However, it should be considered further before implementing these solutions.

6.8 Greenhouse Gas Emissions

The reduction in GHG emissions was calculated for each energy efficiency scenario based on the change in fuel consumption and use of shore power. The results are shown in figure 96. Again, Case 10 was not considered here as this solution had negligible energy savings. Detailed results are shown in appendix K.6.

The reductions are larger for the MGO ship than the LNG ship. This is caused by the GHG emission factor for MGO being higher than for LNG. In addition, the MGO ship uses more fuel for boilers due to a lower heat recovery efficiency for the engines, and it therefore has a larger potential for reductions.

The reduction in GHG emissions is directly related to the fuel consumption, as shown in figure 94 for the MGO ship. As expected, Cases 6-8 had the largest reductions in GHG emissions. Case 5 with PCM in walls had a negligible reduction in emissions due to very small reductions in fuel use. Case 9 with PV panels also had a small reduction in fuel consumption and GHG emissions due to the relatively small area of PV panels installed on the ship.

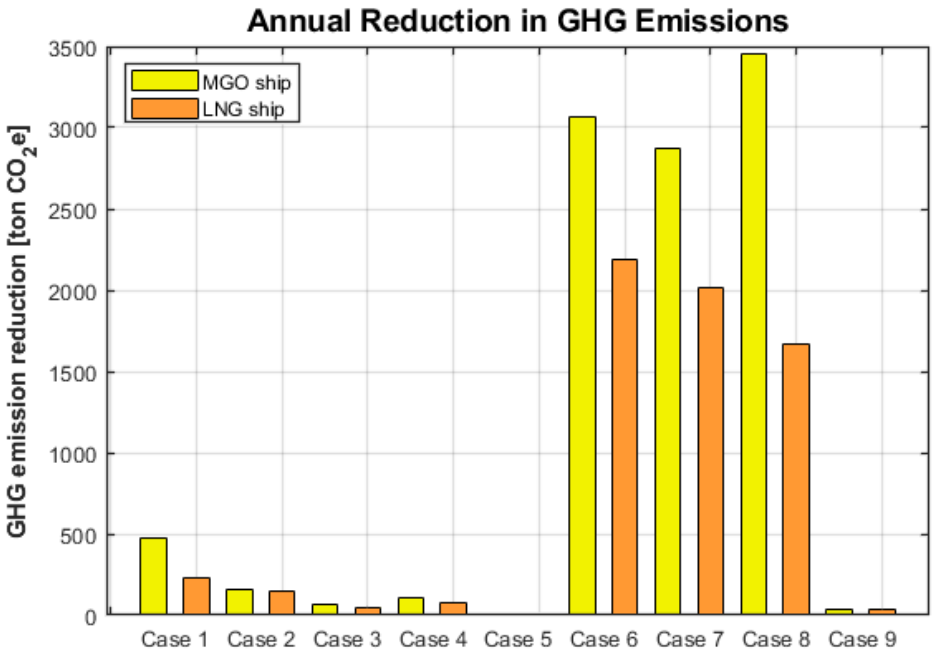

Figure 96: Annual reduction in GHG emissions for the energy saving solutions for the MGO and LNG ships.

For the base case, the total GHG emissions were 71,952 tons CO_2e/year for the MGO ship and 63,463 tons CO_2e/year for the LNG ship. Case 8 on the MGO ship has the largest reduction in GHG emissions, at 3457 tons CO_2e/year. Compared to the base case, this is a reduction of 4.8%. For the LNG ship, Case 6 had the largest reduction in emissions, at 2185 tons CO_2e/year. This is a 3.4% reduction compared to the base case.

Even for solutions that are not economically profitable, there can be large reductions in GHG emissions. This is seen in Case 7 with VAV ventilation for the LNG ship. Implementing such solutions could be feasible in cases where the project can be financed through government subsidies or similar solutions.

Only GHG emissions related to fuels and shore power have been considered. Emissions related to the production and installation of the energy saving solutions were not included. This would reduce the benefit of implementing these solutions in an existing ship, as new components must be produced and installed. To investigate this effect, a life cycle assessment would be required.

On ships using LNG as fuel, LBG could be used instead. Considering the emission factor and price for biofuels mentioned in section 2.10, this would drastically reduce GHG emissions and increase fuel costs. As LBG might become more price competitive in the future, this solution could become a possibility.

7 Discussion

7.1 Sources of Error

When the cruise ship was modelled, several assumptions, estimations and simplifications were made. Floor areas and heights of the decks were estimated. In addition, the various constructions used in the ship envelope were simplified and uncertain. Temperature setpoints, supply air temperatures, ventilation rates, heat load schedules and propulsion demand could also be different on real ships. Therefore, the model might not be a precise representation of Color Fantasy or other cruise ships.

After adjusting the occupancy schedules, the total number of people on the ship is representative of a fully booked ship. However, the ship will likely not be full the whole year, and the average number of people on the ship should therefore be lower. The effect this has on the energy consumption will vary depending on the strategies used. If heating is turned off in empty cabin areas, the energy use would go down. But if the heating stays on, the energy consumption could increase due to lower internal heat gains from occupants. Therefore, the energy use in the reference ships might not be directly comparable to the simulated ship.

One of the largest sources of error is the calculated energy consumption for hotel systems on the reference ships. This is mainly due to lack of information about how much of the energy consumption goes to the hotel system, and what energy users are included in the "other" categories. In addition, the energy consumption varies significantly between different cruise ships. It is therefore difficult to know if the model was calibrated appropriately.

When it comes to comparing the peak demands for heating, cooling and DHW to Birka Stockholm, the method used for finding typical winter and summer days in the reference report was not used here. The values that were compared to Birka Stockholm's peak demands are therefore estimated and uncertain.

Seeing as the integration of the hotel system with the energy supply system was done through post processing in MATLAB, the interaction between these systems was simplified. The hot water storage tank was also simplified by neglecting heat losses from the tank and assuming a uniform temperature. In addition, the tank delivers as much heat as needed at any time as long as it is not fully discharged. The behaviour of a real tank would differ from this, for example through time delays in the system. The potential use of a real tank might therefore differ from the results presented.

7.2 Limitations of IDA ICE

The building simulation tool IDA ICE has limitations related to the movement of the ship through space. As mentioned, it is not possible to vary the orientation of the model during a simulation, and post processing was therefore required to take the varying orientation into account. In addition, the location data for the model cannot be changed during a simulation. This means that the position of the sun was not properly represented. This could also be handled in post processing, but would require the combination of six different simulations in this case. Other challenges include the limited modelling options for the ship's propulsion system and for steam demand in galleys and laundry.

Some of these aspects could quite easily be implemented into the IDA ICE software. For example, the orientation of the building could be varied using a schedule. However, it is unlikely that such ship specific features will be included, as IDA ICE has not been used much for modelling ships, and the need is therefore low.

8 Conclusion

The aim of this master's thesis was to analyse the energy use on passenger ships and investigate possible energy saving solutions, using the building simulation tool IDA ICE.

The initial IDA ICE model was calibrated by increasing the demand for domestic hot water (DHW) and reducing the ventilation rate in large galleys. This gave a total annual energy consumption of 19.2 MWh/passenger for the ship's hotel system. The energy demand for propulsion is 0.156 kWh/ALB-km.

In the fan coil sizing, the resulting thermal environment was similar when using design day data in heating and cooling simulations and when using the maximum heating and cooling power from a one year simulation. For both cases, the air temperatures were largely within the desired range. For most zones apart from the laundry room, the fan coils could be significantly undersized without affecting the thermal environment. The fan coil sizing did not significantly impact the ship's annual energy use.

The ship's energy supply system, consisting of engines and boilers, was considered through post processing using a MATLAB script. A hot water storage tank of size 150 m^3 was also included. Two different fuels were considered: marine gas oil (MGO) and liquefied natural gas (LNG). Due to a higher heat recovery efficiency for LNG engines, all energy saving solutions had smaller reductions in fuel consumption and were less profitable on the LNG ship than on the MGO ship.

Applying heating setback in port and at night, and turning off vehicle deck heating in port, gave a reduction in boiler fuel consumption on the MGO ship of 4.5 and 1.5%, respectively. With low investment costs and a relatively high maximum permissible investment (MPI), these solutions are likely to be profitable on both the MGO and LNG ships.

Implementing increased insulation, improved windows and phase change material (PCM) layers in walls gave very small reductions in fuel consumption, which led to a low MPI. Seeing as these solutions would require large renovations to implement in an existing ship, they are unlikely to be profitable.

For the MGO ship, ventilation heat recovery reduced the boiler fuel consumption by 30%. For both ships, the net present value (NPV) was more than two times larger than the investment costs. This solution should therefore be implemented in ships that do not already have ventilation heat recovery.

Variable air volume (VAV) ventilation gave a 23% reduction in boiler fuel consumption on the MGO ship. The solution is barely profitable on the MGO ship and not profitable on the LNG ship. For the MGO ship, relatively small changes in investment costs and fuel costs would make the solution unprofitable. Based on this, the solution was not considered beneficial to implement.

Using an air-to-water heat pump gave the largest reductions in boiler fuel consumption, with 66% for the MGO ship. The engine fuel consumption increased by 2.6%. On the MGO ship, the NPV was more than three times larger than the investment costs. This indicates that a heat pump solution would be profitable, though it would be more appropriate to use the engines' cooling water as a heat source.

Photovoltaic (PV) panels gave small reductions in fuel consumption and shore power due to a small PV panel area. The solution was not found to be profitable in either ship due to relatively high investment costs. For the MGO ship, a 55% reduction in investment costs would make the solution profitable.

To cover all heating demands and eliminate the use of boilers in port, the size of the storage tank had to be increased to 1105 m^3. A smaller tank of 600 m^3 could cover 97% of the heating demands in port and could therefore be more realistic. Due to negligible energy savings, this case would not be profitable.

In conclusion, the most suitable solutions for cruise ships were found to be heating setback, ventilation heat recovery and heat pumps. A large storage tank could be implemented if the goal is to reduce emissions in port.

9 Further Work

In further work, it would be beneficial to obtain more detailed energy use data for a reference ship. This could make it more clear how much of the total energy use goes to each energy user, which could in turn give a more accurate calibration of the model. Ideally, the same reference ship should be used for the modelling and for comparison of the results.

As a part of the calibration phase, the heating demand as a function of temperature could be compared to energy signature curves for hotels. The thermal mass of the ship construction could then be adjusted to change the slope of the plots.

One could investigate the use of outdoor temperature compensation in supply air temperatures and in the supply water temperature for heating. The effect on energy consumption and thermal environment should be taken into account.

In the application of the hot water storage tank, it would be beneficial to take heat losses into account to get a more accurate picture of the tank's effect on the energy consumption. In addition, temperature stratification in the tank could be considered by modelling several temperature layers. More detailed sizing of the hot storage tank could be done, including required pipe sizes and flow rates to deliver the necessary heat to and from the tank. In order to reduce the necessary size of the hot storage tank, PCM could be used instead of water. This would be especially useful in cases where a large storage capacity is needed.

It could be useful to model the hotel system and the energy supply system together in the same simulation tool, in order to achieve better integration of the two systems. This could be done by modelling the cruise ship's energy supply system in the advanced level of IDA ICE or in a different simulation tool. In the heat pump case, this would make it possible to utilise unused recovered heat before running the heat pump, which reduces the amount of wasted heat.

As a more suitable heat pump solution for cruise ships, one could investigate the use of low temperature water on board as a heat source. This would also require detailed modelling of the cruise ship's energy supply system. An analysis could be conducted using different power coverage factors for the heat pumps, to investigate what is the most profitable.

The energy efficiency scenario Case 1 with heating setback could be improved upon to achieve larger reductions in energy consumption. The strategy could be expanded to include the summer months by adjusting the supply air temperatures based on the outdoor temperature. One could also reduce the heating in cabins whenever guests leave the room, or turn off heating in larger groups of empty cabins.

More energy saving solutions could be implemented in the model and investigated. This could include grey water heat recovery and solar thermal collectors. In addition, it could be interesting to investigate a combination of heat pumps and thermal energy storage, or the use of steam producing heat pumps. For all solutions, the economic profitability should be analysed to make sure that the solutions are beneficial both in terms of energy use and economy.

It could be useful to perform a life cycle assessment to take into account the GHG emissions related to production and installation of the energy saving solutions. In addition to the GHG emissions, one could consider SO_x and NO_x emissions. This would give a better understanding of the energy saving solutions' effect on the environment and human health.

References

[1] Sturla Ingebrigtsen. *Compendium TEP4315 and TEP4245: Ventilation Technology*, chapter 2.2.1, 4.1, 8.1.3, 8.1.4, 11.1.1, 11.2, 11.4. Kompetansebiblioteket, (Accessed: 19.10.20, 19.03.21).

[2] Cecilia Gabrielii. "CruiZE - Cruising towards Zero Emissions". `https://www.sintef.no/en/projects/cruize-cruising-towards-zero-emissions/`. (Accessed: 07.12.20).

[3] Color Line. "Color Fantasy Facts". `https://www.colorline.com/kiel-oslo/facts-about-color-fantasy`. (Accessed: 19.06.20).

[4] Color Line. "Rutetider". `https://www.colorline.no/rutetider`. (Accessed: 30.09.20).

[5] Color Line. "Color Magic Facts". `https://www.colorline.com/kiel-oslo/facts-about-color-magic`. (Accessed: 19.06.20).

[6] CruiseMapper. "Color Fantasy ferry". `https://www.cruisemapper.com/ships/Color-Fantasy-ferry-1884`. (Accessed: 03.10.20).

[7] Color Line. "Lugarer Oslo-Kiel". `https://www.colorline.no/oslo-kiel/lugarer`. (Accessed: 25.06.20).

[8] Color Line. "Color Line Fantasy". `https://tourmkr.com/F1kVlcNnMa/`. (Accessed: 19.06.20).

[9] Oslo Havn KF. "Handlingsplan for fremtidig nullutslippshavn". `https://www.oslohavn.no/no/arkiv/arkiv-2019/handlingsplan-for-fremtidig-nullutslippshavn/`. (Accessed: 17.02.21).

[10] PORT OF KIEL. "Shore Power Facility". `https://www.portofkiel.com/blue-port-en/shore-power-facility.html`. (Accessed: 07.05.21).

[11] Francesco Baldi, Fredrik Ahlgren, Tuong-Van Nguyen, Marcus Thern, Karin Andersson. "Energy and Exergy Analysis of a Cruise Ship". *Energies*, pages 4, 10, 17, 2018.

[12] CruiseMapper. "MS Birka Stockholm". `https://www.cruisemapper.com/ships/MS-Birka-Stockholm-750`. (Accessed: 06.03.21).

[13] Giovanni Barone, Annamaria Buonomano, Cesare Forzano, Adolfo Palombo, Maria Vicidomini. "Sustainable energy design of cruise ships through dynamic simulations: Multi-objective optimization for waste heat recovery". *Energy Conversion and Management*, pages 5–8, 10, 17–18, 20, 2020.

[14] Matti Nurmi. "Improving the energy efficiency of a cruise ship stateroom". Master's thesis, Aalto University, 2017.

[15] M.A. Ancona, F. Baldi, M. Bianchi, L. Branchini, F. Melino, A. Peretto, J. Rosati. "Efficiency improvement on a cruise ship: Load allocation optimization". *Energy Conversion and Management*, pages 44–47, 51–53, 2018.

[16] Cecilia Gabrielii, Research Scientist at SINTEF Energy Research. E-mail communication, 18.02.21, 31.05.21.

[17] Torbjørn Krogh, Manager Interior & HVAC Dept. at Fosen Design & Solutions AS. Meeting on Microsoft Teams, 19.06.20.

[18] Torbjørn Krogh, Manager Interior & HVAC Dept. at Fosen Design & Solutions AS. E-mail communication, 30.06.20.

[19] International Labour Conference. *Maritime Labour Convention*, page 44. 2006.

[20] DNV. "Offshore Standard DNV-OS-D301: Fire Protection", October 2008. `https://rules.dnvgl.com/docs/pdf/DNV/codes/docs/2009-10/Os-D301.pdf`.

[21] DNV GL. *Rules for classification Ships*. "Part 6 Additional class notation: Chapter 5 Equipment and design features", pages 43-44, 2020.

[22] Bjørn J. Wachenfeldt. Utredning av alternative ventilasjonsløsninger for ny ungdomsskole på Mæla i Skien, 2004. https://www.sintef.no/globalassets/upload/smartbygg/utredning-av-alternative-ventilasjonslosninger-for-ny-ungdomsskole-pa-mala-i-skien.pdf.

[23] DNV GL. *Rules for classification Ships*. "Part 6 Additional class notation: Chapter 8 Living and working conditions", pages 22-23, 2015.

[24] Standard Norge. *NS-EN ISO 7547: Ships and marine technology - Air-conditioning and ventilation of accommodation spaces - Design conditions and basis of calculations*, pages 6, 8–9. Norsk Standard, 2005.

[25] Sigbjørn Tyssen, Business Development Manager at Teknotherm. E-mail communication, 27.11.20.

[26] SINTEF Byggforsk. Byggdetaljer 552.315: "Ventilasjon og avfukting i svømmehaller og rom med svømmebasseng", 2003.

[27] DNV GL SE. *Rules for Classification and Construction, Ship Technology*. "Ventilation", page 29, 2014.

[28] Torbjørn Krogh, Manager Interior & HVAC Dept. at Fosen Design & Solutions AS. Meeting on Microsoft Teams, 04.09.20.

[29] Sigbjørn Tyssen. "Technical Specification: HVAC systems", Teknotherm, 2020.

[30] SINTEF Byggforsk. Byggdetaljer 552.340 Del I: "Varmegjenvinnere i ventilasjonsanlegg", 2002.

[31] Systemair. "Systemair prisliste: Januar 2021". https://www.systemair.com/fileadmin/user_upload/systemair-b2b/Local/Norway/Price_list/Systemair_prisliste_2021_nett.pdf. (Accessed: 27.01.21).

[32] SINTEF Byggforsk. Byggdetaljer 552.324: "Behovsstyrt ventilasjon (DCV) Krav ved innkjøp og kontroll ved overlevering", 2016.

[33] Vegard Stokke. "Demand Controlled Ventilation in office buildings - Evaluation of profitability". Master's thesis, University of Stavanger, 2014.

[34] Wolfgang Kampel, Bjørn Aas, Amund Bruland. "Energy-use in Norwegian swimming halls". *Energy and Buildings*, page 183, 2013.

[35] Juha Kivimäki. "Effects of electronically commutated motors used in passenger cabin air conditioning on low voltage network of a cruise ship". Master's thesis, Tampere University of Technology, 2016.

[36] Guangrong Zou, Mia Elg, Aki Kinnunen, Panu Kovanen, Kari Tammi, Kalevi Tervo. "Modeling ship energy flow with multi-domain simulation". Proc. CIMAC 2013.

[37] DNV GL. "(Future) Fuels & Fuel Converters". https://www.ntnu.edu/documents/20587845/1266707380/01_Fuels.pdf/1073c862-2354-4ccf-9732-0906380f601e. (Accessed: 30.01.21).

[38] International Maritime Organization (IMO). "IMO 2020 – cutting sulphur oxide emissions". https://www.imo.org/en/MediaCentre/HotTopics/Pages/Sulphur-2020.aspx. (Accessed: 30.03.21).

[39] DNV GL. "Assessment of Selected Alternative Fuels and Technologies", 2019. https://www.dnv.com/maritime/publications/alternative-fuel-assessment-download.html.

[40] DNV. "Current price development oil and gas". https://www.dnv.com/maritime/lng/current-price-development-oil-and-gas.html. (Accessed: 30.03.21).

[41] Espen Halvorsen Verpe, Sverre Stefanussen Foslie. "Project memo, Reference cases and waste heat". pages 7, 9. Internal document SINTEF Energy Research, 2020.

[42] Cecilia Gabrielii, Research Scientist at SINTEF Energy Research. E-mail communication, 04.03.21, 16.03.21.

[43] Odne Stokke Burheim. *Engineering Energy Storage*, pages 47–48. Academic Press, 2017.

[44] Cecilia Gabrielii, Research Scientist at SINTEF Energy Research. Meeting on Microsoft Teams, 16.03.21.

[45] Natasa Nord. Lecture notes TEP4245 - HVAC Engineering, "Design and Sizing of Domestic Hot Water Systems", 2020.

[46] Marco Manzan, Amedeo Pezzi, Ezio Zandegiacomo de Zorzi, Angelo Freni, Andrea Frazzica, Bianca Maria Vaglieco, Zentilomo Lucio, Deluca Claudio. "Potential of thermal storage for hot potable water distribution in cruise ships". *Energy Procedia*, pages 1108–1109, 2018.

[47] Alexis Sevault. "What are Phase Change Materials? (Will they be the next big thing in Norway?)". https://blog.sintef.com/sintefenergy/energy-efficiency/phase-change-materials-pcm/. (Accessed: 19.03.21).

[48] Walter Frei. "Thermal Modeling of Phase-Change Materials with Hysteresis". https://www.comsol.com/blogs/thermal-modeling-of-phase-change-materials-with-hysteresis/. (Accessed: 19.05.21).

[49] Yantong Li, Natasa Nord, Qiangqiang Xiao, Tymofii Tereshchenko. "Building heating applications with phase change material: A comprehensive review". *Journal of Energy Storage*, pages 4–6, 2020.

[50] Mohammad Saffari, Alvaro de Gracia, Cèsar Fernández, Luisa F. Cabeza. "Simulation-based optimization of PCM melting temperature to improve the energy performance in buildings". *Applied Energy*, pages 420, 423, 2017.

[51] Jørn Stene. Lecture notes TEP4260 - Heat Pumps for Heating and Cooling of Buildings, "Heat Sources and Heat Source Systems for Heat Pump Plants", 2021.

[52] Jørn Stene. Lecture notes TEP4260 - Heat Pumps for Heating and Cooling of Buildings, "Heat Pump Plants for Heating and Cooling of Large Buildings", 2021.

[53] Jørn Stene. Lecture notes TEP4260 - Heat Pumps for Heating and Cooling of Buildings, "Dimensioning of Heat Pump Plants for Heating and Cooling", 2021.

[54] Jørn Stene. Lecture notes TEP4260 - Heat Pumps for Heating and Cooling of Buildings, "Investment Analysis for Heat Pump Systems", 2021.

[55] Global maritime energy efficiency partnerships (GloMEEP). "SOLAR PANELS". https://glomeep.imo.org/technology/solar-panels/. (Accessed: 22.01.21).

[56] Otovo. "Lønnsomhet og tilbakebetalingstid for solceller". https://www.otovo.no/blog/solcellepanel-solceller/lonnsomhet-og-tilbakebetalingstid-for-solceller/. (Accessed: 06.05.21).

[57] Solcellespesialisten. "SCCS Sunpower 360W X22". https://solcellespesialisten.no/nettbutikk/solcellepanel/monokrystalinsk/sunpower-360w.html. (Accessed: 22.01.21).

[58] EQUA Simulation AB. *User Manual: IDA Indoor Climate and Energy, Version 4.5*, 2013.

[59] EQUA Simulation AB. "Ice Rinks and Pools". https://www.equa.se/en/ida-ice/extensions/ice-rinks-and-pools. (Accessed: 24.03.21).

[60] MathWorks. "MATLAB". https://se.mathworks.com/products/matlab.html. (Accessed: 06.03.21).

[61] CruiseMapper. "Color Fantasy ferry deck plans". https://www.cruisemapper.com/deckplans/Color-Fantasy-ferry-1884. (Accessed: 25.06.20).

[62] CruiseMapper. "Tracker". https://www.cruisemapper.com/. (Accessed: 07.10.20).

[63] Google. [Google Maps image showing the area between Oslo and Kiel]. https://goo.gl/maps/pN8XvWDgD5cLUAjY6. (Accessed: 30.09.20).

[64] Ørsted. "Ørsted Offshore Operational Data Sharing: Anholt and Westermost Rough LiDAR Data Documentation". https://orsted.com/en/our-business/offshore-wind/wind-data. (Accessed: 20.10.20).

[65] Google. [Google Maps image showing the area between Stockholm and Mariehamn]. https://goo.gl/maps/V1hCZ52qrhLNkkSh7. (Accessed: 06.03.21).

[66] Google. [Google Maps image showing the Mediterranean Sea]. https://goo.gl/maps/GZpxfJYW9V7kFk74A. (Accessed: 06.03.21).

[67] Google. [Google Maps image showing the Caribbean Sea]. https://goo.gl/maps/UCx6bGdDmvmFMFK46. (Accessed: 06.03.21).

[68] ASHRAE. "ASHRAE Handbook - Fundamentals (SI): Design conditions for OSLO/FORNEBU, Norway", 2005. http://cms.ashrae.biz/weatherdata/STATIONS/014880_s.pdf. (Accessed: 05.04.21).

[69] Titan LNG. "Titan LNG Weekly Prices". https://titan-lng.com/weekly-prices-premium-zone/. (Accessed: 30.03.21).

[70] Ship & Bunker. "Rotterdam Bunker Prices". https://shipandbunker.com/prices/emea/nwe/nl-rtm-rotterdam#MGO. (Accessed: 30.03.21).

[71] Statistics Norway. "09007: Electricity price, grid rent and taxes for households 2012 - 2020". https://www.ssb.no/en/statbank/table/09007/. (Accessed: 24.04.21).

[72] SINTEF Byggforsk. Byggdetaljer 473.020: "Nullutslippsbygninger (ZEB) Retningslinjer og beregningsmetoder", 2017.

[73] Francesco Baldi, Fredrik Ahlgren, Francesco Melino, Cecilia Gabrielii, Karin Andersson. "Optimal load allocation of complex ship power plants". *Energy Conversion and Management*, pages 348–350, 2016.

[74] Morten Simonsen, Hans Jakob Walnum, Stefan Gössling. "Model for Estimation of Fuel Consumption of Cruise Ships". *Energies*, pages 8–9, 2018.

[75] JustFerries. "Passage on ferry COLOR FANTASY, Kiel - Oslo (Color Line)". https://www.youtube.com/watch?v=BW5zml3vCLY&t=1059. (Accessed: 30.09.20).

[76] Color Line. "Restauranter og barer Oslo-Kiel". https://www.colorline.no/oslo-kiel/restauranter-og-barer. (Accessed: 02.07.20).

[77] Color Line. "Aktiviteter Oslo-Kiel". https://www.colorline.no/oslo-kiel/aktiviteter. (Accessed: 02.07.20).

[78] Miko Ha. "Driving into 'Colorlines Fantasy' ferry from Kiel to Oslo.". https://www.youtube.com/watch?v=bU3SY0g2KbI. (Accessed: 14.10.20).

[79] Anders Kirkhus. "Planlegging av parkeringsplasser og garasjeanlegg". https://www.sintef.no/community/fagblogg/poster/planlegging-av-parkeringsplasser-og-garasjeanlegg/. (Accessed: 14.10.20).

[80] Statens vegvesen. "Motorkjøretøyer". https://www.vegvesen.no/s/bransjekontakt/Hb/hb017-1992/DelA_Dimensjoneringsgrunnlag/01.Dimensjoneringsgrunnlag/01_Motorkjoretyer.htm. (Accessed: 15.10.20).

[81] Engineering ToolBox. "Specific Heat of Solids". https://www.engineeringtoolbox.com/specific-heat-solids-d_154.html. (Accessed: 07.07.20).

[82] Steve McNeil. "The Thermal Properties of Wool Carpets", March 2016. https://www.researchgate.net/publication/298352974_The_Thermal_Properties_of_Wool_Carpets. (Accessed: 07.07.20).

[83] Isover Saint-Gobain. "Product Finder". https://www.isover-technical-insulation.com/products?f%5B0%5D=field_product_er_maket%3A1306. (Accessed: 07.07.20).

[84] Isover Saint-Gobain. "A-15 Bulkhead Steel Standard". https://www.isover-technical-insulation.com/products/15-bulkhead-steel-standard. (Accessed: 07.07.20).

[85] Isover Saint-Gobain. "A-60 Bulkead Steel Standard". https://www.isover-technical-insulation.com/products/60-bulkead-steel-standard. (Accessed: 07.07.20).

[86] Standard Norge. *NS-EN 15232-1:2017: Energy Performance of Buildings - Part 1: Impact of Building Automation, Controls and Building Management*, page 74. Norsk Standard, 2017.

[87] Standard Norge. *NS-EN ISO 7730: Ergonomics of the thermal environment*, page 18. Norsk Standard, 2006.

[88] Standard Norge. *SN-NSPEK 3031:2020: Energy performance of buildings - Calculation of energy needs and energy supply*, pages 38–46, 49. Norsk Standard, 2020.

[89] Clemens Boertz. "Energy demand of a fuel cell-driven cruise ship". Master's thesis, Delft University of Technology, 2020.

[90] ASHRAE. "ASHRAE Fundamentals Handbook (SI)", table 5. 2001. https://timomarquez.files.wordpress.com/2011/08/calorequipos.pdf.

[91] Henrik Alvestad. "Characterization of thermal energy needs of swimming pools using building performance simulation". Master's thesis, Norwegian University of Science and Technology, 2019.

[92] Sjøfartsdirektoratet: Norwegian Maritime Authority. *Regulations on accommodation, recreational facilities, food and catering on ships*, page 24. 2017.

[93] Håvard Pallin Grønning, Project Developer at GK Inneklima AS. E-mail communication, 29.04.21.

[94] Ola Nygaard, General Manager at Fosen Ventilasjon AS. E-mail communication, 27.04.21.

[95] Jørn Stene, SINTEF Energiforskning AS Avdeling Energiprosesser. Varmepumper for oppvarming og kjøling av bygninger, 2000. http://www.ivt.ntnu.no/ept/fag/tep4115/innhold/Laboppgaver/Varmepumpe%20Notat%20J%20Stene.pdf.

[96] Geir Eggen, Geir Vangsnes. Heat Pump for District Cooling and Heating at Oslo Airport, Gardermoen, 2005. https://www.sintef.no/globalassets/project/annex29/installasjoner/gshp_gardermoenhp_no1.pdf.

A Design Day Data for Fornebu

The design day data for Fornebu can be seen in table A.1. This was used in heating simulations. The wet-bulb maximum for the winter and the dry-bulb minimum for the summer were assumed to be the same as for Gardermoen. For the remaining parameters, values from ASHRAE were used [68]. Only the winter design day data for Fornebu has been used, as the location for cooling simulations was set to Holzdorf.

Table A.1: Design day data for Fornebu used in heating simulations.

	Winter	**Summer**
Dry-bulb min [°C]	-17.2	13.3
Dry-bulb max [°C]	-14.5	26.8
Wet-bulb max [°C]	-14.6	17.8
Wind direction [°]	0	170
Wind speed [m/s]	0.8	3.2

B Energy Use for MS Birka Stockholm

Heat recovered from engines

For Birka Stockholm, 25.2% of the thermal power is generated by auxiliary boilers, and the rest is heat recovered from the engines [11]. The share of the engines' fuel consumption recovered as heat was then calculated as follows:

$$4000\ MWh \cdot 0.79 \cdot \frac{74.8\%}{25.2\%} = 9380\ MWh$$

$$\frac{9380\ MWh}{100{,}000\ MWh} \cdot 100\% = 9.38\%$$

Energy use

Using the share of heat recovered from the engines together with the engines' mechanical efficiency gives a total efficiency of 53.4%. The energy use for the whole ship was then calculated as follows:

$$100{,}000\ MWh \cdot 0.534 + 4000\ MWh \cdot 0.79 = 56{,}540\ MWh$$

Share of the total energy use for each category [11]:

- Propulsion: 46.0%
- Accommodation heating: 15.9%
- Fuel/tank heating: 3.4%
- Galley: 3.1%
- Hot water heating: 4.8%
- Accommodation cooling: 0.8%
- Other - low estimate: 7.8%
- Other - high estimate: 23.4%

C LNG Engines

For diesel engines, the share of the fuel consumption recovered as heat was 9.38%. Auxiliary engines on Birka Stockholm have a thermal efficiency of 47% [15], which means that the amount of the thermal energy recovered is:

$$\frac{9.38}{47} \cdot 100\% = 19.96\%$$

The amount of the thermal energy from the engines that can be recovered is typically around 10 percentage points higher for LNG engines [16], and this was therefore set to 29.96%. The thermal efficiency of LNG engines was assumed to be the same as on Birka Stockholm. Thus, the share of the LNG engines' fuel consumption recovered as heat is:

$$29.96\% \cdot \frac{47}{100} = 14.1\%$$

D Temperature Data

Figures D.1 to D.6 show the temperature variation throughout the year for Fornebu, Tjøme, Skagen, Fornæs, Beldringe and Holzdorf. IWEC files from IDA ICE were used. Figure D.7 shows the temperature variation in the custom combined weather file.

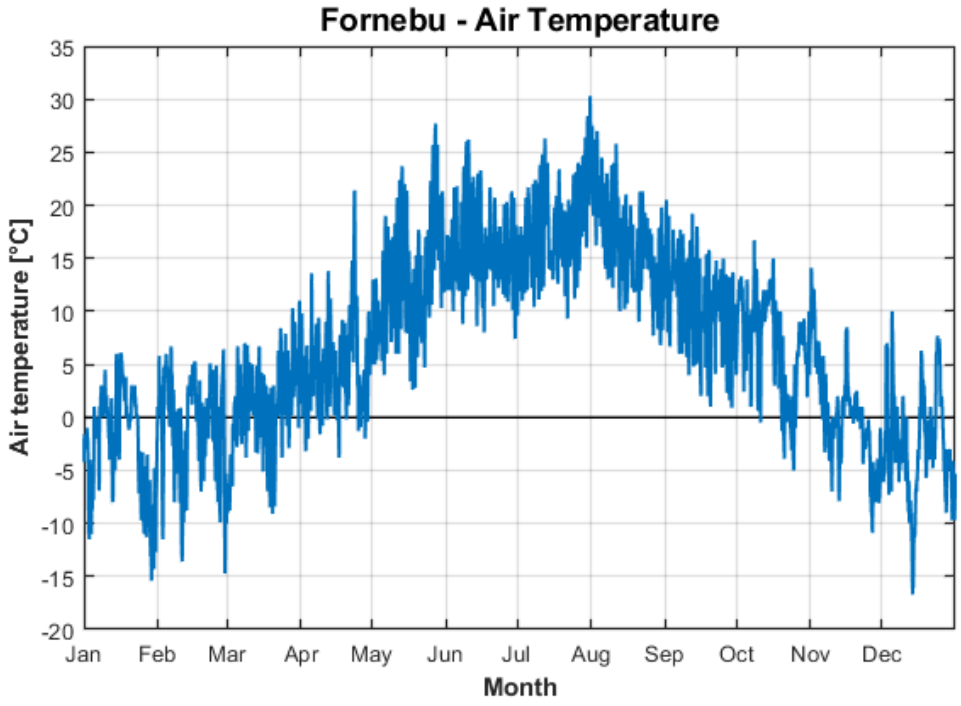

Figure D.1: Temperature variation in the IWEC file for Fornebu.

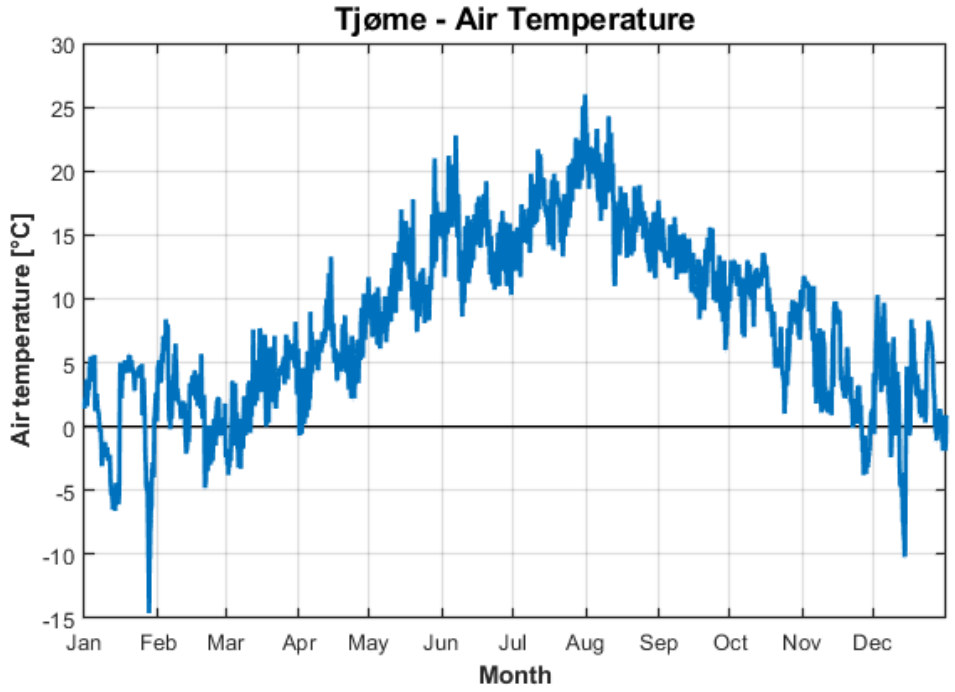

Figure D.2: Temperature variation in the IWEC file for Tjøme.

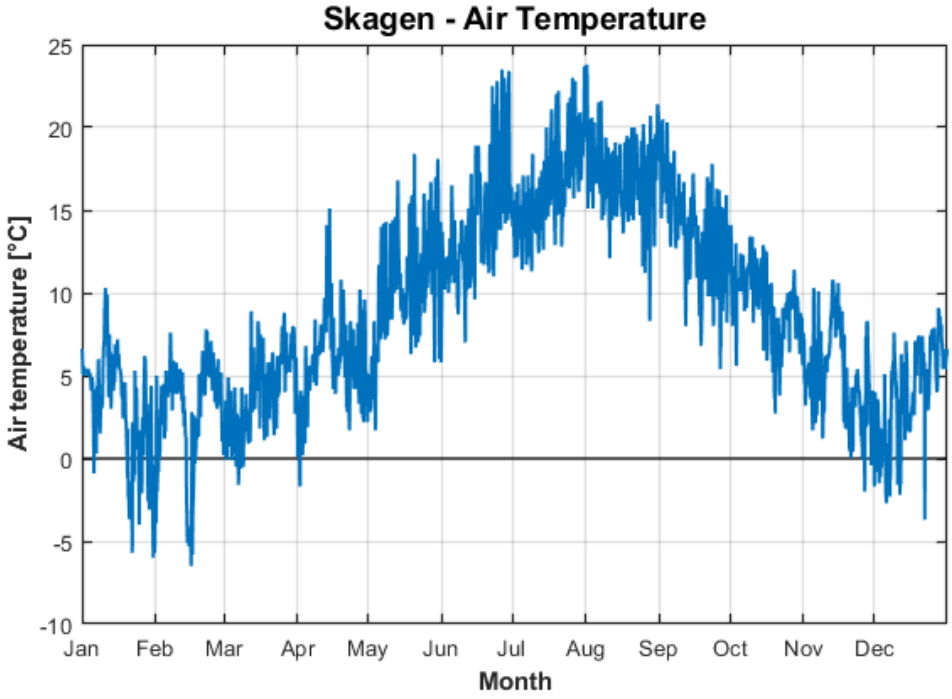

Figure D.3: Temperature variation in the IWEC file for Skagen.

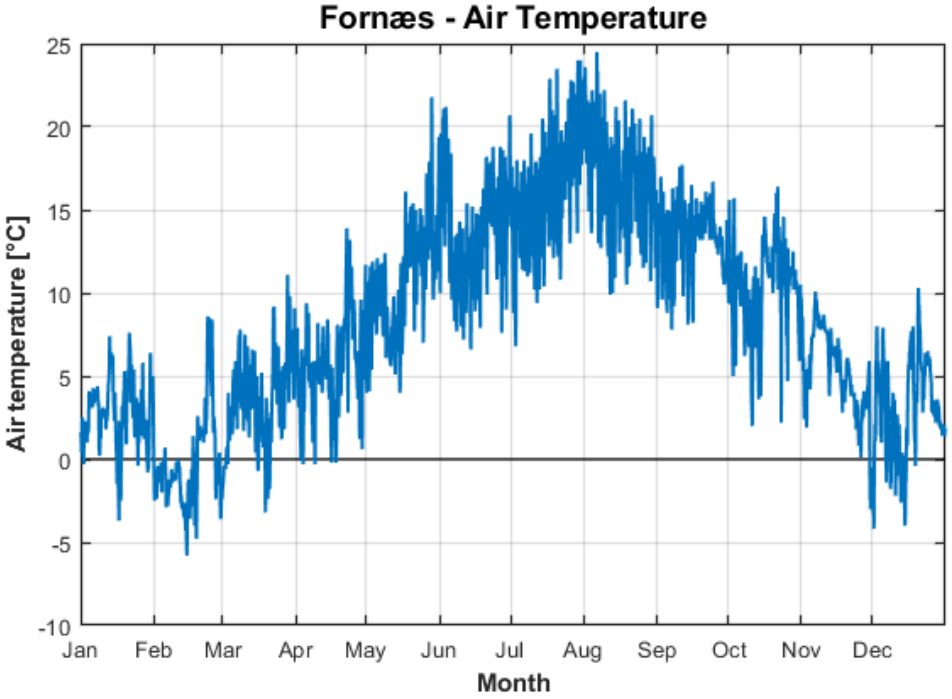

Figure D.4: Temperature variation in the IWEC file for Fornæs.

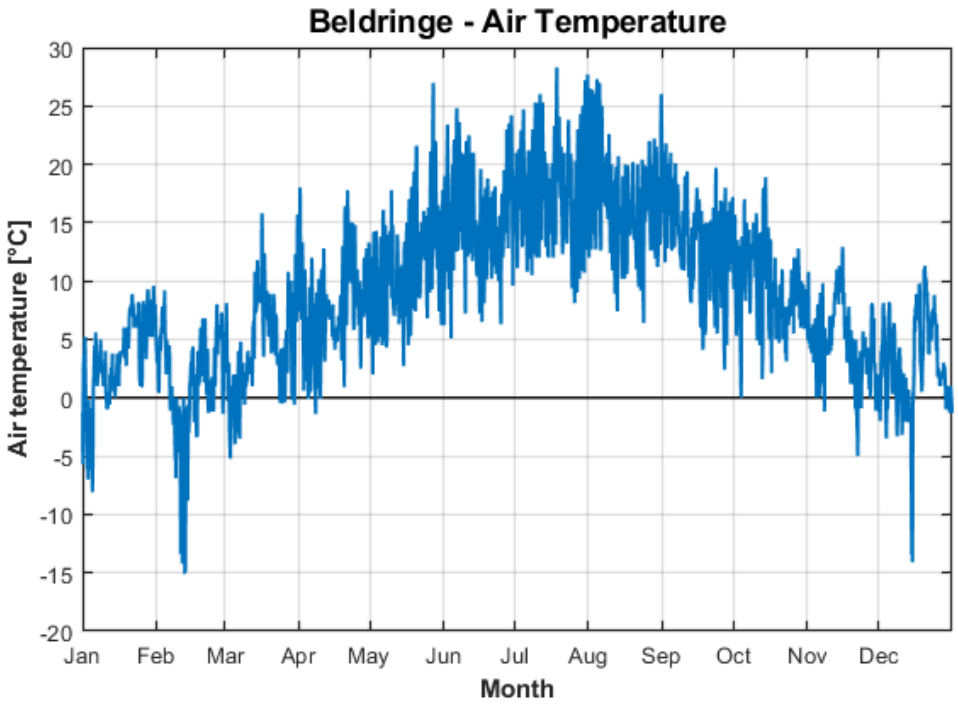

Figure D.5: Temperature variation in the IWEC file for Beldringe.

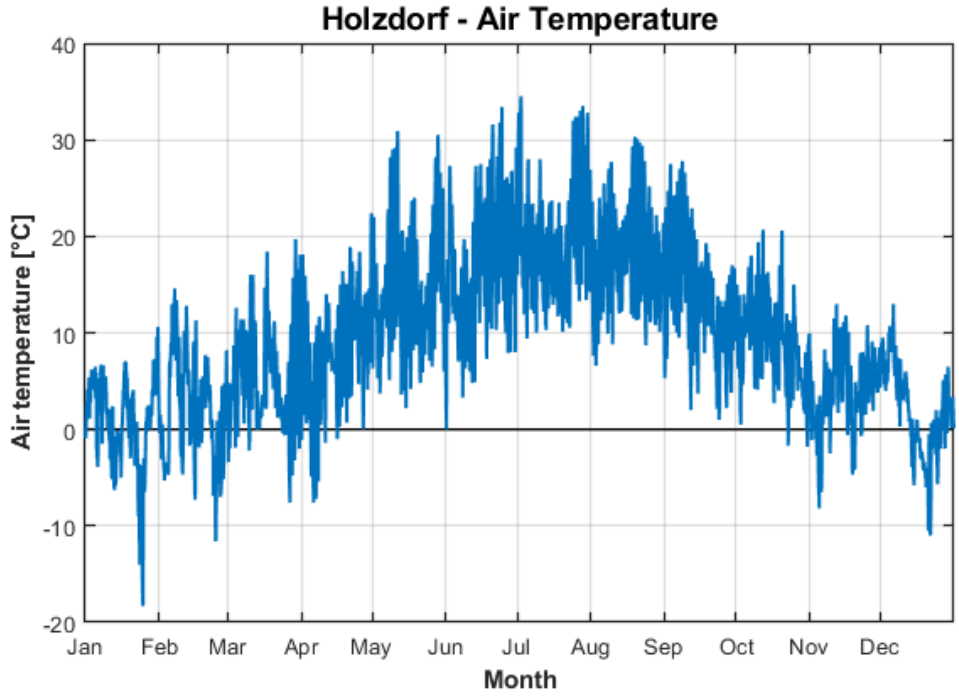

Figure D.6: Temperature variation in the IWEC file for Holzdorf.

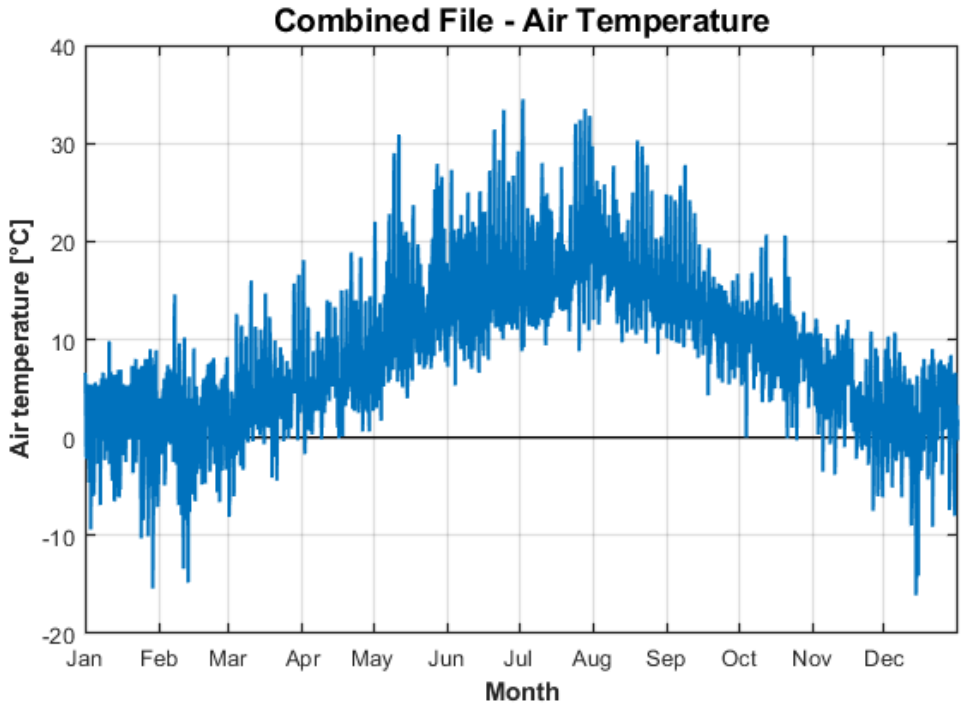

Figure D.7: Temperature variation in the combined weather file.

E Internal Gains Schedules

E.1 Occupancy

Figures E.1 to E.10 show occupancy schedules used for many of the larger zones in the ship.

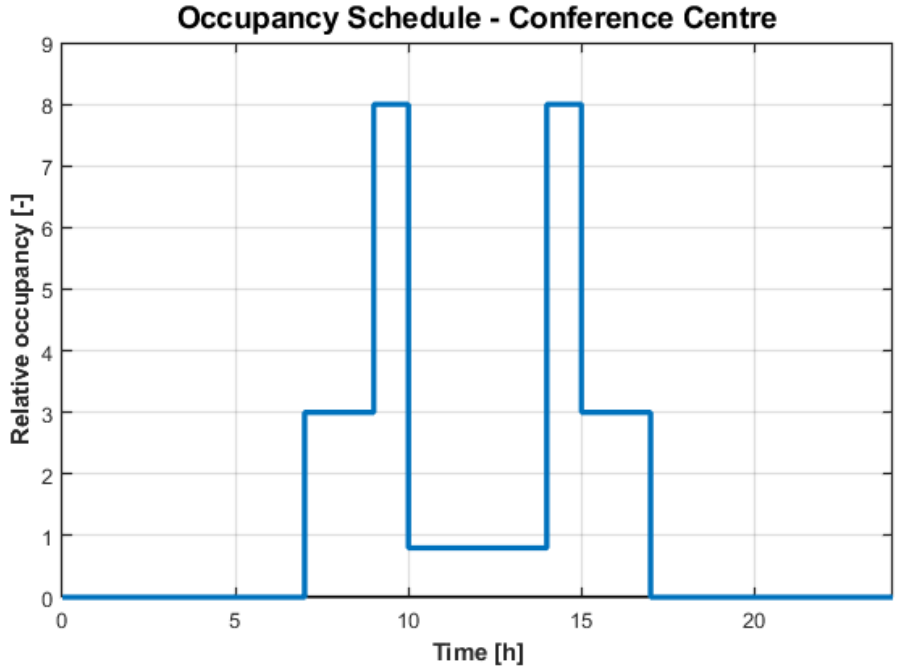

Figure E.1: Occupancy schedule for the auditorium and meeting rooms.

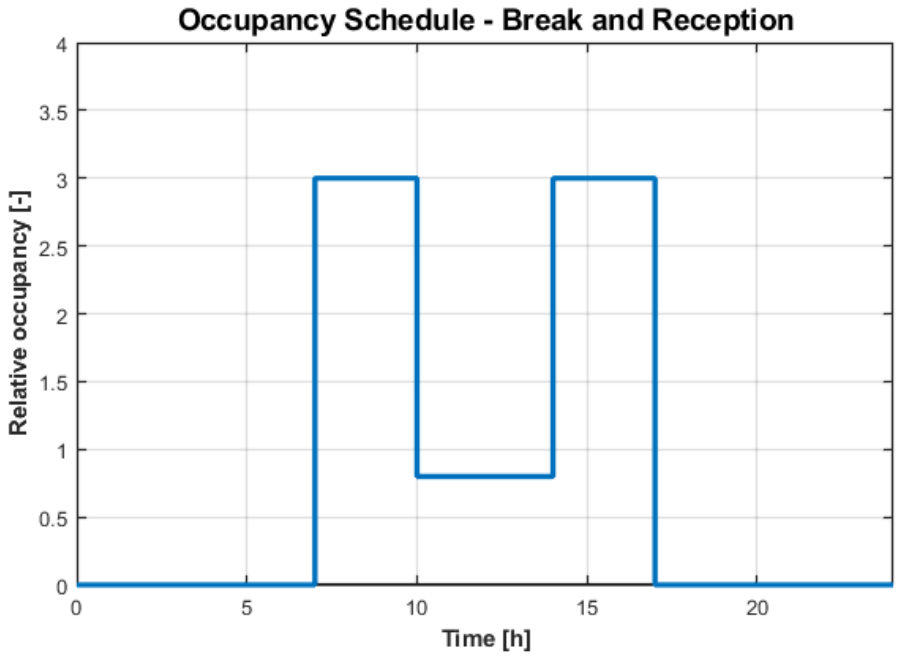

Figure E.2: Occupancy schedule for the break and reception area.

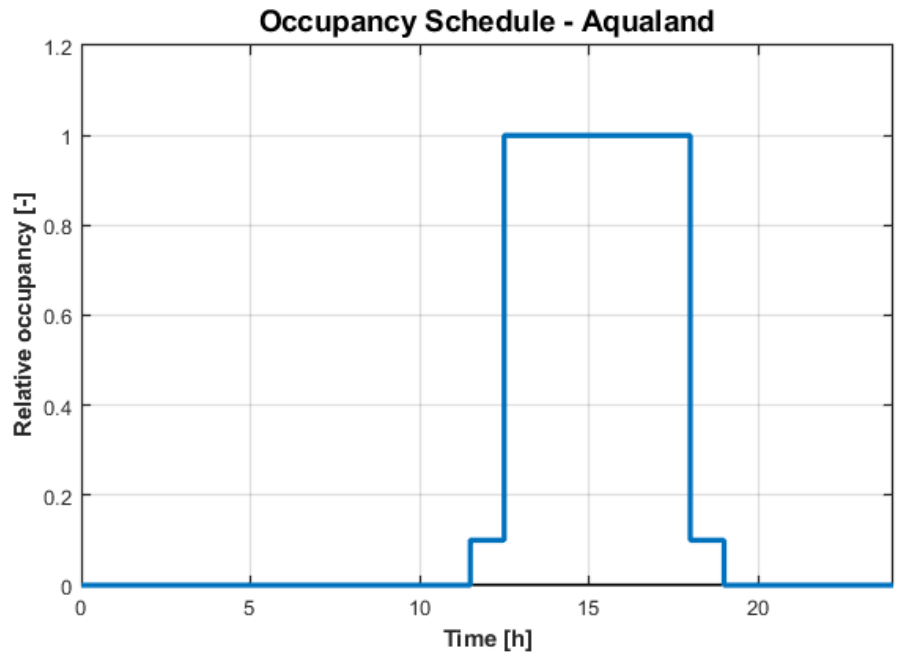

Figure E.3: Occupancy schedule for the Aqualand.

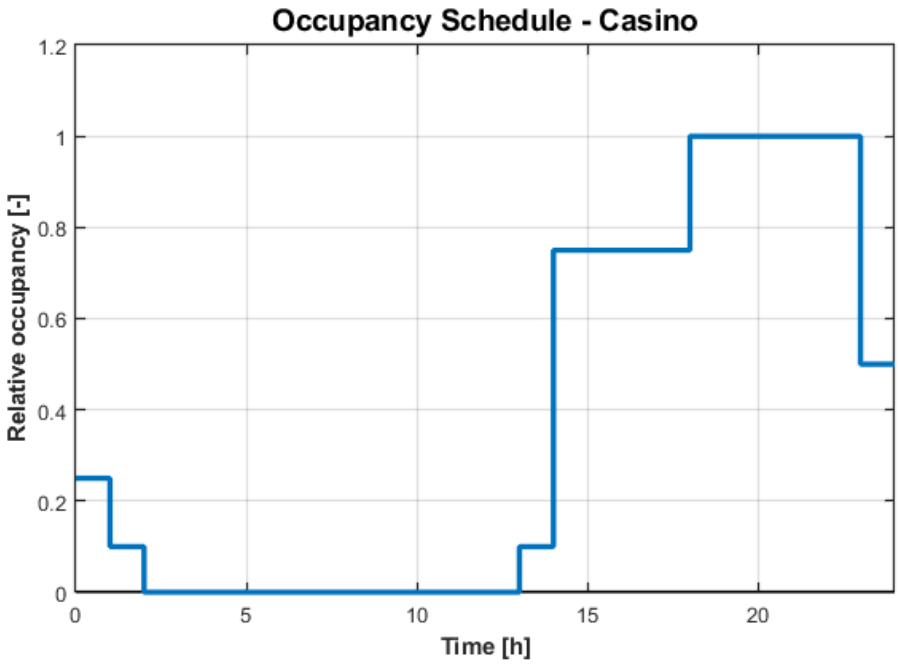

Figure E.4: Occupancy schedule for the casino.

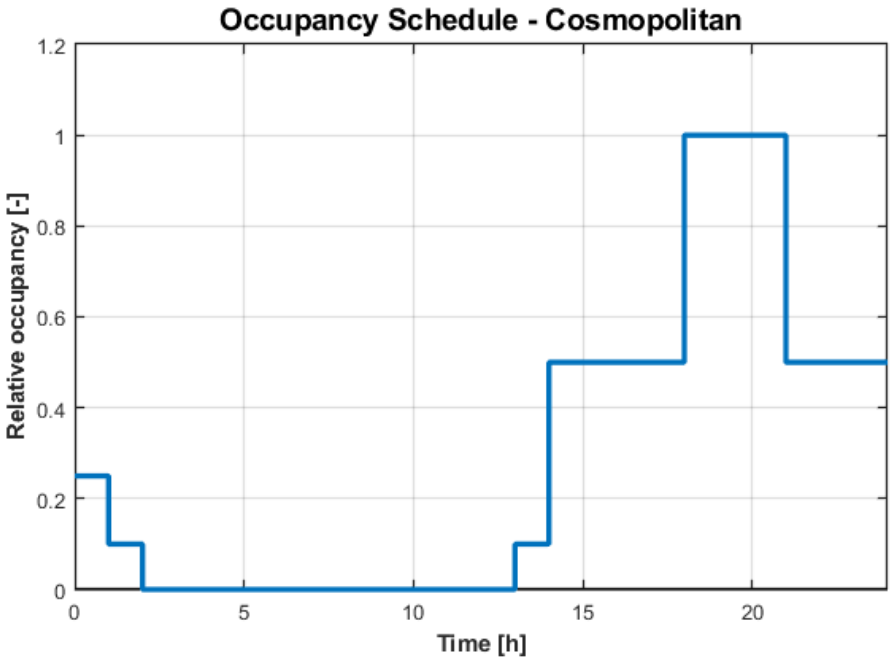

Figure E.5: Occupancy schedule for the Cosmopolitan bar and gourmet.

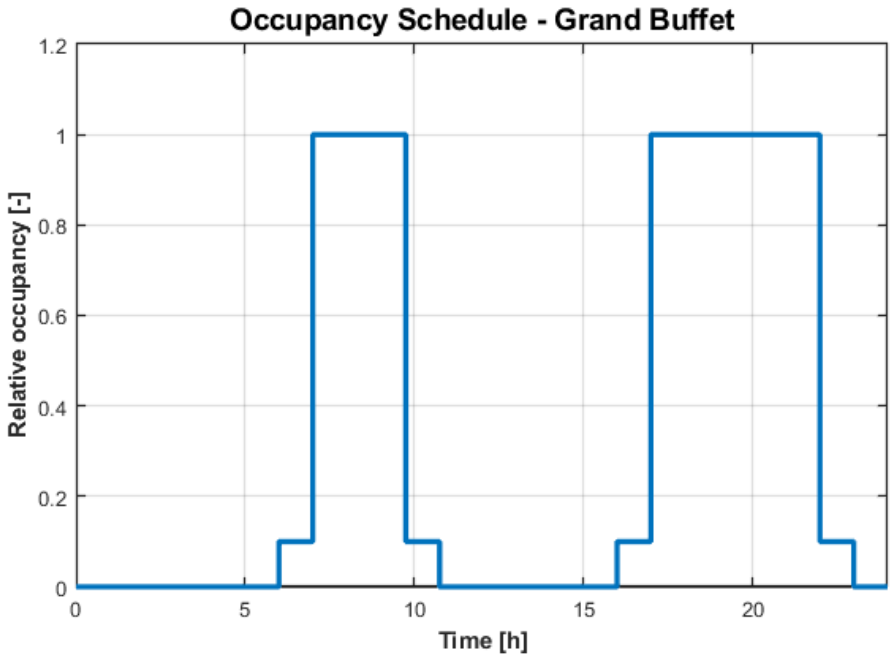

Figure E.6: Occupancy schedule for the Grand buffet.

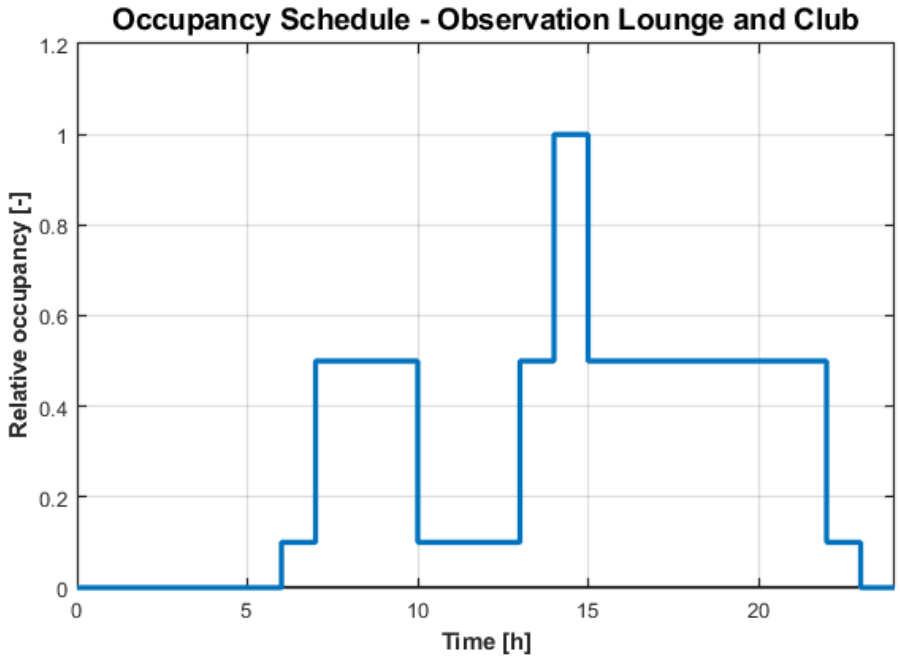

Figure E.7: Occupancy schedule for the Observation lounge and club.

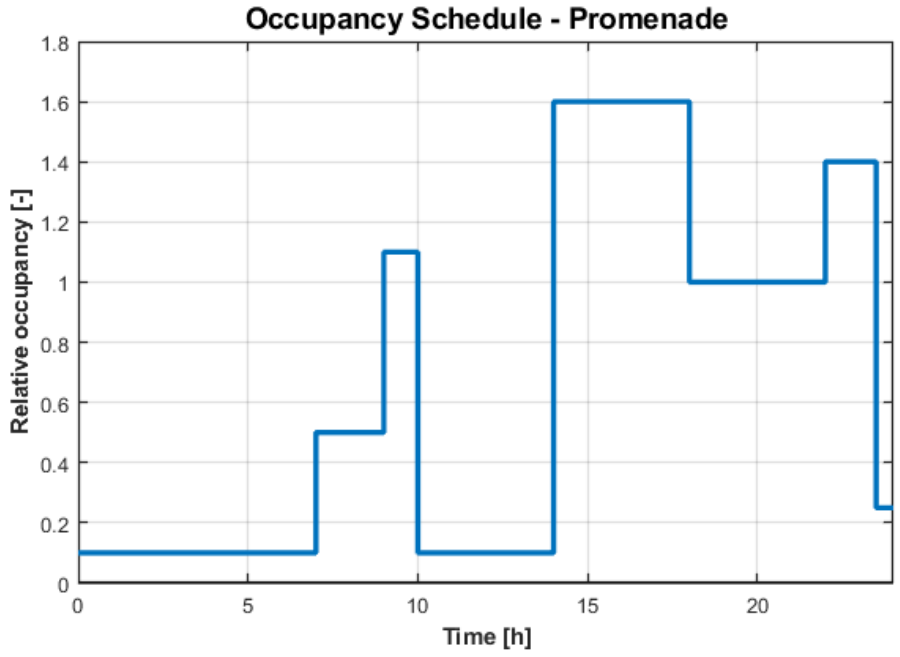

Figure E.8: Occupancy schedule for the promenade, halls and corridors.

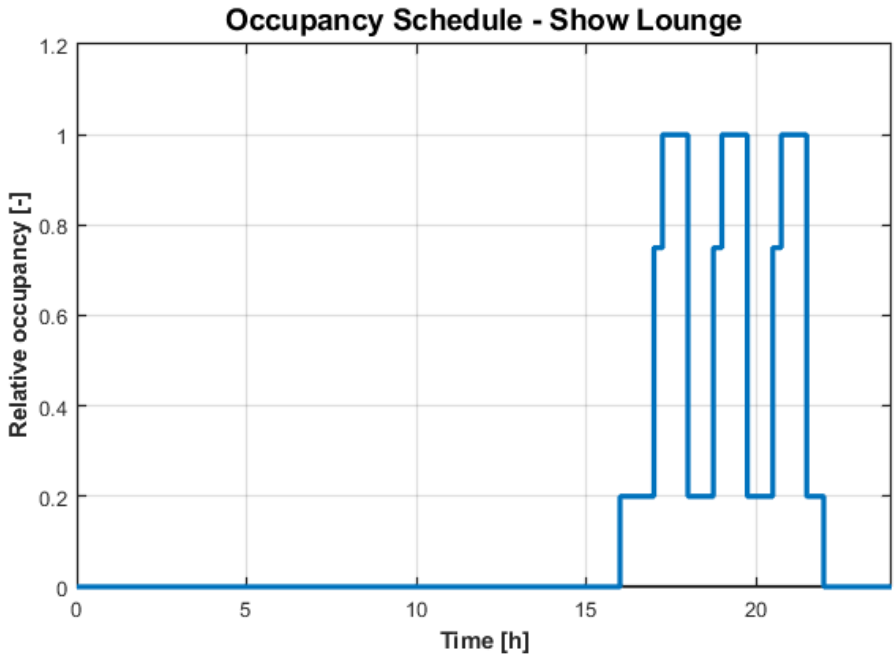

Figure E.9: Occupancy schedule for the show lounge.

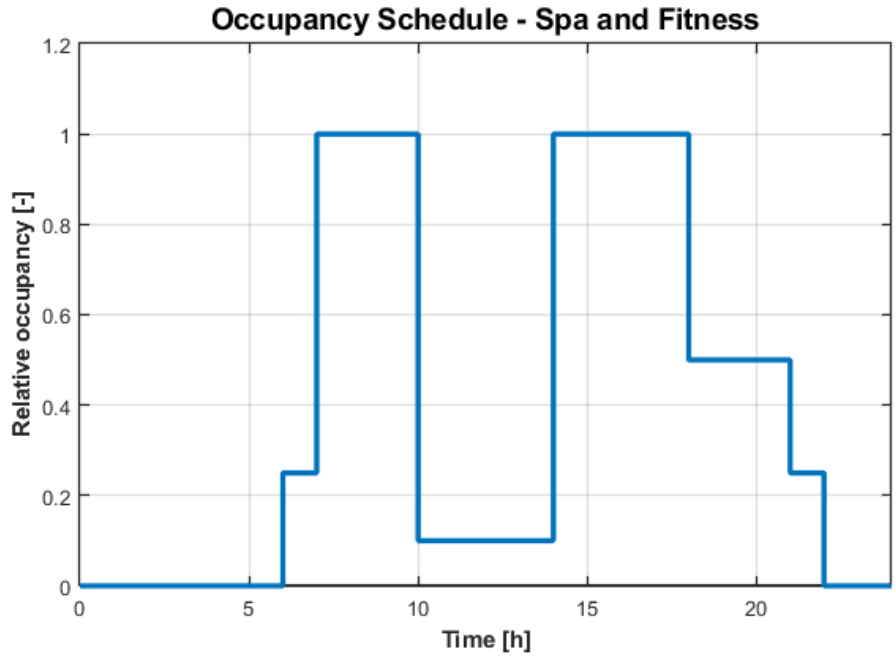

Figure E.10: Occupancy schedule for the spa and fitness centre.

E.2 Lighting

Figures E.11 and E.12 show lighting schedules for office buildings and hotels from SN-NSPEK 3031. These were used as a basis for the lighting schedules in the IDA ICE model.

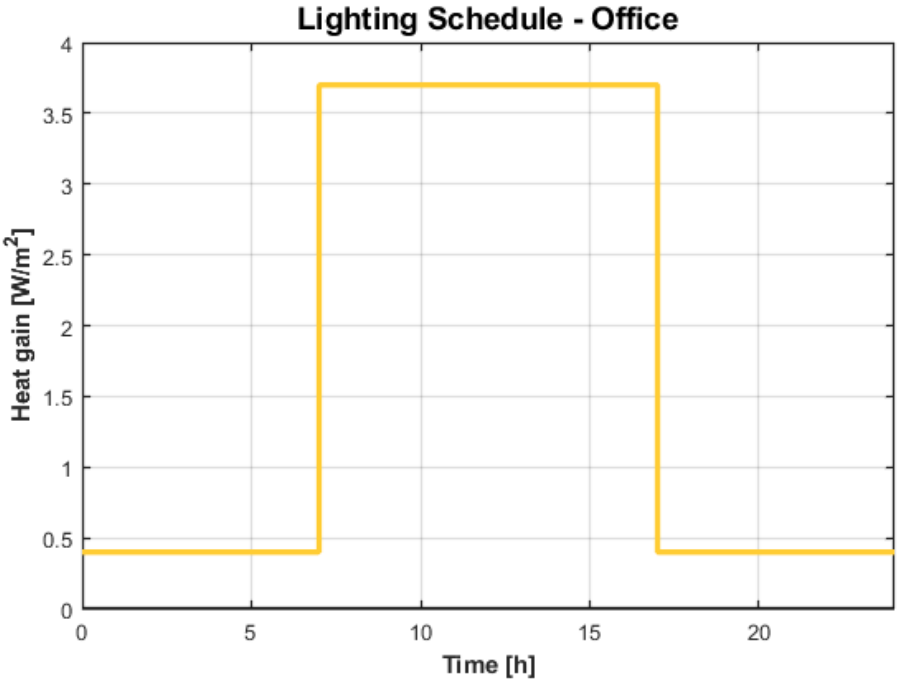

Figure E.11: Lighting schedule for an office building from SN-NSPEK 3031 [88].

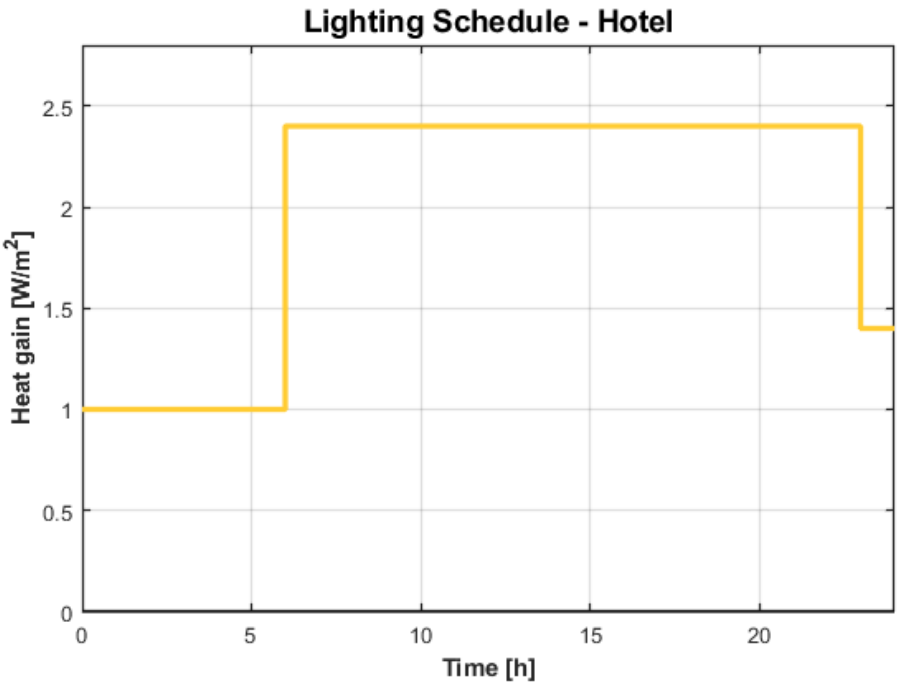

Figure E.12: Lighting schedule for a hotel from SN-NSPEK 3031 [88].

E.3 Equipment

Figures E.13 and E.14 show equipment schedules for office buildings and hotels from SN-NSPEK 3031. These were used as a basis for the equipment schedules in the IDA ICE model.

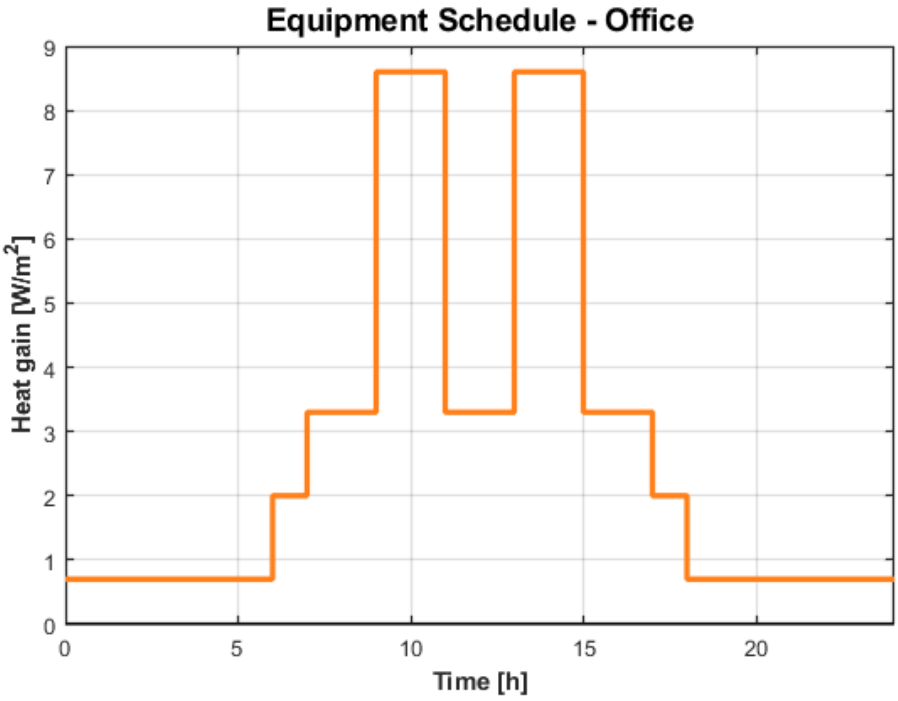

Figure E.13: Equipment schedule for an office building from SN-NSPEK 3031 [88].

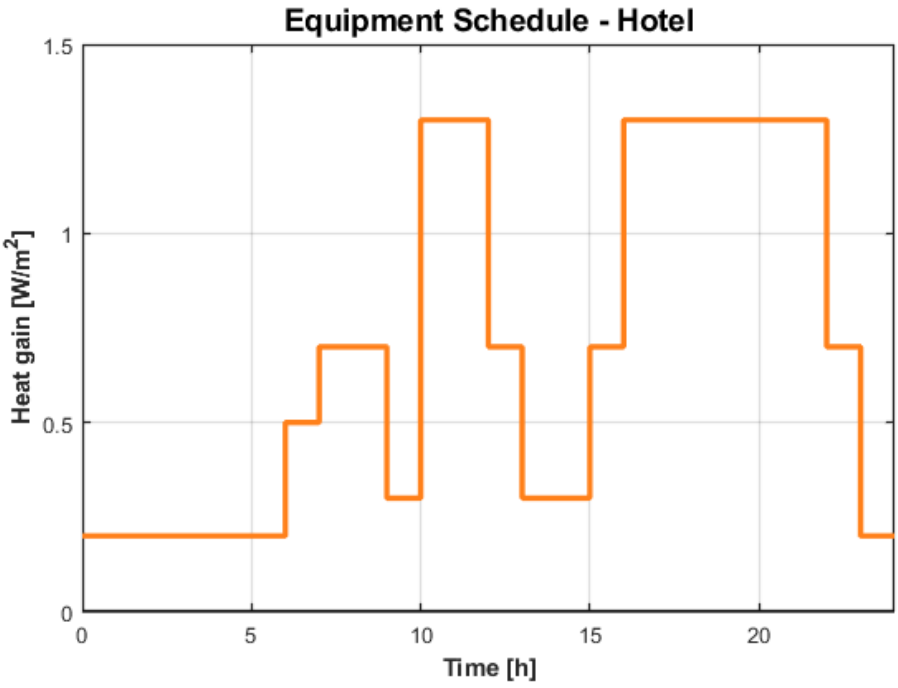

Figure E.14: Equipment schedule for a hotel from SN-NSPEK 3031 [88].

F MATLAB Script for Post Processing

F.1 Base Case

```
% timestep
dt = 0.125; % h

% installed capacity
P_engine_max = 31.6; % MW
P_boiler_max = 12.30; % MW % set as peak boiler demand for the year

% Storage tank
V = 150; % m3
rho = 1000; % kg/m3
cp = 4180; % J/kgK
dT = 30; % max temperature difference in tank
T_max = 80; % °C
T_min = T_max - dT;
E_cap = rho*V*cp*dT/3600/1e6; % MWh

P_charge_max = 3.1; % MW
P_discharge_max = 3.1; % MW

shave_level = P_boiler_max - P_discharge_max; % MW % 3.1 MW below max boiler demand

% Importing data from IDA ICE

A = readtable('caseB.xlsx');

port = A{:,1}; % 1 in port, 0 otherwise
t = A{:,2}; % h
P_el_W = A{:,3}; % electricity demand in W
P_heat_W = A{:,4}; % heat demand in W
n = length(t);

% Initialising vectors

P_el_need = zeros(n,1);
P_heat_need = zeros(n,1);

P_engine_fuel = zeros(n,1);
P_boiler_fuel = zeros(n,1);

x_engine_load = zeros(n,1);
x_boiler_load = zeros(n,1);
eta_el_eng = zeros(n,1);
eta_th_boil = zeros(n,1);
eta_heat_rec = zeros(n,1);

P_el_grid = zeros(n,1);
P_el_engine = zeros(n,1);
P_rec_heat = zeros(n,1);
P_boiler = zeros(n,1);
P_wasted_heat = zeros(n,1);
P_saved_heat = zeros(n,1);
```

```
P_charge = zeros(n,1);
P_discharge = zeros(n,1);
dE_tank = zeros(n,1);
E_tank = zeros(n,1);
dT_tank = zeros(n,1);
T_tank = zeros(n,1);
T_tank(1) = T_max-dT;

P_charge_discharge = zeros(n,1);
E_chargetot = zeros(n,1);
E_dischargetot = zeros(n,1);

for i=2:n
    P_el_need(i) = P_el_W(i)/1e6; % electricity demand in MW
    P_heat_need(i) = P_heat_W(i)/1e6; % heat demand in MW

    if port(i) == 0
        P_el_engine(i) = P_el_need(i); % engines cover el demand at sea
    else
        P_el_grid(i) = P_el_need(i); % shore power covers el demand in port, eta=1
    end

    % engines
    x_engine_load(i) = P_el_engine(i)/P_engine_max;
    eta_el_eng(i) = f_eta_el(x_engine_load(i));
    P_engine_fuel(i) = P_el_engine(i)/eta_el_eng(i);

    eta_heat_rec(i) = f_eta_heat_rec(x_engine_load(i));
    P_rec_heat(i) = P_engine_fuel(i) * eta_heat_rec(i);

    % boiler demand and wasted heat
    if P_heat_need(i) < P_rec_heat(i)
        P_boiler(i) = 0;
        P_wasted_heat(i) = P_rec_heat(i) - P_heat_need(i);
    else
        P_boiler(i) = P_heat_need(i) - P_rec_heat(i);
        P_wasted_heat(i) = 0;
    end

    % Storage

    if i>11520 && i<=58560 % summer
        cl = 0; % charge level
    else % winter
        cl = 1/3;
    end

    % Utilising wasted heat

    if P_wasted_heat(i) > 0 && E_tank(i-1) < E_cap
        if E_tank(i-1)+P_wasted_heat(i)*dt <= E_cap % charge all wasted heat
            P_charge(i) = P_wasted_heat(i);
        else % charge whole tank
            P_charge(i) = (E_cap - E_tank(i-1))/dt;
        end
        if P_charge(i) > P_charge_max
```

```
        P_charge(i) = P_charge_max;
    end
    P_saved_heat(i) = P_charge(i);
    P_wasted_heat(i) = P_wasted_heat(i) - P_saved_heat(i);
end

if P_boiler(i) > 0 && E_tank(i-1) > E_cap*cl
    if P_boiler(i)*dt > E_tank(i-1) - E_cap*cl % discharge down to cl
        P_discharge(i) = (E_tank(i-1) - E_cap*cl)/dt;
    else % discharge covers boiler need
        P_discharge(i) = P_boiler(i);
    end
    if P_discharge(i) > P_discharge_max
        P_discharge(i) = P_discharge_max;
    end
end

% Peak shaving

if i<=11520 || i>58560 % winter
    if P_boiler(i) < shave_level && E_tank(i-1) < E_cap*cl
        P_below = shave_level - P_boiler(i);
        if E_tank(i-1) + P_below*dt <= E_cap*cl % charge all avail power
            P_charge(i) = P_below;
        else % charge up to cl
            P_charge(i) = (E_cap*cl - E_tank(i-1))/dt;
        end
        if P_charge(i) > P_charge_max
            P_charge(i) = P_charge_max;
        end
        if P_charge(i) < P_saved_heat(i) % to save all waste heat needed
            P_charge(i) = P_saved_heat(i);
        end
    end

    if P_boiler(i) > shave_level && E_tank(i-1) > 0
        P_above = P_boiler(i) - shave_level; % boiler demand above shave level
        if P_above*dt > E_tank(i-1) % discharge the whole tank
            P_discharge(i) = E_tank(i-1)/dt;
        else
            P_discharge(i) = P_above; % reduce boiler to shave level
        end
        if P_discharge(i) > P_discharge_max
            P_discharge(i) = P_discharge_max;
        end
    end
end

P_boiler(i) = P_boiler(i) + P_charge(i) - P_discharge(i) - P_saved_heat(i);

% tank energy level and temperature
dE_tank(i) = (P_charge(i) - P_discharge(i))*dt;
E_tank(i) = E_tank(i-1) + dE_tank(i);

dT_tank(i) = dE_tank(i)*3600*1e6/(rho*V*cp);
T_tank(i) = T_tank(i-1) + dT_tank(i);
```

```
    % boilers
    x_boiler_load(i) = P_boiler(i)/P_boiler_max;
    eta_th_boil(i) = f_eta_th_boil(x_boiler_load(i));
    P_boiler_fuel(i) = P_boiler(i)/eta_th_boil(i);

    % total heat rate for charging and discharging
    P_charge_discharge(i) = P_charge(i) - P_discharge(i);

    % cumulative heat rate for charging and discharging
    E_chargetot(i) = E_chargetot(i-1) + P_charge(i)*dt;
    E_dischargetot(i) = E_dischargetot(i-1) + P_discharge(i)*dt;

end

E_wasted = sum(P_wasted_heat)*dt; % MWh
E_saved = sum(P_saved_heat)*dt; % MWh

function eta = f_eta_th_boil(x) % thermal efficiency boilers
eta = -0.118*x^2 + 0.0708*x + 0.7891;
end

function eta = f_eta_el(x) % electrical efficiency engines
eta = -0.0814*x^2 + 0.1612*x + 0.3486;
end

function eta = f_eta_heat_rec(x) % amount of engine heat recovered
eta = 0.189*(0.0812*x^2 - 0.1611*x + 0.5519);
end
```

F.2 Case 10 - Hot Storage Tank for Heat Demands in Port

```
% Storage

% Utilising wasted heat in summer

if i>11520 && i<=58560 % summer
    if P_wasted_heat(i) > 0 && E_tank(i-1) < E_cap
        if E_tank(i-1)+P_wasted_heat(i)*dt <= E_cap % charge all wasted heat
            P_charge(i) = P_wasted_heat(i);
        else % charge whole tank
            P_charge(i) = (E_cap - E_tank(i-1))/dt;
        end
        if P_charge(i) > P_charge_max
            P_charge(i) = P_charge_max;
        end
        P_saved_heat(i) = P_charge(i);
        P_wasted_heat(i) = P_wasted_heat(i) - P_saved_heat(i);
    end

    chargefactor = 0.75;

else % winter
    chargefactor = 1;
end

if port(i)==0 && E_tank(i-1) < E_cap*chargefactor % charging tank at sea
    P_charge(i) = (chargefactor*E_cap - E_tank(i-1))/dt;
    if P_charge(i) > P_charge_max
        P_charge(i) = P_charge_max;
    end
end

if port(i)==1 && E_tank(i-1) > 0 % discharging tank instead of using boiler in port
    if E_tank(i-1) > P_boiler(i)*dt
        P_discharge(i) = P_boiler(i);
    else
        P_discharge(i) = E_tank(i-1)/dt;
    end
    if P_discharge(i) > P_discharge_max
        P_discharge(i) = P_discharge_max;
    end
end

P_boiler(i) = P_boiler(i) + P_charge(i) - P_discharge(i) - P_saved_heat(i);

% tank energy level and temperature
dE_tank(i) = (P_charge(i) - P_discharge(i))*dt;
E_tank(i) = E_tank(i-1) + dE_tank(i);

dT_tank(i) = dE_tank(i)*3600*1e6/(rho*V*cp);
T_tank(i) = T_tank(i-1) + dT_tank(i);

if port(i)==1
    P_boiler_port(i) = P_boiler(i); % use of boiler in port
end
```

G PCM Properties

Tables G.1 and G.2 show the properties for the default PCM in IDA ICE, with the temperature coordinates shifted to give a melting temperature around 24 °C. This material was used in Case 5.

Table G.1: Properties for the PCM used in Case 5.

	Value	**Unit**
Number of temperature coordinates	14	-
Number of partial enthalpies	13	-
Density (solid)	1500	kg/m^3
Thermal conductivity (solid)	0.6	W/(m K)
Thermal conductivity (liquid)	0.6	W/(m K)
Specific heat capacity (solid)	2000	J/(kg K)
Specific heat capacity (liquid)	2000	J/(kg K)
Specific heat capacity during reversing	300	J/(kg K)

Table G.2: Temperature coordinates and partial enthalpies for the PCM used in Case 5.

	Unit
Temperatures coordinates: 15.5, 16.5, 17.5, 18.5, 19.5, 20.5, 21.5, 22.5, 23.5, 24.5, 25.5, 26.5, 27.5, 28.5	°C
Partial enthalpies between temp. coordinates divided by temp. interval (melting): 3000, 3000, 4000, 5000, 6000, 9000, 13000, 38000, 54000, 9000, 5000, 4000, 3000	J/(kg K)
Partial enthalpies between temp. coordinates divided by temp. interval (solidifying): 4000, 5000, 6000, 9000, 20000, 34000, 60000, 5000, 4000, 3000, 2000, 2000, 2000	J/(kg K)

H AHU Investment Costs

Table H.1 shows an estimate of investment costs, including installation, for Systemair's largest AHU, provided by Scandinavian technical contractor GK [93]. These are estimated costs for replacing an AHU in a typical commercial building, excluding VAT.

Table H.1: Estimated investment and installation costs for Systemair's largest AHU, with capacity 5250 m^3/h.

	Cost estimate [NOK]
Demolition	7500
AHU	90,000
New silencers (if needed)	10,000
Installation	15,000
Adaptation of existing ductwork	5000
Insulation	5000
Sum	132,500

I VAV Ventilation

Table I.1: VAV ventilation strategy, floor area, zone multiplier and total costs for each zone.

	Vent. strategy	Floor area [m^2]	Zone mult.	Costs [NOK]
Restaurants				
Oceanic á la Carte	DCV	795	1	559,600
Cosmopolitan bar and gourmet	DCV	673	1	479,200
Private dining	Occupant-contr.	24	1	21,100
Observation lounge and club	DCV	901	1	633,300
Grand buffet	DCV	1533	1	1,055,400
Burger bar	DCV	133	1	117,400
Promenade and shops				
Promenade part 1	DCV	1014	1	707,000
Promenade part 2	DCV	322	1	244,700
Hall 1 deck 6	DCV	582	1	418,900
Hall 1 deck 7-12	DCV	473	1	345,200
Hall 2	DCV	332	1	251,400
Corridor deck 6	DCV	265	1	204,500
Public bathrooms	Schedule	103	2	147,400
Small shop	Occupant-contr.	89	1	61,300
Medium shop	DCV	169	1	137,500
Large shop	DCV	369	1	271,500
Taxfree market	DCV	473	1	345,200
Other public areas				
Adventure planet	DCV	100	1	90,600
Casino	DCV	670	1	472,500
Night club	DCV	200	1	157,600
Show lounge	DCV	801	1	566,300
Teens plaza	DCV	133	1	117,400
Spa and fitness	DCV	607	1	432,300
Extra area	Occupant-contr.	365	57.7	14,361,530
Conference centre				
Auditorium	DCV	324	1	244,700
Meeting room 1	DCV	68	3	211,500
Meeting room 2	DCV	38	5	252,000
Break and reception area	DCV	410	1	298,300
Employee areas				
Small galley	Schedule	221	2	308,200
Large galley	Schedule	438	2	589,600
Laundry	Schedule	187	1	127,300
Cabins				
10.5 m^2 cabins	Occupant-contr.	10.5	658	5,066,600
14 m^2 cabins	Occupant-contr.	14	116	1,670,400
24.5 m^2 cabins	Occupant-contr.	24.5	30	633,000
Total costs				31,600,430

J Fan Coil Heating and Cooling Rates

Table J.1: Heating and cooling rates used for the fan coils in Case A, as well as floor areas for each zone.

	Room unit heat [W]	Room unit cool [W]	Floor area [m^2]
Restaurants			
Oceanic á la Carte	16,867	12,335	795
Cosmopolitan bar and gourmet	12,505	5577	673
Private dining	703	346	24
Observation lounge and club	43,565	36,569	901
Grand buffet	30,893	20,391	1533
Burger bar	3798	2909	133
Promenade and shops			
Promenade part 1	15,935	0	1014
Promenade part 2	2661	0	322
Hall 1 deck 6	4705	5478	582
Hall 1 deck 7-12	14,867	21,002	473
Hall 2	16,874	30,618	332
Corridor deck 6	2057	0	265
Public bathrooms	2890	3186	103
Small shop	592	0	89
Medium shop	1135	819	169
Large shop	1968	1926	369
Taxfree market	3469	1095	473
Other public areas			
Adventure planet	856	323	100
Aqualand	26,643	24,538	547
Casino	4704	1159	670
Night club	9007	3968	200
Show lounge	7067	70	801
Teens plaza	3600	1572	133
Spa and fitness	21,207	21,727	607
Extra area	3221	4211	365
Conference centre			
Auditorium	14,436	11,530	324
Meeting room 1	3292	2901	68
Meeting room 2	3013	2705	38
Break and reception area	15,956	0	410
Employee areas			
Small galley	11,795	231	221
Large galley	28,594	634	438
Laundry	23,464	26,584	187
Navigation bridge	11,175	20,958	165
Officers' quarters	643	885	86
Others			
Cabins, 3-4 stars	41-395	0-175	8-14
Cabins, 5 stars	729-1105	1100-2414	24.5-35
Car deck	1,367,963	0	3125
Trailer deck	1,296,350	0	1778

Table J.2: Heating and cooling rates used for the fan coils in Case B, i.e. the base case, as well as floor areas for each zone.

	Room unit heat [W]	Room unit cool [W]	Floor area [m^2]
Restaurants			
Oceanic á la Carte	13,046	26,132	795
Cosmopolitan bar and gourmet	11,746	17,659	673
Private dining	644	332	24
Observation lounge and club	36,968	47,204	901
Grand buffet	23,793	41,928	1533
Burger bar	3330	5176	133
Promenade and shops			
Promenade part 1	5672	27,277	1014
Promenade part 2	0	4424	322
Hall 1 deck 6	1697	9645	582
Hall 1 deck 7-12	12,343	27,143	473
Hall 2	11,627	30,777	332
Corridor deck 6	0	4512	265
Public bathrooms	ca. 13,400	ca. 3420	103
Small shop	0	1106	89
Medium shop	0	2838	169
Large shop	9	5979	369
Taxfree market	1683	4997	473
Other public areas			
Adventure planet	691	1924	100
Aqualand	36,526	20,077	547
Casino	2792	7897	670
Night club	20,880	3900	200
Show lounge	5568	6793	801
Teens plaza	3117	3233	133
Spa and fitness	17,513	29,548	607
Extra area	1961	5628	365
Conference centre			
Auditorium	40,734	13,422	324
Meeting room 1	2798	3070	68
Meeting room 2	2639	2879	38
Break and reception area	27,108	14,046	410
Employee areas			
Small galley	8429	21,128	221
Large galley	61,145	31,729	438
Laundry	30,809	35,213	187
Navigation bridge	9409	19,776	165
Officers' quarters	288	ca. 1100	86
Others			
Cabins, 3-4 stars	0-960	0-211	8-14
Cabins, 5 stars	706-1009	865-2222	24.5-35
Car deck	1,406,563	0	3125
Trailer deck	1,336,523	0	1778

K Results

K.1 IDA ICE - Exact Results

Table K.1 shows the exact annual energy use obtained from simulations of the initial model, the calibrated model and the base case model. Low and high estimates for energy use for the propulsion and hotel systems on the reference ships are also included.

Table K.1: Exact results obtained for annual energy use for the initial model, calibrated model and base case, as well as low and high estimates for the reference ships. All values are in MWh/passenger.

	Initial model	Calibrated	Base case	Birka Stockholm	Large cruise ship
Propulsion	32.2	32.2	32.2	14.4	22.0
Accom. heating	5.87	5.13	5.13	4.99	0
Fuel/tank heating	0	0	0	1.07	0
Galley	5.98	5.98	5.98	0.974	0
Laundry	3.66	3.66	3.66	0	0
DHW	0.775	1.51	1.51	1.51	0
Cooling	0.469	0.443	0.444	0.251	3.50
HVAC auxiliary	1.98	1.86	1.89	0	4.58
Lighting	0.366	0.366	0.366	0	0
Equipment	0.208	0.208	0.208	0	0
Other - low	0	0	0	2.45	9.46
Other - high	0	0	0	7.35	22.1
Total	51.5	51.4	51.4	25.7-30.6	39.5-52.2

K.2 Post Processing - Exact Results

Table K.2 shows exact results from post processing of the base case with MGO engines and boilers, while table K.3 shows the results for the LNG ship. The tables show electricity and heat delivered by boilers, engines and shore power, as well as fuel consumption for boilers and engines.

Table K.2: Exact results for delivered electricity and heat, as well as fuel consumption, for the MGO ship. All values are in MWh.

	Electricity delivered	Heat delivered	Fuel consumption
Boilers	0	19,917	24,964
Engines	82,262	19,167	203,970
Shore power	1286	0	0

Table K.3: Exact results for delivered electricity and heat, as well as fuel consumption, for the LNG ship. All values are in MWh.

	Electricity delivered	Heat delivered	Fuel consumption
Boilers	0	12,169	15,260
Engines	82,262	28,700	203,970
Shore power	1286	0	0

K.3 Aqualand Energy Use

Table K.4 shows detailed energy use for the Aqualand in the initial model, divided into different energy users. The DHW was calculated assuming the same heating demand as the rest of the ship, at 30.1 kWh/m^2. Considering the area of the pool at 136.8 m^2 gives a total annual energy consumption of 2690 kWh/m^2 ws. A graphical presentation of the energy use is shown in figure K.1.

Table K.4: Annual energy consumption for the Aqualand, divided into energy users.

	Annual energy use [MWh]
AHU cooling	0.447
AHU heating	128.6
AHU fans	11.2
Zone cooling	0
Zone heating	91.3
Equipment	2.37
Lighting	6.99
Pool water heating	110.6
DHW	16.5
Total	368.0

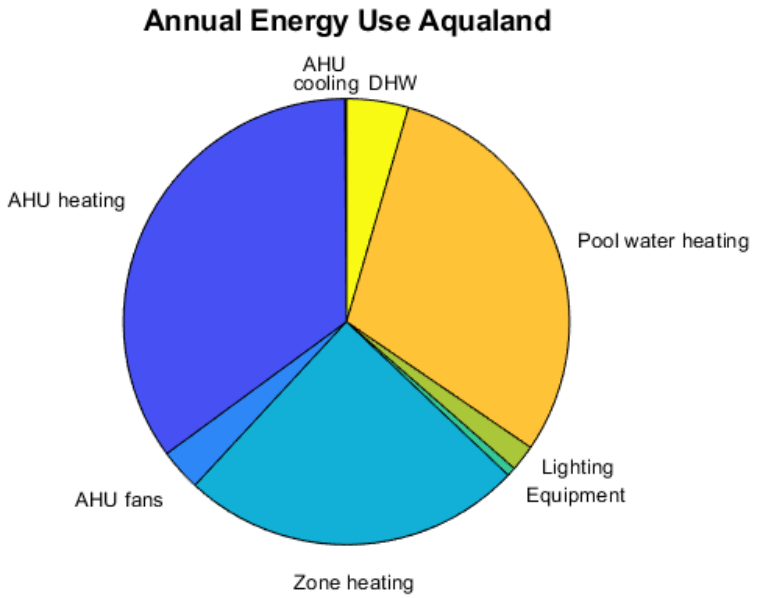

Figure K.1: Annual energy use for the Aqualand, divided into energy users.

K.4 Fan Coil Sizing Analysis

Figures K.2 and K.3 show duration curves for accommodation heating and cooling with unlimited heating and cooling after calibration, and for each of the fan coil sizing cases.

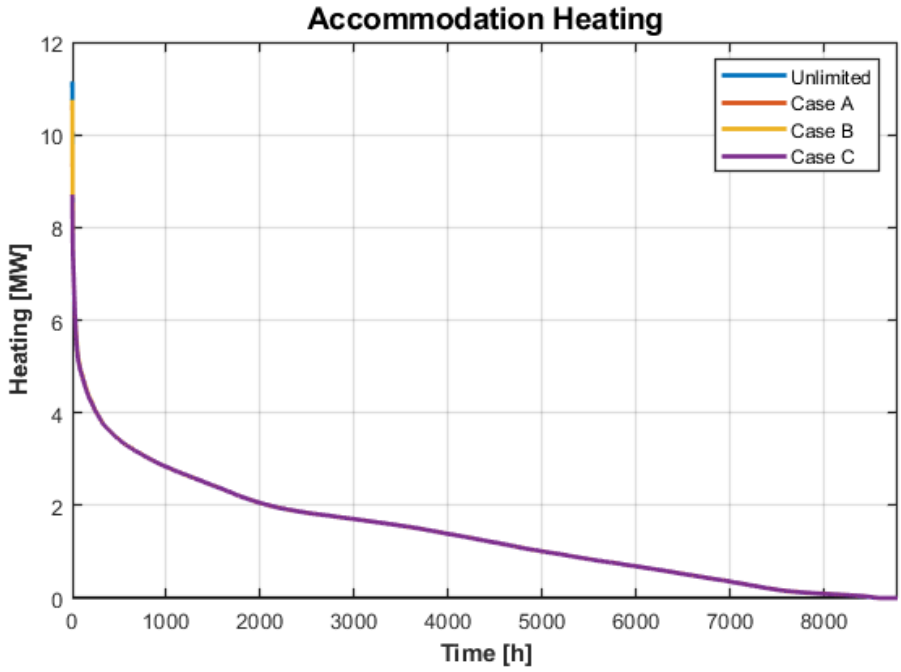

Figure K.2: Duration curves for accommodation heating with unlimited heating and cooling after calibration, and for each fan coil sizing case.

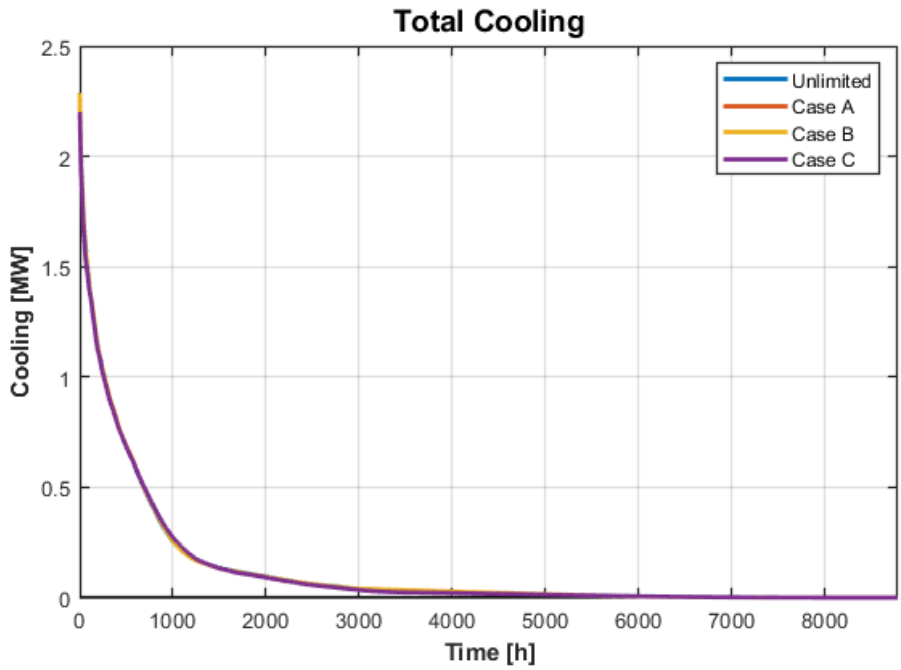

Figure K.3: Duration curves for cooling with unlimited heating and cooling after calibration, and for each fan coil sizing case.

K.5 Energy Efficiency Analysis

LNG Ship

Figure K.4 shows the annual fuel consumption by engines and boilers in each energy efficiency scenario when the ship uses LNG as fuel. The largest reductions in engine fuel consumption occur in Case 6 with ventilation heat recovery and Case 7 with VAV ventilation. Case 8 with a heat pump has an increase in engine fuel consumption due to electricity needed for the heat pump. The most significant reductions in boiler fuel consumption occur in Cases 6, 7 and 8.

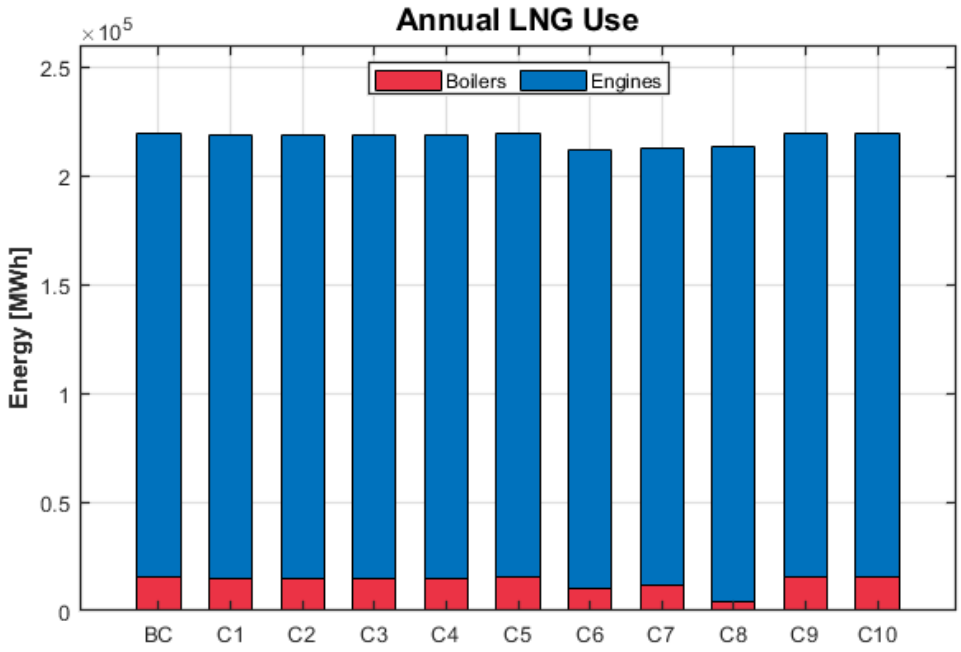

Figure K.4: Fuel consumption for engines and boilers in each energy efficiency scenario for the LNG ship.

Shore Power

Figure K.5 shows the total annual electricity delivered by shore power in each energy efficiency scenario. This was identical for the MGO and LNG ships due to the electricity demand being the same. The shore power equals the hotel system's electricity demand in port. Cases 6 and 7 show a reduction in shore power due to reduced used of fans and pumps and reduced cooling. Case 8 has increased use of shore power due to use of the heat pump.

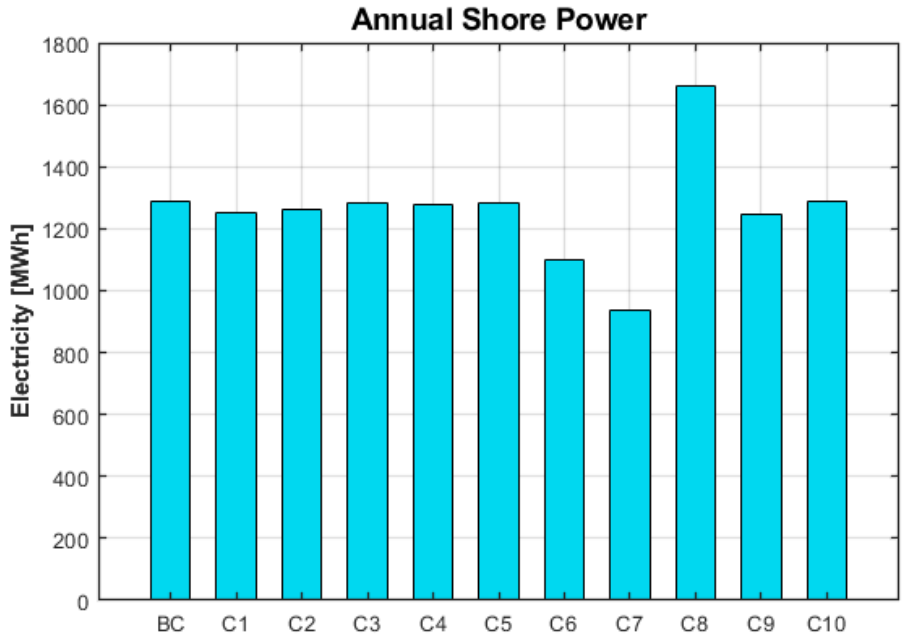

Figure K.5: Annual electricity delivered by shore power for the different energy saving solutions.

K.6 Profitability Analysis and GHG Emissions

Table K.5 shows the prices and GHG emission factors for shore power, MGO and LNG. Table K.6 shows the economic lifetime, real interest rate and annuity factor for the energy saving solutions. Table K.7 shows the investment cost, additional maintenance cost, fuel and shore power saved, and the net annual savings for each energy saving solution. The net present value (NPV), pay-off time, maximum permissible investment (MPI) and reduction in GHG emissions calculated for each solution are shown in table K.8. When calculating the MPI for Case 8 with a heat pump, the additional maintenance cost was set to 2% of the MPI, through iteration.

Table K.5: Prices and GHG emission factors for shore power and fuels.

	Price [NOK/kWh]	CO_2e [g/kWh]
Shore power	0.999	130
MGO	0.388	313.56
LNG	0.259	288.72

Table K.6: Economic lifetime n, real interest rate r and annuity factor a for energy saving solutions.

	Heating setback	Construction	Vent. heat recovery	VAV vent.	Heat pump	PV panels
n [yr]	15	60	15	15	15	25
r [-]	0.05	0.05	0.05	0.05	0.05	0.05
a [-]	0.0963	0.0528	0.0963	0.0963	0.0963	0.0710

Table K.7: Investment cost I_0, additional maintenance cost ΔC_M, fuel and shore power saved, annual savings B.

	I_0 [NOK]	ΔC_M [NOK/yr]	Fuel saved [kWh/yr]	Shore p. saved [kWh/yr]	B [NOK]
C1 MGO	-	-	1,484,000	33,000	608,759
C1 LNG	-	-	797,000	33,000	239,390
C2 MGO	-	-	508,000	24,000	221,080
C2 LNG	-	-	504,000	24,000	154,512
C3 MGO	-	-	209,000	5000	86,087
C3 LNG	-	-	166,000	5000	47,989
C4 MGO	-	-	328,000	10,000	137,254
C4 LNG	-	-	264,000	10,000	78,366
C5 MGO	-	-	29,000	1000	12,251
C5 LNG	-	-	28,000	1000	8251
C6 MGO	6,492,500	0	9,686,000	189,000	3,946,979
C6 LNG	6,492,500	0	7,484,000	189,000	2,127,167
C7 MGO	31,600,430	87,585	9,019,000	350,000	3,761,437
C7 LNG	31,600,430	87,585	6,809,000	350,000	2,025,596
C8 MGO	9,500,000	190,000	11,181,000	-375,000	3,773,603
C8 LNG	9,500,000	190,000	5,954,000	-375,000	977,461
C9 MGO	2,400,000	0	96,000	41,000	78,207
C9 LNG	2,400,000	0	90,000	41,000	64,269

Table K.8: NPV, pay-off time, MPI and annual reduction in GHG emissions.

	NPV [NOK]	Pay-off time [yr]	MPI [NOK]	CO_2e saved [tons/yr]
C1 MGO	-	-	6,318,710	469.6
C1 LNG	-	-	2,484,786	234.4
C2 MGO	-	-	2,294,735	162.4
C2 LNG	-	-	1,603,782	148.6
C3 MGO	-	-	1,629,566	66.2
C3 LNG	-	-	908,398	48.6
C4 MGO	-	-	2,598,121	104.1
C4 LNG	-	-	1,483,413	77.5
C5 MGO	-	-	231,903	9.22
C5 LNG	-	-	156,186	8.21
C6 MGO	34,475,792	1.76	40,968,292	3062
C6 LNG	15,586,766	3.39	22,079,266	2185
C7 MGO	7,442,000	11.2	39,042,430	2874
C7 LNG	-10,575,436	31.0	21,024,994	2011
C8 MGO	29,668,709	2.76	34,068,467	3457
C8 LNG	645,711	13.6	10,034,711	1670
C9 MGO	-1,297,755	-	1,102,245	35.4
C9 LNG	-1,494,196	-	905,804	31.3

NTNU HSE	Hazardous activity identification process	Prepared by	Number	Date
		HSE section	HMSRV2601E	09.01.2013
		Approved by		Replaces
		The Rector		01.12.2006

Unit: Department of energy and process engineering **Date:** 15.01.21

Line manager: Terese Løvås

Participants in the identification process (including their function)**:** Natasa Nord (supervisor), August Brækken (student)

Short description of the main activity/main process: Master project for student August Brækken. "Energy Use and Energy Efficiency Potential on Passenger Ships".

Is the project work purely theoretical? (YES/NO): YES *Answer "YES" implies that supervisor is assured that no activities requiring risk assessment are involved in the work. If YES, briefly describe the activities below. The risk assessment form need not be filled out.*

Signatures: *Responsible supervisor:* Natasa Nord *Student:* August Brækken

ID nr.	Activity/process	Responsible person	Existing documentation	Existing safety measures	Laws, regulations etc.	Comment
1	Literature study on energy and fuel use in passenger ships	August Brækken				
2	Organise data relevant for a hotel system on passenger ships	August Brækken				
3	Collect and develop relevant weather data	August Brækken				
4	Develop energy efficiency scenarios that are relevant for passenger ships	August Brækken				
5	Further develop hotel part of the ship model in IDA ICE	August Brækken				
6	Calibrate the IDA ICE model based on the literature study and data available	August Brækken				
7	Consider the integration of the hotel system with the ship's propulsion and energy systems	August Brækken				
8	Perform energy efficiency analyses for the suggested scenarios	August Brækken				

August Brækken

Energy Use and Energy Efficiency Potential on Passenger Ships

NTNU
Norwegian University of
Science and Technology